Nuclear Waste
Services

NEAR FIELD

2026 Environmental Safety Case for the LLWR

LLWR/ESC/R(26)10171, May 2026

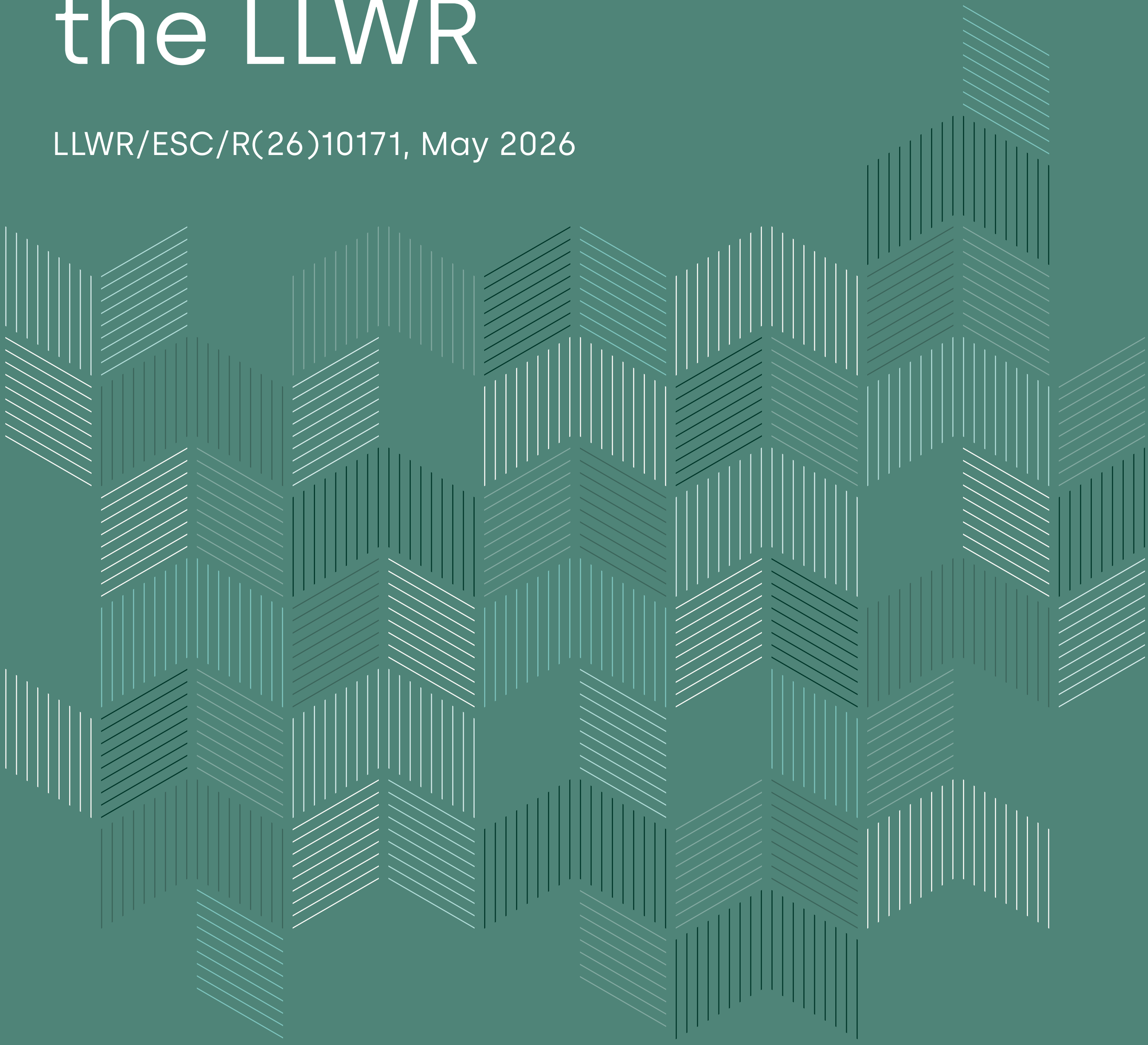

Conditions of Publication

This document is made available by Nuclear Waste Services Limited (NWS). Information on its activities is being made readily available to enable interested parties to have access to and influence on its future programmes.

NWS is a wholly owned subsidiary of the Nuclear Decommissioning Authority (NDA). All copyright, database rights and other intellectual property rights reside with the NDA.

This document may be freely used for non-commercial purposes provided that the source of this document is acknowledged when it is shared with third parties.

Any commercial use of this document including (but not limited to) sharing, distribution, copying and/or re-publication of this document (and/or any extracts thereof) is prohibited. Accordingly, all commercial use of this document requires express written permission from the NDA.

Applications for permission to use the report commercially should be made to the NDA Information Manager.

Although great care has been taken to ensure the accuracy and completeness of the information contained in this publication, neither the NDA nor NWS accepts any liability or responsibility for consequences that may arise from its use or reliance by other parties.

© Nuclear Decommissioning Authority 2026. All rights reserved.

Preface

The Low Level Waste Repository (LLWR) is the United Kingdom's principal facility for the disposal of solid Low Level Waste (LLW). It is a near-surface disposal facility in which waste was disposed in trenches and is now being disposed in vaults excavated into the ground surface. The LLWR is owned by the Nuclear Decommissioning Authority (NDA) and operated on their behalf by a wholly-owned subsidiary division, Nuclear Waste Services Ltd.

We, Nuclear Waste Services, are committed to operating the LLWR as a safe and efficient facility that provides a continuing option for the disposal of LLW in the United Kingdom. This will be achieved consistent with good practice for the near-surface disposal of radioactive waste, in accordance with environmental, health and safety, and security regulation and guidance, and in compliance with the terms of our Nuclear Site Licence and Permit to dispose of radioactive waste. We are also committed to working with the NDA to ensure optimal use is made of the LLWR to support the NDA's mission, in accordance with government policy. This may involve the disposal of a broader range of wastes than just LLW as currently defined in the United Kingdom[1].

One of the means we use to operate the LLWR safely is to maintain and implement an Environmental Safety Case for the site. This is one of the reports presenting the 2026 Environmental Safety Case for the LLWR – the 2026 ESC. The 2026 ESC is a major update based on a comprehensive review of our previous 2011 ESC and subsequent developments. The 2026 ESC addresses both the environmental safety of the disposal facility and the rest of the site. It considers the disposal of both LLW and some less-hazardous Intermediate Level Waste (ILW). Assessing the disposal of some less-hazardous ILW does not imply any decision has been made to dispose of such waste at the LLWR. The work has been undertaken to understand the safety implications if such a decision were made and hence support consideration of the option by the NDA.

The 2026 ESC is issued under the authority of the Nuclear Waste Services' Executive Director of Sites and Operations.

The 2026 ESC consists of documents at two levels:

- A single 'Level 1' report outlines the plan for the development of the LLWR and the main arguments concerning environmental safety and how it is achieved.
- A series of 'Level 2' reports present the evidence that underpins our safety arguments, including descriptions of our management framework, system understanding, design and management choices, assessments and implementation.

---

[1] In government policy, LLW is defined as radioactive waste having a radioactive content not exceeding four gigabecquerels per tonne (GBq t-1) of alpha or 12 GBq t-1 of beta/gamma activity.

This is the Level 2 report ‘Near Field'. The ESC Level 1 and 2 reports are listed in the table below, which also shows for the Level 2 reports the set of arguments for which each report mainly provides evidence. A brief description of the contents of each Level 2 report is also given. The ESC is supported by a large number of technical and scientific reports and references that we refer to as ‘Level 3’ documents. We have also produced a Guide to Key Points of the ESC, to help a wider group of stakeholders understand its nature, conclusions and implications.

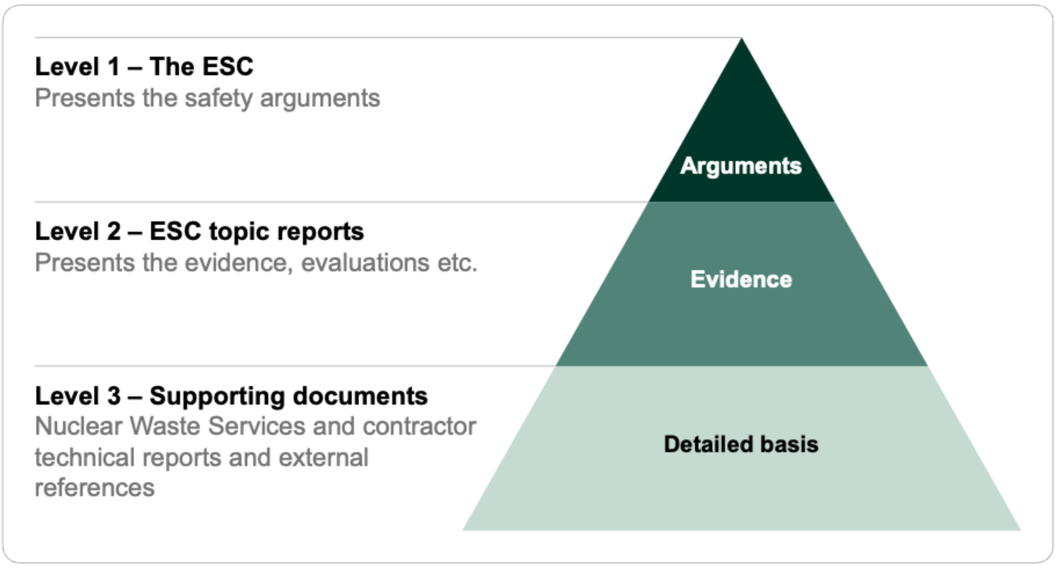

Level 1 – The ESC
Presents the safety arguments

Level 2 – ESC topic reports
Presents the evidence, evaluations etc.

Level 3 – Supporting documents
Nuclear Waste Services and contractor technical reports and external references

Level 1	
Main Report [1]	
Level 2	
Management and dialogue	
Management and Dialogue [2]	Describes our environmental management systems and interactions with regulators and stakeholders
System characterisation and understanding	
Site History and Description [3]	Provides a history and description of the site
Disposal Facility Inventory [4]	Describes the wastes already disposed and wastes that may be disposed at the facility
Engineering Design [5]	Presents the engineering design of the current facility and proposed changes as further disposal vaults are built and the disposal facility is closed

Near Field (this report)	Describes our understanding of the chemical and physical evolution of the engineered disposal system
Hydrogeology [6]	Describes our understanding of the geology and hydrogeology of the site
Site Evolution [7]	Describes our understanding of how the site will evolve, with a focus on coastal erosion
Monitoring [8]	Presents our programme of environmental monitoring supporting the ESC
Optimisation and Site Development Plan	
Optimisation and Site Development Plan [9]	Describes our approach to optimising the design and management of the disposal facility and wider site, and sets out our Site Development Plan
Waste Management Plan [10]	Presents our plans for managing the wastes produced by previous uses and operation of the site
Assessments	
Safety Functions [11]	Presents our understanding of how the different aspects of the repository system and its management contribute to the safety of the facility
Engineering Performance Assessment [12]	Presents our analysis of how the various components of the engineered disposal system will perform, which is an input into our impact assessments
Environmental Safety During the Period of Authorisation [13]	Presents evidence that the LLWR is currently being operated safely and will continue to be so during the period that the facility is permitted
Assessment of Long-term Radiological Impacts [14]	Presents evidence that, if the LLWR is managed in accordance with the Site Development Plan, the site will remain safe in the long term
Hydrogeological Risk Assessment [15]	Presents evidence that the disposal facility protects groundwater from both radiological and non-radiological contaminants in the disposed wastes now and will continue to do so in the future

Assessment of Radiological Impacts on Non-human Biota [16]	Presents evidence that the LLWR does not have adverse consequences for non-human biota populations now and will not in the future
Implementation	
Implementation [17]	Sets out how we use the ESC to manage the site, including setting Waste Acceptance Criteria and other controls on the types and quantities of waste accepted for disposal
Audit	
Addressing Regulatory Requirements and Feedback [18]	Provides a cross-reference between the contents of the ESC and regulatory guidance and feedback

Executive Summary

This report summarises the conceptual model for the evolution of the LLWR near field with particular focus on the physical and chemical evolution and processes influencing the release of contaminants. Overall, these near-field studies demonstrate the application of sound science, underpin our approach to assessment and optimisation, and provide a basis for defining waste acceptance criteria.

Groundwater flow through the near field depends on the evolution of the engineered barriers over timescales of hundreds and thousands of years. Taking account of the performance of the final cap in greatly reducing recharge to the repository, hydrogeological models of the near field predict that unsaturated conditions will be maintained within the vaults and trenches for at least 1000 years and most likely until the onset of coastal erosion disrupts the repository in several hundreds to thousands of years.

The key physical processes influencing the evolution of the near field and, specifically the flow of water through the waste mass, are settlement of the wastes, which for the vaults will depend on container deformation as well as waste degradation processes, and the rate of infiltration through the cap.

The evolution of the wastes in the vaults will depend to some extent on their initial state. We plan to surcharge[2] the existing and committed wastes in half-height ISO freight (HHISO) containers stacked in Vault 8 and part of Vault 9 to express voidage before capping in order to create a stable platform for installation of the final cap. This will involve some damage to the containers. Lower containers will deform at the corner posts, which may create tears along welds, and the lids of the uppermost containers will be damaged. Most HHISO containers will still act with the low permeability grout to largely isolate the wastes from infiltrating water, and flows will predominantly be through the gaps between containers. Future wastes, in stronger containers, will not be surcharged as the containers are designed to carry the capping loads without deformation. Furthermore, stacks of stronger containers will be topped by container protection units that will protect the lids and efficiently divert water into the gaps between stacks.

The initial low infiltration through the final cap means that corrosion of the containers and the waste metals will consume all the infiltrating water until infiltration increases following cap geomembrane degradation. This could take 1000 years or more. As a result, the repository, and the vaults in particular, will be in a state of increasing desaturation until degradation of the cap geomembrane followed by greater infiltration. Higher infiltration rates will lead to increasing saturation in the grouted wastes, eventually a saturated zone at the base of the vaults, and a rise in the water level in the trenches. Before this time, with no continuous

---

[2] Surcharging, or proof-loading, is the practice of loading a surface in order to compress and consolidate the underlying material. In this case, a layer of aggregate materials equivalent to the profile fill and final cap will be used to pre-load the trenches, existing and committed containers in Vault 8, Vaults 9 and 9a [5].

water-filled pathway, there will be very little opportunity for contaminant releases to groundwater from the vaults.

Since the 2011 ESC, we have developed a new generation of reactive transport models in the PFLOTRAN (Parallel FLOw and TRANsport) software that allow us to investigate the evolution of physical and chemical conditions. A key advantage of this software is the ability to account for the highly heterogeneous saturation conditions in the vaults. The models represent different length scales, from a single HHISO container to the full repository. This suite of models allows us to apply appropriate discretisation for the scale of the processes being investigated.

We have improved our understanding and modelling of the cementitious grout used in the HHISO containers. In combination with the lower infiltration rates, arising from the improved cap performance, this has led to revision of the vault chemical evolution with higher initial pH in the grout, compared to the 2011 ESC near field. Other significant improvements include the waste material inventories in Vault 8, and the corrosion rates for stainless steel and carbon steel under a range of different conditions relevant to the trenches and vaults. These changes are reflected in the estimated gas volumes generated by metal corrosion and organic degradation.

The main chemical processes and phases of evolution in the trenches and vaults are summarised as follows:

- Degradation of cellulosic wastes in trench disposals will lead to mildly acidic and sulphate-reducing conditions developing early, followed by methanogenic conditions. Reducing conditions dominated by cellulose degradation will last around 1,200 years to several thousand years depending on the content of organic wastes in different trenches.
- The large quantities of corroding metal in the trenches will ensure reducing conditions are maintained even after cellulose degradation has slowed.
- The main phase of gas production in the trenches lasts for over 2,500 years, with the remaining stainless steel generating low levels of hydrogen for 5,000 years.
- In the longer-term, once corrosion has largely consumed the metal and cellulose is similarly exhausted, the Eh in the trenches will reflect conditions associated with corrosion products and iron minerals, leading to more oxidising conditions. These may mobilise uranium, but coastal erosion is likely to have disrupted the repository before this.
- Corrosion of the external surfaces of the containers will establish reducing conditions in vaults that will last for more than 5,000 thousand years. Anaerobic corrosion of metals will result in a long period when water consumption exceeds infiltration and releases from most containers are restricted to gaseous radionuclides.

- Within the wastes, the grout porewater is initially extremely alkaline with conditions up to pH 13.5. The pH will fall slightly with contact with infiltrating water but will remain at pH 12 or above for several thousand years.
- Cellulose degradation in the vault wastes will proceed largely by alkaline hydrolysis as microbial activity is restricted by the high pH conditions. Without microbial degradation, isosaccharinic acid will increase in concentration. Complexation of isosaccharinic acid with radionuclides such as plutonium will increase their solubility and reduce retardation, thus may affect their mobility once water infiltration rates increase.

The environmental monitoring programme for the trenches has collected data for 50 years from leachate analyses and from probe holes once the interim cap was installed. Consideration of these data has provided valuable insights into the evolution of the system, particularly for gas generation and degradation of organic wastes, and for the behaviour of uranium wastes.

The effectiveness of the near-field processes in minimising the release of contaminants is subject to some important uncertainties related to the following aspects:

- The physical evolution of the cap is important in limiting the infiltration of water. The evolution of the near-field engineering will also affect water inflows from the surrounding geology.
- Focussing of infiltration into the gaps between container stacks relies on the maintenance of high permeability flow paths, while direction of water in the base of the vaults to the underlying geology relies on the undervault drainage blanket. In both cases, there could be clogging by movement of fines or chemical precipitation.
- The physical state and behaviour of the containers depend on corrosion processes in the different environments of the gaps and the grouted waste, both with associated uncertainties.
- The chemical form and distribution of contaminants in the waste materials are important in determining whether and to what extent physical and chemical processes may limit their release from the primary wastes.
- The effects of physical and chemical heterogeneity in the waste and wasteform at the scale of the HHISO container are important to assumptions that are required in modelling of the near field. There are uncertainties about the impact of the biogeochemical conditions that may occur in waste initially isolated from grout and also the impact of transport through cracks in the wasteform.
- The solubility and sorption that limit the migration of the key chemically active radionuclides in the near field are dependent on the local chemical conditions that may be heterogeneous and vary in time.

We have investigated these uncertainties in the near-field modelling and, where relevant, also in the assessment calculations in order to consider their potential impacts.

On the basis of our conceptual model, assessment models have been developed in the probabilistic modelling software, GoldSim, to represent the release of radioactive gases and dissolved contaminants in groundwater from the near field.

The groundwater assessment reference case model considers 'uniform flow' through the wastes. This does not account for the expected system in which flows occur mainly in the unsaturated gaps between containers rather than through the saturated but low permeability waste mass. A variant 'dual porosity' model is used to investigate this heterogeneous transport system. Other features of the model include:

- In the uniform flow model, the near field is modelled as a series of well-mixed compartments in which average waste properties (e.g., density and porosity) are assigned to each compartment.
- Water flows through the repository are modelled, accounting for infiltration through the cap as a time-varying boundary condition, and potential inflows into the repository from the surrounding geology. Water flows are calculated using a Compartment Flow Model (CFM) that is informed by more detailed hydrogeological modelling.
- Radionuclides are assumed to be instantaneously released from their associated wasteform and immediately available for dissolution in infiltrating water.
- Contaminants are subject to solubility limits and linear, reversible sorption parameterised appropriately for the chemical conditions in the trenches or vaults.
- In the 'uniform flow' model, each vault is modelled as a single component, whilst the trenches are sub-divided into a series of components.
- Under the 'uniform flow' model for the vaults, it is assumed that all porosity within the compartments is accessible to water and it is further assumed that water flows through this connected porosity.
- Under the alternative “dual porosity” model for the vaults, there are no water flows through the containers and contaminants diffuse out of the waste stacks into the gaps between the stacks. Water flows from these gaps into the underlying geology. In this model, individual stacks of containers are considered as well-mixed compartments, and one well-mixed compartment represents the gaps between the stacks.
- The model calculates concentrations of contaminants in near-field compartments, which become fluxes with the CFM flows between near-field compartments and thence to the geosphere compartments.

The simplifications adopted in the GoldSim model result overall in a cautious representation of the near field. This is demonstrated for some simplifications, such as neglect of any barrier function from the containers, by the corresponding results of PFLOTRAN modelling.

Two GoldSim assessment models are used to represent radon releases and C-14-bearing gas releases, respectively. The key processes in the radon model are:

- emanation of Rn from the wastes;
- transport of Rn in the bulk gas phase generated by metal corrosion, and also by cellulose degradation in the trenches;
- focussing of gas releases through the defects in the cap geomembrane. This has the effect of increasing the velocity of radon transport between the wastes and the biosphere, thus greatly reducing the time for decay;
- after geomembrane degradation, uniform bulk gas and radon release through the cap resulting in slower travel times, more decay and reduced impacts.

The key processes for the C-14 gas model are:

- experimentally determined waste material C-14 release rates and speciation for the primary releases, including gas;
- gaseous C-14 releases are assumed to be instantaneously transferred to the biosphere;
- restriction of microbial activity in the grouted wastes so that dissolved organic C-14 species persist in porewater;
- infiltration rates are assumed to be too low until geomembrane failure for there to be a significant release of dissolved C-14 from the containers to the gaps;
- fast leaching of dissolved C-14 species from porewater in the surcharged containers following infiltration rate increase;
- diffusion of dissolved C-14 out of perforations in the walls of stronger containers into water flowing in the gaps;
- all C-14 released to the gaps is assumed to undergo microbial degradation to gas and instantaneously transfer to the biosphere;
- in the trenches, all C-14 released from the wastes is assumed to be metabolised to C-14-bearing gas and to be released to the biosphere.

These simplifications in the GoldSim model for the gas assessment result in a cautious representation of C-14 gas releases in which there are no C-14 releases to groundwater. The groundwater assessment does not use the assumption of complete microbial degradation, and dissolved C-14 in the gaps is released to the groundwater.

Uncertainties in both the gas and groundwater models have been treated in several ways:

- by undertaking supporting studies to demonstrate that the uncertainty has a limited effect (for example, enhanced transport as a result of colloids);

- by making cautious assumptions in assessment calculations (for example, by assuming all C-14 in the gaps is metabolised to gas in the gas assessment, and all C-14 in the gaps is released to groundwater in the groundwater assessment);
- for the groundwater pathway, by addressing parameter uncertainty within a probabilistic calculation (for example, uncertainties in the solubilities and sorption distribution coefficients for radionuclides, or the parameters describing the engineered barrier properties);
- for the groundwater and gas pathways, by undertaking variant deterministic calculations to explore the impact of the uncertainty (for example, reduced sorption and enhanced solubility of radionuclides in solution, as a result of the presence of complexants).

We have identified some key near-field uncertainties where we believe it would be appropriate to undertake further work to build understanding and further confidence in our models. In addition to further development of the PFLOTRAN models, for example, to implement sorption of ISA on grout, future work will include:

- Revisiting bulk gas generation and modelling of gas release in order to provide better support to the engineering team for the optimisation of the gas vent design and gas management strategy.
- Long-term near-field experiments at medium to large-scale to provide support for the modelling of the unsaturated system.

Despite the outstanding uncertainties, we are confident that our near-field understanding is sufficiently well-developed and robust to support to the ESC.

Table of Contents

1 Introduction

1.1 Objectives

The objectives of this report are to present a description of the Low Level Waste Repository (LLWR) near field including evidence supporting our understanding of the physical and chemical evolution of the waste and how this affects contaminant behaviour. The report presents information from site monitoring, experimental studies and modelling investigations that have been used to develop the conceptual basis for the 2026 Environmental Safety Case (ESC) assessment models and to provide some specific data inputs.

The report is relevant to several of the requirements in the environment agencies' 'Guidance on Requirements for Authorisation for Near-Surface Disposal Facilities on Land for Solid Radioactive Wastes' (the GRA) [19]:

Requirement 4: Environmental safety culture and management system

'The developer/operator of a disposal facility for solid radioactive waste should foster and nurture a positive environmental safety culture at all times and should have a management system, organisational structure and resources sufficient to provide the following functions: (a) planning and control of work; (b) the application of sound science and good engineering practice; (c) provision of information; (d) documentation and record-keeping; (e) quality management.'

Requirement 8: Optimisation

'The choice of waste acceptance criteria, how the selected site is used and the design, construction, operation, closure and post-closure management of the disposal facility should ensure that radiological risks to members of the public, both during the period of authorisation and afterwards, are as low as reasonably achievable (ALARA), taking into account economic and societal factors.'

Requirement 11: Site investigation

'The developer/operator of a disposal facility for solid radioactive waste should carry out a programme of site investigation and site characterisation to provide information for the environmental safety case and to support facility design and construction.'

Requirement 13: Waste acceptance criteria

'The developer/operator of a disposal facility for solid radioactive waste should establish waste acceptance criteria consistent with the assumptions made in the environmental safety case and with the requirements for transport and handling, and demonstrate that these can be applied during operations at the facility.'

Requirement 14: Monitoring

'In support of the environmental safety case, the developer/operator of a disposal facility for solid radioactive waste should carry out a programme to monitor for changes caused by construction, operation and closure of the facility.'

Under Requirement 4, the application of sound science is highlighted

> *6.2.26: All work that supports the environmental safety case needs to apply sound science. The developer/operator needs to able to make informed judgements about the quality of the science being applied and to make sure that timely scientific investigations are carried out to remedy any deficiencies in understanding of especial relevance to the particular disposal facility. The developer/operator also needs to maintain awareness of scientific developments, both within and outside the UK, that may have a bearing on the environmental safety case for the facility.*

We consider that this report provides evidence of our commitment to the application of sound science by demonstrating our efforts to improve on the approaches, models, software and data used in the 2011 ESC where it was judged to be appropriate (that is, taking account of the principle of proportionality). We have undertaken studies in many areas, in addition to the near field, to ensure that we have taken account of any relevant developments in scientific understanding, and have also drawn on the work of other waste management organisations where possible.

In this report, we present:

- our understanding of the near field, which underpins our estimates of environmental impacts. Near-field studies also support our approach to optimisation (Requirement 8) and waste acceptance criteria (Requirement 13);
- our programme of past and ongoing experimental research, which underpins our modelling studies, demonstrates the application of sound science, which is an important aspect of Requirement 4;
- the use of data from the near-field research programme, monitoring programme and site investigation programme to support development of a conceptual model (Requirements 11 and 14).

1.2 Scope

This report summarises our understanding of the evolution of the LLWR near-field environment, with particular focus on the behaviour of the key barriers to the release of radioactive and chemotoxic contaminants. The report presents a conceptual model of the important features and processes of relevance to near-field evolution. The conceptual model is based on sound scientific understanding of the processes and is supported by the results of our near-field chemical-transport models in the PFLOTRAN software, site monitoring data and the results of experimental studies.

We use the output of the near-field models to underpin the assessment models in the GoldSim software, but the near-field models are not used in the assessments directly. We have summarised the approach to representation of the near field in the assessment models and impact calculations in this report.

The near field encompasses:

- the waste mass in the trenches and the grouted waste containers in the vaults;
- any infilling materials around the containers;
- the directly disposed, large waste items in the vaults and any surrounding grout;
- the engineered components of the vaults;
- the interim cap over the trenches;
- the closure engineering, including the cut-off wall, and the final cap.

The wastes include existing disposed low level waste (LLW), future LLW and intermediate level waste (ILW) that is judged to be acceptable. Accepting wastes exceeding LLW limits would be consistent with government policy on the management of radioactive waste but is not currently permitted at the LLWR by the Environment Agency. The inclusion of less-hazardous ILW in the scope of the ESC is a means of engaging with stakeholders on the most appropriate use of the site, consistent with government policy. It does not imply that any decisions have yet been made.

Our consideration of the physical barriers provided by the wastes and wasteform has also been developed to include consideration of the heterogeneity of the wastes and the water saturation behaviour.

We consider that, together, the application of scientific understanding, modelling approaches, the site monitoring programme, and experimental studies that are presented provide an appropriate and sound underpinning to the ESC in general. More specifically, the understanding and modelling results described in this report underpin our performance assessments, particularly as presented in the ‘Assessment of Longterm Radiological Impacts’ [14] and ‘Hydrological Risk Assessment [15] reports.

A list of ESC reports is given in the table in the Preface.

1.3 Major Improvements Since the 2011 ESC

There have been several major improvements and associated changes to our understanding of the near field since the 2011 ESC [20] as well as significant changes to the disposed and future inventory. These are discussed where relevant in the following sections. Here, we highlight the major changes and identify where they are discussed in the sections:

Understanding of cap performance and evolution of infiltration	Subsection 3.2.1
Modelling of unsaturated conditions using PFLOTRAN	Subsection 6.1
Composition of the water infiltrating the cap	Subsection 6.2.1
Understanding of the grout chemistry and evolution	Subsection 4.3.1
Generation and impact of isosaccharinic acid	Subsection 4.5.4
Material inventory and gas generation	Subsection 7.1

1.4 Structure

Following this introduction, the report has the structure described below.

- Section 2 provides a brief description of the LLWR, highlighting the features of relevance to the near-field evolution.
- Section 3 considers the expected physical evolution of the near-field closure engineering and wasteform features and the effects on the near-field hydrogeology.
- Section 4 describes our conceptual understanding of the near-field chemical evolution.
- Section 5 sets out our conceptual understanding of gas generation and the release of radioactive gases.
- Section 6 describes the modelling of chemical conditions within the vaults and trenches, and the key results.
- Section 7 describes the results of the modelling of gas generation and transport.
- Section 8 presents a summary of the representation of the contaminant release processes in assessment models for the gas and groundwater pathways.
- Section 9 considers the uncertainties and future work.
- Section 10 provides the conclusions of the report.

A general glossary for the ESC is appended to the ‘Main Report’ [1].

2 Description of the LLWR Near-field

2.1 Overview

The LLWR has been the UK's principal facility for the disposal of LLW since 1959. The LLWR receives waste from a range of consignors, including nuclear power stations, fuel cycle facilities, defence establishments, isotope manufacture sites, hospitals, universities, and from the cleanup of historically contaminated sites.

Two distinct disposal systems are present within the LLWR site (Figure 2.1), consisting of:

- seven trenches; and
- two engineered concrete vaults, with historic disposals to Vault 8 and ongoing disposals to Vault 9, and space for a further five vaults.

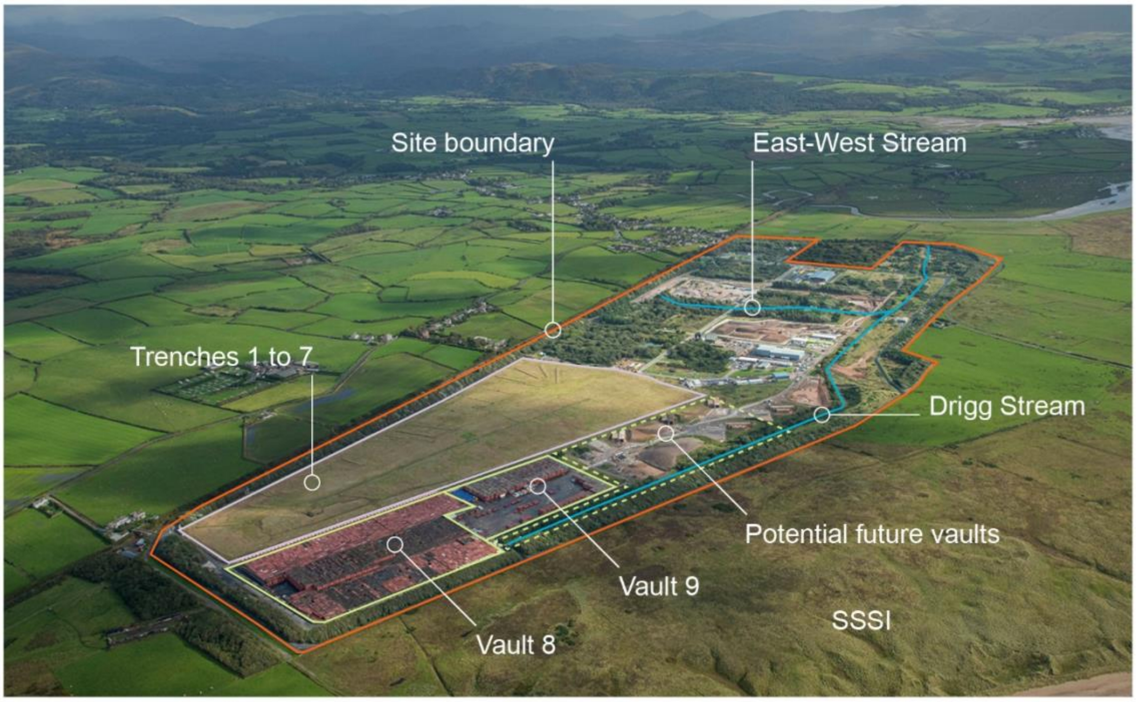

Figure 2.1: Aerial view of the LLWR site looking southeast

From 1959 until 1995, waste was tumble tipped into seven trenches. The base of each trench was generally excavated into a low permeability clay-rich layer at a depth of 5 to 8 m below ground level. In some regions of the trenches, the base clay layer was augmented with bentonite. Trenches 1 to 6 have typical widths between 10 and 20 m and lengths ranging from 480 to 715 m. Trench 7 has an irregular, approximately triangular shape. No compaction of the waste was undertaken other than that which occurred through the weight of the overlying waste and soil cover layer. A total volume of approximately 800,000 m^3 of waste was disposed in the trenches, but the wastes have since degraded and compacted down to an estimated volume of around 500,000 m^3 [5]. Prior to installation of a final cap, it is proposed to surcharge the trenches with a load that is equivalent to the weight of the profile fill and the final cap, to express any remaining voids and provide a stable substrate.

Since 1988, waste has been disposed of in engineered, concrete disposal vaults, initially Vault 8 and more recently Vault 9 (Figure 2.1). This upgrade to the disposal operations was aimed at improving management practices and making more efficient use of the site area. At that time, remedial work was conducted on the trenches, including the installation of a low permeability cut-off wall to limit the lateral movement of groundwater and contaminants, the interim capping of the filled trenches, and the refurbishment of the leachate drainage system.

For disposal in the vaults, waste is packaged in carbon steel half-height ISO (HHISO) containers and surrounded by cement-based grout to reduce package voidage. A significant proportion of the waste in Vaults 8 and 9 was also compacted before packaging on consignors' sites. The full introduction of the revised wasteform, and the phasing out of trench disposals, was not completed until 1995, when new grouting facilities at the LLWR site commenced operation and the interim cap over Trench 7 was finished.

The vaults are designed to accommodate grouted HHISO containers as well as items of waste that are too large for these containers. The original practice was for four layers of containers to be stacked in Vault 8, corresponding to a total capacity of about 200,000 m^3. Higher stacking of HHISO containers in Vault 8, so the tops of stacks followed the approximate dome of the eventual cap, was then planned to provide an additional capacity of around 100,000 m^3.

Vault 9 commenced operation in 2010 for disposal of the HHISO containers, although it was used for storage of containers in 2009. The current site plan allows for the construction of up to five additional vaults (Vaults 10 to 14, referred to collectively as the "future vaults"). A small strip of land adjacent to the west wall of Vault 9 is the location of Vault 9a which, once built, will be operated in parallel with Vault 9.

The planned higher stacking of containers in Vault 8 and for the existing containers in Vault 9 will not now be implemented, although there is a small area in the centre of Vault 8 where containers are stacked 5-high. Instead, it is proposed to surcharge the existing containers in Vaults 8 and 9 prior to installation of the final cap [5]. This proposal recognises that some of the existing containers might not be strong enough to support the loads that would be associated with overlying containers, the profile fill, and the cap. The surcharge procedure is designed to express container deformations and any associated settlement before installation of the final cap, to ensure a stable foundation for the low-permeability layers of the cap.

By around 2030, most LLW will be packaged in updated, strengthened HHISO containers, which will differ from the current design only in that they have slightly thicker vertical corner posts [5]. The strength of these containers will be sufficient to support the loads associated with overlying containers, the profile fill and the cap. Additionally, reinforced concrete 'container protection units' (CPUs) will span the topmost container in each stack [5]. The aim of the CPUs is to protect the lid of the uppermost container during capping operations and to divert infiltration to the gaps between stacks in the post-closure phase.

Work undertaken at the request of the NDA, in line with its strategy to consider alternatives to geological disposal for appropriate wastes, has identified the possibility of disposing of some ILW at the LLWR in the future [9]. If ILW disposal in the vaults is taken forward, then any ILW that can be managed as LLW could be packaged in strengthened HHISO containers. Transport requirements (e.g. limits on specific activity, need for a transport container) mean, however, that most disposals of ILW are likely to be in smaller containers: the standard waste transport container (SWTC)-compatible strong box [5]. Any ILW packages that require additional measures compared to LLW (e.g. to manage operational doses), would be placed inside shielded modules within Vault 10 or another of the future vaults. The shielded modules would consist of corridors with walls of reinforced concrete to reduce operational doses, with reinforced concrete roofs of sufficient thickness to support the cap.

Current projections suggest that disposal operations at the LLWR will continue to approximately 2135, and capacity up to Vault 12 will be sufficient to accommodate all future wastes. Notwithstanding, Vaults 13 and 14 are retained in the design to provide sufficient capacity given uncertainties about the inventory.

2.2 Near-field Engineering

The “Engineering Design” report [5] describes the engineered components that are currently planned to manage and optimise the performance of the LLWR in controlling the release of contaminants. The site is at present in an operational phase, during which disposal activities are carried out alongside the preparatory activities to support the installation of the first tranche of the final cap, over Vault 8 and the northern trenches.

Following the completion of waste emplacement and the closure of the final vault, the LLWR site will be subject to a period of active institutional control, expected to last for 100 years. For the LLWR, the term is synonymous with Period of Authorisation (PoA). During this period, active measures will be undertaken to control the disposal site. A site boundary will be maintained to prevent access by the public, and land use will be controlled. Active leachate collection and management will continue. Monitoring to meet regulatory requirements, and to provide reassurance that the facility is performing safely and as expected, will also continue during the PoA [8, 13]. Remedial actions, such as addressing any problems with the active drainage system, will be taken if required. Following withdrawal of control over the facility by the operator, the LLWR will enter a “post-closure” phase.

The main engineering features present at the LLWR include (see Figure 2.2; also Figure 2.4):

- Trenches 1 to 7;
- the interim cap over the trenches;

- a cut-off wall around the north-west and north-east margins of the trenches;
- Vaults 8 and 9; and
- a leachate management system.

Details of these features, beyond what can be included here, are presented in the Engineering Design report [5] and supporting references.

The interim cap is undergoing remediation to replace the southern part of the interim membrane (southern trench interim membrane or STIM) to ensure that the sections of the trenches that will not be capped in the first tranche are adequately protected from precipitation.

Site development will alter the existing engineering structures at the site and add new features [9]. A design for the future vaults has been developed [5] (Subsection 2.2.3), based on extensive hydrogeological studies and optimisation.

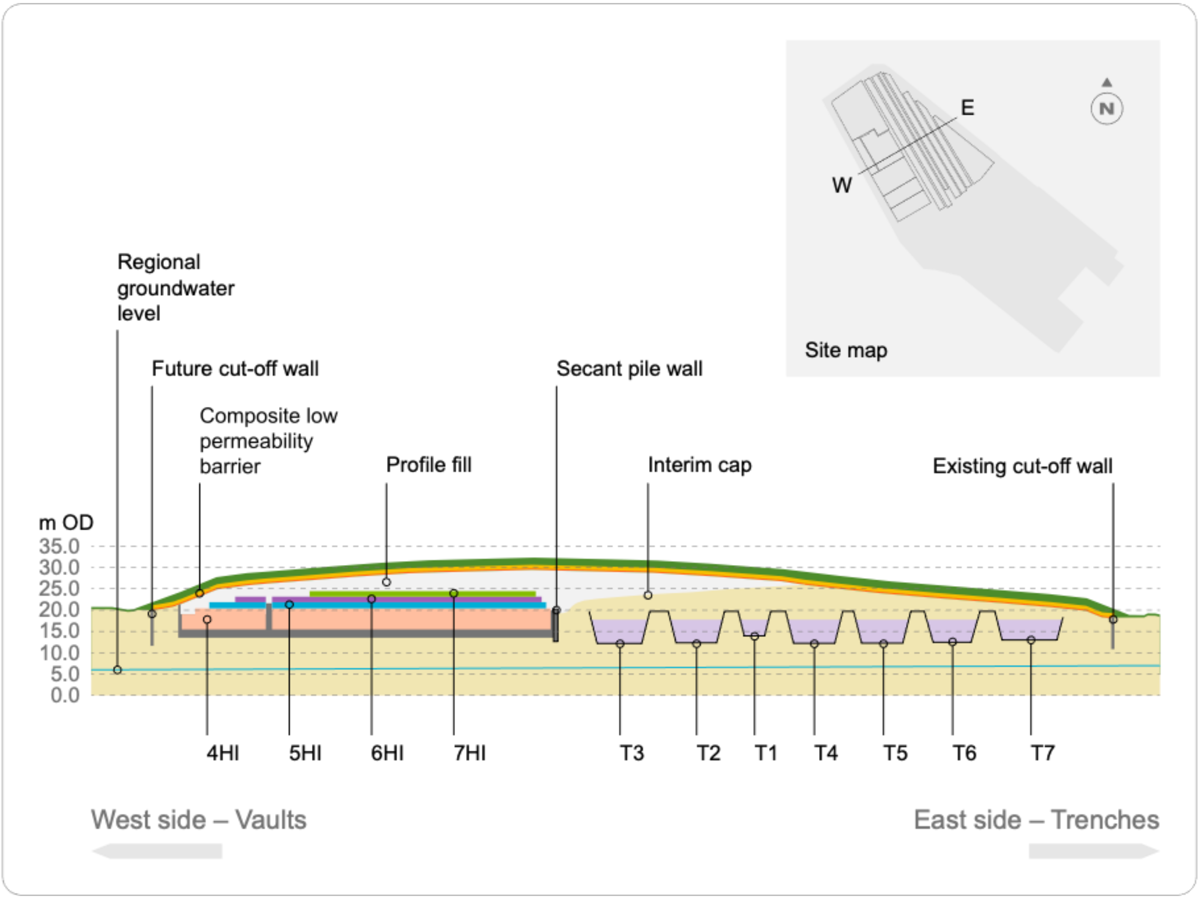

Figure 2.2: Cross section through Vaults 9a (left) and 9, and the Trenches (T1 to T7), showing many of the main engineering features at site closure [5]. The summit of the cap is approximately 13 metres above ground level. (HI: number of HHISO containers in a stack, as in 4-high etc.)

The Reference Design for the repository includes both current and future vaults, the final cap and other structures present at closure and forms the basis of the ESC. The main engineering features at the LLWR at site closure will include [5]:

- Trenches 1 to 7;
- Vaults 8 and 9;
- the future vaults;
- the final cap; and
- the cut-off wall.

Schematic illustrations of the near-field engineering at site closure, identifying key features and their spatial relationship, are provided in Figure 2.2 to Figure 2.4.

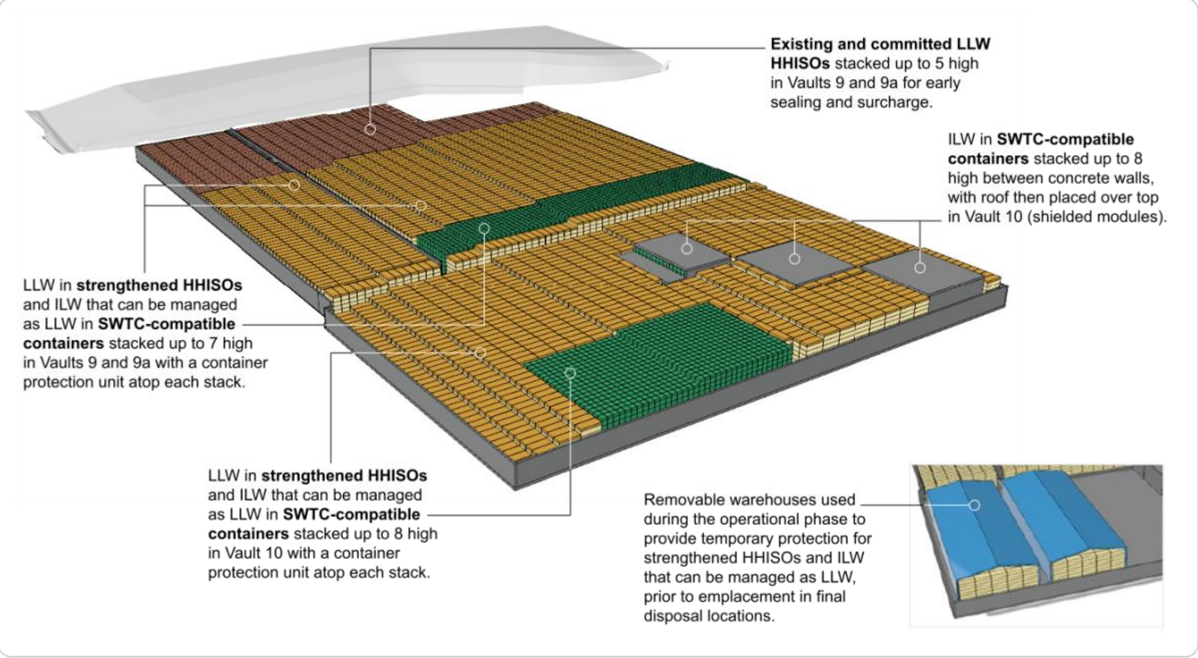

Figure 2.3: Illustration of the optimisation outcomes for Vaults 9, 9a and 10, illustrating shielded modules and temporary warehouses [9]

2.2.1 Vault 8

The wastes in Vault 8 are primarily disposed within half-height ISO containers that have been infilled with grout. There are, however, populations of two-third-height and full-height ISO containers. A small population of large, reinforced concrete, WAGR (Windscale Advanced Gas-cooled Reactor) boxes has also been disposed and, along the eastern edge of the vault, approximately one thousand 500-litre TRS (Treated Radwaste Store) drums from the Winfrith site have been placed in a narrow space against the vault wall. Around the margins of the vault, or in spaces too small for ISO containers, large items such as Magnox spent fuel transport flasks have been grouted *in situ*.

Gaps between stacks of containers are typically centimetre-scale but up to about 60 cm in Vault 8 (see Figure 2.10). Where possible, these gaps between stacks will be infilled with an inert, granular material such as gravel before placement of profile fill.

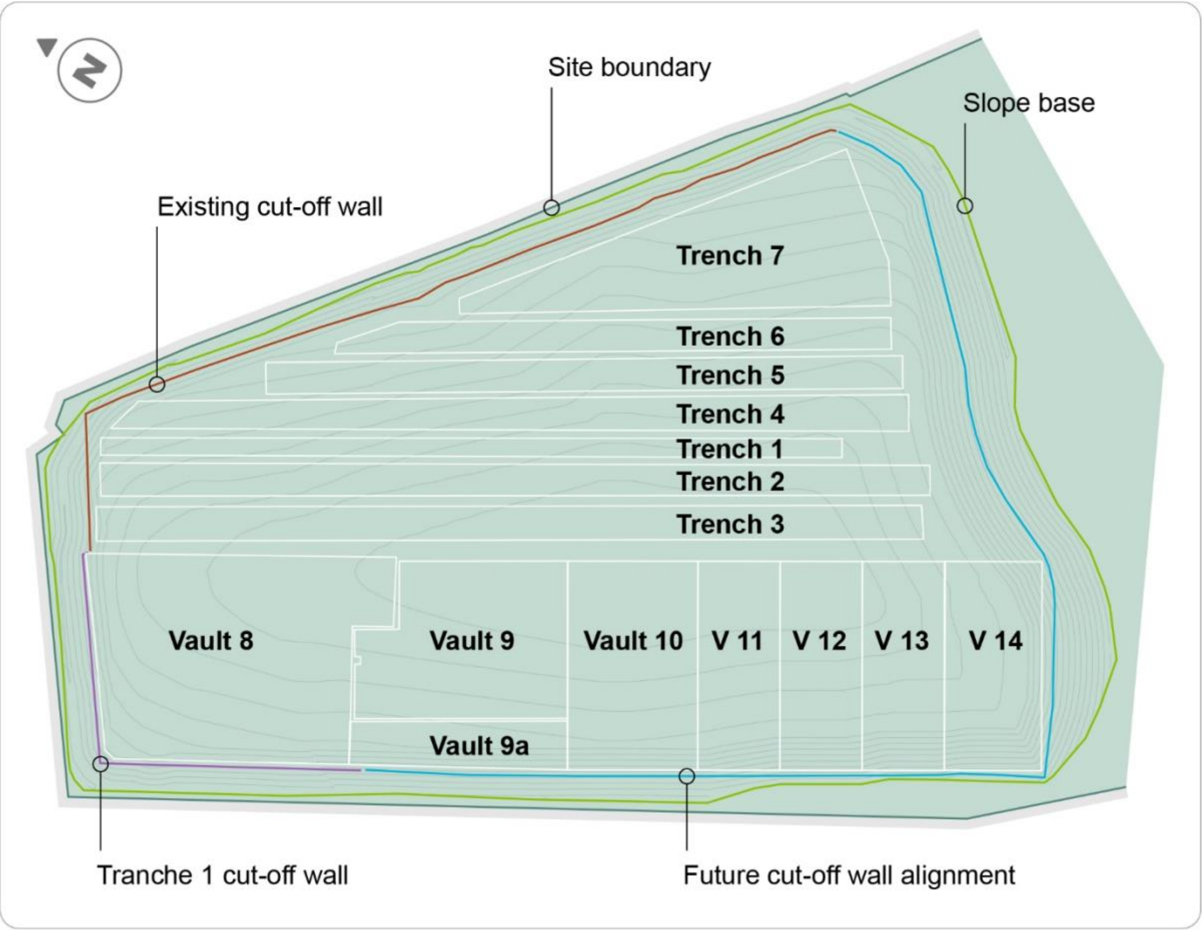

Figure 2.4: **Overview of trench and vault locations with illustrative cap contours (1m spacing) and showing the layout of trenches and vaults. The cut-off wall will follow the edge of the cap. The maximum cap height is 33 m above Ordnance Datum (OD) [5]**

Vault 8 has a reinforced concrete slab that provided a vehicle running surface for disposal operations. The slab was cast in sections with joints and is expected to sustain some cracking on loading by disposals. However, it was not intended to provide a long-term, low-permeability barrier. Rather, water management is provided by in-vault drains, together with underlying, low-permeability clay layers. For Vault 8, natural clay-rich sediments were originally intended to provide the low-permeability element of the base. However, the clay was found to be intermittent and, where it was missing or otherwise insufficient in either quantity or quality, bentonite enhanced sand (BES) was emplaced before the concrete slab was cast.

Vault 8 also includes reinforced concrete walls, and a secant pile wall adjacent to the trenches intended to provide support for the trenches along the interface. The base slabs and walls include drainage arrangements for leachate collection during operations.

2.2.2 Vault 9

The design of Vault 9 uses broadly the same basic principles as Vault 8, with a reinforced concrete base founded on low-permeability materials. In the case of Vault 9, however, a double composite liner was installed beneath the slab, with each composite comprising a 2 mm HDPE geomembrane overlying a 500 mm layer of BES. A granular drainage material layer was installed between the two composites, to provide the facility to monitor the performance of the upper layers and to detect leaks Figure 2.5.

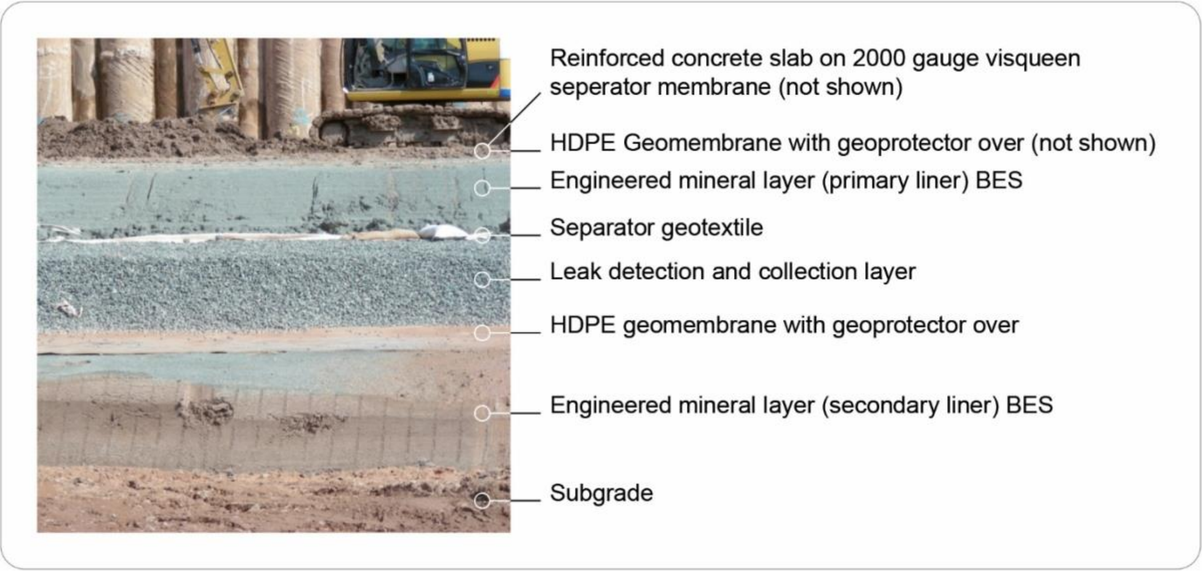

Figure 2.5: View of the Vault 9 basal liner system during construction

To the east, Vault 9 is bounded by a secant pile wall, running parallel with the trenches, and an adjacent reinforced concrete wall, while on the other sides of the vault there are reinforced concrete walls (Figure 2.6). The original intent was to line the outer surfaces of the walls with a geomembrane and a BES layer, but during construction it was decided to omit the geomembrane and BES layer above the 1 m level. At closure, arrangements will be made to allow drainage through the walls above the 1 m level to facilitate leachate flow to the drainage blankets that will underlie the future vaults.

As for Vault 8, some cracking of the concrete element of the base is anticipated during container placement and during closure processes, but the BES layer is expected to remain intact. The Engineering Performance Assessment (EPA [21, 12]) concluded that cracking will not challenge the performance of the base as a means of collecting leachate.

The Reference Design includes disposal capacity up to Vault 14, and even though current inventory estimates suggest that Vaults 13 and 14 may not be required [4], all the vaults are retained in the design for flexibility.

The first new vault planned is Vault 9a along the western side of Vault 9. Vault 9 and Vault 9a are often referred to in tandem as it is also planned to operate them in parallel. This means that existing and committed ISO containers of the current design will be emplaced at the north end of Vault 9a, adjacent to the existing and committed containers at the north side of Vault 9. This will allow these containers to be surcharged in a single tranche across the end of Vault 8 (see Figure 2.3). The remainder of Vault 9a will then be filled with the stronger containers at the same time as Vault 9 is operated.

Figure 2.6: View of the base and walls of Vault 9 [22]

2.2.3 Future Vaults

As Vault 10 and the other future vaults are developed, the secant pile wall on the east side will be continued southwards to provide support to the adjacent Trench 3, and the levels of the bases will fall to match the existing topography. The design of the future vaults, including Vault 9a, is expected to resemble that of Vault 9, apart from the vault bases.

In the case of the future vaults, the bases are required to perform two functions:

- to provide a suitable surface for moving and emplacing the waste packages; and
- to support water management during disposal operations.

The bases of the future vaults will be constructed with a reinforced concrete slab overlying a composite geomembrane and BES layer. The double composite liner of Vault 9 will not be replicated, because a single low-permeability composite liner is judged to be sufficient. This change to the bases also reflects updates to the drainage concept since Vault 9 was designed; the BES layer will be founded upon a drainage blanket, composed of a free-draining granular material, which will form part of a passive drainage system.

Careful design and construction of the final cap will minimise infiltration to the vaults for as long as possible. Once the cap begins to degrade in the longer term, however, higher infiltration will lead to the vaults gradually filling with water. To prevent the vaults filling to a level close to the ground surface, which could lead to discharges to either the shallow groundwater systems or to the surface drainage systems, the western and eastern walls of the future vaults will be limited to 1 m in height. The northern and southern walls will be slightly higher than 1 m, so that water will drain preferentially to the other sides. Any overtopping leachate will flow through drains to the drainage blankets that will underlie each of the future vaults, and from there onward to the deeper, regional groundwater system.

Vaults 8 and 9 do not have drainage blankets, and so any water above 1 m in height in those vaults will be directed to the drainage blankets via other routes, most likely via drainage connections through the walls of Vaults 8 and 9 to the future vaults.

2.2.4 Cut-off Walls

In 1989 a cement-bentonite slurry cut-off wall was constructed around the north and east of Trenches 1 to 6, and in 1995 it was extended along the east of Trench 7. The original cut-off wall was reported to be 1 m wide, from 7.3 to 9.4 m deep, with a much lower permeability than the surrounding geology.

As part of the closure engineering, the existing cut-off wall will be extended to provide a vertical, low-permeability barrier around the whole perimeter of the facility. The new cut-off wall will extend upwards from 2 m below the base of each vault. Where it intersects the final cap, it will be keyed into the BES layer to give continuity of the low-permeability barrier.

The final cut-off wall is intended to minimise lateral flows into the disposal system, especially the trenches and the drainage blankets underlying the vaults. It will also help to direct leachate from the LLWR preferentially downwards to the deeper groundwater system.

2.2.5 Profile Fill and Engineered Cap

The final cap will be a 3 m-thick multilayered structure (Figure 2.7) with a single dome that covers both the trenches and the vaults (Figure 2.4).

The cap will be underlain by at least 2 m of profile fill, and its main features, from bottom to top, will include:

- a gas collection layer to transport gas to a vent (Figure 2.8), which is expected to remain open at least throughout the PoA;
- a composite system comprising a 2 mm geomembrane over a BES layer to reduce infiltration to the repository;
- layers to encourage drainage;
- layers to protect against erosion, as well as intrusion by plants and animals; and
- layers to promote evapotranspiration.

The gas vent is created by the extension of the gas collection layer through the barrier layer (Figure 2.8) and forms an ellipsoidal annular structure approximately 80 m by 20 m and 3 m wide [23] below the crest of the cap above Vault 10 (Figure 2.4). The current assumption is that the gas vent associated with the cap will be sealed before the end of institutional control, but the vent system has not yet been optimised.

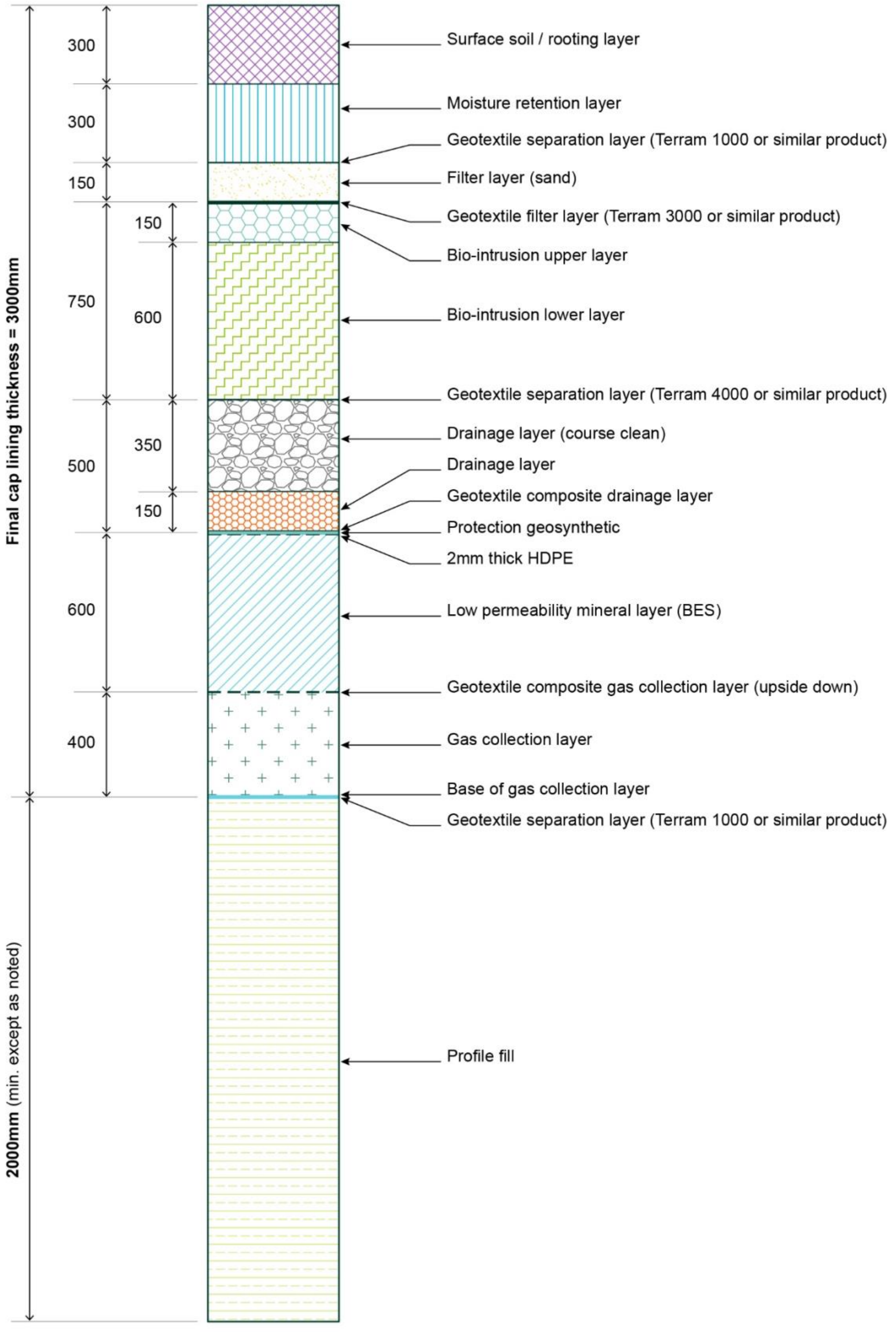

Figure 2.7: Layers of the Final Cap [5]

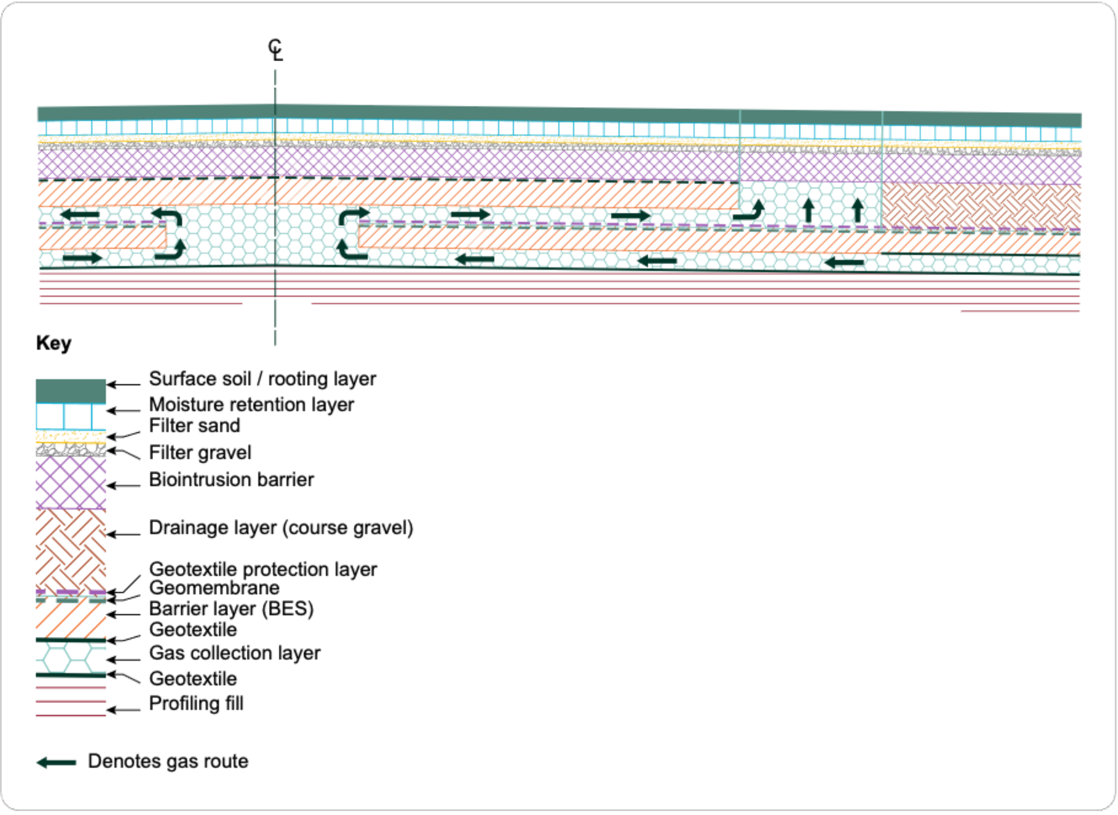

Figure 2.8: Detail of the gas collection layer and vent, showing the intended gas pathway [5]

It is planned that a post-2026 ESC optimisation programme will revisit the design of the vent, and incorporate the findings from recent performance assessments, particularly those relating to the generation, migration and release of bulk and radioactive gases. Consequently, changes to the current venting approach should be expected as part of the next iteration of engineered barrier design. This is discussed further in Subsection 7.2 along with the results of modelling gas generation and transport in the repository.

2.3 Inventory

From the perspective of near-field evolution, the waste inventory is dominated by the large volumes of bulk materials with which the radionuclides are associated. In addition, the disposal practices for the trenches and the vaults involved very different wasteforms, which mean that physical and chemical conditions in the two regions of the repository will evolve very differently (Section 4).

Within the trenches, the waste was generally unconditioned (Figure 2.9). Typically, it was packaged inside plastic bags or carbon steel drums, although some items, such as pipes and redundant laboratory equipment, were disposed of directly into the trenches. No mechanical compaction was carried out, although some self-compaction and settlement will have occurred since disposal. The trenches were filled with waste up to about a metre below the ground surface, and then they were covered with approximately 1 m of backfill, which was mainly derived from the excavated material.

Within the vaults, the waste has mostly been emplaced in carbon steel, HHISO containers (Figure 2.10) that are infilled with a low-viscosity, cementitious grout to fill the remaining void spaces around the waste. The waste occupies approximately half of the internal volume of the containers, with grout filling the remaining volume, although there is significant variation in grout content between containers.

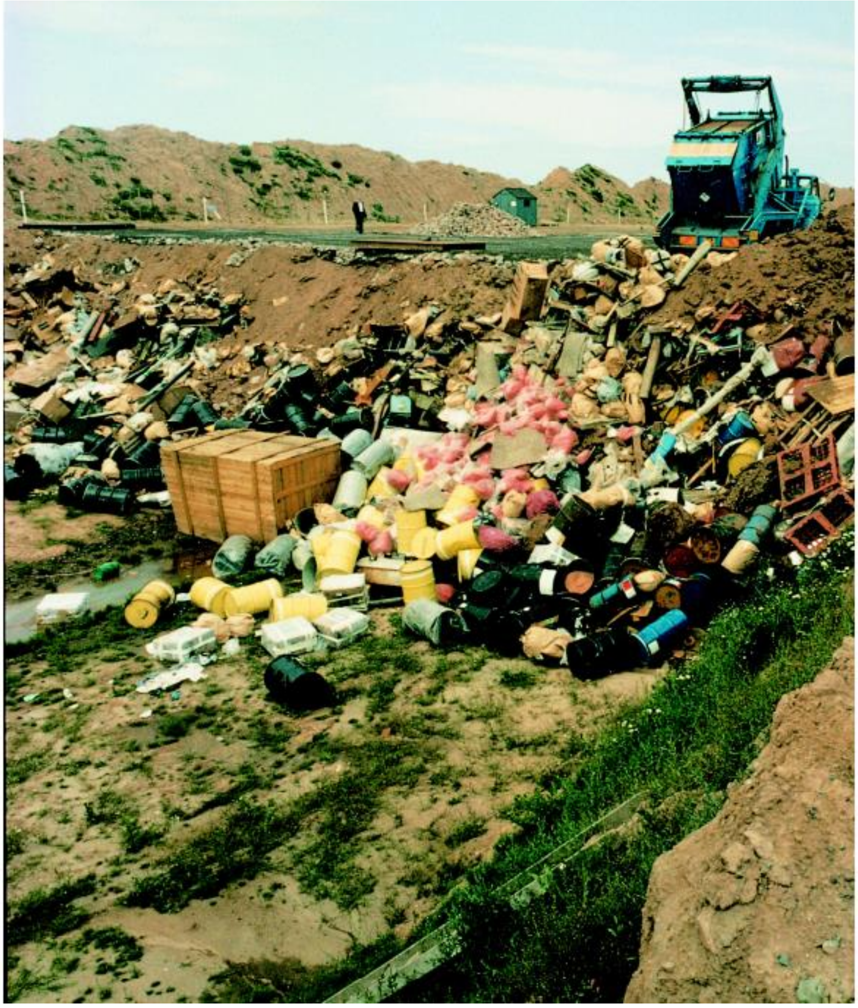

Figure 2.9: Disposal of LLW to the trenches [20]

The waste contains both radioactive and non-radioactive contaminants. The inventory of these contaminants and their distribution between disposed wastes, committed wastes and future waste arisings are described in the 2026 ESC Inventory report [4].

Disposed wastes are those already at the repository in the trenches or Vaults 8 and 9. Committed wastes arise up to and including FY2029/2030 in the ‘further reduced’ UKRWI arisings profile [24]. These wastes are expected to be disposed of in the current HHISO container designs. These packages will be treated like the waste already in Vaults 8 and 9.

Figure 2.10: Existing stacks of half-height ISO containers in Vault 8 [25]

Future wastes are subject to more uncertainty. The 2011 ESC Inventory report [26] noted that '*A variety of inventories can be derived for LLWR using the same arising data by making different assumptions about waste routing and the nature and extent of waste processing*'. The approach and assumption used in derivation of the inventory for the 2026 ESC are described in the Inventory report [4]. For the purposes of the present report, the future LLW differs from the disposed and committed wastes in that it will be packaged in the new stronger containers. Future wastes may also include some suitable ILW in the small, SWTC-compatible strong boxes (referred to as 'strong boxes' hereafter).

The updated disposed waste inventory [4] was derived from:

- review of historical trench records, which hold information about waste volumes as well as their distribution within the trenches;
- rederiving the disposed vault inventory to reflect an improved understanding of radionuclide and material composition;
- the LLWR eMWaste tracking system, which records the contents of every container in Vaults 8 and 9, and provides more detailed data for recent consignments, enhancing the level of detail and the comprehensiveness of the LLWR disposed vault inventory.

The future waste inventory [27] was based on:

- Information in the 2022 UK Radioactive Waste Inventory [28], including all LLW that is expected to arise within the UK that will not be disposed to a suitably permitted landfill site or Dounreay’s LLW disposal facility. This includes LLW that will be directly disposed and LLW that is subject to supercompaction, metallic treatment or incineration, noting that these treatment routes sometimes result in reduced or zero waste volumes and activities being received at the LLWR.

- Some waste streams associated with Nuclear New Build (NNB) power stations and several opportunity wastes and decay-stored streams that have been identified as being suitable for disposal at the LLWR.
- Radiological and non-radiological contaminant capacities and waste acceptance criteria derived from the 2011 ESC assessment calculations [29] and subsequent updates (e.g. the 2018 Hydrological Risk Assessment [30]).

2.3.1 Bulk Waste Materials

For the purposes of modelling the near field, we only require information about a subset of the materials in the waste inventory [4], but we require that information at the level of an individual trench or vault. The near-field models have focussed on the following materials:

- **Metals**
    - Carbon steel
      Note that the inventory [4] categorises carbon steel as "Other Ferrous Metal".
    - Stainless steel
    - Aluminium
      After the steels, aluminium is the next most abundant metal in the inventory, by volume fraction. It is also a relatively reactive metal. For both these reasons, aluminium deserves consideration.
- **Cellulosic materials**
    - Paper and cotton
    - Wood
    - Other / unknown cellulosics.

The justification for this selection is that the degradation of cellulosic materials and the corrosion of metals are known to be important processes when modelling the evolution of waste disposal sites, such as landfills and geological disposal facilities. Moreover, the materials that are listed above are present in the repository in large enough quantities or could degrade sufficiently quickly, to have a significant effect on near-field conditions (see Section 4).

The categories of 'Unknown metals' and 'unknown ferrous metals' are expected to comprise largely carbon steel and have been added to the carbon steel inventory in some cases, for example, for modelling bulk gas generation. Similarly, 'other / unknown cellulosics' are treated as 'paper and cotton' as a greater proportion of these materials, compared to wood, is degraded.

Figure 2.11 to Figure 2.13 show the volumes of these key materials, including packaging for the containers in the vaults, that have either already been disposed of in the repository or will be disposed of in the future vaults. Note that these are disposed waste volumes and, as described above for the trenches, are compiled based on historic disposal records dating from before material information was required for each consignment. The disposed material volumes do not easily correlate with masses, since volumes of pipework, for example, include the voids in the pipes. Consignment records for the vault disposals are increasingly detailed and there is more confidence about the masses of materials disposed.

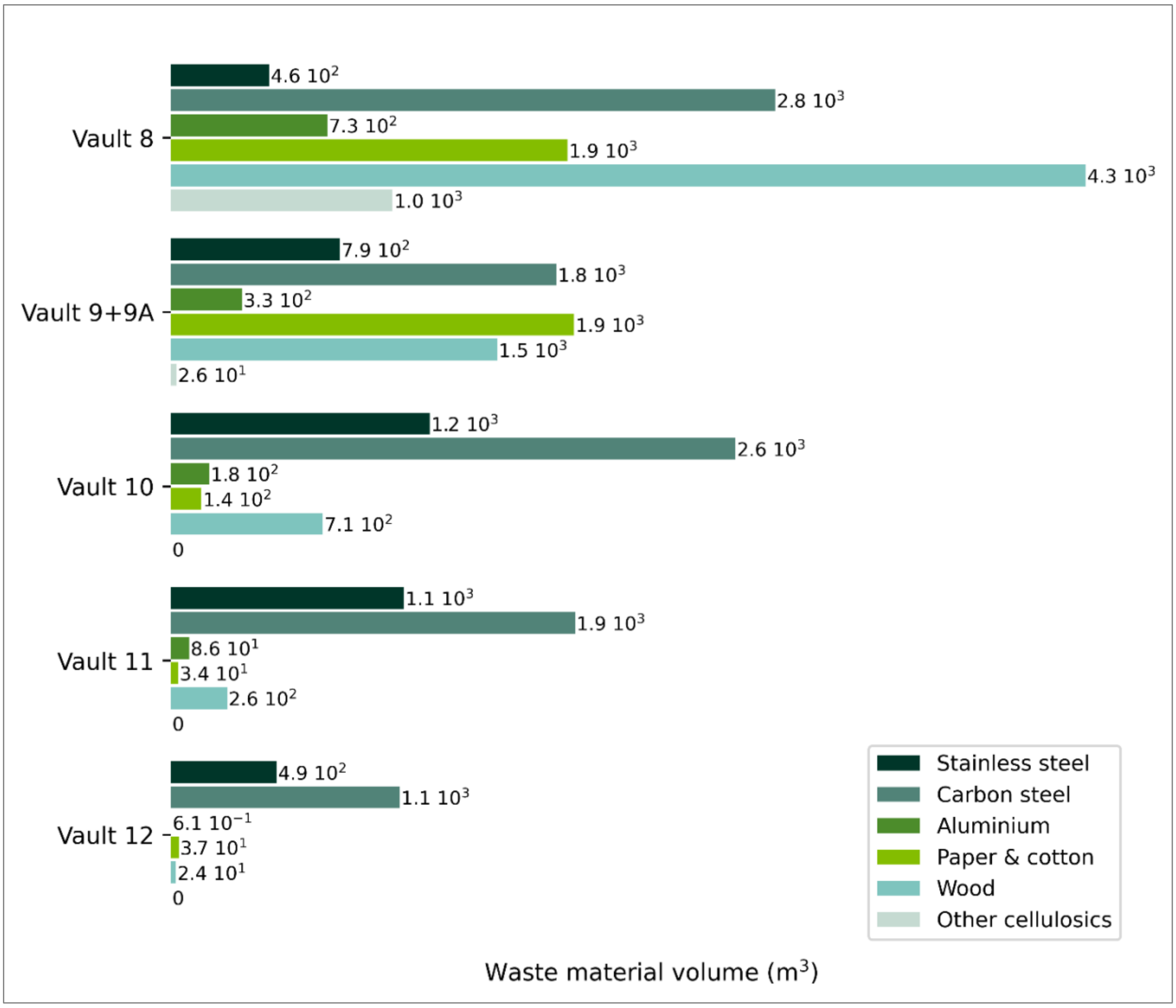

Figure 2.11: Inventory of waste metals and cellulosic materials in the vaults [24]

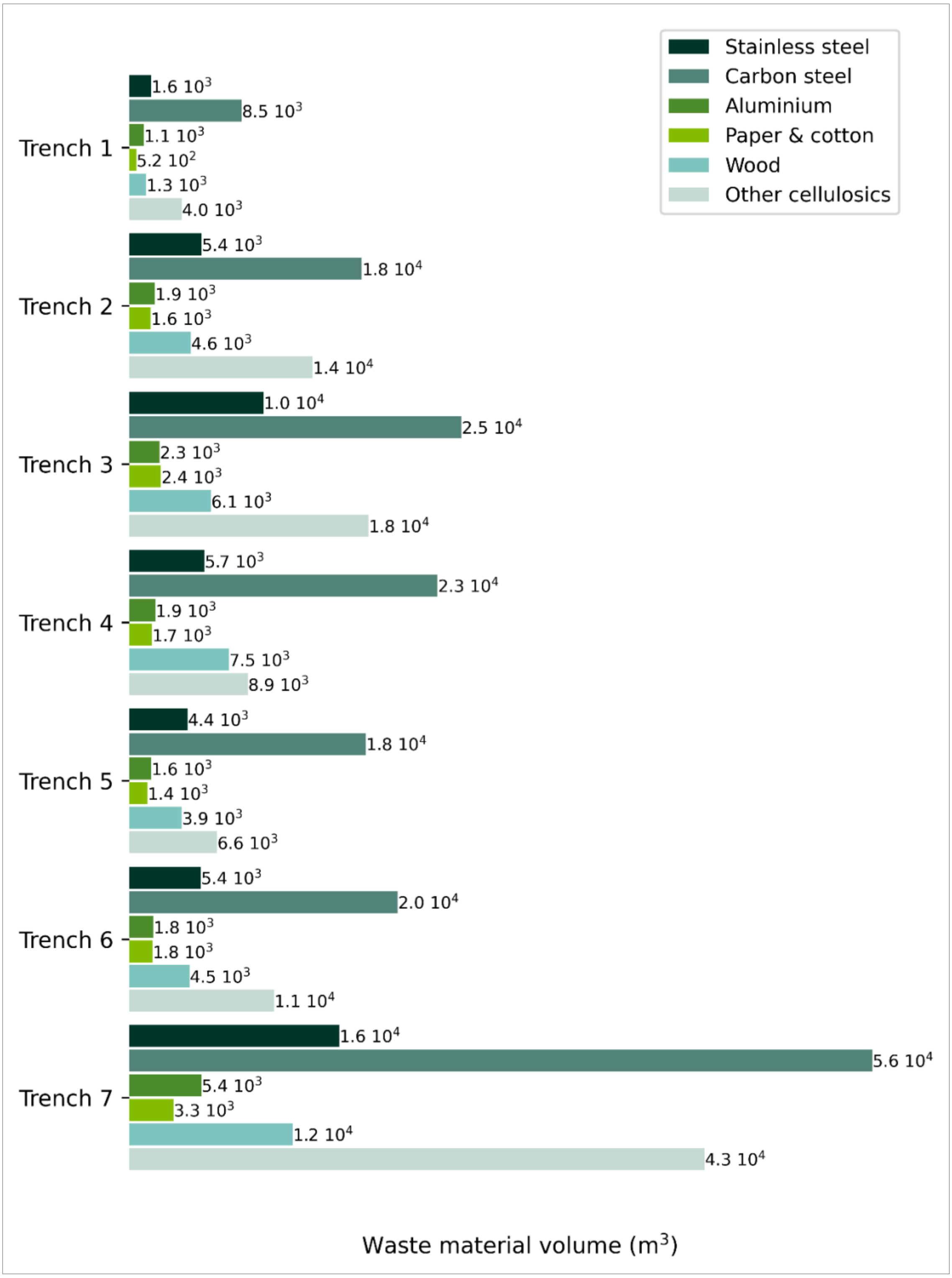

Figure 2.12: Inventory of waste metals and cellulosic materials in the trenches [24]

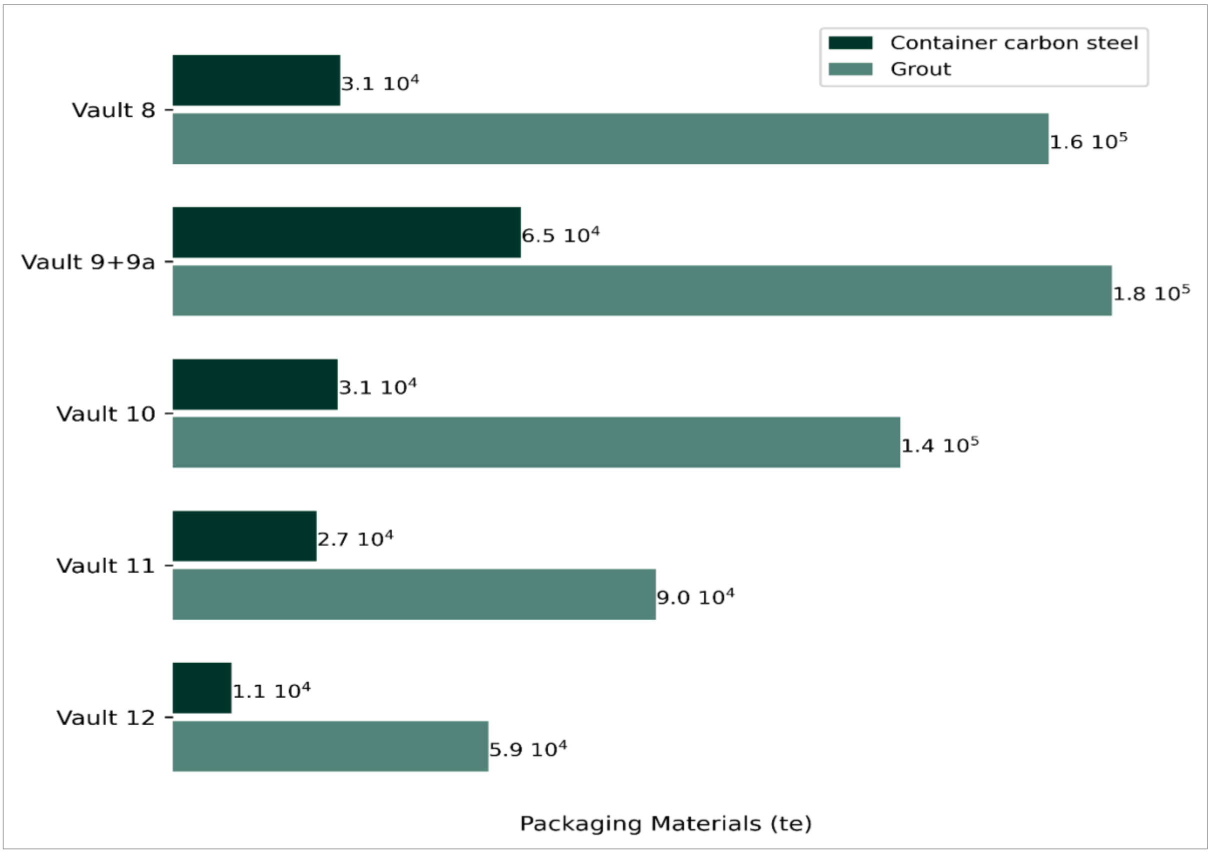

Figure 2.13: Inventory (in tonnes) of container metal (carbon steel) and conditioning grout in the vaults [24]

2.3.2 Radioactive Contaminants

Considering contaminants in the groundwater pathway, the 2011 ESC [31] identified that carbon-14, technetium-99, and uranium isotopes (U-234 / U-235 / U-238) were examples of radioactive contaminants which could have important radiological consequences, but whose migration would be sensitive to chemical conditions in the near field. Therefore, these radionuclides were included in the near-field modelling work that was performed for the 2011 ESC [20]. They, as well as a tracer, are again included in this latest update of the near-field models (Section 6). The inventories of these radionuclides are shown in Figure 2.14 for the trenches and Figure 2.15 for the vaults.

In the gas pathway, the key contaminants are tritiated hydrogen gas, C-14-bearing gases (e.g. $^{14}CO_2$, ^{14}CO, $^{14}CH_4$), and radon. We have not modelled the transport of these species. The relatively short half-life (i.e. 12.32 years) of tritium means that its inventory will have decayed away in less than a hundred years. In the case of radon, the gas assessment includes a simple model of the radon travel time to the biosphere but this is based purely on the advection of the bulk gas. Similarly, the gas assessment accounts for the rate at which the C-14 will be released from the wastes and its speciation in the near field based on experimentally-determined data.

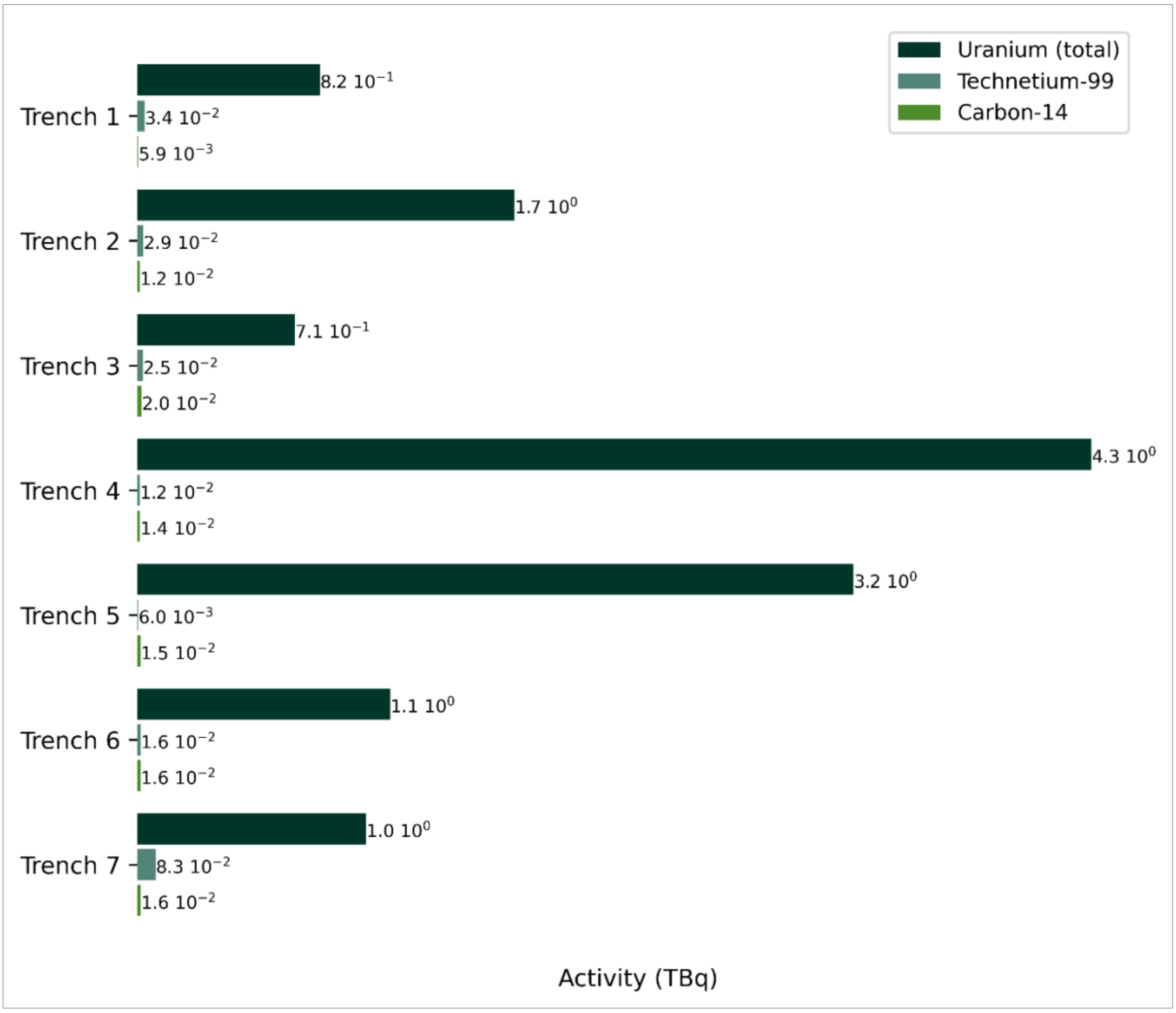

Figure 2.14: Inventory of some key radionuclides in the trenches [32]

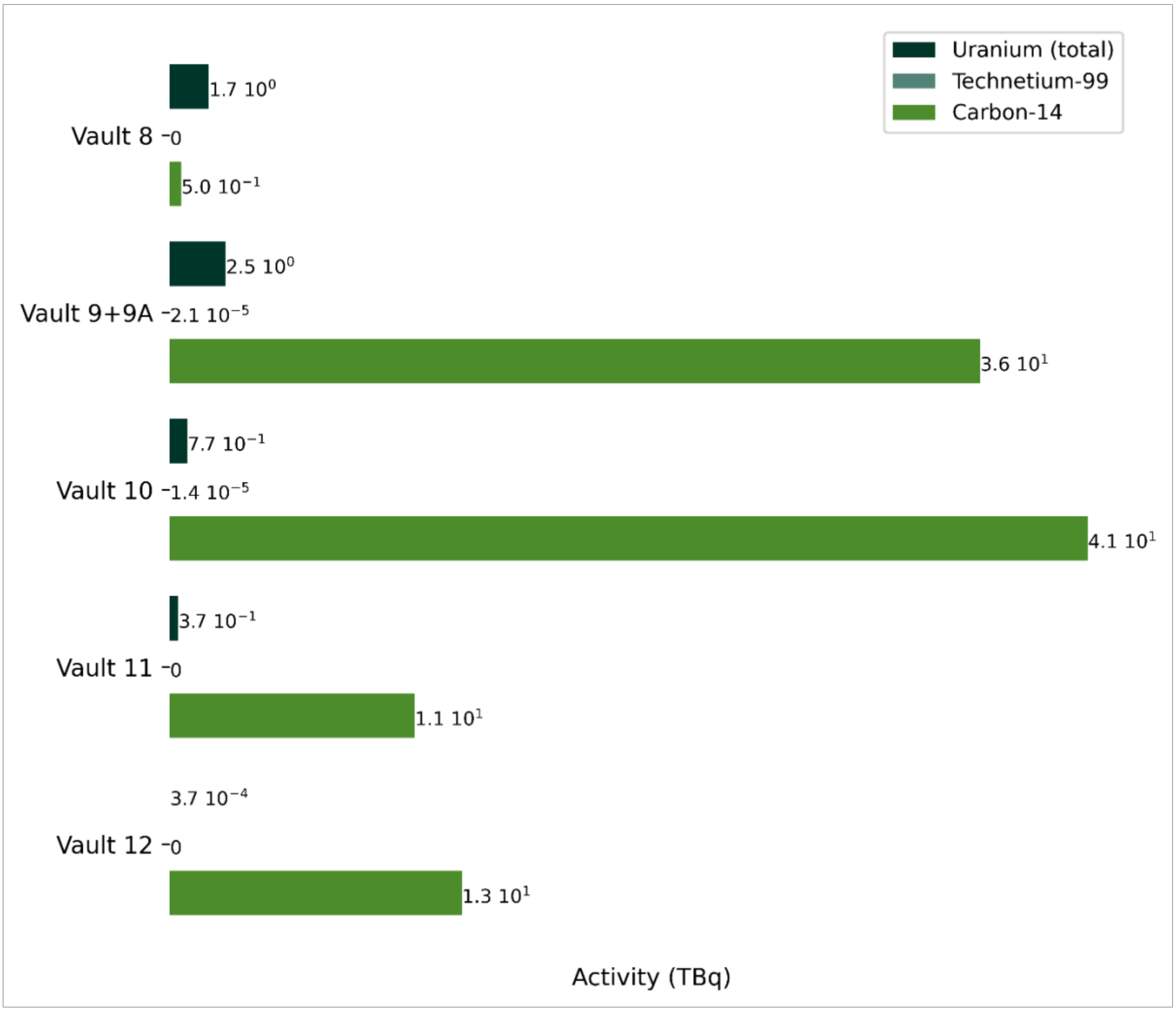

Figure 2.15: Inventory of some key radionuclides in the vaults [32]

2.3.3 Non-radioactive Contaminants

A large set of hazardous substances and non-hazardous pollutants is considered within the Hydrogeological Risk Assessment [15] (Subsection 4.5.1). Most of these are present in the wastes in very small amounts or have previously been shown to raise little concern. In the near-field modelling, we have focussed on those non-radiological contaminants that previous assessments [30] have suggested will be important.

Our near-field models include four non-radioactive species (Figure 2.16 and Figure 2.17):

- Stable lead (Pb) is a hazardous metal, which is declared in the waste inventory [4] and has been disposed of in significant amounts to the trenches and Vault 8. Moreover, it has been detected in leachate from both the trenches and Vault 8 [8]. Reference [33], for example, reviewed historical site monitoring data, and observed that for samples of leachate which were collected between 2008 and 2010, the average lead concentration was 2.74 μg l^{-1} (1.3 10^{-8} M), while the maximum was 18 μg l^{-1} (8.7 10^{-8} M); of the 44 samples, 16 were below the limit of detection

(< 1 µg l^{-1} (4.8 10^{-9} M)). Monitoring between 2012 and 2021 has detected low levels of Pb in leachate from both the vaults and trenches. The maximum detected was 4.3 µg l^{-1}, the average 1.8 µg l^{-1} and a third of samples were below the limit of detection [34].

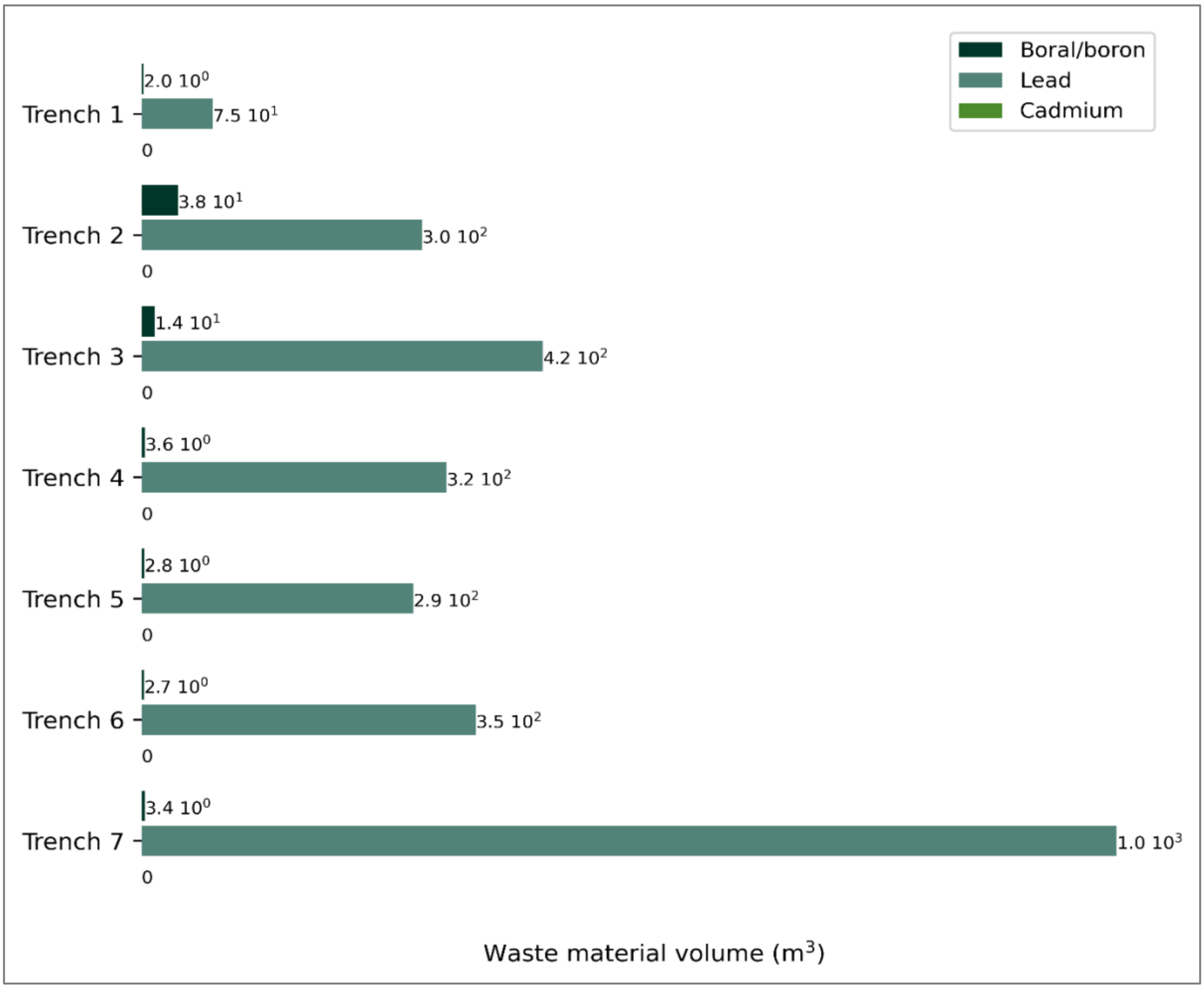

Figure 2.16: Inventory of key non-radiological contaminants in the trenches [32]

- Boron (B) is a non-hazardous pollutant, which is declared in the waste inventory [4] where it is listed as elemental boron as well as in the form of Boral® (a boron-aluminium alloy with between 3% and 10% boron in the form of boron carbide sandwiched between Al sheets). Borosilicate glass (laboratory equipment) has also been disposed in the trenches and Vault 8. Boron has been detected in leachate; up to 2011, its concentration was reported as being ~500 µg l^{-1} (4.6 10^{-5} M) in samples from the trenches and ~260 µg l^{-1} (2.4 10^{-5} M) from Vault 8 [35]. More recent monitoring data, summarised in reference [36], found up to 150 µg l^{-1} of boron in vault leachate and around 400 µg l^{-1} in the trenches.

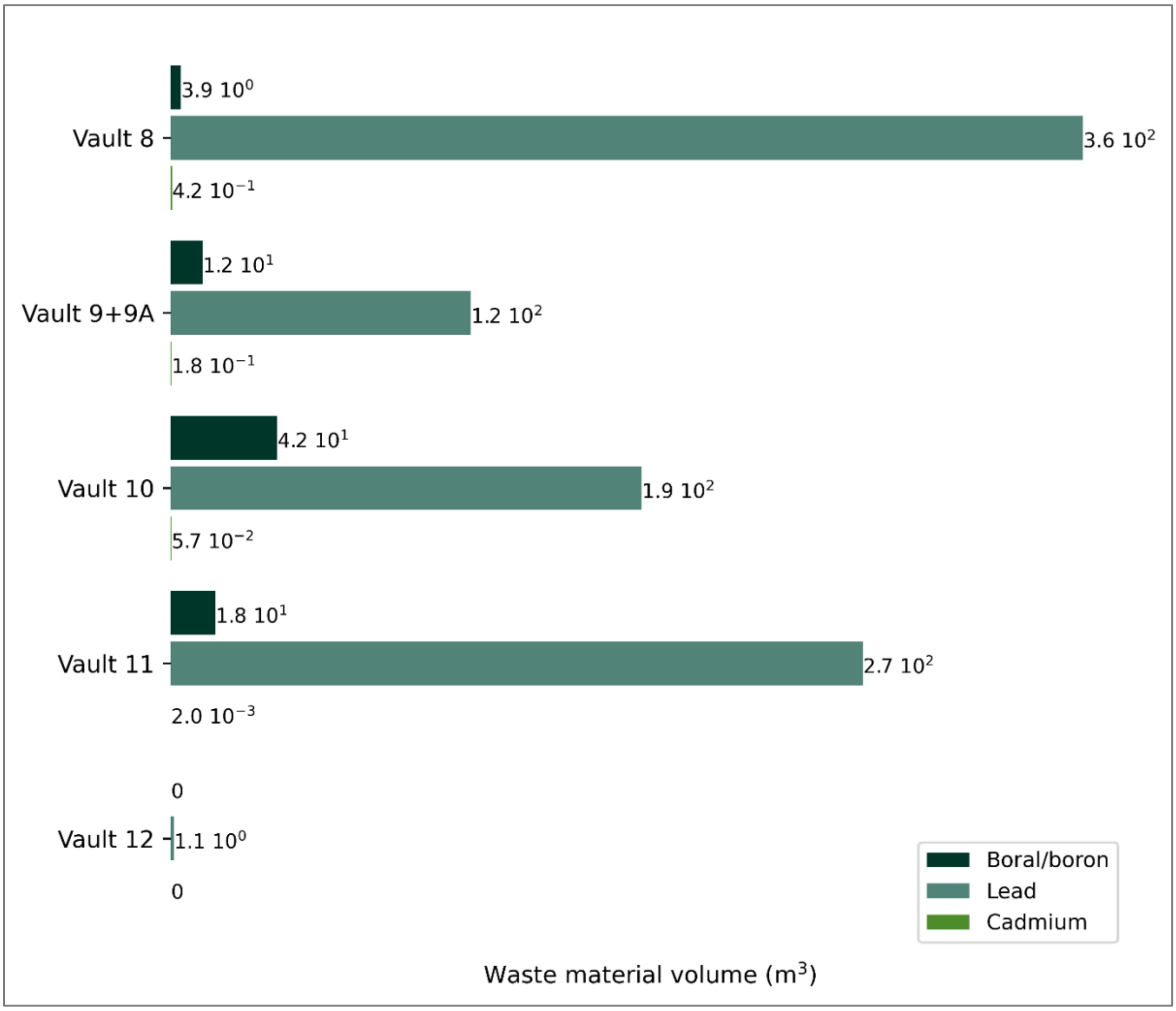

Figure 2.17: Inventory of some key non-radiological contaminants in the vaults [32]. Additionally, small amounts of mercury and mercury compounds have been declared, mostly in waste consigned to Vaults 9 and 9a

- Cadmium (Cd) is a non-hazardous pollutant, which was not declared in the waste inventory [4] but has occasionally been detected in leachate from Vault 8 at low levels with a mean of 0.3 µg l^{-1} (2.7 10^{-9} M) to a maximum of 0.4 µg l^{-1} in 45 samples [37]. The cadmium is likely to have originated from rechargeable nickel-cadmium batteries.
- Lastly, mercury (Hg) is another hazardous substance, which, like cadmium, was not declared in the waste inventory [4] but has been detected in leachate from Vault 8. Reference [37] reported that in 45 samples there were occasional instances above the limit of detection (0.2 µg l^{-1} or 1 10^{-9} M) with a mean of 0.2 µg l^{-1} and maximum of 0.3 µg l^{-1}. Monitoring of the vault leachate between 2012 and 2021 has only resulted in four further findings above the limit of detection. Some of the potential sources of the mercury include thermometers, mercury switches and relays, and fluorescent lamps.

3 Physical Evolution

The processes of physical evolution covered in this section concern the changes to components of the repository that affect fluid flow. Water containing dissolved contaminants, termed leachate, is generally considered to be the main route for contaminant releases from the repository. Fluxes of gases can also give rise to releases, the potential impacts of both radioactive and toxic gases must be accounted for, as well as the hazards associated with releases of flammable gases (Subsection 7.4).

Some of the processes are apparently purely physical, such as loading of the vault bases causing cracking, or settlement in the trench wastes. It is often difficult, however, to disentangle physical processes from chemical processes (Section 4). For example, chemical degradation of the concrete of the vault bases makes them more vulnerable to cracking, and degradation of the trench wastes causes voids into which settlement occurs. As a result, the description of the physical evolution of the repository components in this section anticipates the more detailed description of the chemical processes in Section 4 and gas generation from waste degradation in Section 5. The present section concludes with an introduction to the modelling of transport processes (Subsection 3.5) that allows us to examine the implications of the physical, and chemical, evolution on contaminant releases.

3.1 Initial State of the Wastes

To describe the evolution, we first need to describe the initial state. For the engineered structures such as vault bases, the cut-off wall and the final cap, the initial state is the 'as-built' state that is the starting point for the Engineering Performance Assessment [21] (summarised in reference [12]). The initial state of the trenches and vaults is more complicated. The disposed wastes in both will have been evolving before the installation of the final cap, but the durations, interim conditions and results will vary between vaults and trenches, and even between different vaults as protective measures are introduced for future wastes. Therefore, we start the story of the wastes at the time of disposal to provide a qualitative description up to installation of the final cap. This is then the 'initial state' for consideration of the evolution in the post-final capping phase.

3.1.1 Initial State of the Waste in the Trenches

The trench waste was not compacted during its disposal, and, given the high biodegradable material content, the potential for settlement was high during the period when each trench was being operated. Figure 2.9 illustrates the physical nature of the LLW disposed of in the trenches. The trench waste was covered by soil at the end of the day's disposals operation, as is apparent in Figure 2.9. The soil cover was expected to provide some level of infilling of void spaces and compaction.

While the trenches were operating, and prior to installation of the interim cap, rainwater was free to infiltrate and saturate the trench waste. Trenches 1 to 6 were covered by the interim cap in 1989 and Trench 7 in 1995. Monitoring data suggest that the interim cap partially reduced the infiltration of rainwater to the trench waste and the water levels have gradually been falling (see Subsection 4.2.1).

The degradation of organic wastes, the cellulose-rich materials in particular, will lead to a reduction in the solid volume as gas and soluble degradation products are lost. This creates voidage that can trigger settlement of the overlying wastes. Similarly, corrosion of thin-walled carbon steel is likely to have been fast enough under these conditions that small drums and containers (see Figure 2.9) may have degraded to the extent that they have been crushed by the overlying load.

Estimates of the initial voidage in the trench waste were as high as 66%, but this was expected to fall to around 50% as the wastes degraded and compacted during trench operations [38].

Trench 1 began operations in 1959 but it was not covered by the interim cap until 1988 meaning that wastes were subject to annual precipitation (of around 1 m per year [3]) for more than 30 years. Conversely, Trench 7 began operations in 1985 and was covered by the second phase of the interim cap in 1995, so barely a decade of exposure to rain and atmosphere.

As a result of these different timescales, we might expect considerably more waste degradation in the early trenches, particularly degradation of cellulosic wastes and corrosion of carbon steel. This could lead to more settlement and self-compaction in the early trenches, compared with Trench 7. Some trenches, particularly Trench 2 and Trench 4, are deeper than others, however, which means there is a greater load imposed on the waste mass. Also, the composition of the wastes varies considerably (Figure 2.12). The proportion of steels in the trenches is quite consistent between 25% and 30% of the trench volume, whereas cellulosics vary considerably from less than 15% in Trench 1 to more than 25% in Trench 7. Furthermore, the proportion of less reactive materials, such as concrete, rubble and soil, that will undergo settlement also vary between about 20 % and 45 %. There is also the question of heterogeneity - these proportions are averages for the whole trench and will inevitably vary between disposal bays. Overall, it is difficult to predict the changes in porosity in the trench wastes at early times with a high degree of confidence. Interim capping has caused some compaction and more is expected during surcharging ahead of the final capping [39].

Despite this uncertainty in the details of individual trenches, it is clear that being open to the atmosphere will have allowed oxygenated rainwater to percolate through the trench wastes. The degradation that occurred is likely to be a mixture of aerobic corrosion and organic degradation in shallower and less saturated regions with slower anaerobic processes in the fully saturated deeper regions.

In addition to reducing infiltration, the interim cap also reduced the connection between the unsaturated regions of the trenches and the atmosphere, thus limiting the amount of oxygen available for degradation. As the remaining oxygen was consumed, the conditions became anaerobic relatively quickly. The result is that methane dominates the gases generated from cellulose degradation. In addition, hydrogen can be generated by steel corrosion, although it can also react with CO_2 to form CH_4 (see Section 5 for a discussion of these processes). This is the state we observe in the monitoring of the trenches with methane and carbon dioxide and low levels of hydrogen ([40] and Subsection 4.2.1).

3.1.2 Vault 8 and Vault 9 Existing and Committed Wastes

The Vault 8 waste comprises compacted wastes produced by the Waste Assessment, Monitoring and Compaction (WAMAC) facility at Sellafield, together with wastes that contained solid objects and other non-compactable drummed, or loose, granular materials loaded directly into HHISO containers by waste producers. The waste containers were then infilled with grout, designed to fill void space efficiently, at the LLWR site.

A range of waste types consigned to Vault 8 is illustrated in Figure 3.1 in a non-active container that was used to demonstrate the efficacy of the grouting process [41]. The study estimated that the remaining void space was less than 1.5%. This is considered to be optimistic, however, as other studies have estimated that the total potential voidage in containers may be of the order of 19% on average [42]. This includes ‘ullage’ voidage at the top of containers, which is the residual space that was not completely filled with grout (although some ullage may also arise from the grout causing settlement in the waste before setting).

The containers in Vault 9 benefitted from improved grouting methods, such as use of an inclined table to reduce the ullage, so less compaction is expected with these containers than the older population in Vault 8. Grout ports are now also sealed after grouting.

The presence of the grout in the containers has limited contact of the waste with rainwater in the containers with open grout ports, explaining the minimal release of contaminants from the vaults to date. It is worthy of note, however, that the grout porosity will initially be close to saturation even in containers that have not been open to water ingress. The excess water after setting of the grout was expected, on mass-balance grounds, to result in the porosity being 70% to 80% water-filled [43] and this has recently been confirmed by measurements [44].

The presence of water in the containers will allow corrosion and degradation of the wastes. The grout may also isolate the wastes from the atmosphere so that the reactions which consume oxygen may result in anaerobic conditions developing within the wastes even before capping.

Many of the containers in Vault 8 have been exposed to atmospheric conditions for decades and show signs of corrosion where the paint coating has been damaged or degraded [45]. To date this has not led to many instances of perforations in the metal walls of the containers [21, 12] but it is clear that these corroded areas will be vulnerable to continued corrosion following capping and earlier loss of containment. The existing containers in Vault 9 will be exposed for more than a decade before being covered by the second tranche of the final cap, thus will show similar signs of corrosion.

(a) Absorbent blocks (left) and soil/rubble (right), which shows little ingress and mixing of grout into the soil

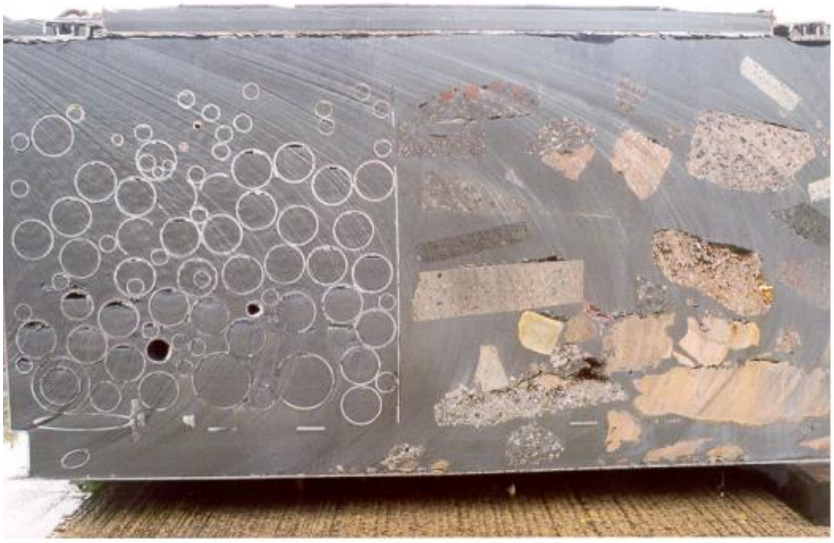

(b) Metal pipes, which are filled by cement grout, but with some enclosed void space (left), and concrete blocks (right)

(c) Compacted waste, originally contained in 1 m^3 steel boxes and 200 dm^3 drums. Voidage is visible beneath the ISO lid due to settling of grout prior to curing.

Figure 3.1: Photographs of sectioned test-grouted ISO containers, showing the distribution of grout, which fills most of the void spaces [20]

As described in Subsection 2.1, it is planned to surcharge these existing and committed wastes in Vaults 8 and 9 (and most likely the north end of Vault 9a) before final capping. The EPA [12] has considered the level of damage to the containers that will occur. We expect that the surcharging process will load the corner elements of containers beyond their capacity, leading to deformation and the expression of available voidage in the wastes. The available voidage will be limited, however, and the void fill and other stacks will prevent major deflections in terms of stack alignment or sides buckling. Overall, the expectation is that the containers will remain in place in their stacks as somewhat 'squashed boxes' whose containment function will be damaged, but not entirely removed (Figure 3.2).

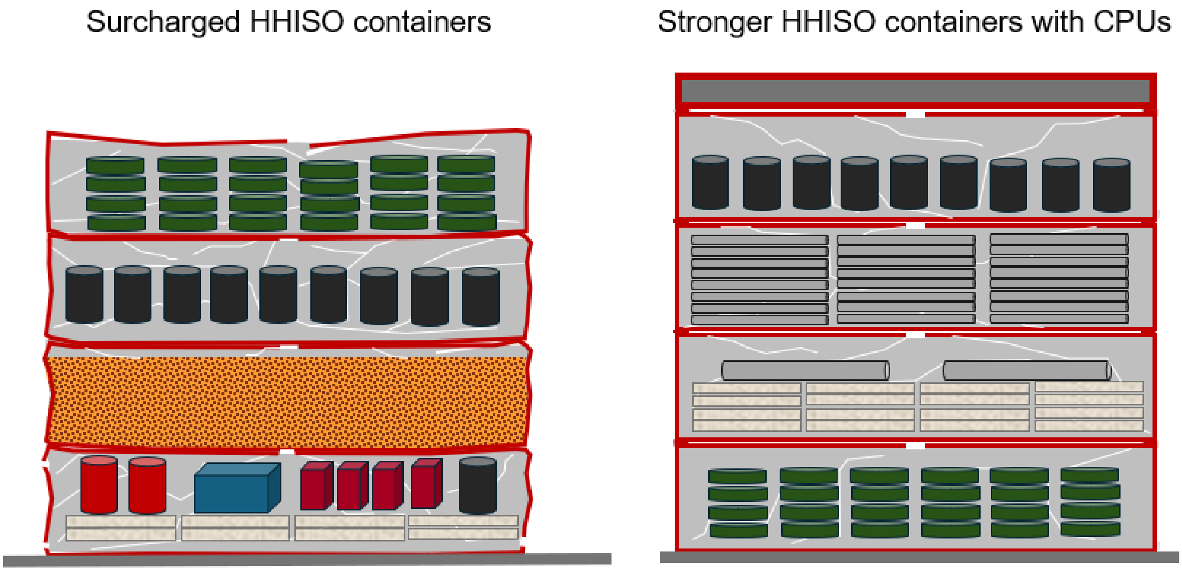

Figure 3.2: Schematic illustrations of the surcharged HHISO containers (left) and the stronger HHISO containers with CPUs (right). Different types of waste items and materials are shown schematically in cracked grout within the containers. Adapted from reference [46]

The containers at the tops of the stacks will be impacted the most as the surcharge process will damage the lids. The fill material will then enter the container and compact the wastes within. In essence, this will accelerate the compaction of the wastes previously anticipated to occur as the result of degradation over the first hundred or so years after closure [12].

3.1.3 LLW in Vault 9 and the Future Vaults

The future LLW in Vault 9 and the further vaults will be packaged in the strengthened HHISO containers and, in addition, container protection units will be placed on the top of each stack to prevent damage during the capping process (Figure 3.2). The grouted containers will also be protected before emplacement in the vaults by storage in temporary warehouses to minimise subaerial weathering and degradation.

These measures will ensure that the containers are in better condition after capping than the existing containers, and likely to retain their containment function for a longer period. The presence of the CPUs will also have the effect of diverting rainfall and, following capping, infiltration from the containers and into the gaps between the stacks.

The future LLW will be grouted but the composition of the grout may be changed in response to difficulties in supply of the current grout components, PFA particularly, and the need to use more sustainable materials. The grout development programme is currently investigating replacing the PFA with commercially available volcanic ash [47]. Although the components will change, the requirements of the grout will remain the same. Thus, the key parameters, such as porosity, permeability, initial pH and chemical evolution, will be kept very similar to the current formulation (see [47] and references therein). As a result, we expect that the future LLW grout will also initially contain excess water allowing degradation and corrosion to commence immediately after grouting.

The future LLW is expected to have lower levels of initial voidage as the result of grouting to the top of the container and waste acceptance criteria (WAC) that will help minimise voids in the disposed wastes. Future vault wastes are projected to contain lower proportions of organics and higher proportions of secondary wastes (slags, shot blasting grit etc.) from metals recycling. Concrete from decommissioning and graphite from reactors will also feature in future waste streams. These wastes will reduce the development of secondary voidage during waste degradation.

3.1.4 ILW in the Future Vaults

The ILW for disposal in the vaults would mainly be packaged in the smaller strong boxes but, as these are painted carbon steel, they will also benefit from protection from subaerial weathering and degradation.

Temporary warehouses would be used for ILW managed as LLW, whereas the ILW that needed additional shielding would be placed directly in the shielded modules. Once a bay in the module is filled, it would have the roof emplaced, providing protection similar to or greater than the temporary warehouses. The shielded modules will also provide protection from infiltration following capping, as the sloping roofs will divert water into drainage gaps between the bays. As a result, the ILW containers in the shielded modules may corrode more slowly than containers in the vaults as there is likely to be a significant delay before they are exposed to flowing water.

The shielded modules will also protect the containers from the load of the profile material and final cap so that the containers are only subject to the loads from stacking within the modules, and this is also expected to prolong the period of containment they provide.

The ILW that can be managed as LLW and emplaced in the open vaults will also have CPUs placed on the stacks of strong boxes and there will be little difference in their behaviour compared with the larger strengthened HHISO containers.

3.2 Evolution of the Engineered Barriers

The engineered barriers currently in place (e.g. the vault bases), or which are planned to be present at site closure (e.g. the final cap), comprise combinations of man-made and natural engineering materials. These barriers will influence the near-field hydrology for the period before the repository is disrupted by coastal erosion. In the EPA [12], the evolution of the engineered barriers is considered over a period lasting 5,000 years after the present.

Results from previous assessments, as well as recent analyses of the performance of the closure engineering planned for the LLWR [12], have shown that key components of the engineered system at the LLWR are:

- the vault bases and walls;
- the cut-off wall; and
- the final cap.

Of these, the final cap is the most important, because it restricts water infiltration from rainfall and is the primary control on water flows and levels within the LLWR.

3.2.1 The Final Cap

The final cap determines the infiltration rate of water to the repository. It largely depends on the performance of the composite barrier comprising a BES layer and the overlying 2 mm-thick high-density polyethylene (HDPE) geomembrane (Figure 2.7). In the BES layer, the montmorillonite clay in the bentonite component swells on contact with water to fill the pore spaces between the sand grains and create the low permeability behaviour of the layer. The overlying geomembrane provides an additional very low permeability barrier and also acts to protect the BES layer. The two layers work in concert such that water percolating through any defects in the geomembrane will spread out along the interface with the BES before slowly permeating downwards. The geomembrane provides a low permeability function for a period before its performance deteriorates due to oxidative degradation [48, 49]. The BES is expected to function well over the long term, although it will also undergo some deterioration, mainly due to cation exchange on interaction with water.

The processes that lead to degradation of performance of these two components are very different. The EPA [12, 21] has carried out a systematic consideration of the evolution of the components of the cap based on a detailed analysis of the processes of degradation, drawing on system-specific design and understanding, together with the latest experimental data in the literature, and expert elicitation.

For the 2011 ESC, infiltration values were essentially elicited directly by experts on the basis of expectations of performance. Now, use of relevant international data and understanding in the literature allows for a much better underpinned approach using calculations based on accepted methodologies. The estimation of infiltration based on these methodologies has resulted in the expectation that the cap will perform better, and for a longer period, than previously assumed [48].

We have derived a probability distribution for the infiltration through the cap [48]. The calculated mean infiltration rates over the 5000-year period post-installation are summarised in Table 3.1. These values illustrate the change between the very low initial rates when both the geomembrane and BES are functioning well, to the significantly higher rates once the geomembrane has degraded and the BES alone determines the infiltration. The mean value for the time of onset of degradation (1500 y after cap installation) and for complete failure (1650 years) are used for the infiltration prescription shown in the table. This is the rate of infiltration used for the modelling described in later sections.

Table 3.1: Cap infiltration rate in mm per year after installation [48]

Time (years)	0	500	1000	1500	2000	2500	3000	4000	5000
Case A: Mean infiltration rate (mm y^{-1}) with geomembrane degradation beginning at 1500 y and complete by 1650 y.									
Mean infiltration	0.002	0.008	0.023	0.041	28	34	38	52	63
Case C: Mean + 2 standard deviation (95th percentile) infiltration rate (mm y^{-1}) with geomembrane degradation beginning at 1500 y and complete by 1650 y.									
High infiltration	0.01	0.11	0.39	0.69	630	794	933	1320	1620

The timescale for geomembrane failure overlaps with that for disruption of the facility by coastal erosion. Projections suggest a timeframe of several hundreds to a few thousand years for initial disruption, that is, the onset of disruption and breaching of the vaults [7], with a reference value of 1250 years used in assessment calculations. This implies that the vaults may be affected by coastal erosion before the geomembrane fails. As is clear from Table 3.1, the repository would have experienced low infiltration over that period and, as discussed in Subsection 3.5, this will have further consequences for the saturation of the repository as well as the corrosion of the containers in the vaults (Subsection 3.4.2), and waste degradation (Subsection 3.4.3).

Finally, in considering the evolution of the cap, the heterogeneity of infiltration in the period before the geomembrane degrades must be recognised. The calculated infiltration rates for this period are averages over the whole cap but the 2mm-thick HDPE used for the geomembrane is effectively impermeable and water inflows can only occur where there are defects. These defects may be pinholes arising during the manufacturing process, larger holes or small tears caused during emplacement, gaps in the welded seams, or holes associated with wrinkles [49]. The key point is that some of these defects will be present initially and others, such as holes associated with wrinkles, will develop over time in response to the load of the overlying cap or strain as the cap settles. The elicitation of cap properties considered the initial number and the evolution of these defects [49] and made use of work reported previously on the type and size of such defects [50].

For the near field, and especially the vaults, before geomembrane degradation, some areas will experience higher infiltration than others as a result of the distribution of the defects. We have examined the contributions made by different types of defects to the overall infiltration [51]. The findings indicate that at early times, the pinhole defects are most significant in terms of their contribution to infiltration since they occur most frequently, whereas, as geomembrane degradation proceeds, the larger defects ('long stress cracks') come to dominate. We can use this information to estimate the different amounts of infiltration an individual stack or small group of stacks close to a defect might experience compared with stacks located away from such defects. At early times, when the overall infiltration rate is low, this could result in differences to the evolution of the waste packages in the vaults (see Subsection 3.4.1).

3.2.2 Evolution of Vault Bases and Walls

The role of the vault base liner during active institutional control of the site is to ensure that leachate can be collected and its release can be managed. Under passive control, after the end of the PoA, the relative performance of the base liner and the final cap is important. Too much water accumulating in the vaults could cause over-topping and contaminant releases to the shallow groundwater. To avoid this, the water must drain at a faster rate than it enters through the cap. Drainage may either occur through the base liner, by over-topping the low walls and draining through the underlying drainage blanket or, in the case of Vaults 8 and 9, through connections to Vault 9a.

The reinforced concrete slabs have not been specifically designed to function as a hydraulic barrier but nevertheless have very low permeabilities and will therefore provide a significant barrier to flow during the early lifetime of the vaults. The base slabs will gradually degrade with time, leading to higher permeability. The inter-slab movement joints are anticipated to degrade more rapidly than the concrete, most likely within 100 years, which may lead to through-slab vertical pathways that allow increased leachate flow into the underlying drainage blanket. Once open, these joints may then become preferential conduits for leachate flow, which may further increase their rate of deterioration. However, clogging of these joints may similarly occur due to the accumulation of particulates on the vault base from the degrading waste and containers. The net change in the overall hydraulic performance of the base slab may therefore be negligible.

Once the concrete deteriorates in contact with the leachate from the wastes, corrosion of the steel reinforcement bars could lead to expansive corrosion products and further cracking of the concrete. The rate of corrosion of the reinforcement is expected to be slow, given the protection afforded by the concrete cover, the anaerobic conditions at the base of the containers and the long period of low infiltration rates.

3.2.3 Evolution of the Cut-off Wall

The primary function of the cut-off wall is to prevent lateral infiltration into the trenches and vaults. The cut-off wall is expected to stop water running off the cap, infiltrating the surrounding soil, and then percolating laterally into the waste. In addition, as the cut-off wall extends deeper than the trenches and the drainage layers beneath the vaults, it will promote release of leachate to the deeper groundwater system, avoiding contaminant releases into shallow groundwater.

The cut-off wall consists of a concrete and bentonite slurry wall extending two metres below the base of the vaults and at least 2m into the clays beneath the trenches (Figure 2.2). The main degradation mechanisms are leaching of the cement and washing out of the bentonite from the slurry wall.

The EPA concluded that some washout of bentonite / cement and localised increase in permeability through cation exchange would occur in the 500 years to 1000 years after the PoA. Combined with areas of local deterioration in vicinity of construction joints and areas of wall thinning, these effects would reduce the effective performance of cut-off walls from the as-built condition. However, the overall performance of the cut-off wall, with sufficient permeability contrast, will remain as water flows will be too low to result in significant washout and the rates of cation exchange too slow to greatly impact the permeability [12].

3.3 Trench Waste Evolution

On the basis of the cellulose degradation rate [52] and modelling of waste degradation in the trenches [53] it is considered likely that these degradation processes could take as long as 2000 years to be substantially complete. Depending upon the proportion of more easily degraded wastes in each trench, the first 50 % of cellulose degradation by mass could occur within the first 500 years. As noted in Subsection 3.1.1, this will vary across the trenches as the materials are heterogeneously distributed and local conditions will differ.

In evaluating the longer-term porosity of the trenches, for use in assessment calculations, the potential volume changes arising from the degradation of cellulose and other organic materials that may eventually degrade have been taken into account. The estimated average porosity after the surcharging period and placement of the final cap is around 44 % and this is not expected to change significantly in the longer term [38]. In specifying the requirements for the final cap, up to one metre of settlement has been allowed for [42]. In general, it is anticipated that total future settlements will be up to a few hundred millimetres and will not affect the performance of the cap [21, 42]. This includes ‘average’ results for Trench 7 which has the largest proportion of cellulosic materials.

Following installation of the final cap, the very low infiltration will lead to the water levels in the trenches falling and a general drying out, especially in regions with higher water levels currently (see Subsection 4.2.1). We do not anticipate that the desaturation will be to such an extent that degradation and corrosion reactions are restricted due to lack of water (see further discussion in Subsection 6.4.1). This is because under the drying conditions, where water is being consumed by corrosion and degradation reactions more quickly than supplied by infiltration, water vapour may be drawn into the trenches from the surrounding geology which remains saturated.

3.4 Vault Waste and Wasteform Evolution

3.4.1 Infiltration and Flow within the Vaults

In Subsection 3.2.1, we described the evolution of the cap and the effect on the infiltration rates. Here we consider the implications for the wastes in the vaults.

In the period when the geomembrane is effective, the infiltration will be localised to places where there are defects in the geomembrane. The consequences of the heterogeneity in infiltration will be amplified by the very low infiltration rates. Some container stacks will have sufficient water in the vicinity that container corrosion occurs continuously over this period while, for other stacks, conditions will be much drier and container corrosion may be slowed or even stopped by lack of water.

The concrete vault bases and underlying unsaturated drainage blankets mean that, unlike in the trenches, movement of water vapour in response to the drying conditions in the vaults will be much more restricted. Within the containers, however, the grout will provide a significant source of water to maintain corrosion reactions.

The effect of localised infiltration on stacks of surcharged containers in Vaults 8 and 9 is illustrated schematically in Figure 3.3. Only the central stack in the illustration receives direct infiltration due to the defect located above it. The damage to the lid of the uppermost container means that most of the water will initially drain into this container, fully saturating the grout matrix, then any cracks along with voids in the wastes. After this container is fully saturated, only then will further water spill over into the gaps and run down the walls of the lower containers. Some of these may already have damage that allows water to drip into the container and increase the saturation of the grout.

In the vaults with stacks of stronger containers and the small strong boxes, localised infiltration will be diverted into the gaps by the CPUs on the tops of stacks (Figure 3.2). The majority of these containers will only be able to take up water, other than possibly water vapour through the gas vents, when corrosion has perforated the walls so water flowing in the gaps can percolate into the grout.

The shielded modules would act to divert the water into the drainage gaps between the bays. Containers in these modules will not experience water flows unless the module roof fails due to degradation of the reinforced concrete by the infiltration through the cap. This degradation was considered in an EPA elicitation. It was estimated that an increase in permeability of the concrete roofs from 10^{-12} m s^{-1} to 10^{-7} m s^{-1} would occur over 5000 years as cracking penetrated the full thickness of the concrete, but the experts suggested that failures of the units would be rare before disruption by coastal erosion [12].

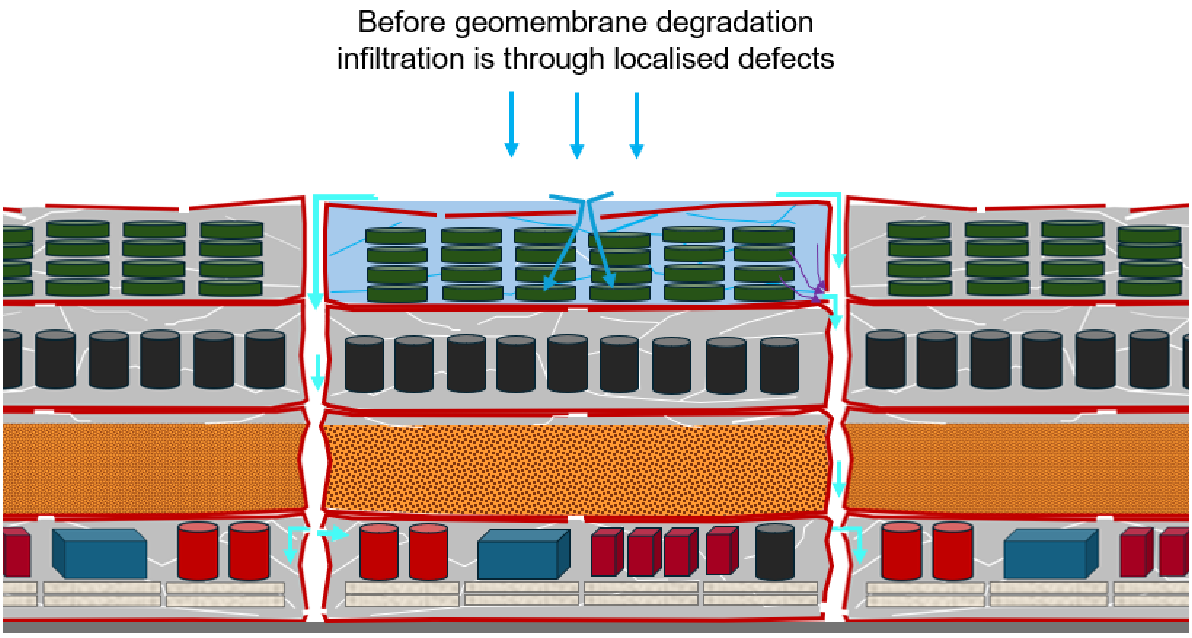

Figure 3.3: Schematic illustration of localised infiltration for surcharged containers in Vault 8. The upper containers in stacks under inflows will gradually saturate and overflow. Adapted from reference [46]

In all cases, the amount of infiltration at early times is so small that even localised releases will not be large volumes of water. For example, the average frequency of defects is approximately one per 400 m^2 initially. For the as-built cap mean infiltration, this equates to less than 1 litre of water per defect per year on average. Even at 500 years, it is only a few litres per year. At this rate, it would require several hundred years merely to fully saturate the grout in the uppermost container in a surcharged stack, unless the top container is one that was topped up by rainwater before capping.

This estimate neglects the effect of water consumption by corrosion. Corrosion of the external surfaces of the containers alone will consume all the infiltration in Vault 8 for at least 500 years [54] and longer for vaults in which the containers are more closely spaced and higher stacked, so that there is more container surface area per square metre of cap, thus more corrosion relative to the infiltration rate. The effect of water consumption by corrosion is discussed further in Subsection 6.4.1.

In the surcharged wastes, the picture is one of large variations in the saturation of the wastes. Containers at the top of stacks under or near defects may receive sufficient infiltration that the saturation of the grout increases faster than water is consumed by metal corrosion in the wastes. The high capillary suction of the grout means, however, that no water will drain from the grouted wastes until the grout is fully saturated. Thus, even if the top containers are perforated and leaky, the other containers in those stacks may receive little or no infiltration for several hundred years. The lack of water flows from the containers also means that dissolved contaminants will be retained within the containers for this period.

The stacks further away from infiltration at defect locations will receive no water inflows until the geomembrane fails and infiltration is more uniform over the vault area.

In the near-field modelling, we have examined the implications of this heterogeneity in infiltration for the evolution of the containers and wastes in the vaults (Subsection 6.6). The impact will be much less significant in the trenches because they approximate a continuous porous medium with few barriers to water movement within an individual trench.

3.4.2 Container Corrosion and Lifetime

On final capping, the conditions in the vaults, and especially in the open gaps between stacks, will initially be similar to those in the open vaults, i.e., humid and oxygen-rich, but they will quickly evolve as oxygen is consumed. Corrosion of the container surfaces may be enhanced initially by chloride remaining from the previous subaerial conditions.

Although most containers have a surface coating to reduce atmospheric corrosion, the period over which this will maintain its protective function is very uncertain. We noted in Subsection 3.1.2 that containers in Vaults 8 and 9 are already showing signs of corrosion. While the future containers will be protected by the use of temporary warehouses for as long as possible before capping of the vault, the effectiveness of the coating is still uncertain. As a result, we do not account for the presence of the container coatings in the near-field modelling.

We expect the corrosion rate of the steel containers in the capped but still aerobic vaults to be around 3 μm y^{-1} [55]. At this rate, aerobic corrosion of the containers in Vault 8 could consume all the oxygen in the vault beneath the cap in around two to three years, driving the gaps to anaerobic conditions. This may occur more quickly in other vaults in which containers are higher stacked, or stacked more closely, so more of the volume beneath the cap is occupied by containers. This results in a greater surface area of metal to corrode and a smaller volume of air-filled voids. Conversely, where the surface coatings on the containers are in better condition, corrosion will affect a smaller area initially, and the oxygen consumption will be slower. Aerobic corrosion over a few years is unlikely to contribute significantly to degradation of the containers, compared with a decade or more in the open vaults[3], and the longer-term anaerobic corrosion will most likely determine the timescale for general perforation of containers.

Neglecting the presence of the surface coating, we estimate the time for general corrosion to perforate the walls of the containers to be several thousands of years [54], based on the combination of elicited corrosion rates for the external and internal surfaces of the containers [55] (see Subsection 4.3.2 for discussion of corrosion inside the containers). Even allowing for a period of subaerial corrosion in the vaults before capping, it is likely that the containers will be largely intact when the vaults are breached by coastal erosion.

General corrosion is not the only process that could lead to the formation of holes in the containers. Reference [54] discusses the other processes, such as galvanic corrosion, or the reaction with dissolved sulphide that could occur in the lower pH environment of the gaps

---

[3] The best estimate corrosion rate for open vault conditions is around 30 μm y^{-1} [55].

where microbial activity could occur. These processes could lead to more localised perforations in the containers.

The key point is that neither general corrosion nor more localised processes are likely to lead to sufficient degradation that the containers become structurally unsound. The population of surcharged containers in Vaults 8 and 9 will already have been deformed by the surcharge process, but container corrosion is unlikely to create the potential for significant further settlement. For the stronger containers used for future LLW and ILW, perforations of the side panels may occur but, in general, corrosion will not be so extensive as to weaken the structural elements sufficiently to cause collapse of stacks over the period before coastal erosion disrupts the vaults.

3.4.3 Vault Waste and Grout Degradation

Wastes in the vaults, like the trenches, will undergo corrosion and degradation of cellulosic wastes. The chemical environment in the grouted wastes will, however, change the cellulose degradation process. As discussed in Subsection 4.3.2, the grout pH will severely limit microbial activity within these wastes so that microbial degradation processes will be restricted to isolated niches, such as within the compacted pucks. Where the cellulose wastes are in contact with the grout porewater, the degradation products are dominated by isosaccharinic acid (ISA) and acetate formation rather than the gases produced by microbial processes. The result, in terms of the volume change in the waste, may be similar, although formation of calcium isosaccharinate complicates the issue. Depending on where this solid precipitates, the increased volume of the solids may partially offset the volume of cellulose lost by degradation. This is not certain if, for example, the precipitate is distributed in the porous grout matrix, increasing the density of the grout. In general, however, we expect that as the cellulose wastes degrade and form either soluble species or gases, the voids and lower density regions may allow overlying waste to settle, forming cracks through the grout.

Corrosion of metals results in an increase in volume. For example, with steel (Fe) corroding to form magnetite (Fe_3O_4) there is an approximately 50% increase in the volume of the oxide over the metal. Thus, as the waste metals corrode, the grout around them is likely to become cracked by the expansive corrosion products.

The low infiltration rates mean that degradation of the grout by leaching is unlikely to cause significant changes to density or porosity on the timescale of interest (see Subsection 6.5.2). Instead, mechanical processes associated with waste degradation will be the main driver of changes to the grout.

For the surcharged containers, the grout is expected to have been cracked to some extent by the load imposed and the settlement down the stack as the corner posts deform. For this population of containers, the additional cracking associated with waste degradation may produce relatively little additional change except perhaps to increase the frequency of small-scale cracks such as around corroding metal items. For the stronger containers, however, there will be no equivalent to the surcharge loading, and cracking of the grout will be associated with waste degradation.

In both cases, the result of cracking will be to increase the permeability of the wasteform. The grout itself has sufficiently low permeability that any flow through the containers will be focussed through cracks in the grout rather than the intact grout matrix.

3.4.4 Implications of Wasteform Evolution for Assessment of Site Disruption

We have considered the physical properties of the vault waste and wasteform in assessing the impact of site disruption by coastal erosion [7]. For the 2011 ESC, the expected evolution of the HHISO containers was considered in an elicitation [56], which concluded that the HHISO containers may retain their physical form for around one thousand years while recognising that the timescales of the stages of physical evolution are uncertain. As discussed, above, the implications of the newly elicited corrosion rates and revised cap performance are that the stronger containers will remain largely structurally intact with only minor corrosion perforations after this time. The surcharged containers will have been corroded to a greater extent as the result of their longer period of subaerial exposure but are also likely to still retain their physical form on this timescale.

The timescale of coastal erosion is uncertain. The initial disruption of the repository site, affecting the western edge of the vaults, could occur within a timeframe of 500 to 2,000 years after the present [7]. We now conclude that even with the later timescale, the containers will largely retain their form and, in the case of the stronger containers and particularly containers protected by the shielded modules, some may have experienced only limited corrosion.

There may, however, be a period of decades to several hundreds of years between first breaching of the cap and exposure of containers at the erosion front, depending on their location. In this period, atmospheric oxygen, moist air laden with salt and rainfall will penetrate the vault environment. This will accelerate corrosion of containers. We have elicited corrosion rates for steel under conditions relevant to the eroding vaults (i.e. atmospheric conditions with high chloride levels) as well as for the open vaults (i.e. atmospheric corrosion with low chloride deposition). The mean corrosion rate is around 25 to 40 μm y^{-1} but rates up to 1 mm y^{-1} are possible in some localised environments [55]. With aerobic corrosion in the presence of chloride from seawater, a few decades will drastically change the state of the container walls, resulting in widespread deterioration even where there was limited corrosion under anaerobic conditions.

As a result, we expect that the containers would have insufficient mechanical strength to prevent the physical breakdown of the waste in a coastal erosion scenario. Containers located at the base of the vault stack in both anaerobic, low infiltration conditions and post-breaching aerobic conditions may have experienced reduced rates of corrosion and could therefore be relatively intact if exposed by coastal erosion. However, once in contact with seawater, the carbon steel container would only have a lifetime of a few tens of years.

The waste and packaging materials that may be exposed on a beach as a result of coastal erosion range from fine disaggregated grout and waste soils at one extreme to large waste metal objects and other large items of waste. Metallic wastes, particularly carbon steel, will corrode more rapidly once exposed to seawater and erosion processes. Residual organic materials, such as waste wood, would be physically broken apart and dispersed in the coastal environment.

The grout is designed to fill void space in the containers and has low mechanical strength. It would also be subject to chemical degradation processes involving sulphate and chloride present in seawater. Thus, we consider it unlikely that large blocks of grout would remain intact. It is more likely that large blocks of concrete waste would remain intact, as construction-grade concrete materials will likely have been formulated for mechanical strength and resistance to chemical degradation.

3.5 Evolution of the Saturation in the Vaults

Taking account of the initial conditions in the vault after capping, changing infiltration rates through the cap and the water balance discussed above, we can distinguish three periods of saturation and water flow within a vault. Starting from the earliest to the latest after repository closure, these are as follows.

First period:

There is a small quantity of residual water in the vault that has drained from the overlying profile fill, but infiltration levels are very low. A shallow wetted zone might exist at the bottom of the vault for a short period. Water entering the vault below a defect in the geomembrane will flow off the CPUs and around the strengthened HHISO containers and small strong boxes, which will be structurally intact (but corroding). Infiltration at defects above the surcharged stacks will largely percolate into the uppermost containers through the damaged lids. Once the oxygen in the vaults is used by corrosion reactions, consumption of water by anaerobic corrosion of the containers, as well as water consuming reactions in any failed containers, will exceed the average infiltration rate and lead to a drying of the vault. This period is expected to be transient, of the order of a decade.

Second period:

Infiltration levels are slightly greater than in the first period but still low and water consumption by container corrosion still exceeds the rate of infiltration. In locations beneath defects in the geomembrane, there may be sufficient water available that it will begin to resaturate the grout in any HHISO containers that have failed lids or have corroded through to expose grout. Within intact containers and containers remote from localised infiltration points, metal corrosion and other waste degradation reactions will reduce the saturation in the grout. Conditions in the gaps, especially in regions more distant from defects, may become so dry that corrosion of the surfaces of the containers is inhibited. No water will be present at the bottom of the vault.

Third period:

Infiltration levels are greater than in the second period. Most of the containers in the stacks, especially the stronger containers with CPUs and containers in the shielded modules, are still intact but with increasing perforations due to corrosion. The infiltration rate exceeds the water consumption rate so there is sufficient water available that grout can resaturate, for example by water inflow through gas vents and grout ports in intact containers. The remaining water will be diverted around the containers to flow through the gaps between containers in most of the vault. The top-most containers in stacks without CPUs will be fully saturated and further infiltration will cause water to either overtop the container and flow down the gaps or, where the containers have failed, flow through cracks in the grouted wastes to holes in the container sides or base. The water levels in the vault will rise over time.

Before the third period, transport of dissolved contaminants out of the containers will be extremely limited by the absence of continuous water-filled pathways between wastes and the geosphere.

Having identified these three periods, we would like to understand their durations, and this is one of the subjects of our near-field modelling studies (Section 6.5.1).

3.5.1 Hydrogeological Modelling

A programme of hydrogeological modelling has been carried out to support the groundwater assessment [6, 57]. The results of these studies are also of use in providing boundary conditions for the representation of the near field in the PFLOTRAN modelling presented in Section 6 of this report.

The CONNECTFLOW software [57] has been used to investigate the current hydrogeological behaviour of the site and to develop the hydrogeological conceptual model. The CONNECTFLOW model represents flow on a regional scale but is refined in the area of the site to allow a detailed representation of the flow through different engineering components. After calibrating the model for current conditions, a representation of the engineering components that will be present in the repository at closure was included. The model was then used to investigate the influence of the repository on the hydrogeology, and to examine the long-term behaviour of the site as a whole [57].

A simplified version of the hydrogeological conceptual model is shown schematically in Figure 3.4, illustrating the vertical flows in the B2 unit underlying the repository and the horizontal flows towards the coast in the underlying Unit B3.

Currently, the water table at the LLWR is 5 to 8 m OD [57]. In the region above the water table, the saturation is less than 1 and the effective hydraulic conductivity is lower than it would be under saturated conditions. The distribution of the saturation and the effective hydraulic conductivity in the unsaturated region above the water table depend on properties, particularly capillary pressure and relative permeability, of the medium through which the water is flowing.

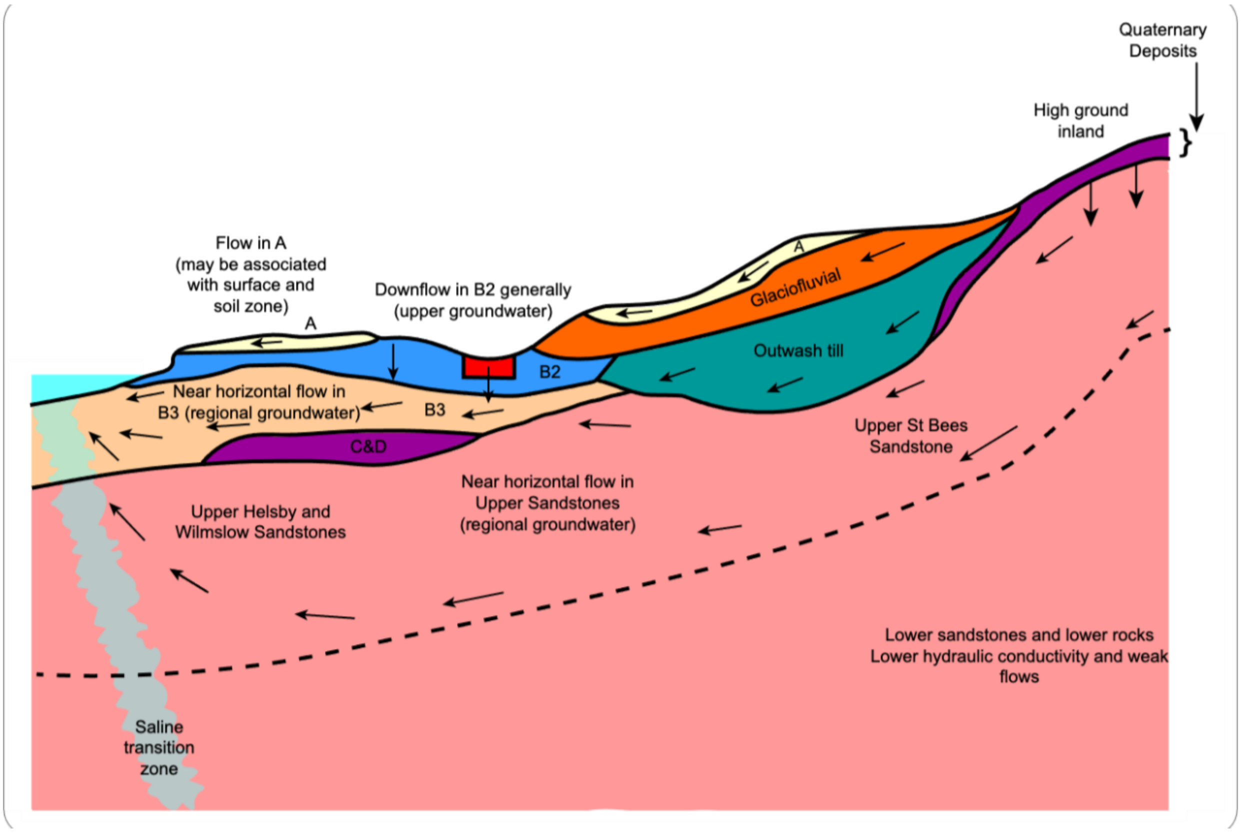

Figure 3.4: **Schematic, simplified representation of groundwater flow in a vertical section through the LLWR perpendicular to the coast. (The arrows show only the direction of the flow, not its magnitude) [6]**

The properties of the engineered structures, and their evolution, have been determined as part of the EPA [12] and these are used as input to the CONNECTFLOW models.

Figure 2.2 shows a schematic overview of the model of the site, including the implementation of the future repository engineering including the cut-off wall.

The results of the CONNECTFLOW groundwater flow simulations are illustrated by Figure 3.5 and Figure 3.6 that show the modelled effective saturation on a vertical section parallel to the coastline passing longitudinally through the repository and the underlying Quaternary sedimentary units (Figure 3.5) and a more detailed section through the vaults Figure 3.6. The simulations begin at 2130 AD, which is the date of completion of the closure engineering [5] and continue to 3280 AD when coastal erosion will begin to disrupt the repository in this climate scenario [57].

The initial time point in Figure 3.5 (2130 AD) shows the results when the infiltration of water through the cap is 0.002 mm per year (Table 3.1). By the last time point at 3280, the infiltration rate is still very low at about 0.25 mm y^{-1} (Case A in Table 3.1) as the cap geomembrane is still intact. Sea level is several meters below the repository at the first time point and rises slightly over the period before coastal erosion impacts the repository.

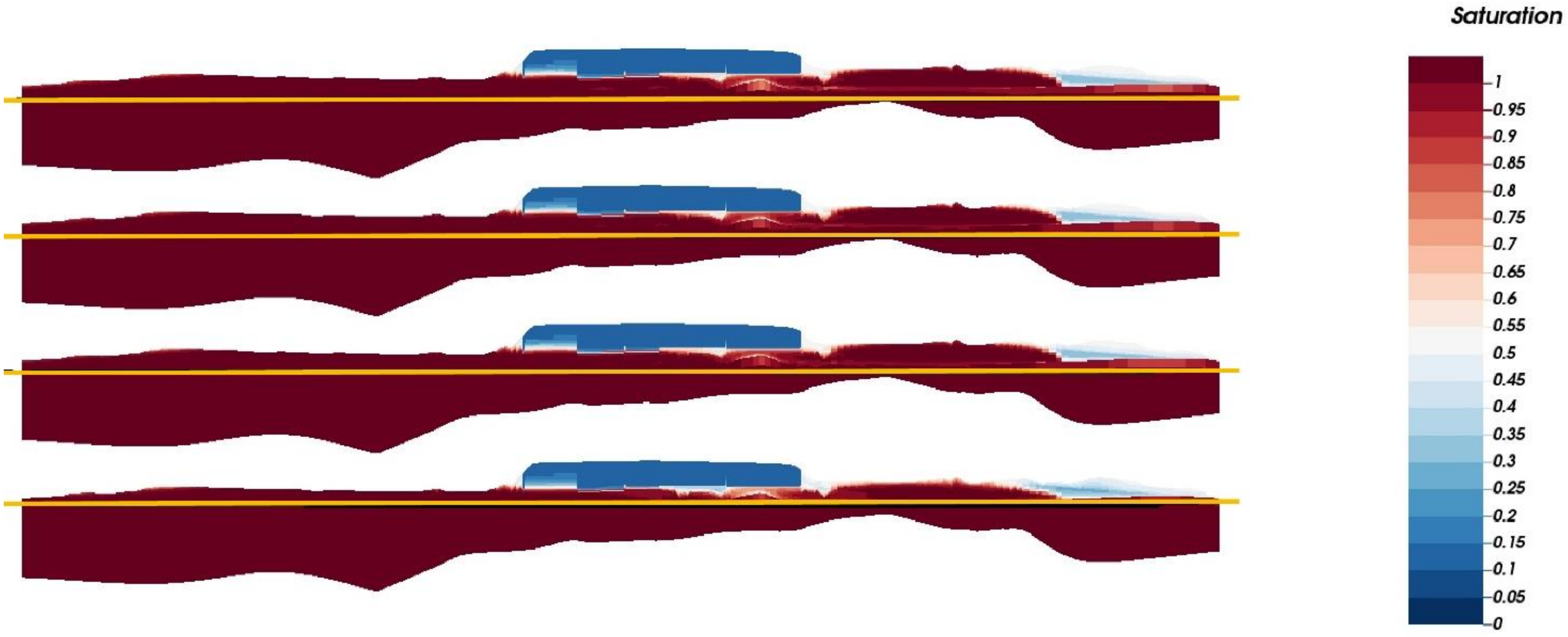

Figure 3.5: **CONNECTFLOW simulation of the evolution of saturation in the repository and underlying geological units for the reference climate scenario. The figures show a vertical section parallel to the coastline through the Vault 8 (left) to Vault 14 (right) for each of four time snapshots at (from top to bottom) 2130 AD, 2230 AD, 2430 AD and 3280 AD. The sea level is denoted by a yellow line. A vertical exaggeration of 5:1 is applied [57]**

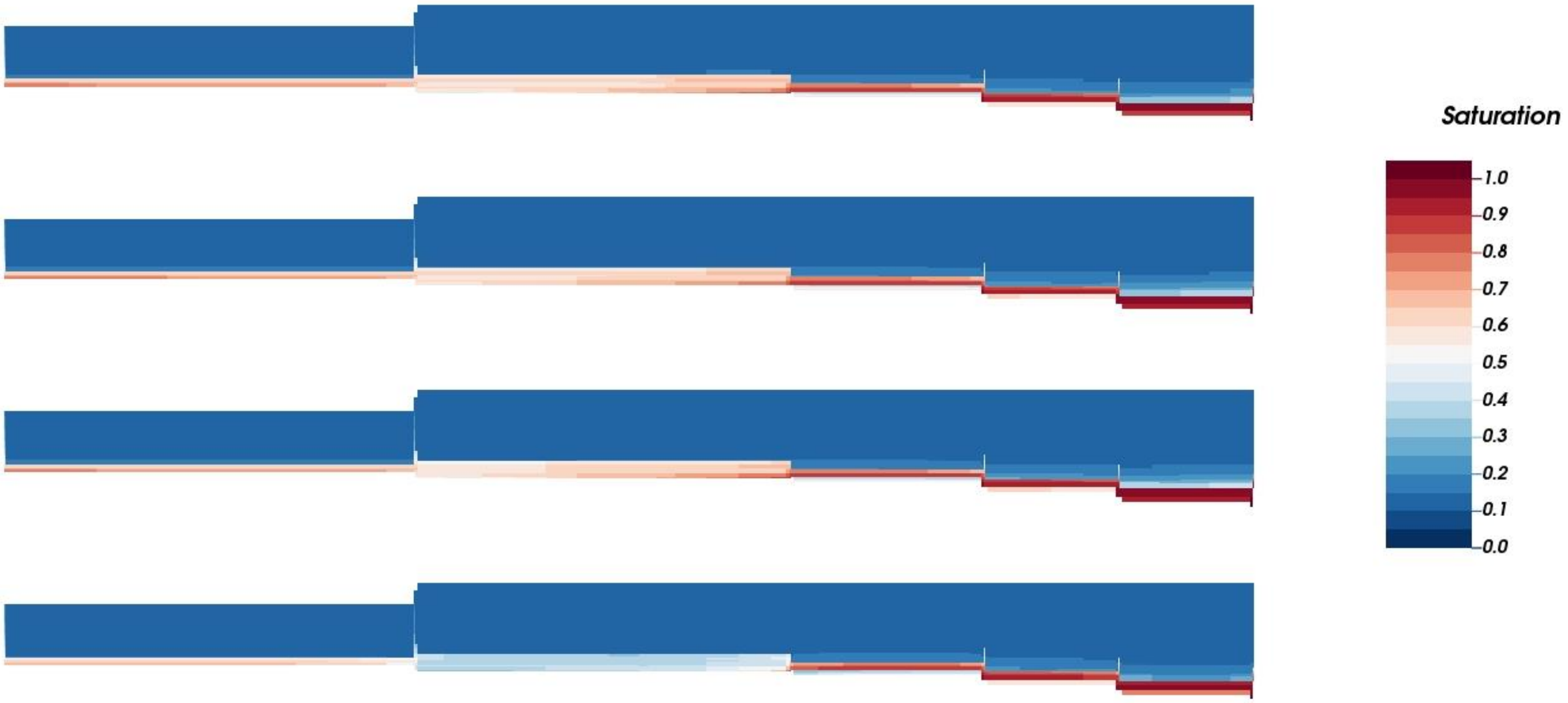

Figure 3.6: **Detailed CONNECTFLOW simulation of the evolution of saturation in the vaults for the reference climate scenario [57]. The figure shows a vertical section parallel to the coastline through the waste stacks in Vault 8 (left) to Vault 12 (right) at each of four time snapshots at (from top to bottom) 2130 AD, 2230 AD, 2430 AD and 3280 AD. A vertical exaggeration of 5:1 is applied**

The vaults are unsaturated over the whole period and the unsaturated zone beneath the vaults increases slightly, demonstrating the drying conditions with no recharge. This is shown most clearly in Figure 3.6 where the Vault 9 base is increasingly unsaturated by 3280 AD.

Water infiltrating the cap, once in excess of consumption reactions, would flow down through the waste mass, then through and around the vault and trench bases, ultimately reaching the B2 lithofacies unit below. This has a relatively low vertical hydraulic conductivity but one that is nevertheless high enough to enable the small amount of infiltrated water to be drained readily through B2 to the Regional Groundwater [6].

A consequence of the reduction in recharge due to the presence of the cap is a lowering of the water table within the repository, relative to the area outside where infiltration overwhelms the drainage capacity of B2 and the water table rises close to ground surface. In this situation there is a positive head difference between the surrounding area and the interior. In the absence of the cut-off wall, this would drive lateral flow into the repository. The cut-off wall has the effect of preventing lateral flows at a depth where they would intercept the waste. Lateral flows still occur at greater depths, below the cut-off wall, but these are also below the vaults and trenches.

Lateral flows through the cut-off wall

It is possible that there will be small flows through the cut-off wall, especially as its performance degrades over time, and these are accounted for in the hydrogeological modelling. Waste in the trenches and vaults close to the periphery would be particularly exposed to this flow. There are two mitigating factors, however. The gap between the cut-off wall and the vault walls or east side of Trench 7 (Figure 2.2) is largely filled by lithological Unit A, which is a sandy, high permeability sediment, that overlies the more clay-rich B2 unit. The result is that any water percolating through the cut-off wall into the unsaturated Unit A will tend to drain downwards to the B2 rather than flowing laterally into the vaults or trenches, so that the level at which it intersects them is below the wastes. The vaults, other than Vault 8, will also be surrounded by the gap adjacent to the 1 metre-high walls that allows water building up in the vaults to flow down to the drainage blanket. Water flows from outside the vault would be intersected by this gap with the result that water percolating through the cut-off wall reaching the vault walls would be diverted to the underlying unit B2. The low wall and gap to the drainage blanket are not used in Vault 9 but the presence of Vault 9a, along its western boundary, will have the same result.

4 Chemical Processes

This section presents a summary of our understanding of the processes that influence:

- the chemical evolution of the wastes consigned to the trenches and vaults;
- the release of radionuclides and non-radiological contaminants from the wastes and near field to groundwater.

Processes affecting the engineered barriers (except for the containers in the vaults, see Subsection 3.4.2) are not considered here but are discussed in the EPA [12]. The chemical evolution of the near field is also of relevance to gas generation and the release of gaseous radionuclides, which are considered in Section 5.

4.1 Overview

A wide range of chemical processes are involved in the degradation of waste and engineering materials during the evolution of the LLWR near field. Many of the chemical, microbiological and corrosion processes are interlinked and coupled to the physical evolution of the near field and groundwater and gas transport processes.

The chemical processes significant for the release and transport of contaminants in the near field have been identified through previous assessments and supporting research [20, 58, 53] and re-examined as part of the current work in support of the 2026 ESC.

The processes and factors influencing the release of contaminants from the trenches are:

- waste degradation, waste metal corrosion and microbiological processes;
- water movement, including precipitation during the operational period and infiltration through the interim trench cap and final cap;
- pH and Eh evolution as a result of the above;
- radionuclide and non-radiological contaminant release processes;
- contaminant sorption and solubility, complexation and colloids;
- spatial heterogeneity in the occurrence of these processes and in the distribution of wastes.

For Vault 8 and the future vaults, additional processes and factors relate to:

- pH buffering by the grout and the carbonation of the grout;
- the effects on Eh of the quantities of steel comprising the half-height ISO containers and small strong boxes;
- the heterogeneity in conditions within and between the waste containers;

The analysis and identification of these chemical features and processes of significance to the ESC has considered information from the inventory, site monitoring data, the engineering performance assessment [12], the results of previous assessments as well as the first phase of the current assessments. We also draw on the analysis of near-field features, events and processes (FEPs) carried out for those assessments as a consistency check.

4.2 Trench Biogeochemical Evolution

An understanding of the biogeochemical evolution, that is, due to the combination of chemical, geological and microbiological processes, of the trench near field is important as this controls the evolution of the local chemical environment and therefore, to a large extent, the behaviour and release of radionuclides within the disposed inventory.

The evolution of the trench near field is a result of a complex set of interactions involving waste degradation, metal corrosion, microbial reactions and water. As a consequence of the nature and chemical composition of the organic and metallic content of LLW, the principal degradation process will involve oxidation[4]. It is well established that microbial processes mediate and catalyse these slow waste degradation processes, particularly of organic materials. Iron corrosion processes are recognised to occur spontaneously. Where metal corrosion proceeds by reduction of water, hydrogen will be produced. This may be readily utilised by microbes and microbial action can lead to enhanced rates of localised corrosion. The corrosion of other metals present in the waste will also occur under the trench conditions. Understanding the processes of waste degradation is important in characterising the chemical environment over various timescales. Site monitoring studies (see, for example, Subsections 4.2.1, 4.5.3 and 4.5.4) and waste simulation experimental studies have been undertaken to support the development of this understanding. The experimental studies are described in detail in the 2002 PCSC [58] and in a review undertaken for the 2011 ESC [59]. A recent report on cellulose degradation reviews the experimental results in the context of LLWR monitoring data and landfill evolution [52].

The redox potential of the near field will be controlled primarily by the redox reactions between the major elements present in LLW and the near field; hydrogen, carbon, nitrogen, oxygen, sulphur and iron. In the trenches, the redox reactions will be mediated by microbiological processes and the pH will also be influenced by these reactions.

Within the trenches, the degradation of cellulosic material and the corrosion of waste metal are expected to lead to reducing and mildly acidic conditions and to promote methane gas generation. Evidence for such conditions is observed in the trench monitoring data including detection of acetate and other carboxylic acids[5], measurement of variable carbonate, sulphide and sulphate concentrations (Table 4.1), reflecting variations in pH and Eh and generation of gases with significant methane content (Figure 4.1) [8].

---

[4] 'Oxidation' in this context includes the use several sources of oxygen in microbial reactions, including gaseous and dissolved oxygen, sulphate, nitrate and water, and the oxidation of metals by water reduction.

[5] These are fermentation products resulting from microbially-mediated cellulose degradation and are important electron donors for processes of iron and sulphate reduction and methanogenesis.

Table 4.1: Historic leachate measurements [20]

(a) Data from sampling of 9 vent probes in Trench 7 during 1997 [60]				
	Carbonate	Sulphate	Sulphide	Acetate
	mol l^{-1}	mol l^{-1}	mol l^{-1}	mol l^{-1}
Minimum	$1.91\ 10^{-3}$	$8.33\ 10^{-5}$	$3.03\ 10^{-6}$	$2.22\ 10^{-4}$
Maximum	$1.17\ 10^{-2}$	$4.48\ 10^{-3}$	$1.30\ 10^{-4}$	$4.20\ 10^{-3}$
Mean	$3.98\ 10^{-3}$	$1.00\ 10^{-3}$	$3.22\ 10^{-5}$	$2.21\ 10^{-3}$

(b) Ranges of acetate concentration (mol l^{-1}) measured in trench vent probes prior to 1993 [61] (single measurements listed as maximum)		
Trench probe	Minimum	Maximum
Trench 2, probe 2.07	-	$5.83\ 10^{-4}$
Trench 2, probe 2.10	$3.33\ 10^{-4}$	$6.67\ 10^{-4}$
Trench 3, probe 3.02	-	$1.00\ 10^{-3}$
Trench 5, probe 5.01	$2.75\ 10^{-3}$	$2.83\ 10^{-3}$
Trench 5, probe 5.03	-	$1.28\ 10^{-2}$
Trench 5, probe 5.07	-	$3.33\ 10^{-4}$
Trench 5, probe 5.08	$2.50\ 10^{-4}$	$3.42\ 10^{-4}$
Trench 5, probe 5.09	-	$3.83\ 10^{-3}$

Biogeochemical evolution is a dynamic process and the extent and longevity of these conditions will depend on a number of factors, including the relative amounts of the different waste materials and the rate of groundwater flow through the near-field environment.

Radionuclides such as uranium and technetium and toxic metal contaminants (for example, chromium) can exist in several oxidation states. These contaminants can, therefore, exhibit different solubility and sorption behaviour depending on the redox potential and pH. A range of redox potential and pH conditions may occur in the trench environment, reflecting both local heterogeneity of conditions and longer-term changes in response to infiltration rates and depletion of organic waste materials.

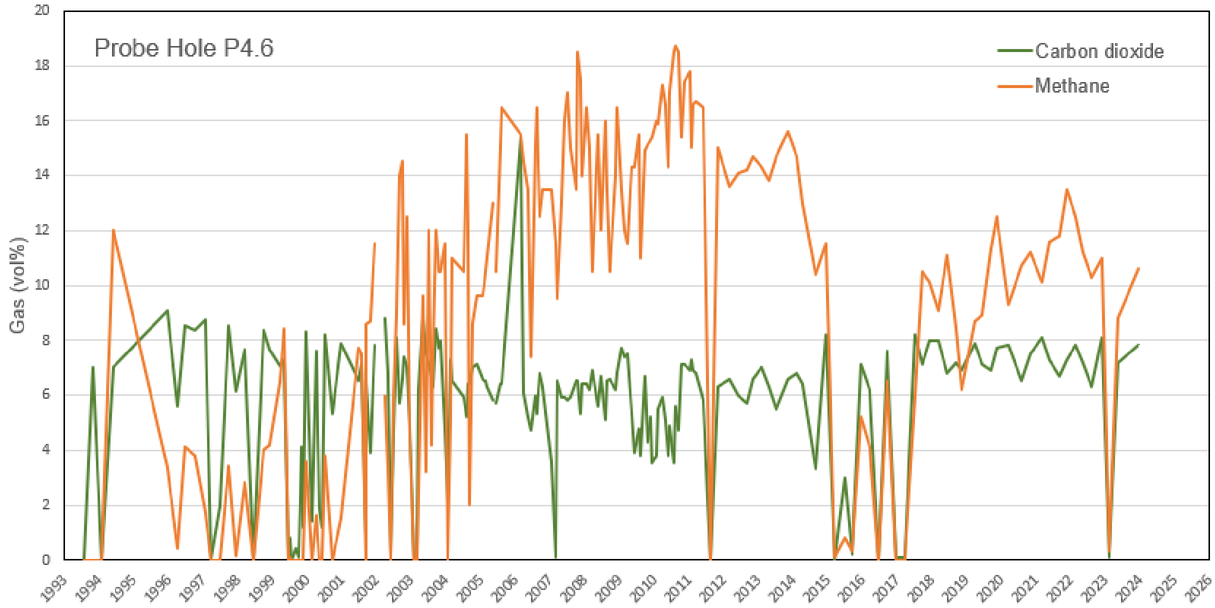

Figure 4.1: Methane and carbon dioxide measured in Trench 4 (sealed probe hole P4.6) over the period 1993 to 2024 as part of the LLWR EMP [8]. These results are discussed further in Subsection 4.2.1

Carbon-14 can either be present in oxidised inorganic forms (carbonate), or in more reduced organic forms. Compared to the redox reactions of metal contaminants, for example, U(IV)/U(VI), which tend towards equilibrium, the reactions between organic and inorganic forms of C-14 are slow and C-14 speciation is primarily influenced by the biogeochemical processes, such as methanogenesis, involving stable carbon present in LLW and the near surface environment. Biogeochemical processes also cause degradation of organic materials, leading to both the release and natural attenuation of organic contaminants such as formaldehyde. This is generated by degradation of cellulose and other waste organics, but also metabolised by microbial activity.

4.2.1 Making use of Monitoring Data

The LLWR environmental monitoring programme (EMP) is designed to monitor the performance of the site and to assess its potential impact on the surrounding environment [8]. Many of the objectives relate to confirmation that the repository system is not giving rise to unacceptable environmental hazards by direct measurement of its impacts. Most relevant to the understanding of the near field, is the objective "*To develop and build confidence in the models of the repository system by collecting data that may be used to refine conceptual models or in model parameterisation, calibration or validation*" [40].

In the descriptions of the trench biogeochemical evolution, above, contaminant release processes (Subsection 4.5) and, particularly, gas generation (Sections 5 and 7), we discuss the monitoring data from the trenches that has been important in testing our conceptual models and validating modelling results.

The monitoring of the trenches since 1995 through the interim cap by a series of open or sealed probe holes provides location-specific information that gives more insight into the variability and heterogeneity of processes than is possible from the leachate collected at the end of the trench drainage system. The measurement of landfill gases in these probe holes is particularly important in examining the current state and evolution of the trenches.

Some of the results from the landfill gas monitoring in the sealed probe holes are shown in Figure 4.2. The gas analyses are for Trenches 4 (P4.6), 5 (P5.8) and 7 (P7.4A), respectively. The values for CO_2, CH_4 and O_2 are given in gas volume percentages, but H_2 analyses are given as parts per million (ppm). While the patterns for the various gases from the three trenches (and other probe holes, not shown) have some similarities in terms of the sudden changes between periods with oxygen and with methane, there are also some differences between the trenches.

A change in analytical method post-2009 resulted in H_2 results being given as 'low' without a numerical value. Also, the interim cap over Vault 7 was installed after the cap over trenches 1-6, leading to a delay, compared with other trenches, in starting the monitoring programme.

The monitoring of leachate in probe holes has indicated that the trenches are generally drying with falling water levels. This is illustrated by Figure 4.3 which shows the leachate level in Trench 4 probe holes.

The intermittent readings with around 20% oxygen appear to be ingress of atmospheric gases into the probe holes (Figure 4.2). Furthermore, the total gas analyses in most results are less than about 25 vol% and suggest that there is a residual atmosphere of nitrogen which makes up the largest portion of the gas phase in the trenches.

We regard this as the result of the state of the interim trench cap. Water balance data suggest that the interim cap over the trenches is not performing as intended and a larger fraction of annual precipitation than originally expected is entering the trenches [62]. In 2012 a Best Available Techniques (BAT) study [63] was commissioned to examine options for the trenches in light of the strip capping approach planned for the whole repository. The installation of the final cap in sequential sections over part of the trenches and the adjacent vault following completion of operations in that vault would mean the southern trenches would not be finally capped until after 2100 [5]. Over the period between 2012 and 2018 the initial BAT study was reviewed and updated following investigations that uncovered damage to the interim cap membrane. The final outcomes of the BAT process were reported in 2019 for the Repository Development Programme (RDP) Tranche 1 [64].

The damage to the cap uncovered during investigations included quite extensive tears and holes in the membrane [65] that would permit air ingress, particularly at times when the overlying soil cover was dry. This may explain the presence of oxygen in monitoring measurements on an approximately annual basis in P5.6 Trench 5 (Figure 4.2).

The observations of oxygen ingress in the Trench 4 and 7 probe holes (Figure 4.2, top and bottom graphs) are less frequent since 2004 and may correspond with periods of perturbation due, for example, to activities on the cap.

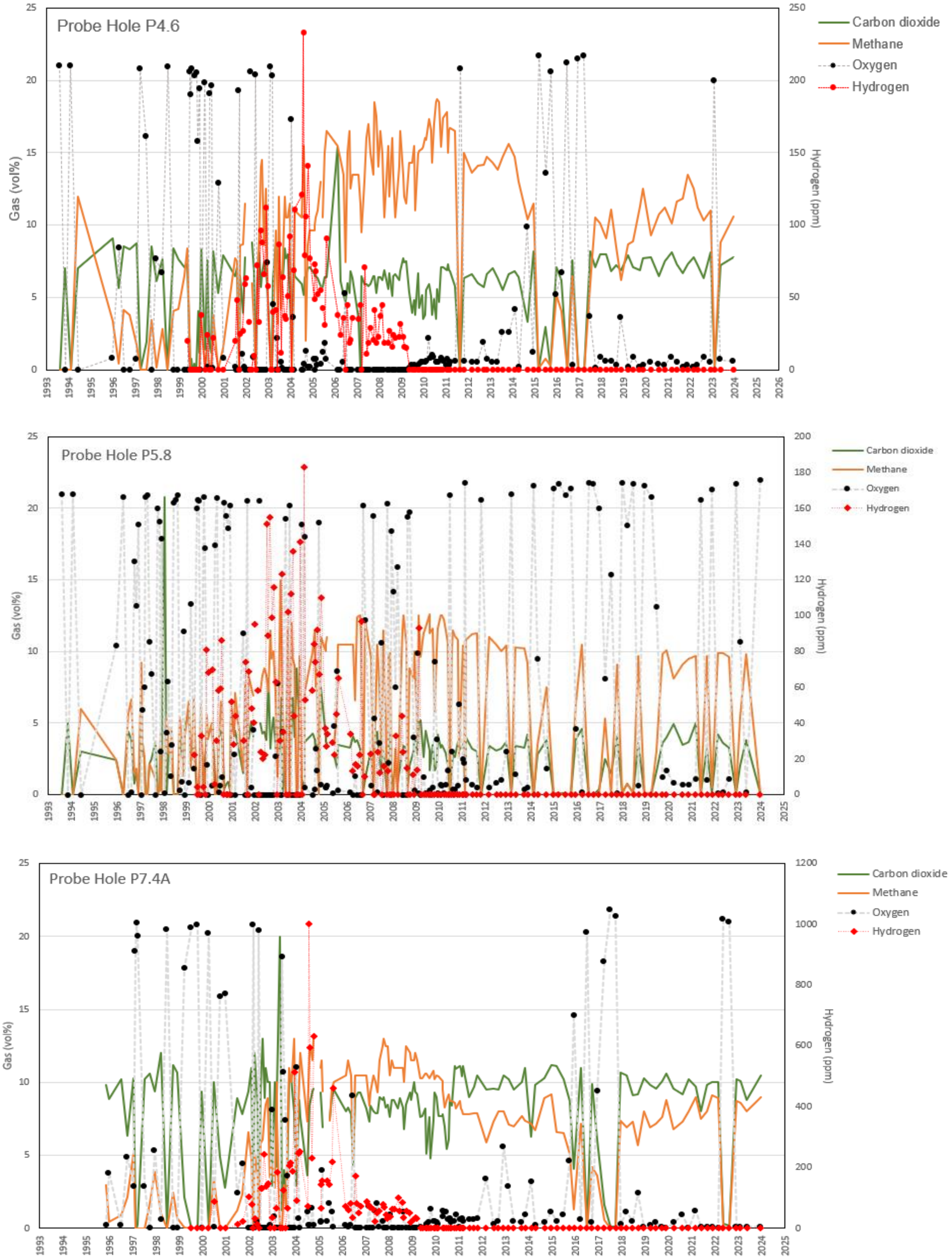

Figure 4.2: Gas monitoring data from sealed probe holes (see text) [34]

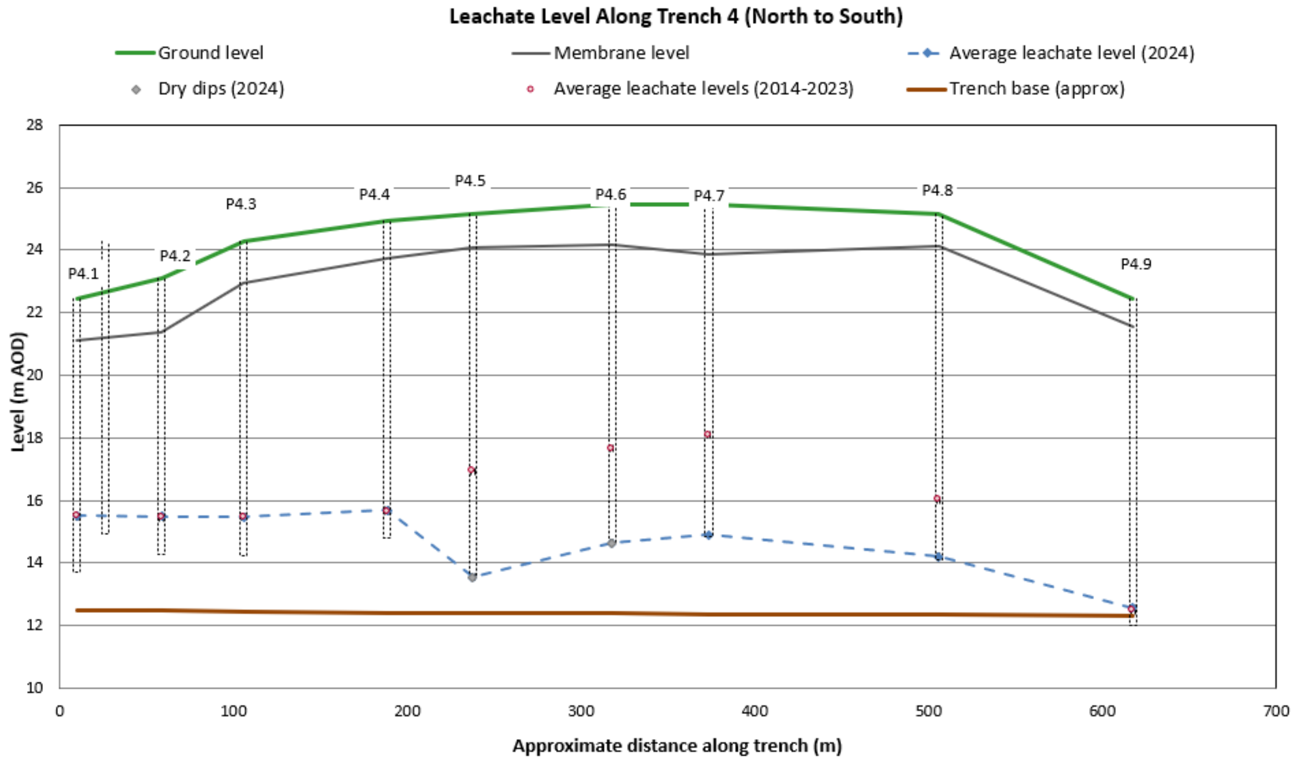

Figure 4.3: **Current and average leachate levels over the last decade and location of the probe holes in Trench 4 [34]**

The results of monitoring of landfill gases show a clear pattern in all the trenches with periods of methane and CO_2 generation alternating with observations of oxygen when the CH_4 and CO_2 are much lower to absent. The quantitative hydrogen measurements before 2010[6] show a similar pattern with H_2 present mainly with methane and CO_2, albeit at much lower levels. Interestingly, there are times in both Trench 4 and Trench 7 where all four gases are present at the same observation and, after 2010 where oxygen is present at low percentages with higher levels of CO_2 and CH_4. As methane would not generally be expected to be produced or to persist in the presence of oxygen (see Subsection 5.1), these observations suggest a mixed system where wastes in part of the trench are degrading anaerobically, but another part is at least intermittently aerobic. Two discrete systems may correspond to the unsaturated and saturated portions of the trenches (Figure 4.3), respectively.

The evolution of separate biogeochemical zones within the trenches may explain the low hydrogen content in the gases which, given the large amounts of metal in the trenches (Subsection 2.3.1; Figure 2.12), should be a more significant gas, possibly at the expense of CO_2 (see Subsection 5.1.3). The hydrogen may be consumed by microbial processes in the unsaturated zone, especially if conditions are not anaerobic. The condition of the interim cap does, however, raise the possibility that hydrogen could have been lost preferentially from

---

[6] A change to monitoring equipment resulted in no further quantitative data for hydrogen after 2010.

the unsaturated portions of the trenches because it is so much lighter than the other gases, thus subject to significant buoyancy.

Trench 7 (Figure 4.2, bottom graph) also shows an interesting trend of generally higher CO_2 than methane, in contrast to other trenches where CH_4 dominates. Given the persistence of low levels (< 5%) oxygen in the Trench 7 probe hole, this suggests the possibility that methane is being oxidised to CO_2 in the more aerobic conditions.

Overall, the quarter century of gas monitoring data for the trenches are suggesting that their evolution is a lot more complex than simple establishment of anaerobic conditions resulting in methane and carbon dioxide generation from cellulose degradation and hydrogen from metal corrosion. The replacement of the southern trench interim membrane should allow more stable anaerobic conditions to become established that should be observed in future monitoring.

4.3 Vault Wasteform Chemical Evolution and Cementitious Interactions

The different disposal environments will lead to the development of different conditions within the trenches and vaults. This is most marked for the cementitious grout present in the containers, which will result in the establishment of alkaline chemical conditions in container porewater and leachate. These conditions will affect the degradation of organic matter and corrosion in the vault.

4.3.1 Grout pH

The chemical evolution of the LLWR grout has been re-examined since 2011 in the light of better understanding of the behaviour of blended or composite cements [66]. These cements make use of materials such as blast furnace slag and pulverised fuel ash (PFA, also known as flyash) that have historically been cheap and widely available waste products from other industries [67, 68].

The LLWR grout is a combination of ordinary Portland cement (OPC) with PFA in a ratio of approximately one to three. PFA is a by-product of the burning of coal in power stations and is widely used in the cement and construction industry to improve the quality of concretes.

The initial mineralogy of the LLWR grout was determined in an experimental study that also considered the leaching behaviour [69]. On the basis of this work, it was previously assumed that the initial pH in the grout porewater was about pH 11 as a result of early loss of the alkali metal hydroxides (NaOH and KOH) into water infiltrating containers either before or shortly after capping of the vaults [20]. The alkali metals oxides are minor components of OPC and PFA powders, but are highly soluble, leading to high pH, typically above pH 12.5, in the early grout porewater. Experimental leaching of powdered grout samples in large volumes of leachant suggested that the porewater would be conditioned to around pH 11 [69] once the alkali metals hydroxides had been lost.

We have reviewed the experimental results in light of the volume of water required to produce equivalent leaching under repository conditions [66]. In considering the newly elicited lower infiltration rates for the vaults (Subsection 3.2.1), we now account in our chemical model of the grout for the period during which the alkali metal hydroxides are still present in the grout as we expect that this period may be substantial. With the alkali metal hydroxides present, the grout porewater pH is initially around pH 13 (Table 4.2) but will fall as the alkalis diffuse out of the grout into infiltrating water flowing in the gaps.

Containers that are protected from water infiltrating the cap by the containers above them in the stacks or by the CPUs in the future vaults will not experience the volume of water required to leach the alkali metals over the period before coastal erosion disrupts the vaults. It is worth considering that even the containers in Vault 8 at the tops of stacks and with open grout ports will have not experienced sufficiently large volumes of water. From the experimental evidence, leaching of the alkalis to achieve a pH of around 11 requires several pore volumes of water. The volume of grout porosity in a typical container is around 3 to 5 m^3 (based on 30% porosity in the grout [70] and average grout content of around 16 tonnes per container [24]), equivalent to several decades of rainfall at the grouting port. Furthermore, the grout has low permeability, so that large flows of water through the intact matrix are not feasible. Water could flow in cracks in the grout but, like standing water in the ullage space, will only contain the alkalis metals that diffuse from the surfaces of the grout.

We have also improved our chemical model of the grout to represent the mineralogy more completely in the near-field modelling [71, 66] This will ensure that interactions between infiltrating water, waste materials, contaminants and the grout can be evaluated to the best possible extent. The new model for the mineralogy builds on previous work [72, 73] but takes account of more recent work on blended cements and the properties of the PFA in hydrated cements. We have also been able to draw on the results of additional experimental studies to support this work [74, 47].

The major component composition of the initial grout porewater is given in Table 4.2 based on modelling of equilibrium in pure water. The composition corrected for the LLWR annual mean temperature of 11 °C is given alongside the composition at the standard temperature of 25 °C for comparison purposes. In general, when the pH in the near field is cited, it is the temperature-corrected value to which we refer.

4.3.2 Implications of the Grout pH

The chemical conditions with pH of 12.5 to 13 within the containers have implications for the processes of waste degradation, particularly metal corrosion and microbial processes.

Corrosion rates for key waste metals such as carbon steel and stainless steel will, in general, be lower under the higher pH conditions, although the reverse is true for reactive metals such as aluminium (Table 4-3). This will affect the rate of hydrogen gas generation (Subsection 5.1.1).

The pH conditions will also affect the corrosion of the inside of the carbon steel containers and this may influence the deterioration rate of the containers. Overall, however, we expect slower internal corrosion to have relatively little impact. The lower pH in the gaps outside the containers means that the higher external corrosion rates, and the potential for microbial processes to affect corrosion locally, are likely to be more significant in determining container longevity. It is worth noting that the mean external container corrosion rate is 0.34 µm y^{-1} [75], lower than the equivalent value of 1 µm y^{-1} used in the 2011 ESC [20].

Table 4.2: Initial LLWR grout porewater composition at 11 °C (and at 25 °C for comparison) in equilibrium with the mineralogical phase assemblage and accounting for CSH alkali uptake [71]

Variable	100% alkalis in OPC and 15% alkalis in the reacted PFA fraction	
Temperature (°C)	11	25
Ionic strength (M)	0.056	0.057
pH	13.13	12.64
Aqueous concentration (M)		
Al	1.64 10^{-4}	2.19 10^{-4}
Inorganic C as CO_3^{2-}	3.85 10^{-5}	3.43 10^{-5}
Ca	8.02 10^{-4}	9.40 10^{-4}
Fe	3.06 10^{-10}	4.14 10^{-10}
K	3.55 10^{-2}	3.58 10^{-2}
Mg	6.43 10^{-10}	1.12 10^{-9}
Na	1.87 10^{-2}	1.88 10^{-2}
S	2.47 10^{-4}	7.81 10^{-4}
Si	1.27 10^{-4}	2.77 10^{-4}

Despite the slower waste metal and internal container corrosion, the conditions in the wastes will still become strongly reducing once the vaults are capped. For some containers, especially those with high grout contents, the grout may isolate the wastes from the atmosphere. In these containers, degradation processes may consume the available oxygen so they become reducing even before capping.

A potentially more important consequence of the higher pH within the waste is its effect on microbial activity. A recent review of the most current scientific understanding of microbial activity in hyperalkaline environments [76] has shown that at pH above 12.5, in low temperature, anoxic environments, the activity of microbes is restricted to the extent that microbially-mediated reactions can be discounted as a widespread influence on chemical conditions, and particularly establishing methanogenesis, in the grouted waste.

Table 4-3: Mean corrosion rates for key waste and container metals under different grout porewater pH, but assuming reducing redox conditions

Metal	Corrosion rate at 11 °C (µm y^{-1})	
	pH 13 [77]	pH 10 to 11 [55]
Stainless steel	$4.2\ 10^{-4}$	$3.0\ 10^{-2}$
Carbon steel	$4.6\ 10^{-3}$	$4.0\ 10^{-2}$
Aluminium	1.0	$6.0\ 10^{-1}$
Magnox	$1.0\ 10^{-1}$	n.d.

The Eh within the grouted containers will largely be determined by steel corrosion generating hydrogen. At pH 12.5 to 13 at 11 °C, this indicates an Eh around -700 mV, which is not expected to change significantly over the period of interest.

Within the gaps between containers, the situation is more complicated because of the minimal contact with grout for a long period, and then the increase in infiltration once the cap geomembrane fails. The pH is expected to be controlled initially by the infiltrating water composition (Subsection 6.2) and corrosion of the outer surfaces of the containers but to remain near-neutral to moderately alkaline (Subsection 6.5.2). There may be sufficient nutrients (electron acceptors) such as sulphate, nitrate and carbonate present in some locations to allow limited microbial activity utilising hydrogen where there is also sufficient water. As containers are perforated by corrosion, the pH in the gaps will tend to increase, although dilution by increasing infiltration may outpace diffusion from the grout. Over the period before coastal erosion, however, the pH in the gaps will mainly remain in the range of pH 7 to 10. The extent of microbial activity is uncertain but probably variable in time and location, so the precise control on Eh in the water in the gaps is also uncertain. However, it is unlikely that Eh will deviate outside the range between -300 and -500 mV (see also Subsection 6.5).

Without microbial activity, the degradation of organic wastes will not follow the evolution of similar wastes in the trenches. Instead of cellulose giving rise to the fermentation product acetate and gases (Subsection 5.1.2), a major product under alkaline conditions will be isosaccharinic acid and other alkaline hydrolysis products. We have conducted a review of the current understanding of ISA production under alkaline conditions [78] to ensure that in changing our near-field conceptual model to account for higher pH in the grout, we are also accounting for the changes to the waste degradation processes.

ISA can act as a strong complexant for some key radionuclides, such as Pu, Th, Eu and U, thus affecting retardation in the near field. In disposal facilities for cemented LLW and ILW, the potential effect of ISA complexation is typically accounted for in assessment calculations by increasing solubility limits and reducing sorption coefficients for affected contaminants, as described in reference [79] (and references therein).

The 2011 ESC [20] made the case that ISA is not of concern under the vault near-field conditions, because pH 10 to 11 in the grout porewater was less conducive to ISA formation [80] and because microbial degradation was expected to lower ISA concentrations to levels that would have little effect on contaminant transport. With potentially more ISA production under higher pH conditions, and without any microbial degradation, we have revised this conclusion.

The review reported in reference [78] suggested that, as much of the existing cellulosic waste in Vault 8 is in the form of compacted pucks that may evolve in isolation from the surrounding grout and at lower pH, there is a possibility that little ISA would be formed. Furthermore, at least transient microbial activity may also be possible within these isolated niches and this could further reduce the ISA concentration. It is difficult to be certain that this will be the case, however, and percolation of high pH grout porewater into the initially dry or only partially wetted cellulosic wastes could introduce conditions that are more conducive to ISA production and less favourable to microbial degradation of the ISA produced. Therefore, we have adopted the position for our assessments that we need to account for ISA production under the conditions in the grouted wastes [79]. We recognise that this is a conservative assumption that is likely to overestimate the effect of ISA complexation, even taking account of ISA sorption onto the grout and potential precipitation of calcium isosaccharinate.

4.4 Heterogeneity in Vault Wastes and Wasteform

The variability in physical properties of reactive materials in compacted and noncompacted wastes may influence the pH and Eh evolution, as alluded to in the discussion of ISA, above. The inventory of consignments to Vault 8 was considered in reference [81] to establish the physical and chemical form of the principal types of reactive waste materials. The study also considered how the release of the key radionuclides of significance to the ESC would be affected by the interactions between the waste materials, grout and the corroding carbon steel containers. A storyboard discussion was developed for the heterogeneous physical and chemical evolution of a range of waste types comprising:

- directly-consigned loose metal wastes encapsulated in grout;
- directly-consigned loose soil and rubble wastes;
- other directly-consigned loose wastes including non-compacted organic wastes, with grout;
- compacted wastes, encased in grout.

The effects of future changes in LLW management practices including treatment of wastes were also considered [81].

This discussion below has been updated to include consideration of wastes disposed to Vault 8 and to Vault 9 since 2011, the future LLW and potential disposal of ILW, as well as any changes to our understanding from more recent studies.

Directly-consigned and grouted metal wastes

In terms of the proportion of the different types of waste and content of key radionuclides (that is, C-14, Cl-36, Tc-99 and uranium. See Subsection 2.3.2) in the Vault 8 inventory, directly consigned metal wastes are of major importance, especially for C-14. Such materials are likely to be initially well encapsulated by the grout, such that most metal surfaces are coated in grout, as shown when the wasteform is sectioned (Figure 3.1). For the future LLW and ILW, metal wastes are similarly important for C-14 (see Subsection 5.2.1; Table 4.4; Table 4.5).

Corrosion of the waste steels and the disposal containers will be slower under the alkaline conditions buffered by the grout, due to the effect of passivation [77]. The rate of corrosion of the metal waste will control the rate of release of some contaminants (See Subsection 4.4).

Soil and rubble wastes

Directly-consigned granular soil and rubble waste may form large, isolated volumes of material within containers, where the waste is not in direct contact with grout (Figure 3.1). These wastes may contain mainly C-14, Cl-36 and uranium [81]. The pH conditions within the soil and rubble will be largely self-buffered between neutral and mildly alkaline conditions initially, depending on the content of concrete or mortar in the rubble. Percolation of leachate from the grout may increase the pH within the soil waste and, in the longer-term, diffusion between the saturated soil porewater and the grout will also increase the pH. Concrete materials will have a limited pH buffering effect where surfaces are weathered and carbonated, but freshly-broken rubble may be more reactive. The pH buffering behaviour of soils will be dependent on their organic carbon content, the local pH conditions, thus microbial activity, and the degree to which the surrounding grout is absorbing CO_2.

The corrosion of the internal surface of the metal container is likely to be the main influence on Eh in the soil and rubble, providing a source of H_2, which will diffuse into and react with the waste. In the presence of significant amounts of Fe(III) minerals in the soils, more oxidising conditions may prevail locally. Radionuclides in wastes of these types will largely be present as surface contamination. The granular and porous nature of the wastes may promote interaction between the surface contaminants and the container porewater. As infiltration rates to the vaults increase, the contaminants in these waste containers will be vulnerable to rapid loss once the container is subject to infiltrating water flows.

Organic wastes

Directly-consigned waste types that may promote microbial activity include: cellulosic wastes such as wood; other organic waste materials, including plastics and rubber; graphite; ion exchange resins; and reactive sulphate- and nitrate-containing wastes. The biogeochemical processes associated with these materials are particularly relevant to the chemical speciation of C-14 and uranium, which are associated with these waste types. However, the evolution of these wastes will be determined by the grout and high pH porewater. As discussed in Subsection 4.3.2, pH of 12.5 and above will severely restrict microbial activity and in general, since these wastes are surrounded by the grout, we expect that their evolution will be largely abiotic.

Graphite wastes are chemically unreactive and it is considered unlikely that they will significantly affect the chemical evolution of the vault wasteform. A review for the GDF programme of the stability of graphite and pyrolytic carbon (a less crystalline form of carbon) wastes disposed in the ILW vaults concluded that on a 10^5 to 10^6 year timescale, the amount of stable carbon mobilised would be insignificant [82].

Compacted wastes

The organic content of the compacted waste and its isolation by the metal pucks from the surrounding grout provides an environment in which microbial activity could flourish without the limitations imposed by high pH grout porewater. Although, in low porosity pucks, microbial activity may be limited by requirements for space to grow and also by water availability. Where low pH regions do develop in the waste pucks initially, as a result of microbial degradation of the organic wastes, seepage of grout porewater into the pucks may increase pH to the extent that further microbial activity is limited or result in carbonate precipitation at the interface between the puck and the grout. Such precipitation may further isolate the compacted puck and the contaminants present in the waste.

Where microbial activity does occur in the waste pucks, strongly reducing conditions are expected to develop, with sulphate reduction, fermentative and methanogenic conditions. Saturation of the waste in the puck, corrosion of the metal wastes and puck, and gas production in the waste may lead to expansion in the puck inducing cracking of the surrounding grout. Although degradation of organic wastes in the puck may create void space that could accommodate some expansion of corroding metals, gas generation within the puck would be more likely to cause disruption that enhanced cracking in the surrounding grout.

Microbial degradation of cellulose-rich wastes in the pucks producing CO_2 will result in some degradation of the surrounding grout by carbonation, thus potentially allowing later C-14-bearing CO_2 to be released to the biosphere. However, the grout content of consignments of compacted waste before 2011 was estimated to be above 60% by volume (Figure 4.4) [81]. More recent data for disposals between 2014 and 2023 indicate the average content was similar, with18 tonnes of grout and 11 tonnes of waste (including the puck steel drums or boxes) per container. These values suggest that, although carbonation and lower pH could occur locally, there is sufficient grout that the porewater in a typical container of compacted wastes will be maintained at pH >12 (Subsection 6.5.2).

Overall, the behaviour of the pucks is uncertain and there will certainly be a range of outcomes for individual containers, but while the waste remains relatively isolated from the grout environment, contaminant releases will also be limited. Where a puck does develop a microbially-influenced environment, there will be a competition between carbonate precipitation at the puck-grout interface, which tends to increase isolation, while gas production, particularly of methane and hydrogen, will tend to increase the cracking around the puck and improve the connection to water in the grout.

Poorly grouted containers

Reference [81] reports the results of a study that evaluated the grout content of HHISO containers consigned to Vault 8. The difference between the mass of ungrouted and grouted containers was used to estimate the grout volume. The results are shown in Figure 4.4. While the containers with compacted pucks (denoted 'WAMAC'), as noted above, predominantly contain grout filling more than half of the container volume, there are several hundred containers that have grout filling less than a fifth of that volume.

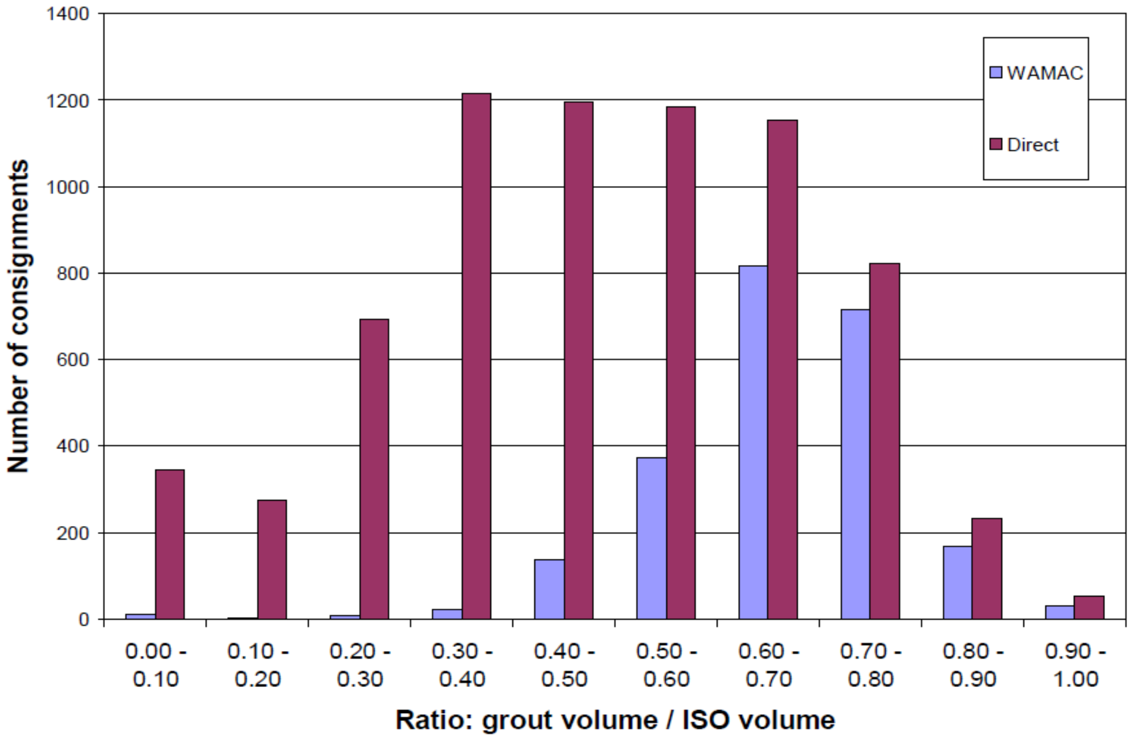

Figure 4.4: Distribution of grout content of directly consigned and compacted (WAMAC) wastes in Vault 8 [81]

The simple metric for grout content does not show how much waste is also present. For example, low grout content could result in an otherwise well-filled container where the grout is excluded from fine porosity, for example, loose soil or absorbent mineral blocks used to stabilise liquid wastes for disposal. However, low grout content can also indicate a container with larger voids such as can occur with metal pipework, or wastes loosely packaged in containers. These examples suggest that the mass of waste might also be small in some cases but the grout generally surrounds the wastes, so the low grout content might not be cause for concern. The analysis of reference [81] suggests, however, that the wastes in the low grout containers are fairly even spread across the categories of metal, wood, soil/rubble, soft plastics, plastics/rubber and other/unknown. This suggests that in some containers, the low grout content means wastes are not well surrounded by grout.

Low grout content could result in a number of different processes that detrimentally affect the retention of contaminants in the waste.

- Less grout means a lower capacity to buffer pH and accelerated loss of high pH conditions once infiltrating water gains access to the container.
- Loss of high pH could, in turn, mean that microbial activity generates CO_2 from remaining organic wastes, such as slow degrading wood and plastics, resulting in carbonation of the grout minerals. This could reduce the retardation of contaminants by sorption on the grout. Carbonate minerals such as calcite do provide some sorption, but it is relatively limited compared with the cement minerals. Some contaminants can also be included in the new mineral phase, for example radium can replace calcium in calcite [83] but the extent is uncertain and we do not try to take benefit from this process.
- Lower pH would also enhance the rate of corrosion of metals, thus releasing contaminants to the pore water more quickly.
- Under lower pH conditions, microbial methanogenesis utilising the CO_2 and carbonate would also be possible. This could affect the speciation, and thus release, of C-14 by transforming dissolved C-14-bearing carbonate to C-14-bearing CH_4 that would by more mobile as a gas (Subsection 4.5.2).

Both degradation of organics and corrosion of metals can lead to volume changes that result in the breaking up of grout, especially where it is present in thin layers between waste items. This could then create preferential flow paths for advection around the waste that reduce the contact between infiltrating water and grout.

We have considered poorly grouted wastes, and the interactions between cellulosic wastes and grout with different proportions of waste and grout, in our near-field modelling (Subsection 6.5.2).

4.4.1 Implications of Future Waste Composition

Effect of changes in LLW management practices

Innovations in waste management practices include treatment processes aimed at reducing waste volumes as well as maximising the recycling of potential resources such as waste metals. Waste treatment technologies including incineration and metal melting will change the physical and chemical form of LLW and affect the chemical evolution of the near field. By reducing the organic carbon content through incineration, the potential to generate methane and organic complexants will be reduced, and metal treatment may reduce the metal content of the waste. The large quantity of container metal in the vaults and the slow corrosion rates mean, however, that smaller quantities of metal wastes are unlikely to affect the development and maintenance of reducing conditions in the vaults in the long-term.

Future LLW and potential ILW disposals

In addition to future LLW, ILW is being considered for disposal in the LLWR vaults. The ILW streams that are included in the Stage 2 reference inventory [24] have not yet arisen as these wastes would need to be packaged in new containers - the small strong boxes (Subsection 2.2.3) - that are acceptable for use in the surface vaults. Existing ILW that has already been packaged in durable GDF containers, for example, stainless steel drums and boxes, has been excluded because the containers will not degrade on a suitable timescale following coastal erosion [84], thus causing waste to accumulate on the storm beach.

Inspection of the inventory data for the ILW identified as suitable for the LLWR shows that the major types of material are similar to the disposed and future LLW [24]. The masses of key reactive waste materials such as steels, cellulosic and other organic wastes, along with grout and container metal are illustrated in Figure 4.5 for disposed LLW, future LLW and future ILW to allow comparison of proportions of materials. The respective total packaged volumes are 2.5 10^5 m^3, 3.9 10^5 m^3 and 8.9 10^4 m^3.

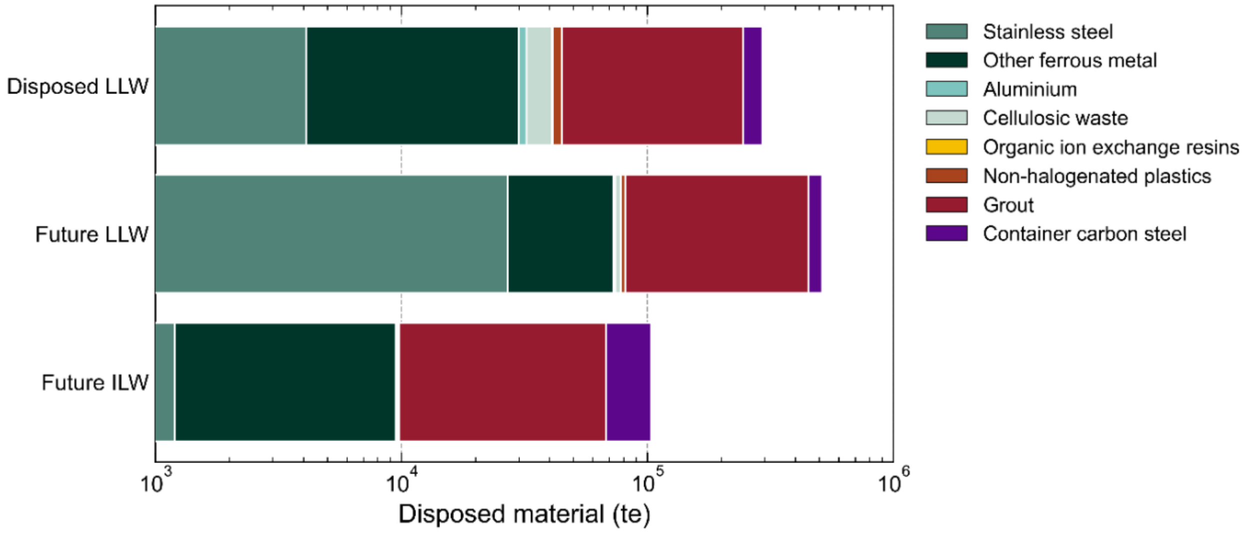

Figure 4.5: Masses of key materials (te) in the disposed LLW and future inventory for LLW and ILW [24]. 'Other ferrous metal' is largely carbon steel

In general, there are proportionately smaller amounts of key reactive waste materials, particularly cellulosic wastes and aluminium, in the ILW than the disposed LLW, when taking the respective waste volumes into account. The difference is small for carbon steel and the ILW has a proportionately greater mass of container steel, because of the smaller disposal containers. The future LLW also has lower aluminium and organic waste content than disposed LLW, but relatively high content of stainless steel and less carbon steel.

These observations suggest that, on the basis of major material composition, there will not be differences in the overall evolution of the vault wastes in future even if ILW is accepted for disposal, although individual containers will inevitably contain different proportions of reactive wastes and grout.

4.5 Contaminant Release Processes

Having discussed the chemical evolution of the near field in the previous two subsections, we now consider the specific features and processes that control the release of the key radionuclides of significance to the groundwater pathway, namely Tc-99, C-14, Cl-36, Tc-99, I-129 and uranium isotopes. This suite of radionuclides includes chemical elements (U, Tc, C) that are chemically reactive and that can exist in a range of species under the chemical conditions of the near field. In contrast, the two halogens (Cl and I) are likely to be present as highly soluble and generally poorly-sorbing monovalent anions. In microporous clay media, Cl and I can be subject to anion exclusion effects, which can enhance mobility. However, in the case of the LLWR, the leachate and contaminant pathways will comprise relatively porous media. Clay is used, in the vault and trench bases for example, to divert water flow, rather than contain contamination.

The features and processes that are important to the release of radionuclides and non-radiological contaminants can be grouped into:

- chemical and physical form of the contaminants;
- mechanisms and processes limiting contaminant release from solids;
- speciation, solubility and sorption effects.

The understanding and evaluation of these processes gained from work supporting the 2011 ESC and advances made by desk studies and research undertaken in support of the ESC is summarised in the following subsections.

4.5.1 Form and Release Processes of Contaminants from LLW

The key contaminants of significance to the LLWR ESC have been determined by consideration of the impact through the groundwater pathway [14], the inventory [4] and previous safety cases, most notably the 2011 ESC [85]. The disposed inventory for the vaults has also been subject to revision since the 2011 ESC. The updated inventory reflects improved understanding of radionuclide and material composition and includes over a decade of additional disposals with better quality and quantity of waste consignment information [4].

Contaminants of interest in the near field include both radionuclides, and stable elements and compounds that are classed as hazardous substances and non-hazardous pollutants. Both types of contaminants may be considered in two categories.

The first category covers radiological and non-radiological species that are bound into a matrix that must degrade or be progressively leached in order for the contaminants to be released into the porewater. This category covers activation products in metals and graphite, and non-radioactive alloying components in steel, for example, chromium, molybdenum and vanadium, as well as contaminants arising from the PFA in the grout, and organic substances present in polymers and plastics such as DEHP (diethylhexyl phthalate). Once released from the matrix, their chemical form will determine their immediate fate. For example, some C-14 may be released from steels and graphite in gaseous form [86]. While C-14-bearing CH_4 has low solubility in water and can escape to the atmosphere, C-14-bearing CO_2 will largely dissolve and then react with grout or other dissolved species. Other contaminants dissolve in the pore solution as they are released from the matrix but their concentration may be limited by solubility, especially under high pH conditions, and also by sorption on grout surfaces, or the soil in the trenches. This category of contaminants can be modelled relatively realistically based on corrosion rates, solubility and sorption parameters specific to the near-field chemical conditions. In quantitative impact assessments, however, more cautious assumptions, such as ‘instantaneous release’, are often used, as discussed in Section 0.

The second category includes contaminants that are assumed to be immediately available to the pore solution. This is a realistic assumption for some contaminants and waste types, for example, surface contamination on a range of materials, where the contaminant is not strongly bonded to the surface. The same assumption is also adopted to account for uncertainty in the physical and chemical form of other contaminants. For example, in considering the behaviour of uranium (U) and technetium (Tc) in the near field, we must account for the fact that the inventory may be spread across many different waste streams in which these radionuclides are in different forms. We do not have sufficient information to model all the variations in detail. Thus, we assume that both metals can dissolve in the porewater to the concentration defined by a solubility-limiting solid phase for the specific chemical conditions. We also take account of their aqueous speciation as these are both redox-sensitive elements.

We have advanced our understanding of the nature of the waste through more detailed consideration of inventory records [4, 87] underpinning research [88, 89, 90, 55] and expert elicitations to characterise specific wastes [56]. As a consequence, there is potential to represent the release of uranium, Tc-99 and C-14 from the wasteform in assessment models. The release processes for the key radionuclides and non-radiological contaminants identified in the ESC and their significance in supporting the ESC, are discussed below.

Uranium

Uranium is present in waste disposed in the trenches and Vault 8 in a variety of chemical and physical forms. However, the majority (approximately 95%) of the inventory comprises residues from uranium metal refining and fuel manufacturing at the Springfields site. Through review of literature dating back to the 1950s [91], it has been possible to develop an understanding of the waste processing practices undertaken at the Springfields site and therefore the nature of the uranium waste disposed within the LLWR trenches. The majority of the Springfields disposals are made up of process residues including:

- filter cake residues of the yellowcake and ore refining process, characterised as insoluble silicate material;
- magnesium and calcium fluoride residues resulting from the reduction of UF_4 to uranium metal.

Information concerning the chemical behaviour of the fluoride residues has been obtained from geochemical interpretation of trench leachate data and a study of analogue fluoride materials (Summary Box 1).

Through routine treatments at Springfields, the residues were subject to an aggressive treatment process, involving leaching in hot concentrated nitric acid, to recover as much uranium as possible before disposal. This treatment process therefore removed the majority of the leachable uranium from the residues, leaving behind only small quantities (around 0.1 to 0.9 wt%) of uranium bound within a fluoride matrix. Experimental leaching studies of analogue fluoride materials [88] (Summary Box 1) indicate that less than half the uranium (0.04 wt% uranium) is present as a soluble residue and that a significant proportion is retained in the poorly soluble fluoride material.

Other notable consignments of uranium-containing waste include [26, 87, 91]:

- disposals to Trench 7 originating from Sellafield operations, where the precise form is unknown, and uranium is thus assumed to be present in a readily leachable form;
- future disposals of uranium hexafluoride (UF_6, “Hex”) cylinders from Capenhurst and Springfields. UF_6 is volatile, reactive and is soluble in water. Thus, it is unlikely that significant quantities of UF_6 would remain after washing of the cylinders. Uranium, however, may be present in the form of surface contamination, resulting from a reaction of UF_6 with the metal surface [81].

There is good evidence from inventory studies [87, 91] and specific research on fluoride residues [88] that uranium release will be limited to an extent by the solid residues in which it is contained, although a significant fraction of the uranium in these materials has been shown to be leachable. Uranium associated with metal wastes comprises surface contamination, which may be readily leached, although subject to anticipated low solubility of uranium under the reducing conditions generated by the corroding metal surface.

There is a range of uranium-containing waste streams in the trenches for which the primary form and release mechanism is more uncertain. This includes metallic uranium, which is likely to oxidise rapidly, as observed in recent characterisation and experimental studies [88]. Collated data and information suggest that uranium release would be limited in instances where the solubility control is lost, for example due to oxidation of the waste. Overall, considering the range of uranium-containing waste streams, we do not consider taking specific account of the effect of a rate-controlled release in models to be justified when the properties of the solid wasteform may limit the release of uranium. Therefore, we represent uranium behaviour in assessment calculations using the concept of solubility and sorption control in the prevailing near-field chemical conditions.

Uranium release from fluoride residues

Trench disposal records indicate that magnesium fluoride residues from uranium metal refining comprise a significant proportion of the U inventory. The residues represent fluoride slags, from the UF_4 reduction process with uranium contents < 0.25 wt% U and which have been acid-milled and acid-treated to recover uranium.

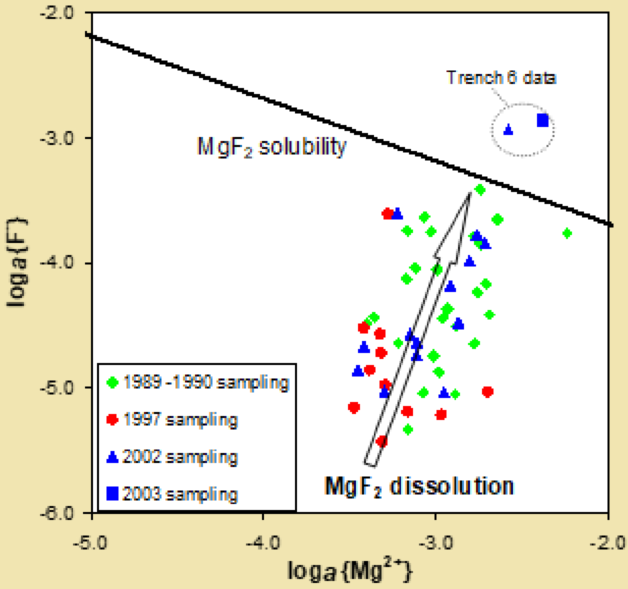

Trench leachate data (left) record elevated concentrations of fluoride and magnesium which are consistent with the dissolution of MgF_2 and its recrystallisation to CaF_2 under the LLWR groundwater conditions. Peak fluoride concentrations occur in samples with highest uranium concentrations. Fluoride concentrations up to 1.6 mg l^{-1} and above groundwater background (> 0.2 mg l^{-1}) are measured in boreholes outside the trench waste region.

Characterisation of analogue samples of raw magnesium slag reveal inclusions of UO_2 enclosed in the fluoride matrix (Fig 1). After reproducing the uranium recovery process uranium is present as sub-micron sized inclusions (Fig 2).

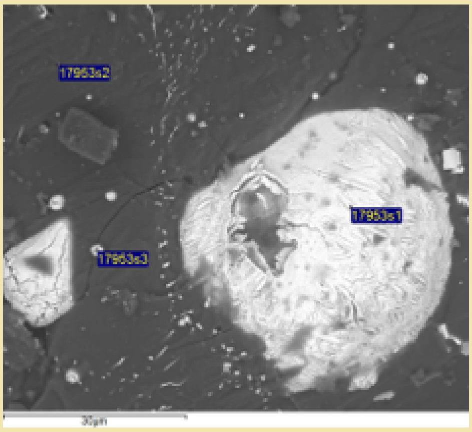

Fig 1. Uranium inclusions in un-treated fluoride

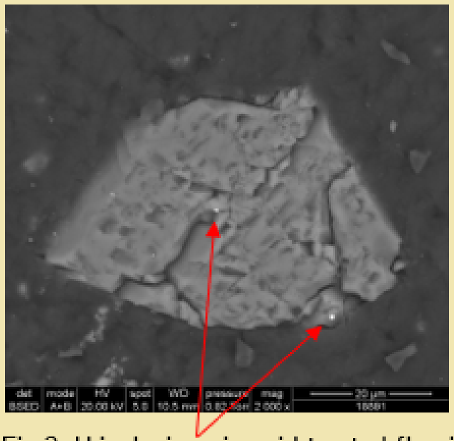

Fig 2. U inclusions in acid-treated fluoride

Leaching experiments of the milled and acid-treated fluoride in deionised water and chloride solutions indicate fluoride solubility comparable to maximum fluoride concentrations in trench leachate and around twice that of MgF_2 mineral phase (sellaite). Uranium data show an easily leached fraction equivalent to around 0.04 wt% uranium. A sample with higher uranium content indicated partial leaching of uranium, with around 0.06 wt% being associated with inclusions in the fluoride. Uranium concentrations of leached fluoride are around 0.4 mg l^{-1} (1.7 10^{-6} mol l^{-1})

Summary Box 1 Nature of uranium fluoride residue in the trenches [20, 88].

Technetium

The fission product Tc-99 is present at low levels in waste streams from the Sellafield site disposed in the trenches and the vaults. The physical and chemical form of Tc in the wastes is not known and Tc is therefore assumed to be present as contamination that would be readily leached on contact with water.

Higher inventories of Tc-99 from Capenhurst occur in Vault 8 wastes and in future disposals. The Tc-bearing wastes in Vault 8 include metal filters from operations at the site. Future arisings comprise Hex cylinders, which are used to store uranium hexafluoride, UF_6, during uranium enrichment. Tc-99 is a metallic by-product of the enrichment of reprocessed uranium that is likely to be present as surface contamination resulting from reaction with the surface of the metal cylinders.

The main Tc-99 inventory is also associated with metallic wastes, where it is present as surface contamination. The reductive chemical mechanism by which Tc-99 contamination accumulates on metal surfaces is likely to limit Tc-99 release under near-field conditions. Under oxidising conditions Tc-99 would be expected to be released, as the more soluble, oxidised Tc(VII) pertechnetate species becomes dominant. The physical nature of the contamination is not expected to limit Tc release, however, and in assessment calculations Tc-99 release is controlled by its solubility under reducing conditions where amorphous Tc(IV) oxide, TcO_2(am), is stable.

Carbon-14

Carbon-14 is a neutron activation product that is present in a range of materials including irradiated metals, graphite and concrete in both LLW and ILW (Table 4.4 and Table 4.5, respectively). C-14 is also present in waste streams comprising ion-exchange resins, cellulosic and soft plastic wastes, where it represents secondary contamination or an effluent residue. C-14 is mainly produced by activation of ppm-level nitrogen impurities and inclusions including air-filled porosity in metals, concrete and graphite. In graphite, however, comparable or greater amounts of C-14 may also result from activation of stable C-13 [90] that comprises 1% of the naturally-occurring carbon isotopes.

Where C-14 is present as a primary activation product, it will be present within the solid material, although its distribution will depend on the distribution of the original N-14 and C-13 and on the irradiation flux and period. For example, for reactor graphite, the type (Magnox or AGR) and operating history of the reactor and the position of the graphite block in the core will determine the radiation dose received but the type of graphite and the manufacturing process will determine the level of original impurities.

In general, the C-14 is found to be distributed uniformly in the graphite, although there is evidence for enrichment of C-14 in carbonaceous deposits on the surfaces of fuel channels in Magnox reactor graphite [92]. This is thought to arise from N_2 adsorbing on the channel surfaces during periodic reactor shutdowns.

Table 4.4: Materials associated with the LLW C-14 inventory [32]

LLW		Total C-14 inventory at disposal (TBq)					
		Graphite	Steel	Organics[1]	Pucks	Slags[2]	Other[3]
Existing and committed disposals	Vault 8	0.1	0.051	0.17	0.094	0	0.076
	Vault 9+9a	0.40	0.018	0.14	0.027	0	0.41
Future disposals	Vault 9+9a	0.68	0.25	0.23	0	0	1.4
	Vault 10	1.13	10.05 [4]	$6.5\ 10^{-6}$	0	0	0.58
	Vault 11	0.59	1.65	0	0	0	0.25
	Vault 12	0.78	0.33	0	0	0	0.44

[1] Organics are mainly organic ion exchange resins.

[2] The slags inventory is small and uncertain and is treated as 'steel' in the assessment.

[3] Other includes soil, rubble, cement/concrete, glass/ceramics, and waste material that is ‘not declared’.

[4] This arises largely from decommissioning and dismantling of Magnox power stations.

There is experimental evidence to indicate that C-14 in graphite is divided into a more strongly bound fraction that results from activation of C-13 present in the graphite crystal structure and a more easily released fraction of adsorbed C-14 resulting from activation of nitrogen gas and carbonaceous deposits [86] [90]. However, the total releasable fraction of C-14 in graphite is small, between about 1% and 5% [86], so that a significant fraction of N_2-derived C-14 must also be bonded into the graphite matrix or trapped in inaccessible porosity.

A significant body of experimental work on irradiated nuclear graphite ([86] and references therein) has determined the pattern of C-14 release from graphite in the presence of an aqueous phase, with an initial fast release followed by a slower but steady release that gradually declines over years. The precise mechanism by which graphite and water interact to cause a release of C-14 has not been determined, and it is unclear whether the water catalyses the release or is involved in reactions with reduced carbon species on the graphite surfaces. Moreover, the experimental Eh and pH conditions only affect the releases insofar as CO_2 dissolves to a greater extent as the pH of the leachant increases [86].

Table 4.5: **Materials associated with the ILW C-14 inventory [32].**

ILW		Total C-14 inventory at disposal (TBq)					
		Graphite	Steel	Organics[1]	Magnox	Al	Other[2]
Future disposals	Vault 9+9a	30.0	1.7	$1.8\ 10^{-6}$	0.10	$3.1\ 10^{-6}$	0.46
	Vault 10	19.9	7.2	$1.7\ 10^{-6}$	0.06	$2.9\ 10^{-6}$	1.66
	Vault 11	0	7.7	0	0	0	0.64
	Vault 12	0	11.3	0	0	0	0

1 Organics are mainly ion exchange resins.

2 Other includes soil, rubble, cement/concrete, glass/ceramics, and waste material that is 'not declared'.

Based on these data, in our assessments, we consider a small component of the C-14, 1% of the releasable fraction, is released rapidly from the graphite [90]. For grouted wastes, this release is assumed to occur during the grouting process and the C-14 to be retain in the grout. A longer-term release rate has also been defined based on the experimental data to account for the remaining C-14 releases [86]. The C-14 is released from graphite mainly as gases, CO_2 predominantly, volatile organic species assumed to be largely CH_4, and minor CO, with a substantial portion of around 30% of the releasable C-14 in the form of small, soluble organic molecules [90].

In metals, C-14 may be generated in carbide inclusions that can subsequently react with water as the metal corrodes to form small organic compounds and gases such as methane [86]. It is likely that C-14 present in irradiated metals will be evenly distributed, unless the metals are particularly thick as neutrons are only attenuated in steels of centimetre-thickness [62]. Rates of release of C-14 from irradiated metals are therefore likely to be controlled by the corrosion process, which will slowly expose C-14 within the metal matrix allowing interaction (diffusion and chemical reaction) with water. Quantification of corrosion-controlled C-14 release rates require data concerning the metal geometry, which is quite uncertain for most LLW. In the assessments, we have made the assumption that activated steels have an average thickness of 10 mm, which is related to the neutron attenuation depth beyond which we would expect the C-14 activity to gradually diminish [93].

Inorganic C-14 (carbonate) can be formed in more oxidised operational conditions and is trapped by anion exchange resins. The category of C-14-bearing materials described as 'Organics' (Table 4.4) largely comprises organic anion exchange resins on which the C-14 is present as inorganic carbonate that is assumed to be readily releasable to water.

There is only a small inventory of C-14 in the trenches (0.1 TBq) but considerable uncertainty about its form and association with waste materials. Recognising this uncertainty, we have chosen to represent the trench C-14 inventory as associated with the same types of materials as in the Vault 8 inventory. That is, the C-14 inventory is assigned to metals, graphite and organics in the same proportion as in the Vault 8 inventory (see Table 4.4) [94]. Pucks, and slags, blasting grit and filters from metal recycling were excluded as such waste treatment practises were not employed at the time of operation of the trenches. The release processes and primary speciation of C-14 are then based on the same understanding used for the assessment of C-14 release in the vaults [46]. The different chemical environment in the trenches is taken into account via the corrosion rate of metals and the fate of the released C-14 species.

Chlorine-36 and Iodine-129

Chlorine-36 is a neutron activation product formed from impurities and inclusions of stable Cl-35 and is found within the solid matrix of irradiated graphite, metals and concrete [56].

In unirradiated graphite, Cl-35 is present in two chemical forms: approximately 70 % is in organic form, bonded with carbon in the matrix, and approximately 30 % in inorganic form as oxychlorine compounds [95]. This suggests that, like C-14, Cl-36 may not be fully released from the graphite matrix. Reference [96] notes that there are few experimental data on Cl-36 leaching for UK graphites. French studies (summarised in reference [97]) are more extensive and leaching experiments suggest that Cl-36 is released at a significantly faster rate than C-14 and that the release is controlled by the saturation and diffusion of water into the porous graphite material. Most importantly, the work reported in reference [98] showed that the graphite chlorine impurity level consistent with the Cl-36 measurements is in the region of a few hundred ppb compared with an initial chlorine content in the non-irradiated graphite of around a few tens of ppm, indicating the significant release of Cl-36 in the reactor. Similar results have been obtained in the UK studies [99]. While some Cl-36 is detected in the coolant gas desiccant, secondary Cl-36 is also observed as a surface contaminant present in metals from reactor coolant circuits. This would be more readily released to the porewater than Cl-36 present in the solid matrix. Following leaching of the graphite or metal with water, Cl-36 is most likely to be in the form of the chloride anion, and transport will not be retarded by sorption processes.

Overall, there is significant uncertainty in the forward LLW Cl-36 inventory as a result of the mobility of Cl-36 and the poor consistency between modelled inventories in ILW graphite and LLW streams from the same reactors. Reference [100] reports an assessment of the treatment of Cl-36 uncertainty in the UKRWI but concluded that that

> *"…for AGRs it is highly unlikely that a significant quantity of any released Cl-36 is currently accounted for in the National Inventory. In the case of Magnox stations, the possibility exists that some or all of the released Cl-36 is accounted for, but the uncertainties are large, and a definitive conclusion is not possible."*

Iodine-129 is a fission product and a significant inventory arises in future disposals from Sellafield, where it occurs in miscellaneous beta-gamma waste, miscellaneous decommissioning waste and general operational waste. I-129 is also forecast to arise from decommissioning activities at the Harwell site. Given that I-129 is a fission product, it is highly probable that this radionuclide will be present as a surface contaminant on a range of waste types. Most of the I-129 inventory is associated with metals, or with slags resulting from waste treatment. The remainder is associated primarily with organic materials, ash resulting from the incineration of organic materials and pucks resulting from the compaction of soft wastes [4].

In the groundwater assessment model, these two chemically unreactive contaminants are represented using the assumption that their inventory is instantaneously released to water and is not solubility limited. For Cl-36, it is considered that this represents a cautious approach and that part of the inventory is likely to be retained in irradiated metals, released only by corrosion processes, and in graphite.

Future waste treatment

Potential innovations in the treatment of LLW, with the aim to reduce consignment volumes to the LLWR, involve the use of technologies such as surface decontamination, metal melting and incineration. Such treatment processes may affect the chemical form of the radionuclides as well as the physical wasteform. Radionuclides will be concentrated in blasting grit, slags, ash, and filter and effluent treatment residues. The residues are expected to require further encapsulation, for example, cementation, to immobilise them during transport and storage.

The overall effects of waste treatment processes on radionuclide behaviour are complicated but, in general, the chemically reactive radionuclides of relevance (C-14, Tc-99 and uranium) may be quite strongly retained in the secondary treatment wastes [89].

Specific consideration of other chemical treatment effluents and reagents will be required. Oxidative treatments, including incineration and chemical decontamination, may result in the formation of higher oxidation states of U and Tc, which have higher solubilities. However, we consider that the prevailing Eh conditions of the near field will control radionuclide solubility. Thermal treatment for graphite is being investigated to reduce the mobile radionuclides, especially C-14. Use of this treatment at scale will require return of the secondary wastes. For C-14, this could be grouted carbonate abatement residues that would provide a suitable wasteform for LLW disposal.

Cl-36, which is retained through the physical properties and nature of the irradiated metals and other bulk materials, may have enhanced mobility in the treatment residues compared to the original metal wastes.

In the assessments, we have taken cautious approaches to evaluating the implications of waste treatment of key waste materials such as metals. In the C-14 gas assessment, for example, it is cautiously assumed that the total future inventory of C-14 associated with metals is returned as LLW when a portion is treated. Slags are treated as (high surface area) metal, on the basis that the C-14 is present as carbides in small metal droplets in the slags, while the blasting grit and filters are treated as 'Other' waste where the C-14 is assumed to be present as inorganic surface contamination [46].

Non-radiological contaminants

The assessment of the impacts of non-radiological contaminants has been updated since the 2011 ESC [31] with the development of the 2018 Hydrological Risk Assessment (HRA) [30]. A new HRA will be presented as part of the 2026 ESC [15].

The 2018 HRA considered a larger range of metals, non-metals and organic contaminants than had been considered previously. In total, the quantitative assessment covered five hazardous substances (arsenic, benzene, lead, mercury and vinyl chloride) and 21 non-hazardous pollutants including 15 metals and 6 non-metals. This list has been further reviewed and extended for the quantitative non-radiological groundwater assessment [101] to include a further six hazardous substances (Cr(VI), benzo(a)pyrene (BAP), styrene, tributyl phosphate (TBP), triphenyl phosphate (TPP) and trixylyl phosphate (TXP)).

The list of non-radiological contaminants considered in the 2026 HRA [15], with their classification, is given in Table 4.6. This is a subset of the contaminants considered in the non-radiological groundwater assessment [101]. A small number of contaminants considered in that assessment have no known inventory, are not expected to be present in declared bulk materials and not present in grout. This means that they have no source term for the HRA [15]. For contaminants with no source-term, but which may have been detected in leachate or site characterisation studies, the results of the non-radiological groundwater assessment are used to calculate a precautionary capacity for future disposals [17].

Some of the contaminants considered in the non-radiological groundwater assessment are organic compounds that may represent mobile degradation products of disposed polymers. Vinyl chloride may be present as unreacted monomer in the polymer (polyvinylchloride, or PVC) and is also a degradation product of chlorinated hydrocarbons [102]. It has been detected in trench leachate and, more recently, in monitoring of volatile organic compounds present landfill gases in the sealed probe holes [103]. In the HRA it is used to represent the range of degradation products of halogenated polymers for which there is less information about inventory or occurrence. Similarly, TBP is used in the HRA to represent the family of organo-phosphate compounds, including TPP and TXP, for which we have no inventory information. Other contaminants are uncommon elements, such as thallium, that may have been detected in leachate and it has been necessary to evaluate their potential impact but they are not included in the HRA [101].

Some of the most common contaminants in the waste may be associated with alloys, such as stainless steel (Fe with Cr, Mo and V), Nimonic (Ni-Cr), Stellite (Co-Cr alloy with W and Mo), composites such as Boral (boron carbide sandwiched between aluminium sheets), but others may be metals, such as Mo and Pb, used in the nuclear industry.

Metals are common constituents of natural mineral phases (for example, Al, Fe, Mg and U) and occur widely in groundwater at concentrations that reflect the local hydrogeochemical conditions [104]. In the repository, they will be influenced by the prevailing chemical conditions (pH and Eh) which control their solubility. For example, elevated concentrations of Mg relative to local groundwater that have been measured in trench leachate are likely to be related to the dissolution of magnesium fluoride residues [91] [88]. Fluoride in trench leachate attains concentrations of around 35 mg l^{-1}, which is consistent with dissolution of fluoride materials in wastes from the Springfields site [88]. The fluoride residues may also contain soluble sources of other metals such as Fe, U and Zn [91].

Metal contaminants such as Cr and Mn are expected to have low solubility when released by steel corrosion in their reduced form under the reducing conditions. Observations in trench leachate monitoring of higher concentrations might also be associated with disposed chemical reagents (e.g. chromate and permanganate) in the trench wastes.

Table 4.6: Classification of non-radiological contaminants considered in the HRA [15]

Classification	Pollutant
Non-hazardous	Aluminium Antimony Barium Beryllium Boron Cadmium Chromium(III) Cobalt Copper Iron Magnesium Molybdenum Nickel Selenium Tin Titanium Uranium Vanadium Zinc Phenol Ammonium Fluoride Phosphate
Hazardous	Arsenic Chromium(VI) Lead Mercury BAP Benzene TBP Vinyl Chloride

4.5.2 Speciation and Solubility of Key Radionuclides

The chemical speciation of radionuclides under the chemical conditions that develop in the LLWR trench and vault regions can be an important control on the release and mobility of radionuclides in groundwater and gas. The principal radioelements of significance to the ESC which are influenced by chemical speciation under the conditions that may develop in the LLWR near field are:

- carbon
- uranium
- technetium.

C-14 is potentially of radiological significance in terms of impacts from both the gas and groundwater pathways. There is a substantial inventory of stable carbon, which is fundamental to a number of biogeochemical processes that determine the chemical evolution of the trench near field but is less important for the grouted wastes in the vaults. In both the vaults and trenches, however, C-14 species resulting from primary release from the waste materials will be subject to further processes that will determine the chemical speciation and partitioning to solid, liquid and gas phases.

In the trenches, C-14 is likely to follow the evolution of the stable carbon components, so microbial processes may metabolise the dissolved fraction of the C-14 and form dissolved organic species, such as acetate, as well as CH_4 gas. The reaction with other electron donors, such as hydrogen generated by corrosion and electron acceptors, such as sulphate and Fe(III) will affect the proportion of organic carbon and CH_4 gas. The dissolved inorganic fraction may form CO_2 gas, dissolved carbonate and carbonate minerals depending on the pH both in the close vicinity of the C-14 waste and in the wider region of the near field through which dissolved C-14 species may migrate.

The fate of C-14 in the vaults depends on whether it is retained in the grouted wastes or can migrate to the voids between container stacks. The high pH within the grouted wastes is likely to restrict microbial utilisation of the small organic molecules or CO_2 so that the latter is retained in the form of solid carbonate minerals and the former can diffuse out of the waste once the container is perforated. We cautiously assume that all primary gaseous organic C-14 species, mainly CH_4, are lost immediately to a mobile gas phase that transports the C-14 to the biosphere where it is oxidised in the soil layer to CO_2 that can be taken up by plants. Once dissolved C-14 species are lost by diffusion or advection in infiltrating water from the waste into the gaps, this hydrogen-rich, lower pH, environment may support microbial activity that metabolises the C-14, generating gaseous species. In general, we assume that microbial activity in the gaps will result in further CH_4 generation (Subsection 5.2.1). It is possible, however, that locally higher pH, for example due to significant interaction of infiltrating water with the grout or lack of nutrients, limits this microbial activity so that the dissolved C-14 species are substantially lost to the groundwater.

The oxidation state of uranium and technetium will control their speciation and solubility. For both radionuclides, the lower oxidation states U(IV) and Tc(IV), generally have lower solubilities than U(VI) and Tc(VII). Under the reducing conditions that pertain in both the vaults and the trenches, U(IV) and Tc(IV) are expected to be their stable forms for the whole period until coastal erosion affects the repository. The oxidation state and speciation of radionuclide species may also influence processes of precipitation and dissolution in secondary phases, sorption and uptake by colloidal particles (see Subsection 4.5.4), and diffusion in the grout.

Aqueous speciation is influenced by temperature and pressure and by various compositional factors including:

- pH
- redox potential (Eh)
- ionic strength
- complexing ligands (see Subsection 4.5.4).

Aqueous chemical speciation and radionuclide solubility can be described by equilibrium thermodynamic models and comprehensive thermodynamic databases are available for both uranium and technetium [105, 106]. A chemical speciation model is included in the PFLOTRAN near-field models, using the ThermoChimie geochemical database (Version 12a) [107, 108] which enables the solubility controls over uranium and technetium to be examined as the chemical conditions of the LLWR near field evolve. Additional solubility and speciation calculations were undertaken for the 2011 ESC to examine and understand effects such as complexation by ligands, including carbonate present in groundwater, and acetate and fluoride present in trench leachate [53]. Expert elicitation was used for the 2011 ESC [56] to identify ranges and distributions for the solubilities of uranium and technetium for use in probabilistic assessment calculations and these have been reviewed and revised for the higher pH conditions in the vaults [109].

As noted above, uranium and technetium solubility are both affected by oxidation state; however, variation in solubility as a consequence of changes in near-field chemistry is of most significance to uranium. The inventory of uranium, if expressed as a concentration in porewater, is several orders of magnitude above U(IV) solubility limits in most regions of the trenches and vaults. In contrast, it is likely that Tc-99 could only exceed solubility limits where there is above average concentration of Tc in disposals to the vaults combined with lower pH conditions. Besides solubility, technetium speciation will have an important influence on its sorption on the grout since it can be present as various anionic forms that sorb poorly.

The speciation and solubility of Tc is less complex than that of uranium and, in the pH range of interest to the 2011 ESC (pH 5 to pH 11), Tc(IV) speciation was considered to be dominated by the $TcO(OH)_2$ species and the TcO_2(am) solid phase controlled solubility at around 10^{-8} M [110]. For the higher pH 12.5 to 13 in the vaults, we have considered the solubility and speciation based on the ThermoChimie v10a thermodynamic database [107]. The results are consistent with the elicited values for Tc(IV) at the lower pH but, above pH 11, the more likely solubility-limiting phase is $TcO_2{:}1.63H_2O(s)$, and the solubility at pH 13 increases to about 10^{-7} M as the anionic species $TcO(OH)_3^-$ dominates the solution [111].

Several solid phases have the potential to control the solubility of uranium under the pH and Eh conditions that are expected to develop in the trenches and vaults. UO_2(am) is considered to represent the chemical form of much of the uranium present in the trenches at the time of disposal; this phase has been identified by X-ray diffraction during characterisation of fluoride residues [88]. UO_2(am) has a solubility of around 10^{-8} M under the pH and Eh conditions of the trenches and this is consistent with measured concentrations of uranium in trench leachate [91]. The strongly reducing conditions developed in the vaults are controlled mainly by iron corrosion and not the microbial reactions occurring under the near-neutral conditions of the trenches. The stability of the U(VI) phase $CaUO_4$ is, however, enhanced under the alkaline and reducing conditions of the cement-buffered vaults so that its presence cannot be excluded (Figure 4.6). Its solubility at pH 13 is lower than under neutral pH and comparable to, or lower than, that of UO_2(am) (around 10^{-8} M). Thus, the potential variation in uranium solubility for the vaults is likely to be lower than for the trenches and may depend more on the pH than the Eh.

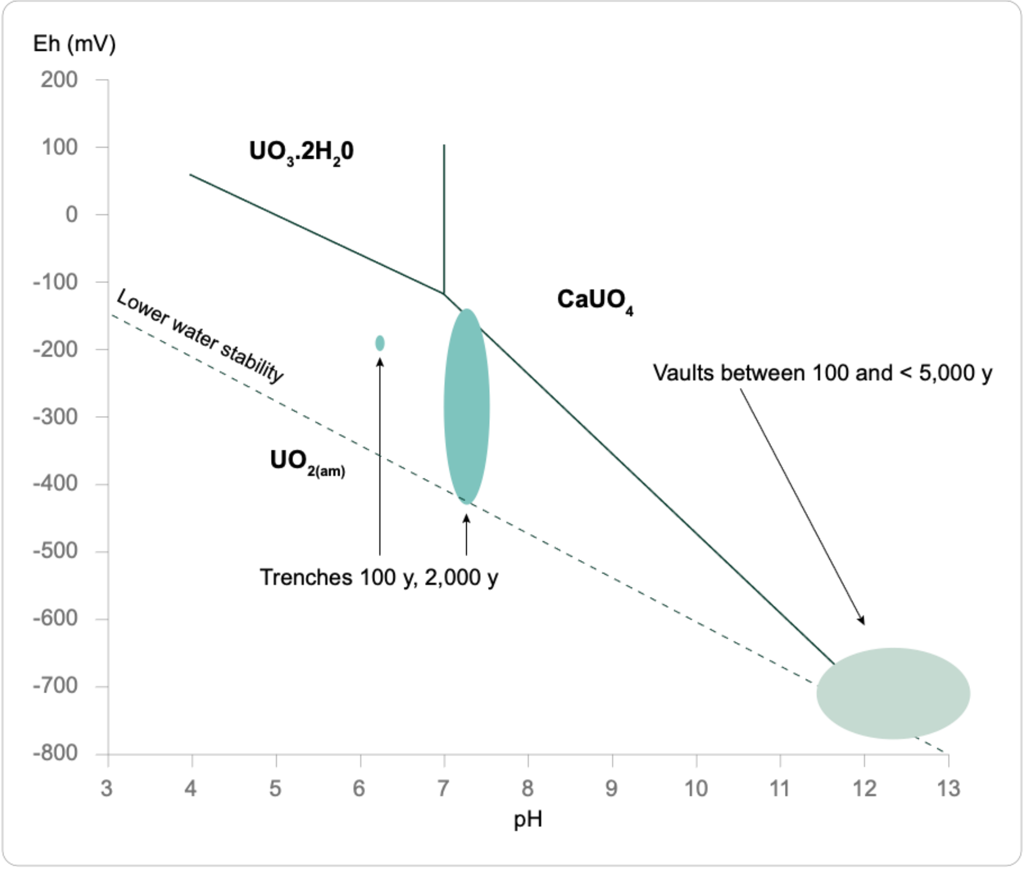

Figure 4.6: Pourbaix (Eh-pH) diagram showing the stability fields of U(IV) and U(VI) phases and the conditions in the trenches and vaults

ThermoChimie includes several U(IV) oxide phases, representing different stages between amorphous and crystalline forms, as well as some mixed U(IV) / U(VI) phases, each of which gives different solubility limits. Assuming the solubility-limit phase is $UO_2{:}2H_2O(am)$, a solubility of ~3 10^{-9} M is calculated for pH 11 and Eh -650 mV [43], which is comparable to the value for U(IV) solubility in the vaults of 10^{-8} M that was elicited for the 2011 ESC [56]. Increased pH, reflecting the high grout pH conditions, has little effect on the U(IV) solubility, consistent with the conclusions of a more recent elicitation [112] that also suggested a value of around 10^{-8} M for U(IV) under pH 13 to 13.5 conditions.

4.5.3 Near-Field Sorption Processes

Following release of contaminants from the primary waste materials, and in regions of the near field where contaminant concentrations are below the solubility of discrete solid phases, sorption processes may control the mobility of radionuclides and other contaminants within the near field. Sorption processes may be specific to:

- the chemical properties of the contaminant,
- the solid sorption substrate, and

- the prevailing chemical conditions.

The principal solid phases that have the potential to act as substrates for sorption in the trenches and vaults were recognised by the 2002 PCSC [58] as:

- soil present as disposed contaminated waste, and also in the trenches as backfill and firebreaks. Drigg soil contains a variety of potentially sorbing mineral surfaces including clay minerals and poorly crystalline iron and aluminium oxides;
- metallic corrosion products comprising oxides, hydroxides and carbonates formed by corrosion of mainly steel waste, and, for the vaults, steel containers;
- plastic and cellulosic wastes and their solid degradation products including living and dead biomass and resulting solid humus;
- disposed inorganic and mineral wastes, including building rubble, concrete and sand. Primary mineral surfaces are likely to consist of silicate and carbonate phases of variable grain size;
- cementitious grout used exclusively in the vaults.

The degree to which each of these substrates may retard contaminant migration will depend on a number of factors, including the affinity each contaminant has for sorption onto the specific substrate and the amount of each substrate in the transport path.

There are large uncertainties in these effects for some of the substrates listed, thus, in the assessment models we follow the precedent set by earlier work and take a cautious approach that considers only:

- sorption onto soil present in the trenches;
- sorption onto the grout present in the vault wasteform.

The neglect of sorption onto corrosion products is acknowledged to be very cautious for the vaults in light of the focusing of infiltrating water into the unsaturated gaps between stacks, where slow flows will largely be over the corroding surface of the steel containers (Subsection 3.4.1). Even so, it is difficult to argue that all contaminants will be exposed to corroding steel surfaces, and a cautious approach is preferred.

Sorption measurements, expressed in the form of a sorption distribution coefficient (K_d, or R_d[7]) for specific radionuclides, have previously been made on representative soils and cementitious materials. Sorption data used in the 2002 PCSC near-field models were derived from these site-specific studies for sorption under appropriate near-field leachate conditions or, in the absence of such site-specific data, from generic data compilations. A shortcoming recognised [58] for both the LLWR site-specific data and the generic data was that it was obtained predominantly under oxic conditions. This introduces some uncertainty

---

[7] R_d refers to a measured sorption distribution ratio which may not represent the equilibrium distribution (K_d).

for redox-sensitive elements, such as the actinides, which may be present in their more reduced form at specific times during the biogeochemical evolution of the near field.

Since 2002, therefore, we have undertaken specific studies of uranium sorption onto grout, soils and corrosion products under anaerobic conditions. These experiments suggest that sorption of uranium under reducing conditions is not distinguishable from sorption under oxidising conditions [113].

For the 2011 ESC, site-specific sorption data and generic sorption data (including data for sorption under cementitious conditions) were considered and the K_ds reviewed using an expert elicitation process [56]. On the basis of this experimental study [113], the U(IV) data were considered applicable to U(VI) sorption under oxidising conditions [56].

In preparation for the 2026 ESC, we have reviewed all of the sorption data used previously, including for both radiological and non-radiological contaminants in the trenches, vaults, and the underlying geological units included in the groundwater assessment [114, 115]. The sorption parameter dataset has been extended to include consideration of the higher pH conditions in the vaults [109], as well as a larger number of radionuclides, to account for the ILW inventory, and the extended suite of non-radiological contaminants [116] (Table 4.6). As far as possible, the K_ds have been described in the form of a pdf (probability density function) in order that they can be used in the probabilistic groundwater assessment cases.

4.5.4 Significance of Colloids and Complexants

Colloids and complexants have the potential to enhance the release of contaminants from the near field and increase their mobility in groundwater.

Colloids are particles with diameter between 1 µm and 1 nm, which are suspended in an aqueous solution. In the context of a disposal assessment, they could comprise radioelement particles/aggregates forming homogeneous colloids (so called 'intrinsic' colloids) and inorganic and organic materials, such as clays, metal oxides, soil humic materials and suspended microbes, upon which radionuclides can sorb, forming heterogeneous colloids ('pseudo-colloids'). Pseudo-colloids may be present in the natural environment or may be produced from waste and engineering materials.

Complexants generally refer to soluble organic ligands, which may be present in consigned waste or may be generated by chemical processes in the near field. Complexants can also include simple common anions such as chloride and carbonate present in groundwater.

Colloid studies for the LLWR

Colloid studies at the LLWR have involved extensive field investigations (1999–2002) into the presence, characteristics, and radioactivity of colloids [117, 118, 119, 120]. A recent review has summarised the outcomes of these studies [121]. The studies found some radioactivity associated with small colloids in the trench near field, but none with geosphere colloids, even in areas marked by high tritium indicating releases of contamination from the trenches. Experimental work indicated that colloids generated in the near field may not be stable when migrating to the more aerobic geosphere, suggesting they do not significantly affect radionuclide transport from the trenches.

The Environmental Monitoring Programme supports these findings, with recent groundwater monitoring showing no notable association between radioactivity and colloid fractions [122]. A 2020 review recommended continued monitoring using improved filtration [123]. Further sampling and analyses carried out since the review have confirmed that colloids present in groundwater are not linked to detectable radioactivity [40], providing more evidence that colloids are not important for contaminant transport from the trenches.

Further planned monitoring, especially following infrastructure upgrades (e.g., membrane replacements and final cap installation), will deliver further long-term insight into colloid behaviour.

For the vaults, current evaluation of colloid impact is limited by lack of leachate that has been in contact with grouted wastes. We have applied a ‘colloid ladder’ conceptual assessment [124], in which a series of sequential questions about colloid stability, mobility, and radionuclide association are used to determine the likely significance of colloids [121]. The early high pH conditions in the grouted wastes suggest that colloids are unlikely to be stable [125], and long periods with dry gaps between stacks of containers means that they will not be mobile in the vaults. Grout pore sizes further inhibit colloid mobility within the waste [47], and releases of dissolved or colloidal contaminants from the wastes are expected to be extremely limited before cap geomembrane failure allows increased infiltration.

Iron-based colloids formed from corroding external container walls are not expected to enhance contaminant release, given that radionuclides would have already been released from the wastes before encountering such colloids. Any potential for colloid-facilitated transport to the geosphere would anyway occur only after geomembrane failure and increased infiltration, which is expected on a similar timescale to disruption of the vaults by coastal erosion.

Overall, evidence and conceptual arguments strongly suggest that colloids are not significant in enhancing contaminant release from the trench or vault near fields. Furthermore, if stable vault-derived colloids do reach the geosphere, their main impact could be to reduce effective sorption, a factor considered in the groundwater pathway assessment [126].

Complexants of relevance to the LLWR

Complexants are soluble ligands capable of dominating the aqueous speciation of radionuclides and other contaminants. Formation of complexes can reduce sorption and increase solubility, thereby potentially enhancing mobility of contaminants. Key types of complexants include common anions such as chloride and carbonate, though these are of minor significance at natural groundwater concentrations, and a range of organic compounds, notably those used in decontamination processes (e.g., citric acid, EDTA) which can be significant even at low concentrations.

Complexants can also interact with sorption processes; for example, uranyl carbonate species can sorb onto static surfaces [127], while some ligands like phosphates may lower solubility of uranium by forming less soluble solid phases [128]. For example, modelling of trench conditions suggests that uranyl fluoride complexes could dominate at fluoride concentrations comparable to maximum observed monitoring values (around 10^{-3} mol l^{-1} [91]). The effect of the uranyl fluoride complexation, or the potential precipitation of the solid phase $UOF_2.2H_2O$, may result in an overall lowering of U(VI) solubility compared to UO_2(am) solubility in the absence of fluoride [53].

In determining sorption coefficients for safety assessments, the effects of common anions are included through supporting speciation calculations. More importantly for the quantitative assessments, we also need to account for the potential impacts of two specific types of waste-derived complexants:

- EDTA, a decontaminant that is disposed in the wastes, particularly from Sellafield, is taken to be representative of the family of similar amino-polycarboxylic acids [129];
- ISA, a cellulose degradation product under the pH 12.5 to 13 conditions (see Subsection 4.3.2).

The impacts of these complexants are integrated into assessments using two quantitative factors [79]:

- Solubility Enhancement Factor (SEF): The ratio of contaminant solubility in the presence versus absence of a complexant. SEF > 1 indicates increased solubility.
- Sorption Reduction Factor (SRF): The ratio of the K_d in the absence of the contaminant and the K_d in the presence of the complexant. SRF > 1 indicates reduced sorption.

Both SEF and SRF depend on chemical conditions, especially complexant concentration, and can be informed by experimental studies and speciation modelling. For EDTA, concentrations in trenches are based on leachate measurements whereas, for vaults, historic disposals are used [130, 131]. ISA concentrations are modelled based on cellulose content, the kinetics of ISA formation, ISA sorption onto grout, and precipitation as calcium isosaccharinate, with significant variations expected between vaults due to differing proportions of cellulose and grouts [79].

This approach, using correction factors to account for organic complexation, has become well established in international safety assessment practice since its development (see [79] and references therein).

Superplasticisers, used as additives in grouts to improve flow and penetration of the waste, have also raised concerns due to their surfactant properties, which could theoretically increase radionuclide mobility [132, 133]. However, experimental evidence shows these molecules are not easily released from the cement matrix [134]. While they may enhance solubility in free solutions, they do not have a measurable effect in expressed porewaters or leachates from intact or crushed grout. In light of these results, and the expectation that contaminant transport from the grout will largely be diffusion-dominated, with minimal degradation of the grout in the period before coastal erosion disrupts the vaults, we do not consider any effect of superplasticiser complexation on contaminant mobility in the assessments.

In summary, organic and inorganic complexants are a key consideration in the assessment of contaminant mobility at the LLWR, with their impacts quantitatively incorporated using SEFs and SRFs. While waste-derived complexants like EDTA and ISA may be significant, the effect of superplasticisers is negligible under site-relevant conditions.

5 Gas Generation

This section considers the processes involved in the generation of gases, both the bulk gas phase in the repository and radioactive gases as a precursor to the discussion of gas modelling (Section 7) and assessment of radiological impacts (Subsection 8.2).

Our understanding of gas generation processes has been developed and validated through consideration of monitoring data (see Subsection 4.2.1). For the trenches, routine gas monitoring is undertaken to measure the rate of gas flow from sample locations in the cap and surrounding area and in the drains. Landfill gases CH_4, H_2, CO_2 and O_2 are monitored on a monthly or quarterly basis [8], along with common chemotoxic species. Rn-222 is measured using probes within the trenches and in Vault 8. Gas samples have also been analysed to determine the C-14 content of CH_4 and CO_2 gases collected from selected sampling locations in the trenches [40].

Monitoring of sealed probe holes for toxic trace components of the landfill gas has also been carried out as part of the triennial enhanced monitoring programme since 2015 [103]. These trace components, including volatile organic compounds, acetaldehyde, formaldehyde, arsenic and mercury, may arise from volatilisation of materials in the waste or can be formed through biochemical reactions associated with degradation processes. In a typical municipal landfill, these trace components may make up less than one percent of the volume of the gas emitted from the waste. However, the impact of some trace gases on human health and the environment may be more significant than that of bulk landfill gases [135].

Hydrogen sulphide and ammonia are the most important chemotoxic gases that are likely to be generated under the anaerobic conditions present in the trenches and also in the vaults where microbial activity can occur. Both are highly soluble and reactive, however, and we do not consider that a significant volume will be released as gas. Older monitoring data from leachate in the sealed trench probe holes show low levels of dissolved sulphide (generally less than 100 µg dm^{-3}). Ammonia was previously (pre-2012) detected in monitoring of the probe holes, at levels of a few tens of mg dm^{-3}, but more recent measurements of trench leachate are less than 1 mg dm^{-3} [34]. These measurements all indicate that gaseous H_2S and ammonia are not present in significant volumes, nor likely to be in future. Some quantitative assessment was carried out previously [136] and this is discussed further in Subsection 7.4.

Significant concentrations of toxic trace components for which analysis is carried out have been found in the landfill gas at some locations. The very low bulk gas flux from the trenches means, however, that all instances are classified as an 'insignificant emission' [103]. Although, some of the detected volatile substances arise from the waste inventory, for example styrene and vinyl chloride from polymers, others such as toluene may result from historic activities on the site [103].

Assessment of the radiological impact of gases released from the LLWR near field includes the tritium, carbon-14-bearing gases and radon-222 [13, 14].

Tritium has the potential to be transported in gas, either as radioactive hydrogen (^3HH), as tritiated water vapour (^3HOH), or possibly as tritiated methane ($^3HCH_3$). The half-life of tritium (12.35 years) is sufficiently short that most of the inventory will decay during operation of the LLWR and it is only considered in the assessment of site safety during the PoA [13].

Radon (Rn-222) also has a very short half-life (3.825 days), but it is generated continuously from decay of its parent, Ra-226 (half-life 1.6 10^3 years). Ra-226 may either be present in the wastes or may be formed from decay of U-238 (half-life 4.5 10^9 years) and its shorter-lived progeny, such as U-234 (half-life 2.4 10^5 years). Due to its short half-life, Rn-222 may decay to sufficiently low levels during its migration out of the repository from where it is generated in the waste that it will not cause a significant radiological risk. Generation of bulk gases from the wastes and container materials in the near field may, however, affect Rn-222 migration through the cap [46], and Rn-222 concentrations are of significance to human intrusion [14].

Carbon-14-bearing gases have been examined in detail in the ESC [13, 14] because of the future inventory of C-14 and the complex chemical and biological interactions of C-14 in the near field and biosphere. C-14 can be present in gaseous form as CO_2 or CH_4 but can also be partitioned between the aqueous phase, solid minerals and the gas phase depending on the local chemical environment.

The generation of the bulk non-radioactive gases (H_2, CO_2 and CH_4) is discussed in the following subsection. The significance of the effect that bulk gas generation has on the release of gaseous C-14, tritium and Rn-222 is then discussed in Subsection 5.2.

5.1 Processes of Gas Generation from Waste

Processes of gas generation from LLW are intimately linked with the biogeochemical and corrosion processes that control the chemical evolution of waste. There are two primary gas generation sources that we consider:

- organic materials, which may generate mainly CO_2 and also CH_4, when microbial activity is involved, and
- anaerobic corrosion of metals, such as steel, which generates H_2.

The differences in chemical conditions and, particularly, microbial activity between the trenches and the vaults discussed in Subsections 4.2 and 4.3, respectively, results in a corresponding difference in the importance of these sources.

Considering the low activity of LLW, radiolytic generation of gases from degradation of wastes and from radiolysis of water is regarded as insignificant compared to the above processes. Studies of C-14 gaseous release from higher activity wastes [137] have also considered the generation of methane and other light hydrocarbons from reaction of carbides present in metals. In terms of the bulk gas generation rate, the amount of hydrocarbon gas generated from carbide will be insignificant compared to the volume that would be generated by anaerobic corrosion and organic degradation processes. However, we recognise that carbide inclusions in irradiated metals may represent a significant source of C-14 in irradiated waste metals, that result in formation of C-14-bearing gases (Subsection 5.2.1).

In the case of the trench near-field environment, the two main processes of gas generation from wastes are expected to be closely interlinked [138] (Figure 5.1) and all three main gases (H_2, CO_2 and CH_4) may be both generated and consumed by microbial processes. Other minor gases that may also result from the suite of microbiological processes include N_2 and NH_3 generated by denitrification processes, and H_2S generated by sulphate reduction. As noted above, H_2S and NH_3 are soluble, and these gases will represent a very low partial pressure of an evolved gas phase. Hydrogen may also be generated by fermentative processes, but overall H_2 will tend to be consumed by the microbial processes occurring during LLW degradation [138].

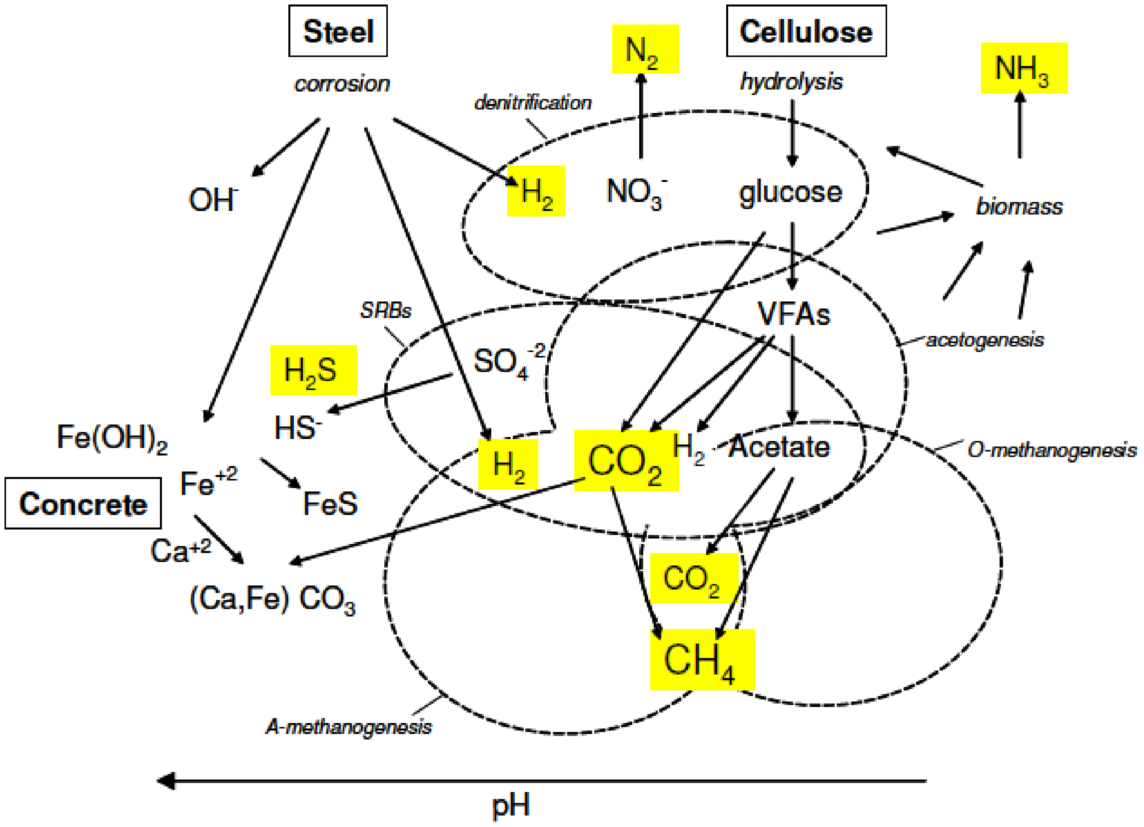

Gases are highlighted in yellow, VFAs: volatile fatty acids, SRBs: sulphate-reducing bacteria.

Figure 5.1: Conceptual model of gas-generating processes from LLW, after reference [138]

In the grout-conditioned porewater in the vault wastes, microbial activity will be strongly restricted so that the generation of CO_2 and CH_4 from organic materials will generally not occur. Anaerobic corrosion of metals will take place at rates significantly different from those in the trench environment. For some metals, such as steels, the high pH will slow corrosion and the generation of hydrogen. For reactive metals, such as aluminium, corrosion is enhanced by the high pH as the surface oxide film is no longer stable enough to protect the metal as it does at near-neutral pH [55].

5.1.1 Generation of hydrogen by corrosion

The generation of H_2 by the anaerobic corrosion of metal is a comparatively simple process that could produce a H_2-rich gas in accumulations of metal waste. In the trenches, it is of prime importance in providing an electron donor for microbial processes including methanogenesis.

Metal corrosion produces hydrogen gas by reaction with water. For the less reactive metals (for example, steel), hydrogen is produced only under anaerobic conditions in the absence of oxygen. Initially most wastes will be in contact with air; steel simply oxidises under aerobic conditions without production of gas. The overall reaction, which will involve steps in which iron hydroxides are formed, in the presence of water, may be approximated by:

$4Fe + 3O_2 \rightarrow 2Fe_2O_3$

This aerobic process, along with aerobic microbiological processes, will consume available oxygen.

Under anaerobic conditions, steel corrosion proceeds by reaction with water. The reaction may be approximately described by conversion to magnetite:

$3Fe + 4H_2O \rightarrow Fe_3O_4 + 4H_2$

Additionally, other corrosion products may be formed, including Fe(II) hydroxide, Fe(II) sulphide and Fe(II)-containing carbonates. All these reactions will liberate H_2 gas.

Experimental studies of gas generation from waste degradation experiments undertaken at the LLWR in support of the 2002 PCSC [58] show low levels of H_2 generated from metal containing simulated LLW. Gas data from the long-term trench experiment indicate that CH_4 is the dominant gas generated. In smaller-scale experiments [139], hydrogen is detected and analyses indicate that a cumulative volume of between 0.2 and 0.9 cm^3 of H_2 was measured compared to substantially higher volumes of between 20 and 40 litres of CH_4 and between 4 and 10 litres of CO_2 generated over a 2,000 day experimental period. In these experiments, H_2 ceased to be detected after around 400 days. Similarly, a study of gas generation from a large scale LLW gas generation experiment at the VLJ Repository, Finland recorded low levels of H_2, considered to be from anaerobic corrosion, during an initial phase of degradation [138].

These experiments indicate that, while the anaerobic corrosion process has the potential to generate H_2 gas, in the presence of electron donors such as sulphate and Fe(III) present in LLW in the trenches, the generated H_2 may be consumed by microbial processes.

5.1.2 Organic sources and microbial control of gas generation

Microbes will mediate the breakdown of many organic materials with the ultimate production of mainly CO_2 and CH_4 gases. At the LLWR, there are several classes of organic materials that could be broken down in this way: cellulosic materials; plastics and rubbers; ion-exchange resins; solvents; oils; and radioactively-labelled molecules. We have followed the approach of the 2002 PCSC [58] and the 2011 ESC [53] in considering only cellulosic materials in models of gas generation. Other organic materials, such as PVC (polyvinyl chloride, present more commonly as soft thin plastic waste than the rigid form) and polystyrene (ion exchange resin beads), are considered to be too recalcitrant and slow to degrade under the low temperature and low irradiation conditions of the LLWR to contribute significantly to gas production [140].

The first step in the microbial degradation of cellulose is its conversion (hydrolysis) into soluble intermediates (for example, glucose), which are then consumed by a complex set of microbial populations. One or other of the microbial populations will be favoured depending on the prevailing geochemical conditions, particularly in the presence of electron acceptors such as oxygen, nitrate, ferric iron and sulphate. Recognising that the dominant population of microbes will switch from aerobic bacteria, to nitrate-reducing bacteria, to iron(III) reducing, sulphate-reducing, and finally to fermentative and methanogenic organisms as conditions become more reducing, the sequence of major gases produced under increasingly reducing conditions are:

- CO_2 under aerobic conditions;
- CO_2 and N_2 in the presence of nitrate (denitrification);
- CO_2 and Fe(II) (solids) in the presence of Fe(III) minerals (iron reduction);
- CO_2 and sulphide (solids) in the presence of sulphate (sulphate reduction);
- CO_2 and CH_4 (methanogenesis);
- H_2 generated by fermentation processes.

In practice, some of these processes will occur simultaneously as a result of the development of localised chemical environments.

The growth of bacteria is driven by the availability of energy sources (electron donors and acceptors) present in the waste. Growth is also affected by environmental conditions and competition between certain populations, for example, sulphate-reducing bacteria (SRBs) may dominate over methanogens [141]. Hydrogen as well as reduced carbon compounds (for example, glucose, acetate and volatile fatty acids) may be utilised as an electron donor by the main terminal electron accepting processes of sulphate and iron reduction and by methanogenesis. The anaerobic corrosion process discussed above provides the main source of H_2 for hydrogen-consuming processes, although acidogenenic microbes may produce H_2 and contribute to a consortium of microbial groups, which co-exist. Autotrophic H_2 consuming organisms may not require a source of organic carbon and can utilise inorganic carbon for biomass growth [142, 76].

Trench monitoring studies have routinely monitored the composition of gases evolved from the wastes through gas vent probes installed in the interim trench cap [8] (e.g. Figure 4.1).

The gas monitoring data confirms the significant content of CH_4 and CO_2 in trench gases and the trace levels of hydrogen may indicate hydrogen consumption by reaction with electron acceptors. In addition, C-14 has also been detected associated with CH_4 and CO_2 gases [40].

5.1.3 Secondary processes affecting generated gases

Once the main gases (H_2, CO_2 and CH_4) have been generated, they may be subject to further chemical and microbiological processes. The case of H_2 consumption as an electron donor has been discussed above, since it is viewed as being integral to the overall biogeochemical processes occurring within localised regions of waste, for example, within compacted waste pucks.

Both CO_2 and CH_4 have the potential to react within the near field during their migration in the gas phase:

- CO_2, being soluble, has the potential to dissolve and react in the aqueous phase and may also react directly with cementitious materials (carbonation);
- CH_4 could be subject to oxidation in more aerobic regions of the near field, such as during its migration through the cap.

Carbonation is the process by which CO_2[8] penetrates a cementitious material and reacts with the calcium-rich cement hydration products, such as calcium hydroxide ($Ca(OH)_2$) and calcium silicate hydrates (CSH), to form calcite ($CaCO_3$). Carbonation may be accompanied by modifications of the microstructure (i.e. clogging of pores) and the water content (i.e. release of chemically-bound water). In the grout, the long-term porewater pH is dependent on the presence of the CSH (Subsection 4.3), so the effect of carbonation is a reduction in the ability of the grout to maintain a high porewater pH.

Carbonation is an important process for the vault wasteform because it is presumed that any C-14-bearing CO_2 generated from the waste will tend to react with the grout and therefore be retained within the near field. The initially high pH conditions in the grout mean that microbial degradation of cellulosic waste will be limited and alkaline hydrolysis more important. This process, however, does not give rise to CO_2, unlike microbial degradation. As a result, much less bulk CO_2 will be produced from cellulosic wastes. In turn, this will result in less carbonation of the grout by bulk CO_2 and increase the retention of C-14-bearing CO_2, released abiotically by graphite and other wastes, in the grout.

We recognise, as described in Subsection 4.4, that some cellulosic wastes may evolve in isolation from the grout porewater, for example, in compacted pucks, so that microbial degradation may be possible, resulting in CO_2 generation and localised carbonation of the grout in the vicinity of the puck. However, considering the excess grout present in most containers and the reaction of CO_2 with corrosion products, there would be adequate capacity to absorb generated CO_2 (Subsection 4.4) [81, 72]. Consequently, we anticipate

---

[8] Dissolved inorganic carbon, in the form of carbonate or bicarbonate species, may also cause carbonation by reaction with cements and grouts in a saturated system.

that little CO_2 will be released from the vaults. We recognise that it is conceivable that there are circumstances where incomplete reaction of CO_2 could occur, depending on the gas transport pathways through the vault wasteform and vault stacks, but this would be a localised effect.

Methane oxidation is a process recognised in municipal waste landfill sites and is considered in estimating overall methane generation rates from such facilities [143, 144]. Methane oxidation may occur as a consequence of oxygen diffusion through the cap. Nitrate and sulphate present in water infiltrating through the unsaturated regions of the cap may, potentially, also provide an electron acceptor for methane oxidation. In terms of the C-14 gas assessment [46] the complete oxidation of methane in the biosphere (for example, in the soil zone) is a cautious assumption since uptake of C-14 by plants is in the form of inorganic carbon. However, in order to be transported to the soil zone, C-14 must be present as CH_4 rather than CO_2, which can dissolve in water and react during transport to the biosphere. While it is possible that methane oxidation might occur in more oxidised regions of the near field, we have taken the more cautious approach of ignoring this process except in the biosphere.

5.2 Implications for Gaseous Radionuclide Release

5.2.1 Carbon-14

Assessments for the previous environmental safety cases [58, 145] have demonstrated that, of the gaseous radionuclides, C-14 is of primary interest. This is because of the expected future inventory and the influence of the physical and chemical processes occurring in the wastes and vault wasteform. C-14 may be present in the form of both CO_2 and CH_4, which are the main carbon-bearing bulk gases that will be generated from the trench and vault wastes. Small amounts of C-14-bearing carbon monoxide (CO) may be released from graphite and steel [86] but are not expected to be stable in the near field and are treated as methane in the gas assessment [46].

C-14 is present in the LLWR inventory in a variety of wastes (Table 4.4). The primary C-14 release processes from these materials (Subsection 4.5.2) will determine initial C-14 speciation and releases to the aqueous and gas phases, but biogeochemical processes and the local chemical conditions, particularly pH, will then affect the partitioning of the remaining C-14 between solid mineral phases, dissolved species and further gaseous CO_2 or CH_4.

Given the experimental and site evidence for the role of microbiological processes in controlling the speciation and reactions of stable carbon in the trenches, we consider that C-14 will undergo similar chemical reactions. The effect of isotopic fractionation is recognised as a minor effect, which may produce a slight enrichment of the heavier isotope in solid carbonate phases, where these precipitate, and a corresponding depletion of C-14 content in microbially-generated CH_4 gas [146]. Some C-14 in the trenches is present in irradiated metals and graphite that will initially generate only small quantities of C-14-bearing gas. The remaining C-14 released to porewater as dissolved inorganic and organic species from these wastes is, however, likely to undergo further microbial reaction to produce C-14-bearing gases.

Cellulose wastes will be the source of larger quantities of gas including both CH_4 and CO_2. C-14 present as surface contamination on cellulose wastes can be released to the porewater and involved in reactions that are not dependent on cellulose degradation. The form and fate of such C-14 is uncertain, however, and the gas assessment cautiously assumes that all C-14 in the trenches is released to the biosphere as gas, but the release rates are determined by the waste material, that is metal, graphite or organic wastes [46] [94].

Within the vaults, the high pH environment in the grouted wastes will affect the release of gaseous C-14 by restricting the microbial degradation of cellulosic waste, thus limiting the formation of CO_2 and CH_4 in favour of dissolved cellulose degradation products (e.g., ISA), and also by the reaction between C-14-bearing CO_2 and the grout. Even for graphite, for which CO_2 is the dominant form of C-14 released, the only releases to the biosphere will initially come from the small fraction of CH_4 (Subsection 4.5.2). As the dissolved organic molecules are released from the wastes into the gaps between containers, the lower pH in this environment may allow microbial degradation to produce additional gaseous C-14 releases in the form of both CH_4 and CO_2. In the hydrogen-rich atmosphere in the gaps, C-14-bearing CO_2 could potentially undergo further microbial reaction to CH_4.

We therefore expect that gaseous C-14 release from the cementitious vaults will be as a methane-rich gas resulting from the combination of abiotic C-14 release processes from the various wastes together with the effect of reactions with grout removing CO_2, and later microbial processes occurring outside the waste containers. We recognise that carbonation might not result in complete reaction of C-14-bearing CO_2 with grout within the container. We do not consider that there is sufficient evidence for the potential oxidation of CH_4 in aerobic regions of the cap, which might reduce the flux of C-14-bearing gas.

With this understanding of C-14 behaviour, based on the behaviour and generation of stable carbon bulk gases, together with inventory data (Table 4.4 and Table 4.5, Subsection 4.5.1) we expect that the primary control on the gaseous release will be the specific activity of C-14 in the primary wastes and the rate of release of C-14 from the wastes, especially graphite and activated metals.

5.2.2 Tritium and Radon

Tritium present in the form of H_2 gas[9] is considered to have little radiological impact, since release of this gas from the trenches is unlikely on the timescale of interest, given the potential biogeochemical reactions that may consume H_2 gas and hence tritium. In both the trenches and vaults, tritium present in water vapour and methane might be transported in gases generated by the main gas-generating processes, linked to corrosion and the degradation of organic matter.

---

[9] This is the form of tritium in Betalight disposals to the trenches, which comprise the most significant tritium waste stream [26].

The short half-life of tritium limits the radiological impact of tritium to the operational period and its impact is considered in the PoA [13].

Radon gas will not be directly associated with bulk gas generation, but its radiological impact can be affected by the proximity of Ra-226 and uranium-containing wastes to gas-generating wastes such as cellulosic wastes and metals. The radiological assessment of radon release has considered inhalation of radon by a representative individual who inhabits a building constructed upon the cap, into which radon migrates [14, 46].

An important effect controlling the radon concentration in the building is the decay of Rn-222 that occurs as it migrates from the waste and through the cap, as a consequence of its short half-life (3.8 days). Rn-222 concentrations in the open air above the trenches are close to background [40]. Rn-222 monitoring data from the trench probe holes have been used along with the distribution of Ra-226 in the trenches to estimate the ratio of radon released from the wastes to that produced by decay of the local inventory of Ra-226 [147]. This ratio of released Rn-222 to generated Rn-222 is termed the radon emanation factor. The data suggested a range in emanation factor of 7% to 15%, that is between 85% and 93% of the radon decays before release to the monitoring point. However, there is some bias in the data because the trench inventory information is uncertain, and there is a short travel distance between the source (Ra-226 in the waste) and the monitoring point (detector in the probe hole), in which radioactive decay can occur. In the vault wastes, we expect that the grouted wasteform and presence of the steel container will have an even greater effect in terms of allowing decay before escape from the container. Consequently, we have used the upper value as the emanation factor for the trench wastes and the lower value for the vaults in the assessment for radon gas [46].

Assessment of the Rn-222 release from the trenches and the vaults has considered the processes affecting gas migration through the cap [46]. The cap design includes a gravel gas collection layer and a gas vent (Figure 2.8) to control gas migration following capping and during the remaining period of authorisation (PoA). The design of the gas vent and the gas management arrangements have not been subject to optimisation and it is not yet clear whether the vent would be closed at the end of the PoA. To account for this uncertainty, the radon gas assessment considers the case where the gas vent is left open following release of the site [46].

The human intrusion assessment includes consideration of the effect of intrusion into the cap, including construction of a building with a deep basement, which might act as a conduit through which radon could migrate into the house [14].

6 Modelling of Near-field Evolution

6.1 Modelling of the Near Field with PFLOTRAN

This section is concerned with the modelling we undertake to understand how contaminants could be transported through the near field and out of the repository. We make use of the concepts of reactive transport in porous media, which have been the subject of several journal articles and textbooks (e.g. [148] and references therein). We use the output of the near-field models to underpin the assessment calculations conducted using GoldSim models [126, 14], for example, in developing the conceptual model for the groundwater assessment, but the near-field model results are not used by the assessment models directly.

Many of the near-field materials are porous media through which both water, including any dissolved contaminants, and gas can flow. The key contaminant transport processes within the near field are advection, which refers to the transport of a contaminant by the bulk movement of a fluid, and diffusion, which is the movement of contaminants in a fluid from areas of high concentration to areas of low concentration. The fluid may be water or gas, since both can carry contaminants. From the perspective of the ESC, however, the candidates for transport in a gas are limited to radioactive gases such as radon and radionuclides that can form gaseous species, such as C-14-bearing methane or tritiated water (^{3}HHO). Chemotoxic gases, such as hydrogen sulphide, are not of concern (see Section 5).

In the discussion of the evolution of the trench and vault wastes, we have focussed on the changes to transport properties. Advection and diffusion will be influenced by the permeability and porosity of the various materials. For example, we expect that the trenches will retain sufficient porosity even after surcharging and settlement that advection will be the main transport mechanism for the release of dissolved contaminants to the groundwater. In contrast, the grout will be largely impermeable to infiltrating water until it is cracked. Contaminant release will depend on slow diffusion through the grout to flowing water, either in these cracks or, once there is sufficient corrosion in the container walls, in the gaps between container stacks. It is important to note that even when cracked, there will be no flows through the grout until it is fully saturated. Before this point, the capillary suction of the grout will draw water into the matrix, resulting in only transient water in cracks.

We have chosen to focus our modelling efforts on the vaults where the changes since 2011 are significant and thoroughgoing. In contrast, our understanding of the trenches has not changed. We do not expect that the lower infiltration rates following capping, nor the different composition of the infiltrating water, will significantly affect the chemical and physical evolution of these wastes. Instead, for evolution of pH and Eh in the trenches, we have relied on the work carried out for the 2011 ESC [20, 53].

6.2 Scope of the Near-field Modelling with PFLOTRAN

PFLOTRAN

A key tool for developing near-field understanding, and particularly contaminant transport, is the modelling of the repository system. For the 2011 ESC, the General Repository Model (GRM) [53] was used to represent the vaults and trenches and model the biogeochemical processes occurring. The GRM made use of a flow field calculated with the Compartment Flow Model (CFM) [57]. For the 2026 ESC, we have developed models using the PFLOTRAN software [149] [150].

The choice of PFLOTRAN was made after review of potentially suitable software products that have the capability to simulate both chemical processes and transport in the partially and variably saturated near field [151].

PFLOTRAN is an open source, state-of-the-art massively parallel subsurface flow and reactive transport code developed over about 25 years [150]. It has been supported by the United States' Department of Energy and National Laboratories and is approved for use on the Waste Isolation Pilot Plant safety assessment, biogeochemical modelling for the Hanford site and studies in support of spent fuel disposal in the US. Internationally, it is also widely used by waste management organisations for modelling of both repository near-field and geosphere, as well as by other research organisations and universities working in diverse fields from CO_2 storage, geothermal energy, groundwater quality and more (see the publications page of the PFLOTRAN website [150] for a more extensive list). As a result of this support, the PFLOTRAN software is both thoroughly verified and well maintained.

ThermoChimie

At the same time as changing to PFLOTRAN, we adopted the ThermoChimie thermodynamic database [107] as development and maintenance of the database is carried out by a consortium of waste management organisations led by ANDRA and including RWM (now NWS). Initially, ThermoChimie versions 10a and 11a were used for the PFLOTRAN modelling but, as the database has been updated, we have moved to version 12a (issued August 2023). We have updated to the latest version 13a (issued September 2025) for the most recent calculations, but not all older calculations have been re-run because of the need to progress documentation and reporting for the 2026 ESC.

Requirements for the modelling

We use the PFLOTRAN models to provide understanding to underpin the assessment calculations conducted using GoldSim models [14, 126].

Using PFLOTRAN, we have developed models at a range of scales, from single container to the whole repository, in order to be able to use appropriate levels of discretisation for the processes we are interested in. This approach addresses concerns about ensuring appropriate discretisation of the system noted by the Environment Agency in their review of the 2011 ESC (ESC-FI-016 [152]).

The PFLOTRAN models were applied to simulate the development of unsaturated conditions in the repository, the ingress of water through the repository cap and its movement through the repository. Further, the PFLOTRAN models were used to investigate the degradation of both cellulosic and metallic wastes within the vaults, and the evolution of chemical conditions, which is coupled to the transport of chemical species through the system.

Parameterisation

The PFLOTRAN software allows us to represent chemistry and transport in unsaturated porous media, but in order to do so, the appropriate parameters to describe the various porous materials are required including:

- the host rock immediately surrounding the repository;
- the soils which are present as cover for the trench wastes;
- the granular material used as profile fill over the trenches and vaults;
- the structural concrete slabs and walls which are present in the vaults; and
- the grout which surrounds the wastes inside the containers.

The derivation of parameters is described in references [43] and [51] but the key points are:

- In the trenches, the wastes will be relatively permeable and the rate at which water will trickle down through the wastes and then into the geosphere is largely determined by the rate at which water will infiltrate the geomembrane and BES layer of the final cap.
- For the wastes in the vaults, the cap will exert similar control but with the difference that the gaps between the stacks of containers will be much more permeable than the grout surrounding the wastes, and so water will tend to flow down through the gaps rather than through the wasteforms.

Thus, while there are uncertainties associated with the unsaturated flow properties of the various near-field materials at the LLWR, those uncertainties have relatively minor implications for the pattern of water and gas flows through the near field.

In the rest of this section, we give the key results from the PFLOTRAN modelling. The full modelling programme is reported in references [51] and [43], where the earlier development and testing of the models is also described.

6.2.1 Improvements to the Conceptual Models since 2011

The near-field models build on work for the 2011 ESC [20], but there have been developments in our understanding of some of the processes and of the rates at which they are expected to occur.

The key changes are to:

- the representation of fluid flows and variably saturated conditions beneath the cap;
- the rate of infiltration through the cap, as well as the infiltrating water chemistry; and

- the rate of steel corrosion.

The 2011 ESC represented the repository using a two-dimensional areal model in which only the flows of liquid water were computed, although each grid cell did have a connection to the overlying atmosphere. Once the wastes in a grid cell had been consumed, the grid cell re-oxidised. In contrast, with PFLOTRAN the models of the repository are three-dimensional, on various length scales, and solve the full set of equations for water and gas flows coupled to the evolution of partially saturated conditions.

A change common to both trenches and vaults is that the final cap is expected to provide more of a barrier to infiltration than has previously been assumed (Subsection 3.2.1). This means that there will be a period, lasting for one to two thousand years, during which the waste degradation reactions will consume water faster than it can be replaced by infiltration. An implication of this timescale for dry conditions is that coastal erosion may have begun to disrupt the repository before infiltration through the cap is great enough to create a saturated zone at the base of the vaults and for there to be releases of leachate to groundwater.

In the PFLOTRAN models, the evolving chemistry of the infiltrating water is derived from a geochemical model of rainwater percolating through the BES layer in the final cap (Table 6.1) [71]. This chemistry is initially more alkaline and less oxidising than the LLWR "reference" groundwater which was used in the 2011 ESC.

Table 6.1: Major element composition of rainwater and infiltration (at 11 °C) at three representative times for the mean infiltration rate (Table 3.1) [153]. LLWR reference groundwater [154] shown for comparison

	Rainwater	Model			Reference groundwater
Year		2080	3500	7000	
pH	6.86	7.72	9.52	9.09	7.33
pe	4	-3.48	4.72	10.39	2.87
Concentration (mol kg_w^{-1})					
Ca	$1.00\ 10^{-5}$	$9.93\ 10^{-3}$	$3.31\ 10^{-5}$	$6.79\ 10^{-5}$	$2.08\ 10^{-3}$
Na	$5.10\ 10^{-4}$	$1.93\ 10^{-1}$	$4.06\ 10^{-3}$	$5.09\ 10^{-4}$	$1.28\ 10^{-3}$
K	$2.00\ 10^{-5}$	$1.25\ 10^{-3}$	$4.38\ 10^{-5}$	$2.19\ 10^{-5}$	$8.20\ 10^{-5}$
CO_3	$1.00\ 10^{-5}$	$2.29\ 10^{-3}$	$2.24\ 10^{-3}$	$1.00\ 10^{-5}$	$5.35\ 10^{-3}$
SO_4	$4.00\ 10^{-5}$	$8.98\ 10^{-2}$	$4.93\ 10^{-4}$	$4.00\ 10^{-5}$	$3.96\ 10^{-4}$

Recent reviews of the rates of waste degradation suggest that the degradation rate of cellulose should be slightly faster than previously assumed [52], whereas the corrosion rates of mild and stainless steel should be slower [55, 77]. Acidic conditions are predicted to develop in the trenches because of the production of acetate and carbon dioxide associated with the degradation of cellulose by microbial processes. The faster degradation rate of cellulose means that acidic conditions in the trenches will persist for only a few hundred years, which is more consistent with landfill experience (Subsection 6.4).

In the case of the vaults, additional changes have been to recognise:

- The dual permeability nature of the stacks of grouted waste packages in the vaults will influence the flows. Water will flow through the highly permeable gaps between the HHISO containers in preference to through the low permeability grouted wastes (Subsection 3.4.1).
- The grouted wastes will be conditioned to a higher pH (i.e. greater than pH 13 at 11 °C) than was assumed in the 2011 ESC (i.e. pH 11).

Both changes have important implications for the vault performance. Thus:

- if water flows through the gaps and not the grouted wastes, then contaminants must diffuse to the gaps before they can be advected; and
- if the pH is greater than pH 12, then microbial activity will be inhibited [76], which means that cellulose will degrade very slowly to form isosaccharinic acid (ISA), with important consequences for the solubilities of some radionuclides (e.g. plutonium).

In addition, recognition of higher pH within the grouted wastes and lower pH in the gaps between container stacks has required re-elicitation of corrosion rates for the key waste metals [77] and for the carbon steel of the containers [55].

6.3 Geometrical Models

We have developed a set of geometrical models, with a range of length scales, to simulate various regions of the repository from package-scale to site-scale [43]. We justify this approach by noting that a site-scale model alone would either be computationally expensive to run or would use a relatively small number of grid blocks to represent the whole repository, in which case it would omit some details.

Furthermore, a consequence of the expected long-lived unsaturated conditions in the vaults (Subsection 3.5) and flow largely confined to gaps between stacks is that containers and stacks of containers will evolve in isolation for a long period. This has led to our emphasis on container- and stack-scale near-field models to examine chemical evolution, and the potential for heterogeneous evolution, in detail.

The set of geometrical models comprise a site-scale model (Figure 6.1), vault-scale models (Figure 6.2), column models representing a stack of six HHISO containers (Figure 6.3 and Figure 6.4), and single package-scale models [43, 51].

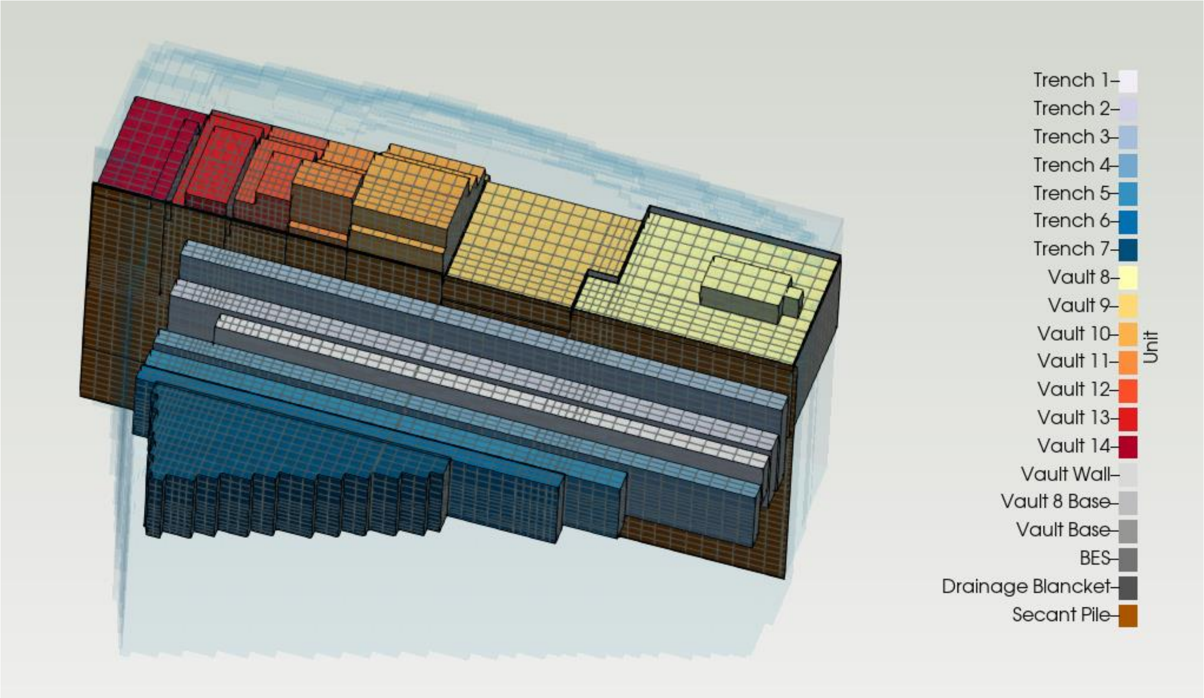

Figure 6.1: **Oblique view of the site-scale model showing the grid blocks colour-coded according to the repository component they represent [51]**

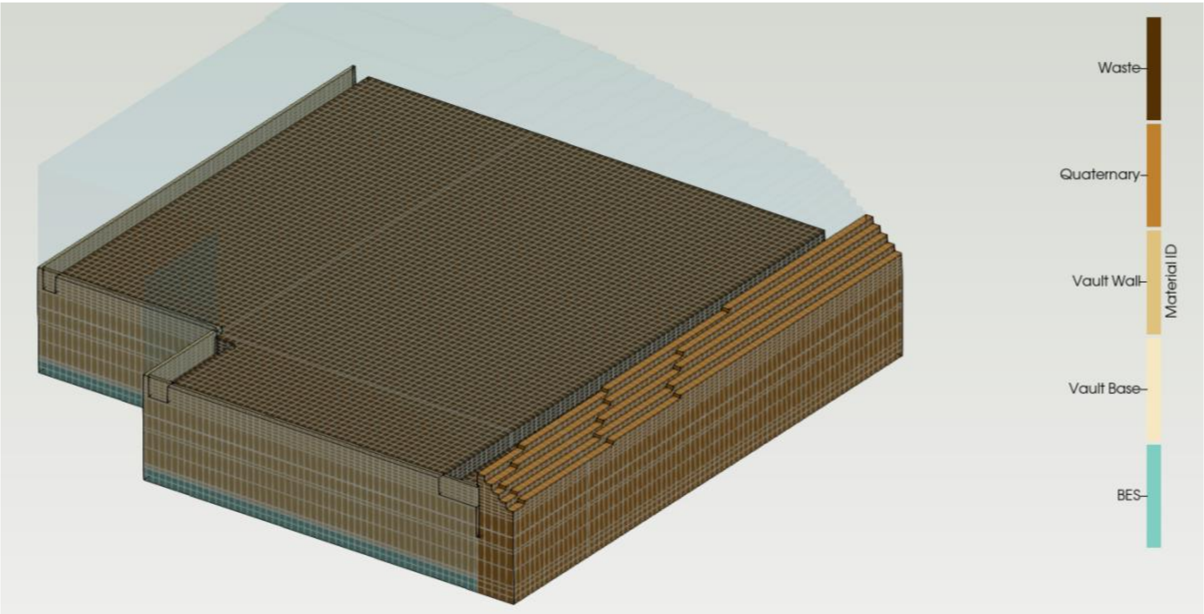

Figure 6.2: **Oblique view of the Vault 9 model grid with Vault 8 (not shown) adjacent to the wall in the left foreground and the trenches beyond the secant pile wall at the back left. Vault 9a is obscured by the representation of the external geology on the right [51]**

A modelling challenge for the site-scale-and vault-scale models is how to represent a very large number of HHISO containers. In order to optimise the running of the models, we have used a MINC (Multiple INteracting Continua) representation to model processes inside the waste containers [43]. This representation has its origins in work to simulate processes in fractured rocks and splits each grid block into a nested sequence of layers. The first layer corresponds to the gaps between the containers, while each of the other layers, five in our case, represents a shell of the grouted waste.

Figure 6.3 illustrates the model for a stack of containers using the MINC representation.

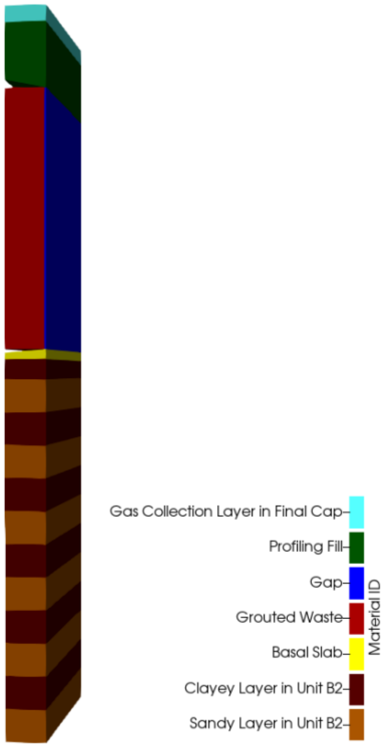

Figure 6.3: Components of the stack-scale MINC model showing schematically that the grid blocks are connected vertically via the gap [43]

The MINC method is computationally efficient, allowing sufficient detail to be represented in the larger-scale models, but means that the presence of the steel containers is neglected. In general, we expect this to be a cautious representation as it neglects any barrier function of the container in minimising contact between waste and infiltrating water. To ensure we understand the implications of this, we have also modelled single containers and stacks of containers using an explicit representation Figure 6.4 [43]. The explicit model also allows us to consider 'failed' containers, that is we can represent the presence of containers that have holes, for example, due to corrosion, in the side panels allowing contact between the grout and water flowing in the gaps. We can vary the total area and number of the holes to investigate the effect on contaminant release [51].

The explicit representation provides a more flexible model that can be used to investigate aspects such as the performance of the containers as a near-field barrier. To this end, some simulations examined the impact of perforations, caused by corrosion, on contaminant transport. Additionally, using two independent models at the package and stack scale provides a useful cross-check and allows comparisons between results from the different representations.

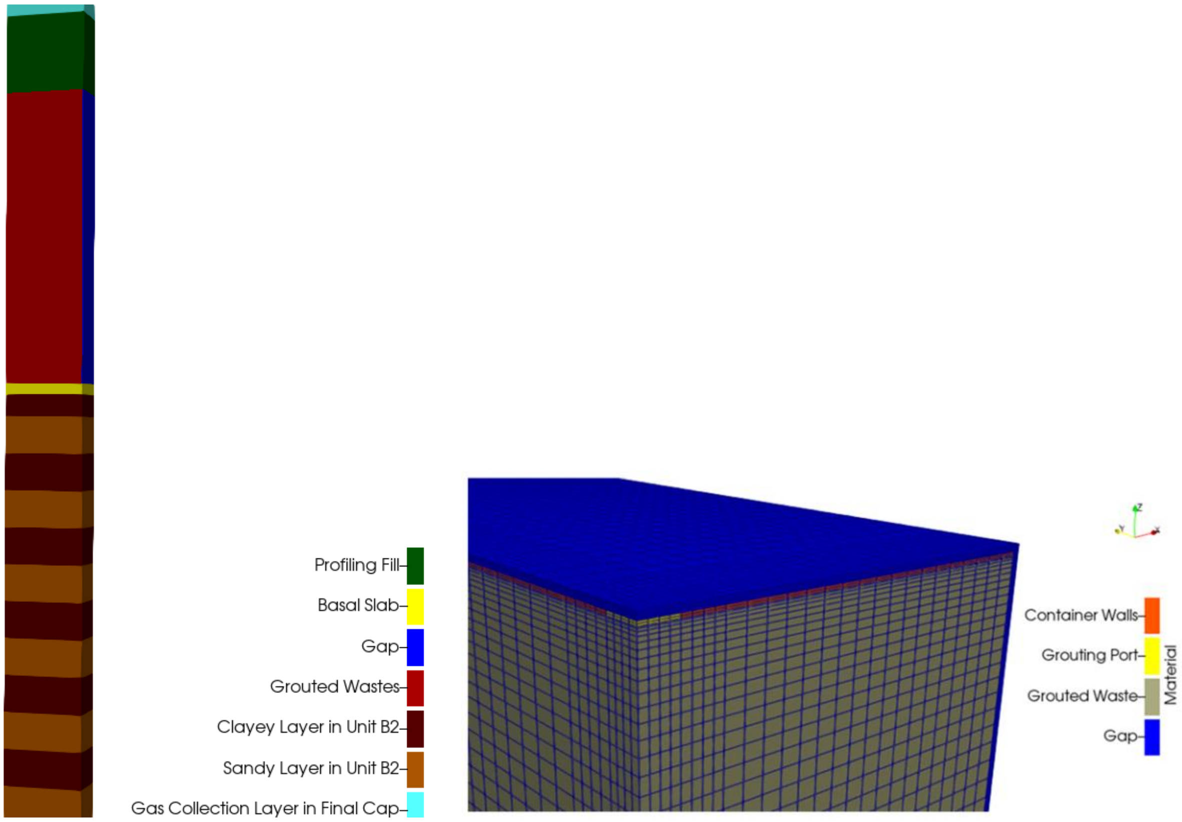

Figure 6.4: **Left: explicit representation of a stack of containers analogous to the MINC model shown in Figure 6.3. Right: detail of the 3-D grid for an explicit representation of a single container with steel walls and a grouting port at the centre of the lid [43]. Many of the explicit models utilise a 2-D cylindrical geometry**

Boundary conditions

In the site-scale model, the bottom boundary condition is based on understanding derived from groundwater flow models of the area [6], which predict that the regional groundwater flow will maintain saturated conditions and relatively constant pressures at a depth of about ten metres below the repository. The boundary condition at the top of the model makes use of an estimate of the evolving rate of infiltration through the cap [48], together with assumptions about the infiltrating water chemistry based on the modelled interaction of rainwater with some of the minerals in the cap (Table 6.1). The sides of the model coincide with the cut-off walls and are assumed to be no-flow boundaries.

For the smaller-scale models, the infiltration through the top boundary is the same as the site-scale model but is scaled for a vault or a stack of containers as appropriate,

6.4 Trenches

The trenches hold a variety of wastes, of which the bulk materials that are expected to influence the near-field conditions most significantly are cellulose and steels. This is partly because of their large inventory and partly because of their reactivity. As a part of the disposal process, the wastes were mixed with soil, which included carbonate minerals such as calcite ($CaCO_3$) and siderite ($FeCO_3$); these minerals are also expected to contribute to the behaviour of the near field.

The near-field conditions in the trenches are important because they will affect the migration of some radionuclides, such as Tc-99 and uranium, as well as some non-radiological contaminants.

6.4.1 Trench Flows and Saturations

The trenches at the LLWR are mostly constructed within the Quaternary deposits. Within this host geology, the flow of water is generally downwards, driven by the difference between the water level and the head in the underlying regional groundwater.

Once the final cap has been put in place, infiltration reduces and, at early times, is much lower than hydrologically effective rainfall. Consequently, water will drain downwards in the region covered by the cap, including from the profile fill which could initially have a significant saturation. The installation of the renewed interim membrane over the southern trenches will have a similar effect in the immediate future.

The downward flow is determined by (a) the water level and (b) the vertical hydraulic conductivity of the underlying geology. The latter is controlled by the clayey layers in the Quaternary deposits, and possibly by the bentonite which was rotavated into some areas of the trench bases. As a result of the water draining downwards, the saturation of the trenches decreases. This was observed in the period following emplacement of the interim cap (Subsection 4.2.1) and further decreases are expected following emplacement of the more effective final cap.

Meanwhile, corrosion of the steel wastes in the trenches consumes oxygen. After a short time, predicted to be of the order of a year or less [155], most of the oxygen beneath the cap is depleted, and thereafter corrosion continues under anaerobic conditions. Anaerobic corrosion of steel is slower than aerobic corrosion and consumes water.

Figure 6.5 compares the rate of infiltration with the rate at which the corrosion reactions consume water. It shows that corrosion of the steel wastes in the trenches will take up all the infiltration, from the point when conditions become anaerobic until the geomembrane in the final cap starts to degrade.

Throughout this period, the trenches remain unsaturated, although the PFLOTRAN model suggests that conditions will be sufficiently humid for cellulose to degrade and metals to corrode at rates which are not much limited by the availability of water. The reason the system does not become even more dry is that water and water vapour are drawn up from the model's bottom boundary, where it is assumed that the regional groundwater flow in the B2 unit will supply whatever water is needed. In reality water may also be drawn laterally from the surrounding sediments, including potentially through the cut-off wall as it degrades over time (see Subsection 3.5.1).

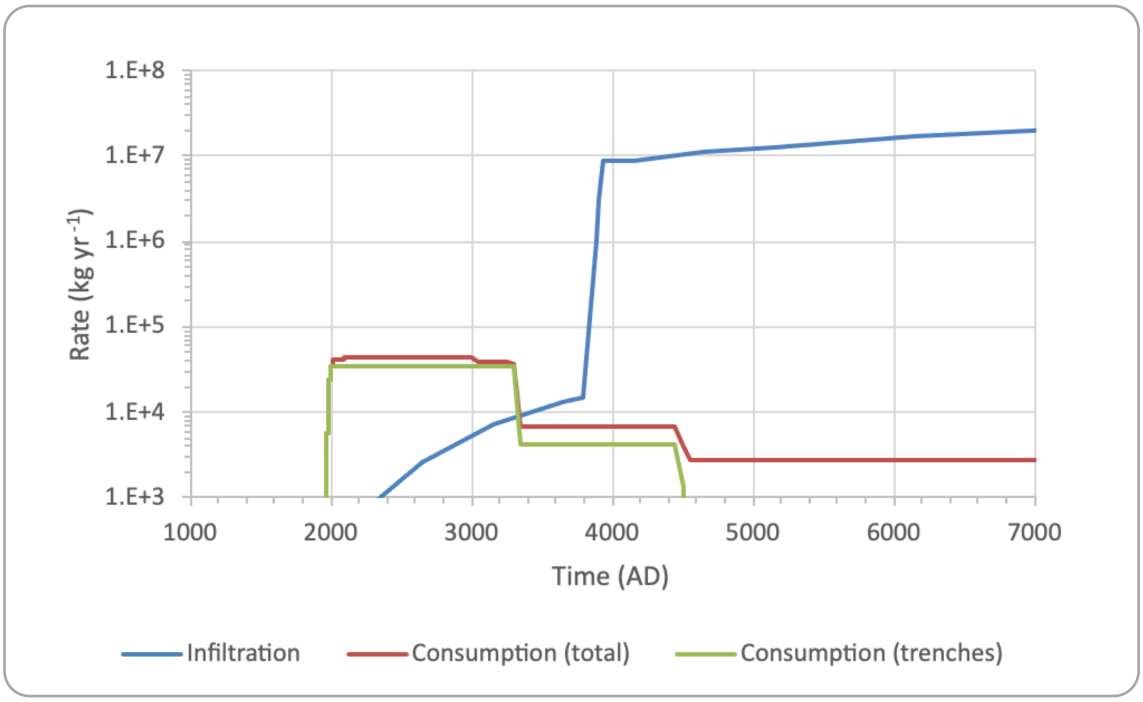

Figure 6.5: **Rate of water infiltration through the whole area of the final cap compared with the rate of water consumption by the metal wastes that are disposed of in the whole repository and in just the trenches. The dominant sink of water is associated with the corrosion of carbon steel wastes in the trenches for the first 1,300 years, and with the corrosion of stainless-steel wastes in the trenches for the next 1,200 years [51]**

Over time, the components of the cap, and especially its geomembrane, degrade and infiltration increases (Figure 6.5). The water levels within the trenches rise in response and water flows out of the trenches down through the underlying geology increase. It is expected that the water level and the downflow will only increase significantly many years (i.e. one or two thousand years) after the end of the Period of Authorisation.

Eventually, after about 2,500 years, all the metal waste has corroded away, and therefore water consumption stops. The water level rises a bit more, but remains below the bottom of the cap. There are two reasons for this behaviour: firstly, the rate of infiltration is less than the rate of hydrologically effective rainfall, and secondly, the vertical hydraulic conductivity of the porous materials overlying the trenches is greater than that of the i*n situ* geology.

Incidentally, Figure 6.5 predicts that the peak rate of water consumption in the repository will be 5 10^5 kg y^{-1}, or 1.37 m^3 per day. This rate of water abstraction is relatively slow, and it is therefore expected to have minimal effect on the hydraulic heads at the bottom boundary of the model, where the flows are controlled by the regional groundwater system.

6.4.2 Trench pH

Microbial degradation of the cellulosic wastes in the trenches will establish mildly acidic conditions for a period of a few hundred years [20, p. 103] after which the pH will return to that of the infiltrating water. The duration of the period of acidic conditions depends mostly on the inventory and the rate constant for cellulose degradation.

The acidity is caused by the generation of organic acids and carbon dioxide. In addition, carbonate mineral phases such as calcite ($CaCO_3$), which are present in the soil materials, will buffer the pH to a minimum value of pH 6.3 [20, p. 103].

Anaerobic corrosion of the steel wastes continues for longer than degradation of the cellulosic wastes, and also modifies the pH of the trenches by generating hydroxide ions. The result is pH values which can exceed those of the infiltrating water.

6.4.3 Trench Eh

The redox potential (Eh) of the trenches is also controlled by the cellulose degradation and steel corrosion processes.

During the first few hundred years, sulphate-reducing and then methanogenic conditions are established in the trenches, with Eh values as low as -400 mV [20, p. 103].

After the cellulose has degraded, anaerobic corrosion of the steel wastes continues, with the Eh determined from the water reduction reaction. At that time, the gas phase is essentially pure hydrogen (with a pressure of approximately 1 atm), and therefore the Eh values throughout the trenches remain low.

Re-oxidation of the trenches results from the slowing of cellulose degradation and corrosion processes after 2,500 years, and the input of oxidising species in the infiltrating water (see Subsection 6.2.1). The Eh increases gradually to around +200 mV [20, p. 103].

6.4.4 Trench Technetium and Uranium Release

The technetium inventory in the trenches is sufficiently low (0.2 TBq or approximately 0.3 kg; see Figure 2.14) that its concentration when completely dissolved in the pore water is below the solubility limit of TcO_2(am). The aqueous phase concentration of technetium is therefore controlled by sorption.

For a few thousand years after disposal, chemical conditions in the trenches stabilise Tc(IV), which will sorb onto the soil. In the longer term, when regions of the trenches may start to re-oxidise as metals are fully corroded, Tc(VII) will become stable, and the poorly sorbing pertechnetate aqueous species (TcO_4^-) will predominate. It is likely that coastal erosion will disrupt the trenches before the metals are fully corroded but, as the inventory of Tc-99 in the trenches is low, this long-term scenario is not expected to have a significant radiological impact [20].

The uranium inventory of the trenches is sufficiently high that its concentration is solubility controlled under the reducing conditions which are established, and where U(IV) is predominant [43]. In the trenches, uranium is solubility controlled by the U(IV) solid UO_2(am) at a concentration of around 10^{-7} mol dm^{-3} [20].

When the cellulose and metal wastes have completely degraded, after around 2,500 years, the trenches start to re-oxidise, and this process is associated with increased mobility of the uranium. However, in addition to the solubility and sorption processes, the release of uranium will also be limited by the slow leaching of uranium from the wastes (such as fluoride residues. See Summary Box 1) or from iron oxide phases that will take up uranium from solution. Moreover, it is likely that coastal erosion will have disrupted the site by the time that re-oxidation occurs, with mobilisation of the uranium in the trenches, and therefore these processes are of limited relevance to the expected evolution scenario.

6.5 Vaults

6.5.1 Evolution of Saturation

Results from the stack-scale and site-scale models implemented in PFLOTRAN can be used to illustrate the evolution of saturation.

Figure 6.6 shows the results of simulating the evolution of saturation in a stack of six containers (see Figure 6.4 and Subsection 6.3 for an explanation of the model geometry).

Many of the models, including the one that is illustrated here, neglect the presence of the containers so that interactions between grout and infiltration are not obstructed, and water can be sucked out of the gaps and into the grout. These models illustrate one end of the spectrum of potential infiltration-grout interactions. We also consider models that account for intact containers where the interactions are reduced to the open grout port (see Subsection 6.5.2).

The waste inventory is based on the average content of a HHISO container in Vault 8 (which has the highest average cellulose content of all the vaults, see Figure 2.11), and the wastes are assumed to be surrounded by the grout, which can interact with the infiltrating water on all four vertical sides of the wasteform.

In Figure 6.6 five time points in the evolving saturation of the system are shown, illustrating the effect on saturation as water is consumed and gas generated by corrosion of the metal wastes as well as the steel containers.

From the results of the modelling [51] we see that:

- For approximately 1,000 years following installation of the cap, the rate of infiltration is insufficient to meet the demand for water associated with the corrosion of the metal wastes and the steel containers (see also Figure 6.7). The humidity in the gap between containers becomes very low such that water vapour may be drawn up from the B2 unit. Although the system becomes dry, it is not so dry that the waste degradation reactions become inhibited to a very great extent. Figure 6.6 (500 y) shows the gradual drying out of the wastes as indicated by the increasing gas saturation.

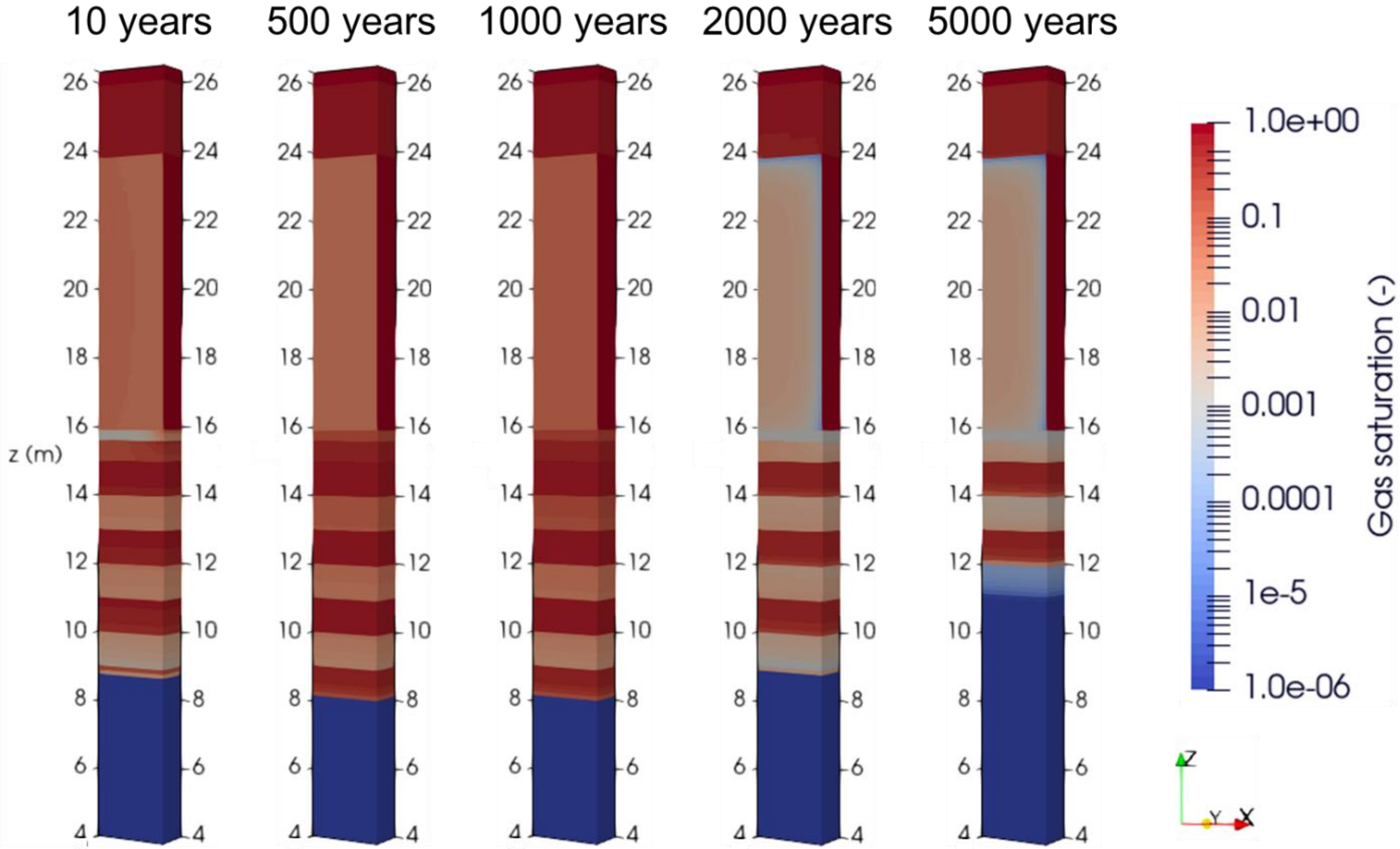

Figure 6.6: Contour plots of the gas saturation at 10 y, 500 y, 1000 y, 2000 y and 5000 y after capping in a stack of grouted containers following the installation of the final cap (neglecting the presence of the containers around the grouted wastes) [51]. [Note logarithmic scale for gas saturation]

- After around 1,000 years after installation of the cap, the rate at which corrosion is consuming water drops because some of the waste metals (notably the aluminium) are becoming exhausted (Figure 6.7). This will clearly depend on the specific inventory. The modelling results shown use the average Vault 8 inventory of materials and differences between vaults will be reflected by differences in the local evolving conditions. The rate of recharge is also increasing because the cap components are degrading. Consequently, the system starts to wet. Some water starts to flow from the gap into the underlying B2 (this assumes cracks in the vault base and that the underlying drainage layer and B2 are unsaturated).
- After around 2,000 years, that is after failure of the geomembrane, the water table starts to rise through the underlying Unit B2. This is illustrated in Figure 6.6 (2000 y) which also shows the increasing saturation of the waste containers as water is drawn into the grout from the gap between container stacks. The gap itself remains unsaturated.
- The increasing infiltration rate is associated with a slowly rising water table as illustrated in Figure 6.6 (5000 y).

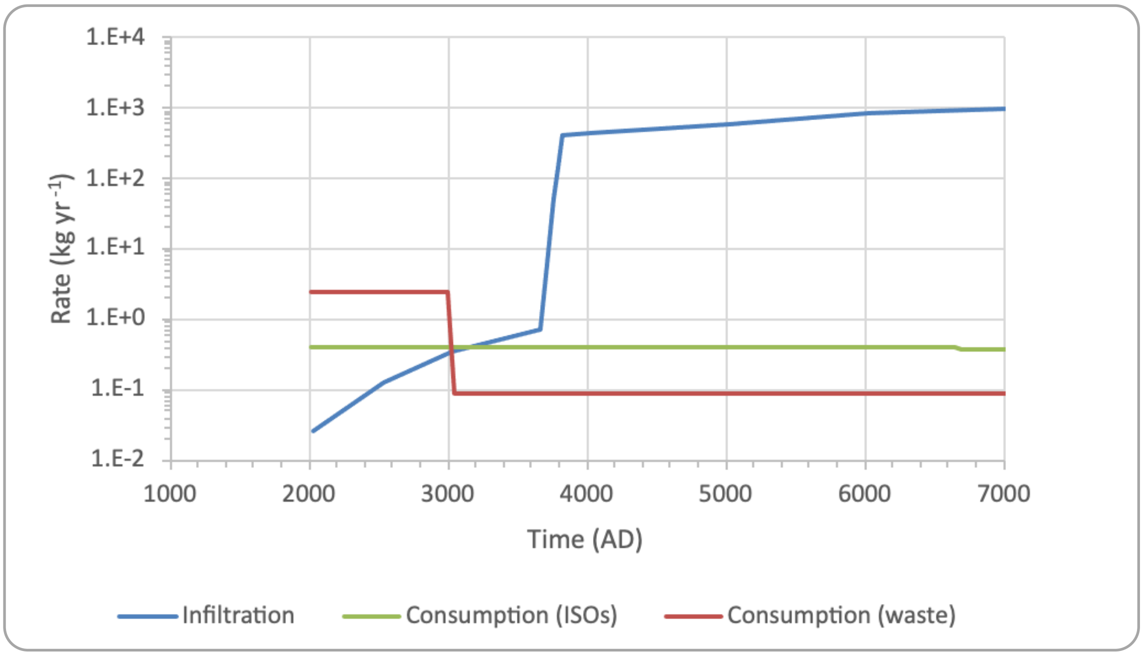

Figure 6.7: Rate of water infiltration through the area of the final cap above a stack of six ISO containers in Vault 8 compared with the rate of water consumption by corrosion of the containers and their metal wastes [43]. The dominant sink of water is associated with the corrosion of aluminium waste for the first 1,000 years, and with the corrosion of the mild steel surfaces of the containers thereafter

Even at the end of the simulation (i.e., at 5000 years), when the cap geomembrane and the BES are assumed to be fairly extensively degraded and therefore the cap is not restricting the rate of recharge to be a small fraction of its undisturbed value, the water table still lies beneath the bottom of the vault.

The conditions in the vaults lead to a long-term depression of the water table in the repository relative to the surrounding geology. This effect is a combination of precipitation diverted by the cap (this results in the local recharge to the surrounding geology being higher than the hydrologically effective rainfall), water draining quickly through the gaps and thence into the drainage layer and the B2 Unit, and the cut-off wall restricting lateral flow from the surrounding B2 Unit to the area beneath the vaults, thus ensuring that the water table is lower beneath the vaults than in the geology outside the cut-off wall.

The timescale for water to accumulate at the base of a vault is uncertain as it is intimately tied to both the performance of the cap and the integrity of the concrete basal slab and its underlying clay layer. Furthermore, our models neglect the presence of the containers, thus will overestimate the amount of water that is drawn into the grout as a result of its strong capillary suction. This will be the case most obviously in vaults with stronger containers and CPUs where damage of the containers due to corrosion is expected to be localised.

Our current modelling indicates that saturated zones at the base of the vaults may not form before the vaults are affected by coastal erosion. In reality, the vaults will evolve differently in response to their distinct containers and alternative base designs, the presence of CPUs or ILW units, as well as spatial variations in the properties of Unit B2 and the performance of the cut-off wall.

The low saturation, within the vaults particularly, does raise the question of inflow through the cut-off wall, especially at longer times as its properties degrade. However, as noted in Subsection 3.5.1, only Vault 8 might be vulnerable to such inflows. All the other vaults will be protected by a hydraulic short-circuit in the form of the drainage gap between the low inner vault wall and the cut-off wall leading to the under-vault drainage blankets. Although Vault 8 does not have this structure, flows through the cut-off wall would, however, need to traverse the unsaturated, permeable Unit A sediments between the cut-off wall and the vault wall. It is likely that these sediments would act to direct the flows down to the underlying B2 unit.

A contour plot of gas saturation for the vaults and trenches simulated in the PFLOTRAN site-scale model [43] is shown in Figure 6.8 for 2000 years and 4000 years after final capping. The line of the section passes through the gaps between containers. These are very dry (coloured red on the figure) but, conversely, the secant wall, to the right of Vault 9 in these figures, and the walls and base of the vault stay rather wet (i.e., shaded blue), because of the low permeability flow properties of the bentonite and concrete used in their construction.

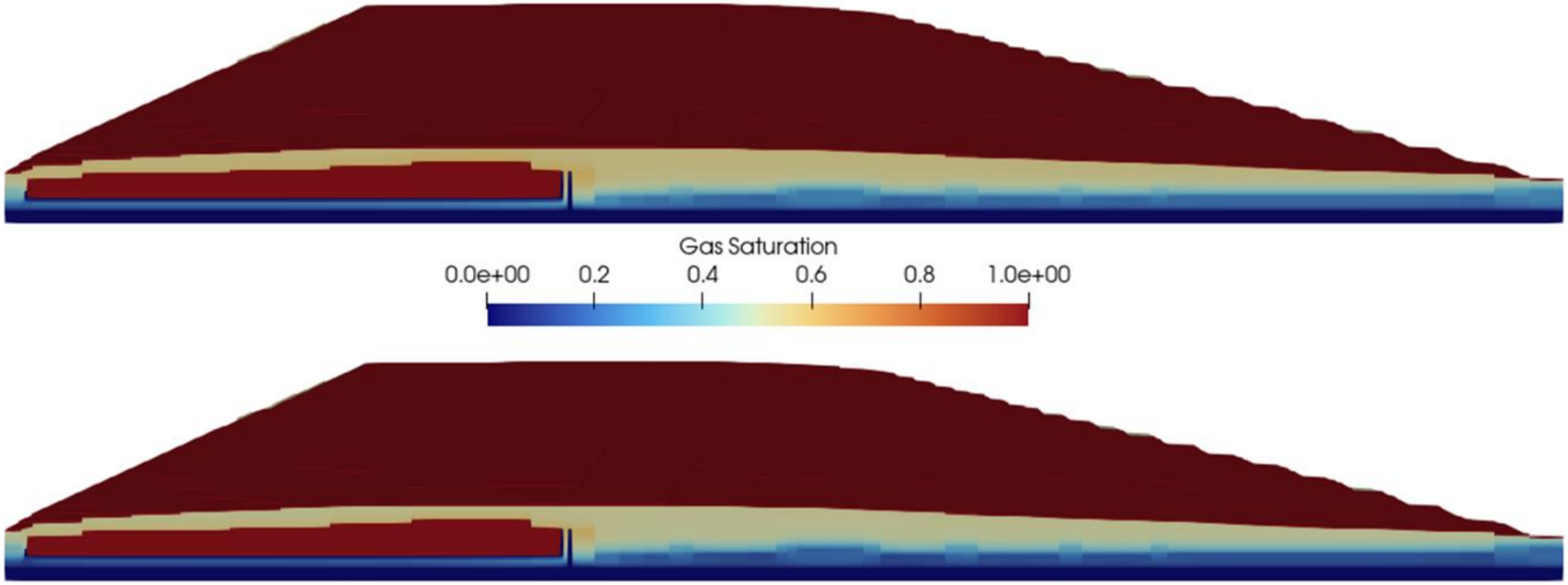

Figure 6.8: **Contour plots of the gas saturation for the 3-D site-scale model at (top) 2000 years, and (lower) 4000 years following the installation of the cap. The contours are shown on a vertical section through Vault 9 (left) and the trenches (right). The section passes through the unsaturated gaps between container stacks in Vault 9 [43]**

This is the period following degradation of the geomembrane when the infiltration rates rise from less than 1 mm y^{-1} to almost 30 mm y^{-1} (Table 3.1). Even with the increased infiltration rates, the gaps between the container stacks in the vaults are shown to be extremely dry, whereas some water is present in the overlying profile fill and capping materials (buff-coloured areas with gas saturation around 0.5 on Figure 6.8) and the trenches are wetter, but not saturated as a result of continued gas generation from waste corrosion and degradation.

It is not readily apparent on these repository-scale figures that the water saturation below the vault increases over this period, as shown in the results from the package stack-scale model in Figure 6.6. However, increasing saturation in the trenches is more evident in the darker blue hues.

Overall, there are strong reasons to expect that the vaults will be largely unsaturated over the period of 5,000 years following capping. This period encompasses the uncertainty in the time of onset of coastal erosion that will eventually disrupt the repository [7].

In summary, we expect that the grouted wastes will be near-saturated initially and remain relatively saturated, while the gaps between container stacks will remain unsaturated until infiltration rates exceed the rate of water consumption by metal corrosion, waste degradation and grout resaturation. This will occur at some time following geomembrane failure, when water will start to flow through the base of the vault and into the geosphere. The precise timing of this is uncertain but is most likely to occur between 1500 and 2500 years after cap installation.

6.5.2 Evolution of pH

Following repository capping, we expect that the pH within most of the grout in the majority of containers will remain above about pH 12 for several thousand years, restricting microbial activity (see Subsection 4.3.2).

Simulations using the PFLOTRAN stack-scale model, representing grouted HHISO containers but without taking account of the metal box, shows that lowering of grout pH is initially restricted to immediately adjacent to the gaps (Figure 6.9) and, conversely the pH increases in the profiling material above the stack. This is where the infiltrating water can contact the grout and where grout porewater species can diffusion into the slowing flowing water. Figure 6.9 shows contours of pH for three time points: the initial state following capping, at 2000 years following the failure of the geomembrane and, finally, at 5000 years. In addition to interaction with infiltrating water, the simulation of the grouted wastes takes account of degradation reactions, including ISA formation from cellulose.

The interaction between the water flowing in the gap and the grout surface leads to the pH in the water in the gaps increasing, while the pH in the grout falls slightly, most markedly in the topmost containers which experience direct contact with the infiltrating water. Since we do not expect there to be much contact between the grout and the infiltrating water until after significant degradation of the containers, this simulation represents a cautious case, but even so the grout remains around pH 12. Figure 6.9 also shows how the evolving water composition in the gaps can affect the conditions below the vault as the water drains down.

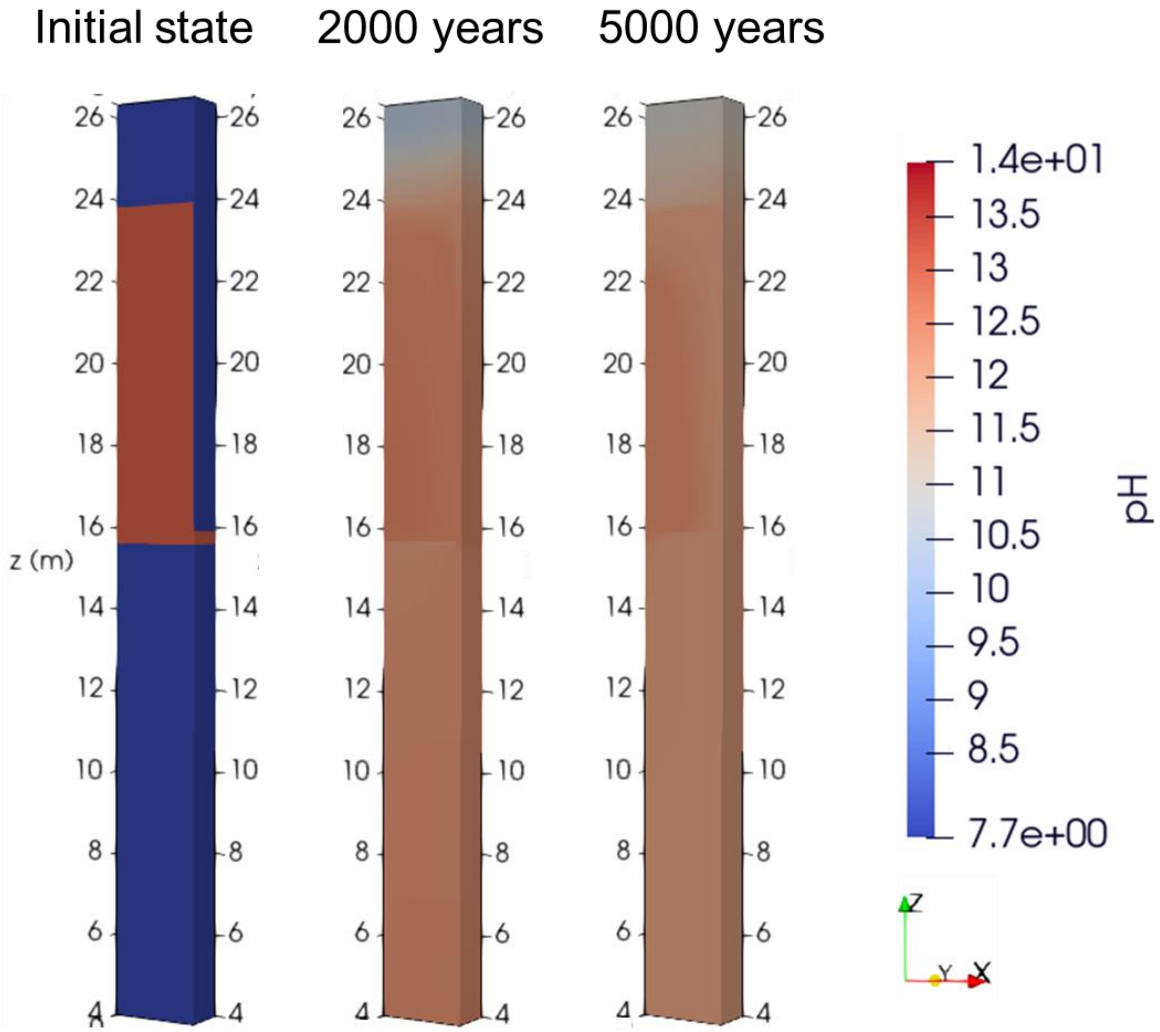

Figure 6.9: **Evolution of pH in the grout (assuming Vault 8 average inventory) over 5000 years, neglecting the presence of the six HHISO containers but including the degradation of cellulosic wastes, which causes a reduction in pH throughout the containers [43]**

The situation illustrated in Figure 6.9 ignores the presence of the containers around the grouted waste in order to illustrate one end of the spectrum of potential infiltration-grout interactions. An alternative is a stack where the containers are intact, and water ingress is initially possible only via the grout port or vent.

This is illustrated in Figure 6.10, which shows the results of pH evolution in a representation of a stack of six containers. Infiltration is incident on the upper surface of the top container and can flow around the surfaces and in the narrow gaps between the top and base of stacked containers. However, interaction between water and grout can only occur at the open grout ports located at the upper left corner of each container in the model stack (as the model uses a plane of symmetry, only one half of each container is represented and the grout port is assumed to be located at the centre of each container). The chemical interactions with the concrete vault floor and the B2 unit are explicitly represented and result in elevated pH occurring beneath the vault. In this model, the degradation of the cellulosic wastes generating ISA causes proportionately more of the pH change than in the case where the ISA can diffuse from the grout into water in the gaps.

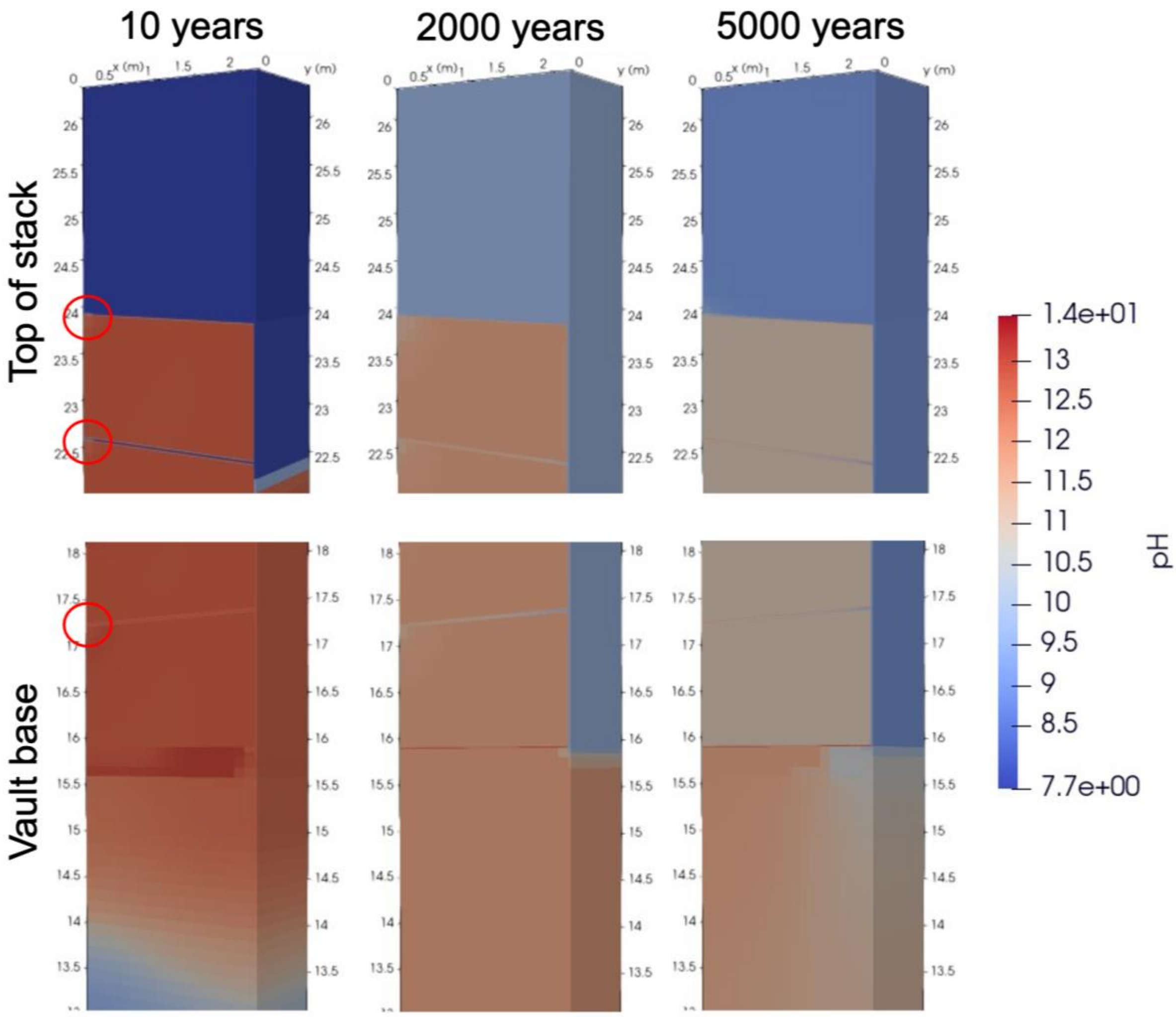

Figure 6.10: **Evolution of pH over 5000 years in a stack of six containers [43]. The presence of the containers is taken into account and interaction with infiltrating water coming into the top boundary of the model can only occur at the grout ports (indicated by red circles), which are located in centre of each container. The gap between the stacks is on the right side of the model and the concrete vault base underlies the stack**

We have also investigated the impact of different amounts of grout in the containers. The results shown in Figure 6.9 use the average wasteform composition for Vault 8 wastes, which includes about 16 tonnes of grout per container. The average for Vault 9 is slightly higher (18 tonnes) and this was used for the 'base case' pH evolution shown in Figure 6.11. In these simulations, the infiltrating water reflects contact with the BES as discussed in Subsection 6.2. From the base case, we reduced the amount of grout in successive simulations to investigate how the pH at the centre of the grout block evolves in the model in which the presence of the container walls is neglected. Figure 6.11 shows the results, which are explained more fully in reference [51]. The key point is that reducing the grout content of a container does not result in a rapid decrease in pH even with cautious neglect of the presence of the HHISO container.

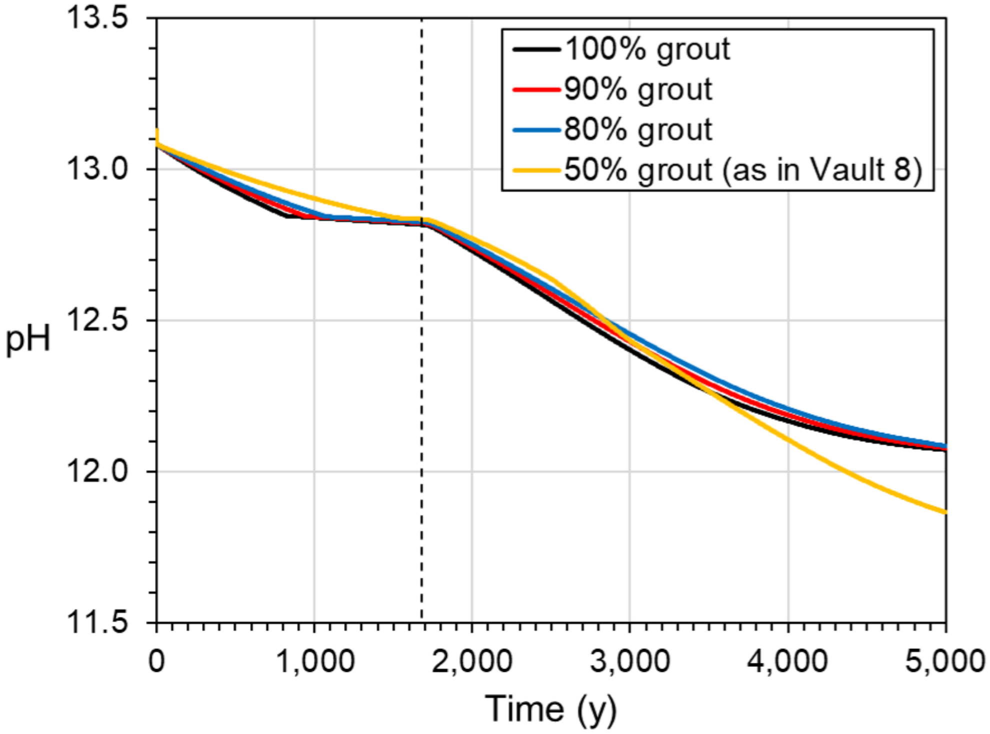

Figure 6.11: Evolution of the pH at a point which is located near the centre of a waste package [51]. The base case (100%) is average Vault 9 waste with 18 tonnes of grout per container. Variant modelling cases considered the use of differing amounts of grout. The vertical dashed line shows the start of degradation of the geomembrane in the final cap

We use these model simulations to support our contention that the grout porewater in most containers will remain above pH 12. This is not to say, however, that there will be no instances of lower pH in the grouted wastes. The heterogeneity of infiltration, especially in the period before the geomembrane fails, means that some container stacks will experience much wetter conditions than others (see Subsection 6.6). This may not significantly affect the stronger container stacks with CPUs because we expect most of these containers to retain their integrity for a long period. For the surcharged stacks in Vaults 8 and 9, the containers at the top of some stacks will have infiltration percolating into the waste through the damaged lids from early times. The result of this early contact will depend on the condition of the grouted wasteform and the integrity of the container as illustrated schematically in Figure 6.12.

In summary, our modelling of the interaction of the infiltrating water with the grouted wastes, and neglecting the presence of the containers, indicates that the grout porewater will remain above pH 12 in most containers over 5,000 years. There will be some containers, especially in the surcharged stacks located under higher inflow points, that will be more affected by leaching and the pH will fall further. These containers are also likely to be those responsible for most of the contaminant releases to groundwater.

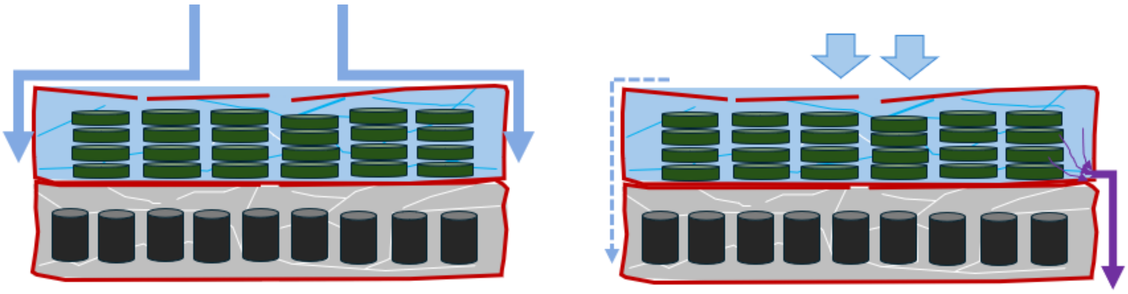

Upper container with failed lid under an infiltration inflow. Grout saturates and excess water spills over into the gaps. Water in the grout is stagnant. The overspill water is alkaline from contact with the grout and may also contain some contaminants. Both pH and contaminants will fall over time in the overspill water.

Upper container with failed lid under an infiltration inflow. Container has perforations on the sides and the grout is cracked. The grout saturates and excess water can flow out of the container creating an advective system. Less water spills over into the gaps.
Water flowing from the perforations will leach the grout, reducing the pH, and is likely to contain contaminants.

Figure 6.12: Schematic illustration of diffusion-dominated grout degradation in intact containers (left) and advective leaching in failed containers (right)

pH evolution in the gaps

The discussion above concentrated on the pH in the porewater of the containers that is the result of conditioning by the grout. In the gaps between the containers, the conditions are substantially different as the composition of the infiltration is rainwater conditioned by the BES, then modified by contact with the iron corrosion products on the container surfaces.

For most of the water in the gaps in areas of the vaults with CPUs on stacks, there will be limited contact with the grout. As a result, in these areas of the vaults, the composition of infiltration will be determined mainly by the BES, with pH between about 7 and 10 (Subsection 6.2.1) and subsequent contact with corrosion reactions on the containers.

For the existing and committed containers that have been surcharged, there will be greater contact between infiltrating water and the grout as the result of the failed container lids on the top container and localised holes in the sides of the containers throughout the stack (Figure 6.12). The results of simulations of interaction between the grouted wastes and the infiltrating water in the gaps are shown in Figure 6.13 for a stack of Vault 9 containers with differing amounts of grout. These pH values are expected to be overestimates because the model assumes unimpeded contact between the grout in all containers and the water in the gap. Higher infiltration rates after geomembrane failure also tend to result in dilution of the water in the gaps as diffusion from the partially leached grout surface can no longer keep pace with the water volume.

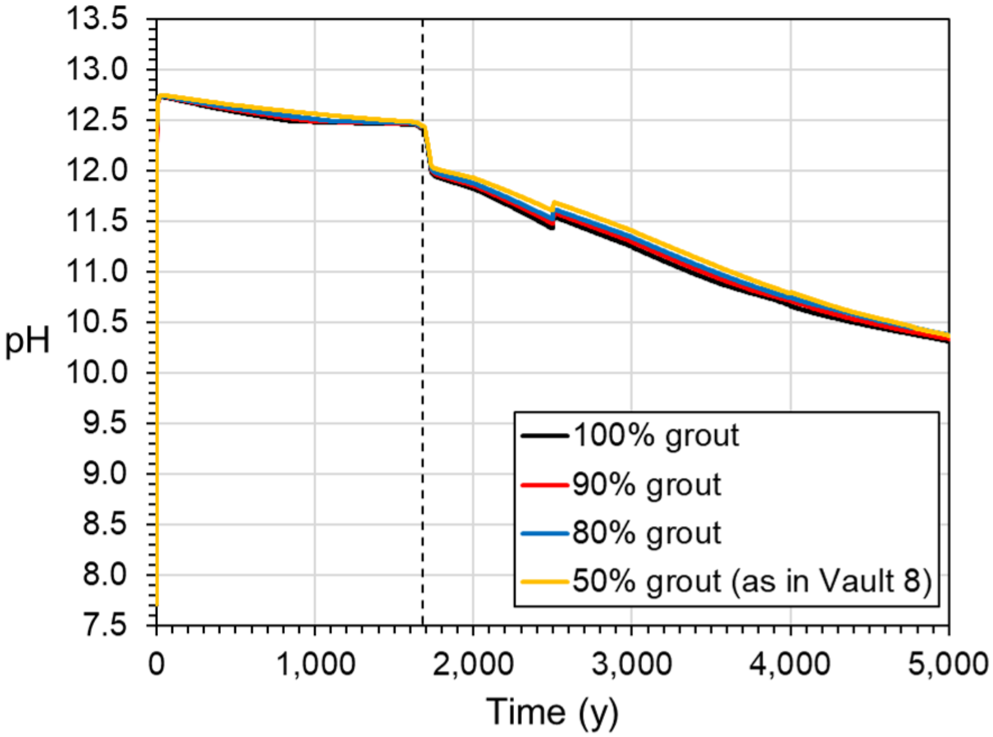

Figure 6.13: Evolution of the pH at a point which is in the middle of a gap between stacks of ISO containers [51]. Variant modelling cases consider differing amounts of grout in the containers relative to average Vault 9 waste (100%). The vertical dashed line shows the point when the geomembrane in the final cap starts to degrade, resulting in an increased flow of water through the gaps

In reality, we expect that the top of stack containers in the surcharged vaults will dominate the evolution of pH from the infiltration composition in the gaps. Underlying containers will only contribute once they are saturated and perforated sufficiently to allow water to contact more grout. Where the stacks have CPUs, limited perforation of containers, at least by the time of geomembrane failure, suggests that the pH of infiltrating water will largely reflect its initial composition modified by contact with iron corrosion products.

The key point is that the pH of water in the gaps will most likely be lower than in the grout but will be heterogeneous and evolve independently in different areas of the vaults. This means that the occurrence of microbial activity in the gaps will also vary and, assuming there are sufficient nutrients, is most likely to occur where the pH is lower and less likely where pH is closer to the grout pH.

6.5.3 Contaminant transport

The PFLOTRAN models have been used to consider the transport and release of a number of contaminants of interest (Subsections 2.3.2 and 2.3.3). Here we report only a subset of the results, including C-14 for which PFLOTRAN models were not used. Reference [51] provides the results for the full set of contaminants considered.

Tracer

We have argued above that diffusion is the dominant transport process by which contaminants will be released from the grout. It is therefore helpful to first consider the release of an inert tracer. If the tracer is present at an initial concentration of 1 M, then Figure 6.14 shows how the tracer will migrate away from a stack of containers and into the geosphere.

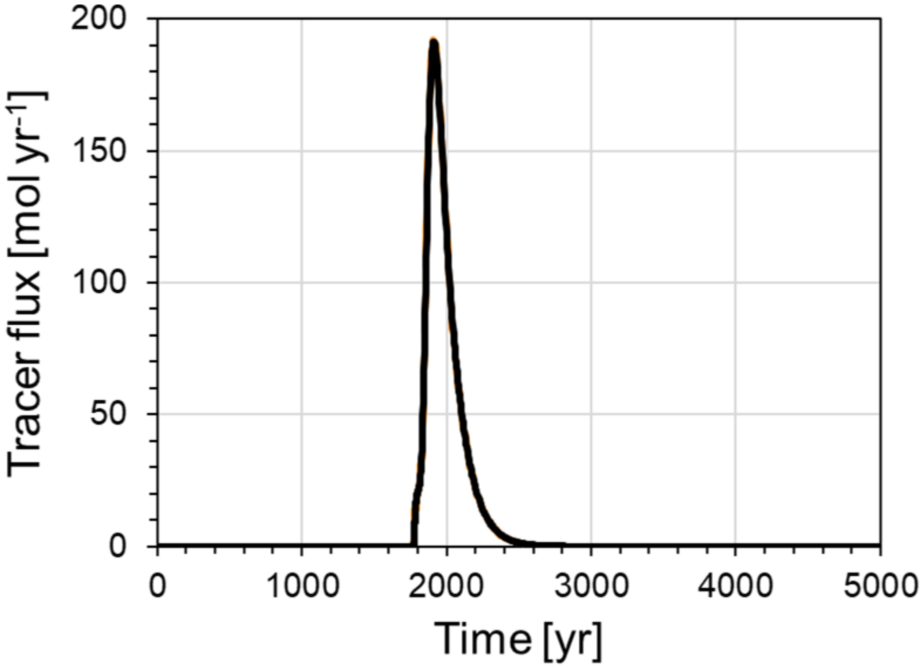

Figure 6.14: Flux of a tracer across the bottom surface for the model using an explicit representation of a stack of grouted containers, but neglecting the presence of the containers around the grouted wastes [51]

Migration of the tracer is negligible until after the geomembrane in the cap has degraded. But once the degradation has occurred, a net flow of water develops downwards through the gaps. The concentration of tracer in the gaps is less than in the wasteform, and so the tracer starts to diffuse out of the wasteform. As the tracer does not have a solid to support the concentration in the grout, the concentration falls, reducing the rate of diffusion into the gaps.

This is a cautious prediction for two reasons.

Firstly, the model assumes perfect contact between the grout and the water flowing through the gaps. In practice, the steel containers will restrict this contact. If only a small fraction of the grout is in contact with the water in the gaps, then the diffusive flux out of the wasteform will be reduced by the fraction, and the timescale over which the tracer is released will be stretched out by the reciprocal of the fraction.

In addition, we have made cautious assumptions when parameterising the rate of diffusion through the wasteform. That is because there is considerable uncertainty around how quickly the tracer will diffuse through the mixture of wastes and grout. To account for this uncertainty, we have chosen parameters that mean the diffusion is more than an order of magnitude faster than it would be for grout alone.

Having discussed the migration of a tracer, we now recognise that the migration of many species will be affected by chemical processes such as sorption and solubility limits.

The inventory of Tc-99 in the vaults means that it will not be subject to a solubility limit, but it will be subject to sorption. It is therefore convenient to consider this radionuclide next.

Technetium

Technetium can take two oxidation states but under the reducing vault conditions, Tc(IV) is expected to strongly dominate over the more oxidised Tc(VII) species.

Based on the expected pH conditions, the solubility limiting phase for Tc(IV) is assumed to be TcO_2(aged) [107, 51]. However, as noted, the inventory of Tc is small, and where average waste concentrations occur, its concentration in porewater will be controlled by sorption rather than its solubility limit (Subsection 4.5.2). This is demonstrated by Figure 6.15, where the amount of available grout determines the pH, thus the sorption and porewater concentration of Tc.

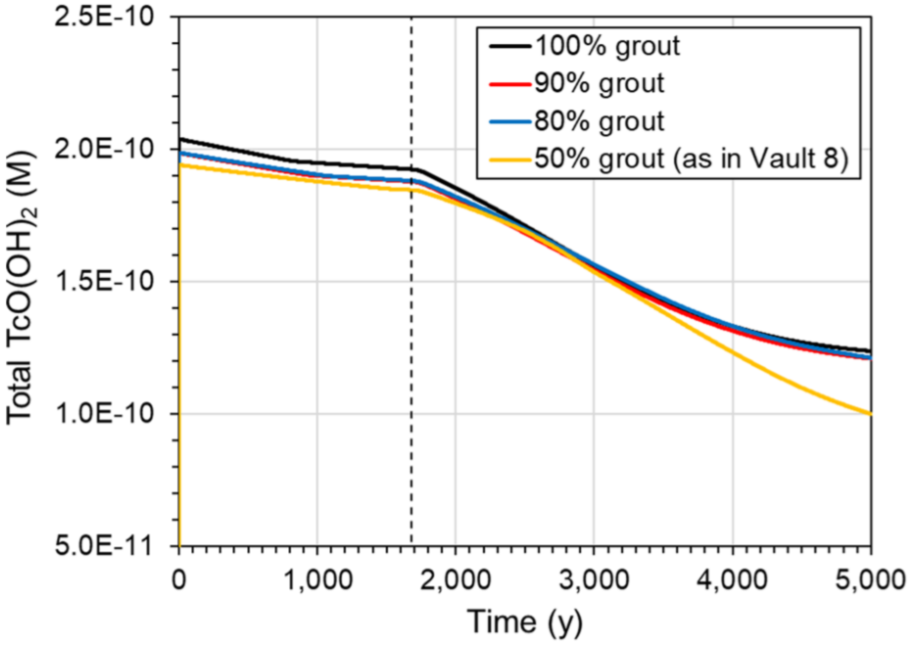

Figure 6.15: Evolution of the Tc(IV) concentration at a point located near the centre of a waste package for varying amounts of grout in the container [51]

Review of the effects of ISA complexation for contaminants of interest [79] suggests that ISA is less important for Tc than for U transport. In fact, Thermochimie contains no Tc-ISA complexes [107]. We have instead compared the release of Tc from container-scale models with and without ISA generation from cellulose wastes. The pH evolves differently in the two systems as the alkaline hydrolysis reactions of cellulose result in a decrease in pH faster than by diffusion into the external water flows alone.

The black line in Figure 6.16 shows the flux of Tc species out of the bottom of a model without cellulose or its degradation to ISA. The pH in the wasteform stays high (i.e. at about 13.2) and very little Tc is released until water starts to flow over the grout surface. Most of the Tc is sorbed, while the aqueous concentration of Tc in the wasteform is about 4.4 10^{-10} M.

The orange line in Figure 6.16 shows the corresponding results for a model with cellulose. The cellulose degrades to ISA, and in the process lowers the pH in the grout. By the time that water starts to flow across the surface of the wasteform, at around 1700 years, the grout pH has dropped to about pH 12. The change in pH affects the chemical speciation and sorption, so the aqueous concentration of Tc in the wasteform is now 2.5 10^{-10} M. And that reduction in concentration is reflected in a lower flux of Tc out of the bottom of the model.

As ThermoChime does not include any Tc-ISA complexes, cellulose degradation can only modify the transport of Tc through the indirect effects on pH.

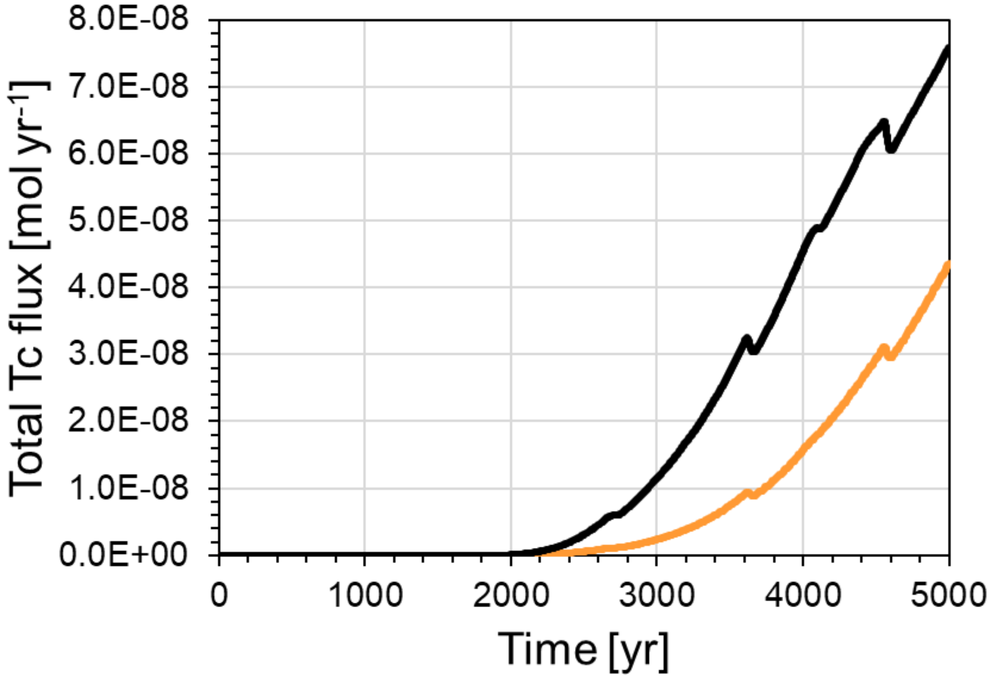

Figure 6.16: Annual flux of Tc(IV) species from the bottom of the model, taking ISA formation (orange line), which lowers the grout pH, into account, and neglecting ISA formation (black line) so that the pH remains high [51]

Uranium

In describing the behaviour of uranium, we make use of a solubility limit that is based on the most likely solubility-limiting uranium solid phase under near-field chemical conditions. The U(IV) phase UO_2:$2H_2O$(am) is assumed in the PFLOTRAN modelling illustrated here, based on work described earlier (Subsection 4.5.2).

U(IV) species are dominant in the aqueous phase. Figure 6.17 illustrates the changing U concentration in the water at the top and bottom of the gap between container stacks. U(VI) is present, as the UO_2^{2+} species, but at a concentration several orders of magnitude lower than the U^{4+} species.

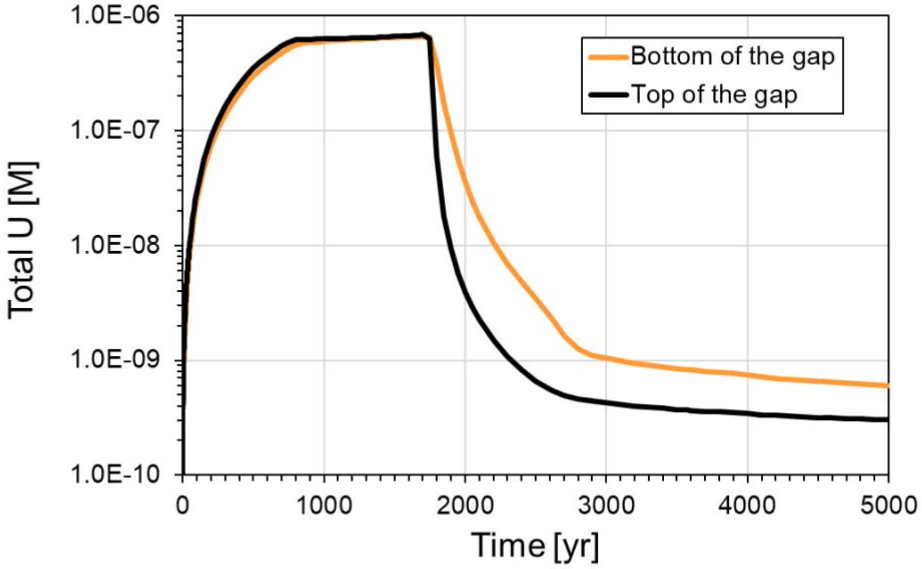

Figure 6.17: Total concentration of aqueous U species in the porewater in the gap adjacent to a 6-high stack of containers (the presence of the containers is neglected). ISA complexation is taken into account, resulting in a higher U concentration than would be the case were it neglected [43]

The U concentration builds up in the porewater in the gap (noting that the gap is assumed to retain some water throughout). At both the top and the bottom of the gap, the U concentration increases to reach a plateau after 700 years. The concentration of the plateau is maintained for about a thousand years. Then, after 1700 years, the U concentration starts to decrease throughout the gap, because the cap geomembrane has degraded, increasing infiltration, and more water is now flowing down through the gap. Thus, the result over a short period is dilution of the water in the gap. Figure 6.17 also shows that the concentration at the bottom of the gap is higher than at the top, because U continues to diffuse into the water as it trickles down the gap.

The results shown in Figure 6.17 include U complexation by ISA. Isosaccharinic acid is generated by alkaline hydrolysis of cellulose within the waste, and its concentration is controlled by both a solubility limit, for calcium isosaccharinate, and by its sorption on the grout (although this is not accounted for in these models). This implies that there is a maximum impact it can have on the uranium solubility and sorption (see also reference [79]). Figure 6.18 illustrates the calculated evolution of ISA concentration in an average Vault 8 container, with the corresponding content of cellulose.

Figure 6.19 shows the flux of U in gap porewater out of the bottom of the model into the underlying geology. As U is solubility limited, concentrations in the grout (as well as in the porewater in the gap) cannot exceed this value. The release of U from the grouted wasteform is also influenced by sorption on the grout phases and complexation by ISA.

Figure 6.19 shows the flux of uranium neglecting complexation by ISA. When ISA complexation is included, the long-term release of U increases by almost two orders of magnitude, as illustrated in Figure 6.20.

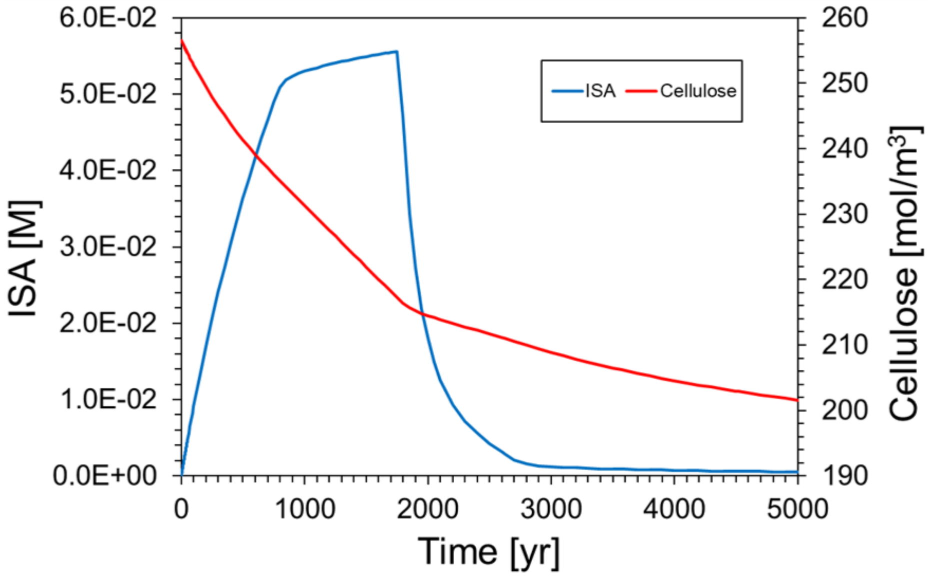

Figure 6.18: Evolution of ISA concentration at a point which is located near the centre of a waste package, and the falling cellulose content in the waste as it degrades. Note that ISA sorption to the grout is neglected [51]

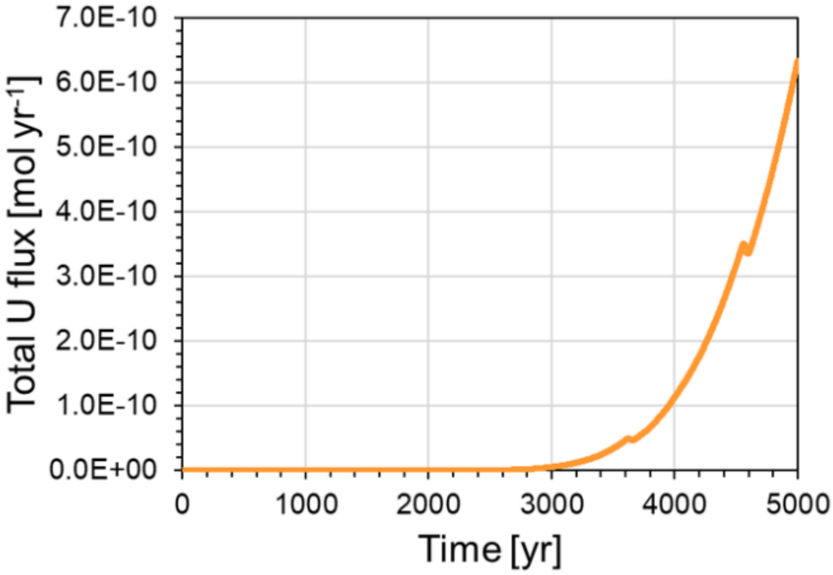

Figure 6.19: Annual flux of U (moles per year) in gap porewater out of the bottom of the model into the underlying geosphere. This simulation neglects U complexation by ISA [51]

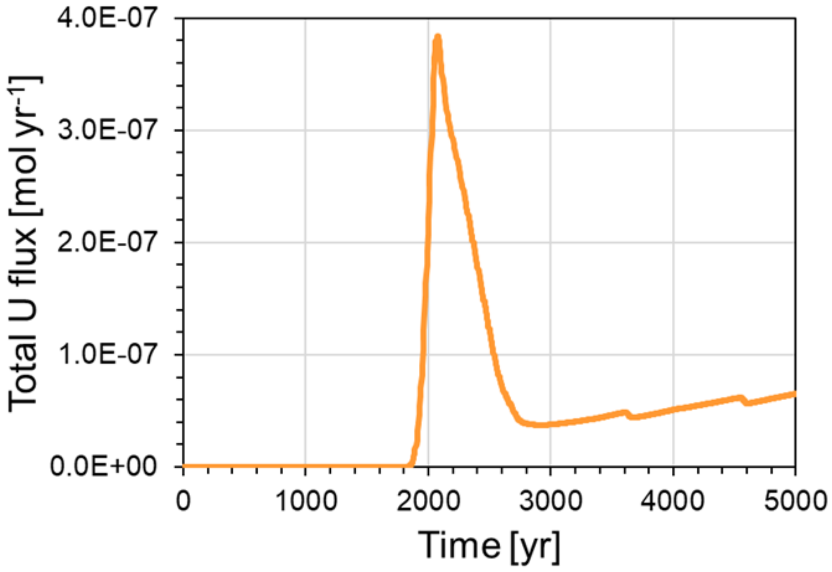

Figure 6.20: Annual flux of U (moles per year) in gap porewater out of the bottom of the model into the underlying geosphere. Complexation by ISA, increasing U solubility, is accounted for [51]

It appears that accounting for complexation by ISA has created two U release regimes.

First, there is a fast release of U complexed by ISA that has built up in the grout porewater. This fast release is like the release of a tracer (Figure 6.14), and is an artefact of our model, which models sorption of U, but not of either ISA or the U-ISA complexes.

Second, there is a combination of the slow release of the other U species, which are affected by sorption, with the remaining, and higher, flux of U-ISA complexes that are not hindered by sorption in our model.

Although the shape of the ISA curve in Figure 6.18 is similar to that of U in the gap (Figure 6.17), the magnitude of the reduction in ISA concentration is much smaller. The total aqueous concentration of ISA after about 3000 y is still ~5 10^{-4} M and, as indicated in Figure 6.18, there is still sufficient cellulose to generate more ISA. As a result, the concentration of U-ISA complexes remains high enough to maintain a greater U flux from containers with cellulose.

As noted, currently we do not account for the sorption of ISA, nor ISA complexes, on the grout in the PFLOTRAN model so that the resulting ISA concentration is higher than would be expected with sorption. We overestimate the influence of ISA in the model, resulting in a total dissolved U concentration of about 5 10^{-7} M (see Figure 6.17) compared with a concentration of around 10^{-9} M with no ISA present and approximately 2 10^{-9} M with ISA present but accounting for ISA sorption on the grout [79]. If ISA sorption on the grout was taken into account, the peak in Figure 6.20 would be lower and the tail higher as sorption would also retard the release of the U-ISA complexes.

The omission of ISA sorption from the model was a pragmatic decision, because further work, and time, will be needed to parameterise the full system comprising grout, U and ISA.

Once the containers fail and the grout saturates, ISA will be released into the gaps along with any complexed uranium. The lower pH environment in the gaps, and the potential for microbial activity there, means that the ISA may be degraded. If the degradation reduces the ISA concentration sufficiently that the complexes with U (and potentially also other metals) are destabilised, some of the U could effectively be stranded in the gaps since its solubility limit in the absence of ISA ($3\ 10^{-9}$ M) might be lower than the concentration reached in the gaps (Figure 6.17). However, as the infiltration increases, this stranded uranium will re-dissolve and, apart from any that sorbs to iron corrosion products in the gaps, will be released into the geosphere.

The maximum flux from the stack of 6 containers, based on the Vault 8 inventory, is around $4\ 10^{-7}$ mol y^{-1}. Summed over the approximately 10,000 containers in Vault 8, this suggests a rather cautious maximum release rate from Vault 8 of less than 10^{-3} mol y^{-1}, or less than 1 g uranium per year. Other vaults have smaller inventories of cellulose and the effect of ISA on the release of U, and other contaminants, is expected to be smaller [79].

Non-radiological contaminants

The inventory of the Vault 8 includes non-radiological contaminants, and their migration is simpler than for uranium. Figure 6.21 shows the evolution of fluxes of boron (B), cadmium (Cd), lead (Pb) and mercury (Hg) out of the bottom of the model as reported in reference [51]. None of these contaminants are significantly affected by complexation with ISA.

The transport of B resembles that of a conservative tracer, as can be seen by comparing Figure 6.21 (a) with Figure 6.14. This is because the solubility limiting phases for this species are uncertain and have not been included in the calculations. Furthermore, the linear sorption coefficient for this metal is negligible, so sorption also plays a minimal role. The model results are expected to be cautious as the majority of the boron inventory in Vault 8 is in the form of Boral, a composite material in which boron is present as relatively insoluble boron carbide particles sandwiched between layers of aluminium [36].

The solubility limiting phases for Hg are also uncertain and have not been included in the calculations. Furthermore, sorption of Hg in cement is an order or magnitude lower than for Cd and Pb, and two orders of magnitude lower than for U and Tc. This leads to a small amount of sorption of this contaminant within the wasteform. For these reasons, fluxes of Hg at the bottom of the system behave rather like a tracer, just with a longer tail (Figure 6.21 (d)). In contrast, Cd and Pb are solubility limited and retarded by sorption (Figure 6.21 (b), (c)).

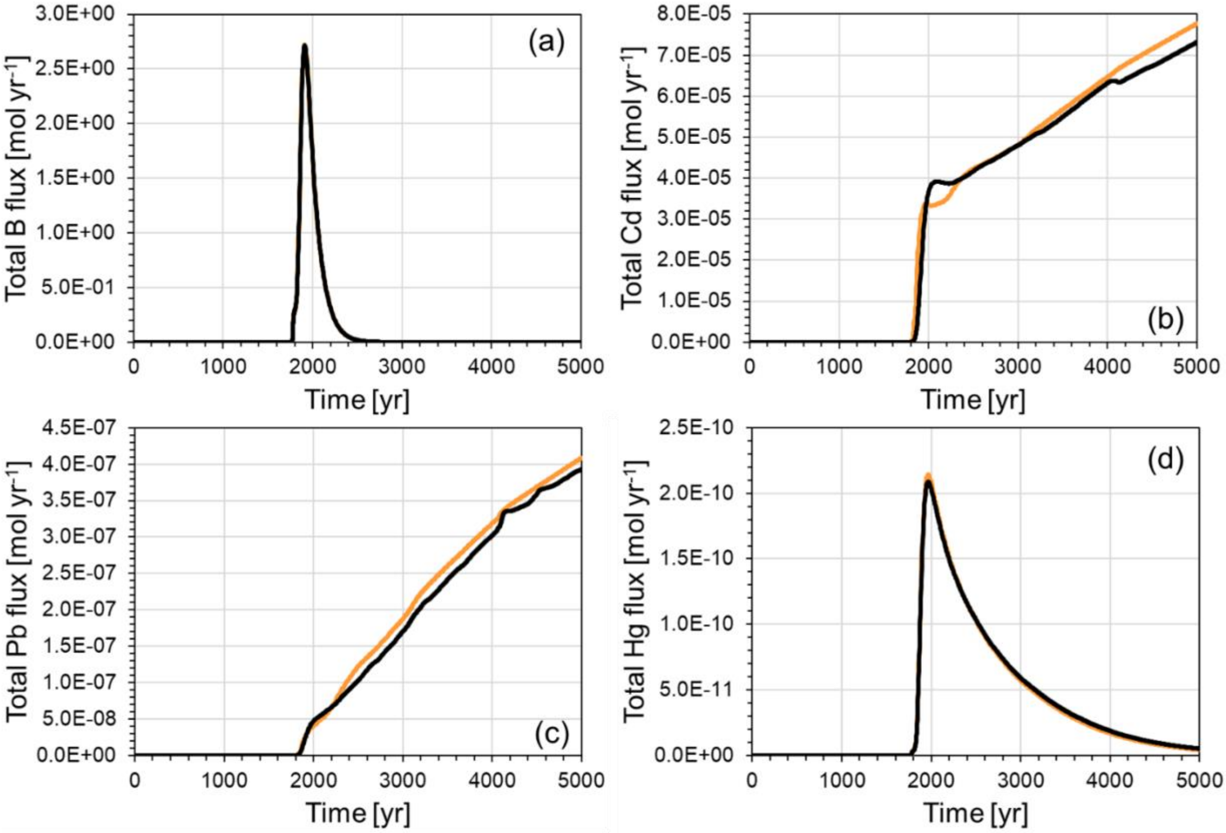

Figure 6.21: Annual fluxes of toxic metals out of the bottom of the model into the underlying geosphere, both taking account of ISA complexation (orange lines) and neglecting ISA complexation (black lines): (a) boron, (b) cadmium, (c) lead, (d) mercury [51]

Carbon-14

The conceptual understanding of the behaviour of C-14 in the vaults has significantly changed from the 2011 view in light of both greater understanding of the form of C-14 in the wastes, particularly graphite and metals, and the other near-field changes already described. The limitation of microbial activity, as discussed in Subsection 5.2.1, means that the only C-14-bearing gas generated from the grouted wastes is the primary C-14-bearing methane released mainly by graphite and metals. Further gas can be generated only when the dissolved C-14 species migrate into the gaps, where the lower pH conditions allow microbial reactions.

We consider that there is such uncertainty about the conditions in the gaps that there is no benefit to be gained from attempting to model this system to provide input to the assessments. Instead, in the gas assessment, we assume the mobile dissolved C-14 species are fully degraded to produce further C-14-bearing gas. For the gas assessment this is a cautious assumption but, for the groundwater assessment, the opposite assumption is adopted so that all dissolved C-14 released to the gaps is lost to the groundwater.

We now account for the partition of C-14 in the vaults into gas, water and mineral phases directly in the gas assessment conceptual model [46], based on the release rates and speciation of C-14 from the different waste materials (see Subsection 8.2).

For the groundwater assessment we have calculated the partition of C-14 releases between groundwater, gas and carbonate. The calculation is based on the same C-14 speciation and release rates for the various waste materials as used in the gas assessment. The partitioning between phases is therefore the same for both groundwater and gas assessments until dissolved C-14 is released to the gaps. At this point, the partitioning for the two assessments diverges as described above.

The results for Vault 8 (Figure 6.22) show the calculated partitioning of the C-14 between the three phases and the residual content of the wastes.

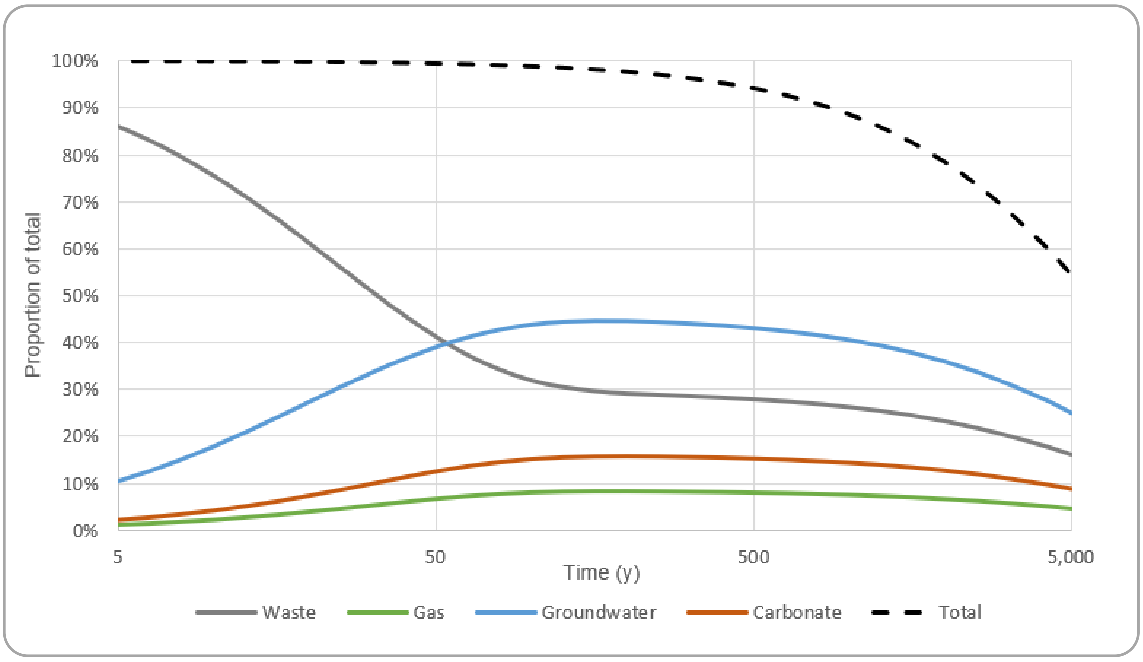

Figure 6.22: The evolving proportions of total C-14 in Vault 8 in the waste, gas, water and mineral phases after closure of the vault [156]

The maximum value for release to groundwater, 45% in this case, in each vault is used to calculate an inventory-weighted average for use in all vaults. This inventory-weighted average is 12.79%, with a minimum value of 0% (equivalent to the gas assessment case with no release to groundwater) and a maximum of 13% [156]. The asymmetric range around the best estimate value reflects the large uncertainty about the extent of microbial degradation of dissolved C-14 species in the gaps between stacks.

Vault 8 is rather atypical compared with the other vaults, because of the large inventory of organic wastes and the pucks that are assumed to release a high proportion of the C-14 in organic form. For comparison, the portion released to groundwater from the future vaults is 11%, reflecting the different materials inventories that are associated with the C-14.

For the small inventory of C-14 in the trenches, we have used SMOGG to provide an estimate of the total release rate for the gas assessment [94]. There is no information on the materials with which the C-14 inventory is associated in the trenches. Previously, an assumption was used that all C-14 was incorporated into cellulose and released as the cellulose degraded [53]. Instead, we have allocated the C-14 inventory to the same materials (steels, graphite, organics) and proportions as used for the Vault 8 inventory, although pucks and metal treatment wastes have been omitted since the operations in most trench predate use of these processes.

Figure 6.23 shows the resulting release rate for C-14 to gas, totalled over all the trenches, starting from the end of operations in Trench 1 (1963). The initial peaks for each trench are due to the quickly released organic fraction that is easily metabolised to methane and carbon dioxide. The gaseous releases from graphite, which in the absence of grout, includes the CO_2, contribute to the later hump, but the slow corrosion of the steels accounts for the releases continuing out to more than 2000 years [94].

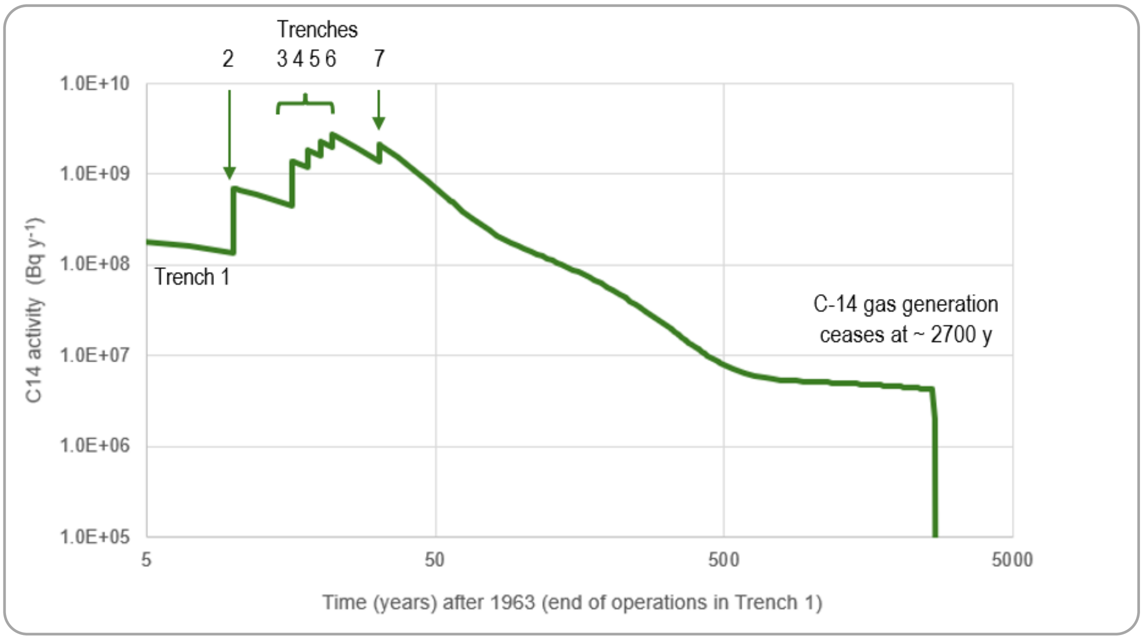

Figure 6.23: Total over all trenches of the C-14 gas release rate (Bq y^{-1}) from the wastes, beginning from the end of operations in Trench 1 [94]

6.6 Heterogeneity and Uncertainty

The results that have been presented above come from computational models, which are a representation of the real repository system.

The usefulness of the computational models relies upon including an appropriately comprehensive selection of the key features and processes. A feature of the real system that we have not discussed much is heterogeneity. Initially, water will percolate through a small number of defects in the geomembrane of the final cap. A fraction of the steel waste containers will develop perforations because of localised corrosion. Over time, the basal slabs of the vaults will crack, because their steel rebar will corrode, forming corrosion products which will exert stresses on the surrounding concrete. All these processes might influence the behaviour of the real repository system and therefore are discussed below.

In addition, the results depend, to some extent, on our selection of the model parameters, some of which are uncertain. A key parameter is the rate of infiltration through the final cap, for which we have determined both a mean value and a range of uncertainty (Figures 5-5 and 5-8 in reference [12]). Other uncertain parameters include the rates of waste degradation, and the permeabilities of the basal slabs in the vaults. Variant simulations were performed to evaluate the potential consequence of the uncertainties. Some results from a couple of variant simulations, one for a higher rate of infiltration through the final cap and another for a more rapid rate of corrosion, are shown below.

Heterogeneity

At early times, before the geomembrane in the final cap has undergone degradation, infiltration will occur through a small number of defects in the geomembrane [12]. We have developed models for the number of defects, and for the flows through each type [51].

When the geomembrane is installed, it will include pinholes (with areas up to 5 mm^2), holes (with areas up to 100 mm^2), and one or two tears. The lower bound, best estimate, and upper bound values for the areal density of these defects were elicited to be 5, 8, and 20 defects per hectare, respectively [49]. For comparison, there are slightly more than 600 stacks of ISO containers per hectare in Vault 8.

In addition, stress cracks will develop in the geomembrane over time. By the time that the geomembrane is just starting to experience more widespread degradation, we estimate that the mean number of small stress cracks (with a width of 1 mm and a length of 10 mm) will be 55 per hectare, and the mean number of larger stress cracks (with a width of 1 mm and a length of 100 mm) will be 25 per hectare [51].

The downwards flow of water will also be affected by the presence of wrinkles in the geomembrane. Wrinkles may develop, for example, because of daily temperature fluctuations leading to expansion and contraction of the geomembrane while it is still exposed at the surface. The key feature of a wrinkle that would potentially affect the flow of water through the geomembrane, is that once a wrinkle has developed there is no longer good contact between the geomembrane and the underlying material. That means where a defect is associated with a wrinkle, the water that flows through the defect can spread out beneath the wrinkle before flowing down through the underlying material. This effectively increases the size of the defect, and hence the magnitude of the flow, considerably. However, wrinkles and defects seldom coincide, with less than 1 per hectare at the time of installation.

The water flows through the pinholes and holes were determined to be initially in the range from 1 kg y^{-1} to 2 kg y^{-1}, and will increase slowly, so that by the time the geomembrane starts to undergo oxidative degradation they will be in the range from 6 kg y^{-1} to 9 kg y^{-1}. Compared with these flows through the pinholes and holes, the flows through the stress cracks will be about double, while the flows that would be associated with wrinkles will be about one and a half orders of magnitude larger.

An important point to notice is that these flows are approximately sufficient to maintain the water consuming (i.e. corrosion) reactions associated with a stack of ISO containers underlying a defect. It appears, from Figure 6.7, that the initial rate of water consumption by one stack of containers would be almost 3 kg y^{-1}, but this would reduce to just 0.4 kg y^{-1} once the aluminium in the waste has fully corroded.

The implication is that the stack of ISO containers located immediately beneath a defect could be relatively wet. However, any excess water would be expected to pool, before evaporating and diffusing as water vapour away from the region to neighbouring stacks of drier ISO containers, where the containers and their metal wastes will be corroding in a humid environment.

Even though water might trickle downwards from a defect over the surfaces of an isolated stack of containers at a significant rate, the migration of aqueous chemical species from the grouted wasteforms to the water is likely to be limited, partly because the flow will be focussed to a small region, and partly because the steel surfaces of the containers will remain largely intact, except perhaps in Vault 8 and Vault 9 where the process of surcharging is expected to buckle some corner posts and deform surfaces.

Interestingly, on the long timescale (i.e. one or two thousand years) that is required for infiltration through the final cap to become widespread, with the potential for onwards transport of contaminants into the geosphere, the components of the basal slabs (i.e. concrete slabs, geomembranes, and BES layers) in the vaults will have evolved as well. The effective permeabilities of the basal slabs will have increased to be only a little less than the vertical permeability of the surrounding geology. This means that although the basal slabs will provide a short-term barrier to the transport of contaminants out of the near field, they will not do so in the long term, when water starts to flow out of the near field.

Uncertainty

Many of the model parameters are uncertain to a greater or lesser extent. The uncertainty in the rate of water infiltration was examined in [51] by performing a variant simulation with an infiltration rate that was equal to our estimate of the mean value plus 2 standard deviations (Case C in Table 3.1) this corresponds to increasing the infiltration rate by a factor of approximately 20.

In this variant simulation, the water level rises once the geomembrane in the final cap has degraded, and most of the vault would become saturated within a few hundred years without the passive drainage system maintaining a lower water level. A comparison of Figure 6.24 and Figure 6.9 shows that alkaline conditions persist in the grouted wasteforms for the higher infiltration rate, with pH values that remain above 11.5 at 5000 years after closure. However, the faster flow of porewater in the profiling material above the stack of containers, in the vertical gap between the stacks of ISO containers, and in Unit B2, means that the pH is lower in those regions compared with the Reference case, falling to between 9 and 10.5.

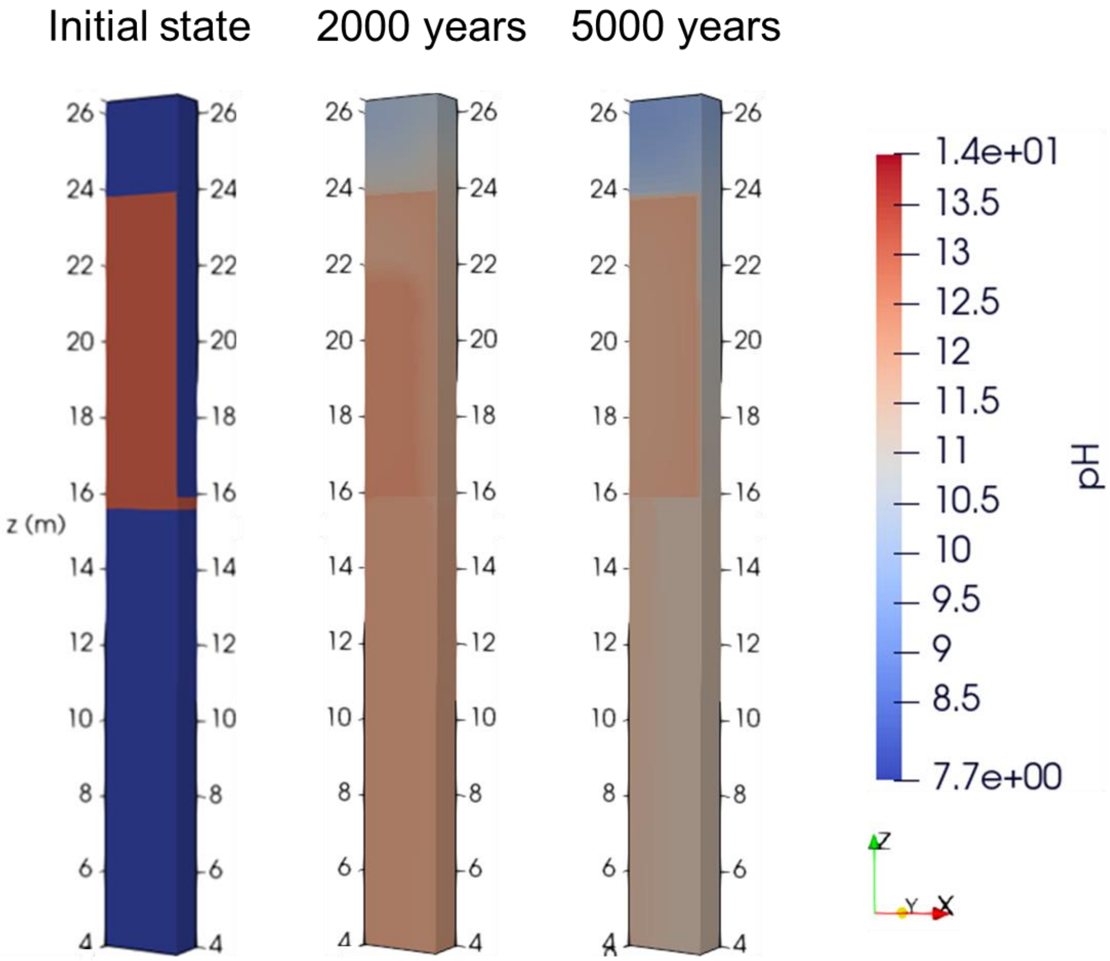

Figure 6.24: Evolution of pH in the grout (assuming Vault 8 average inventory) over 5000 years for the high infiltration (95th percentile) case, neglecting the presence of the six HHISO containers [51]

The uncertainties in the rates of waste degradation have been examined by varying the rates of water consumption and gas generation [51], which are proportional to the rates of metal corrosion.

For a simulation that doubled the rates of water consumption and gas generation, very slightly higher gas saturations develop within the stack of grouted wasteforms. Moreover, the flows of water into, and of gas out of, the grouted wasteforms change, which modifies the transport of contaminants.

Thus, the change in the corrosion rates affects the transport of ISA, as shown in Figure 6.25. This in turn impacts the complexation of uranium, its sorption onto the grout, and consequently the concentrations of aqueous uranium. The combination of different flow and complexation conditions leads to lower concentrations of aqueous U and Tc. With corrosion rates that are two times higher than those of the Reference case, the concentrations of U and Tc evolve as shown in Figure 6.26 (results compared with the Reference case).

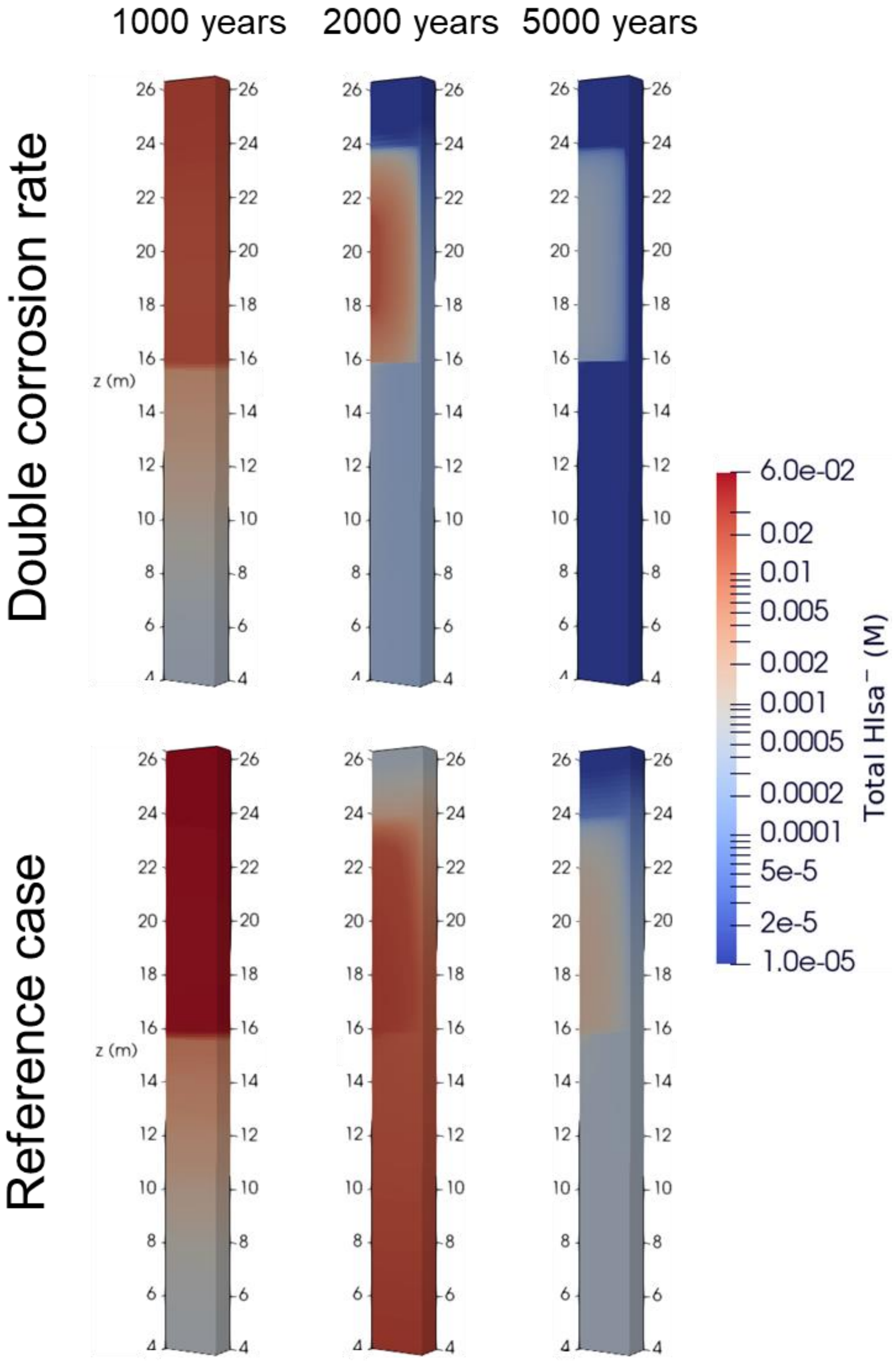

Figure 6.25: **Evolution of total aqueous ISA (assuming Vault 8 average inventory) over 5000 years, neglecting the presence of the six HHISO containers [51]. Concentrations simulated with a doubled corrosion rate (top) are compared with the Reference case (bottom)**

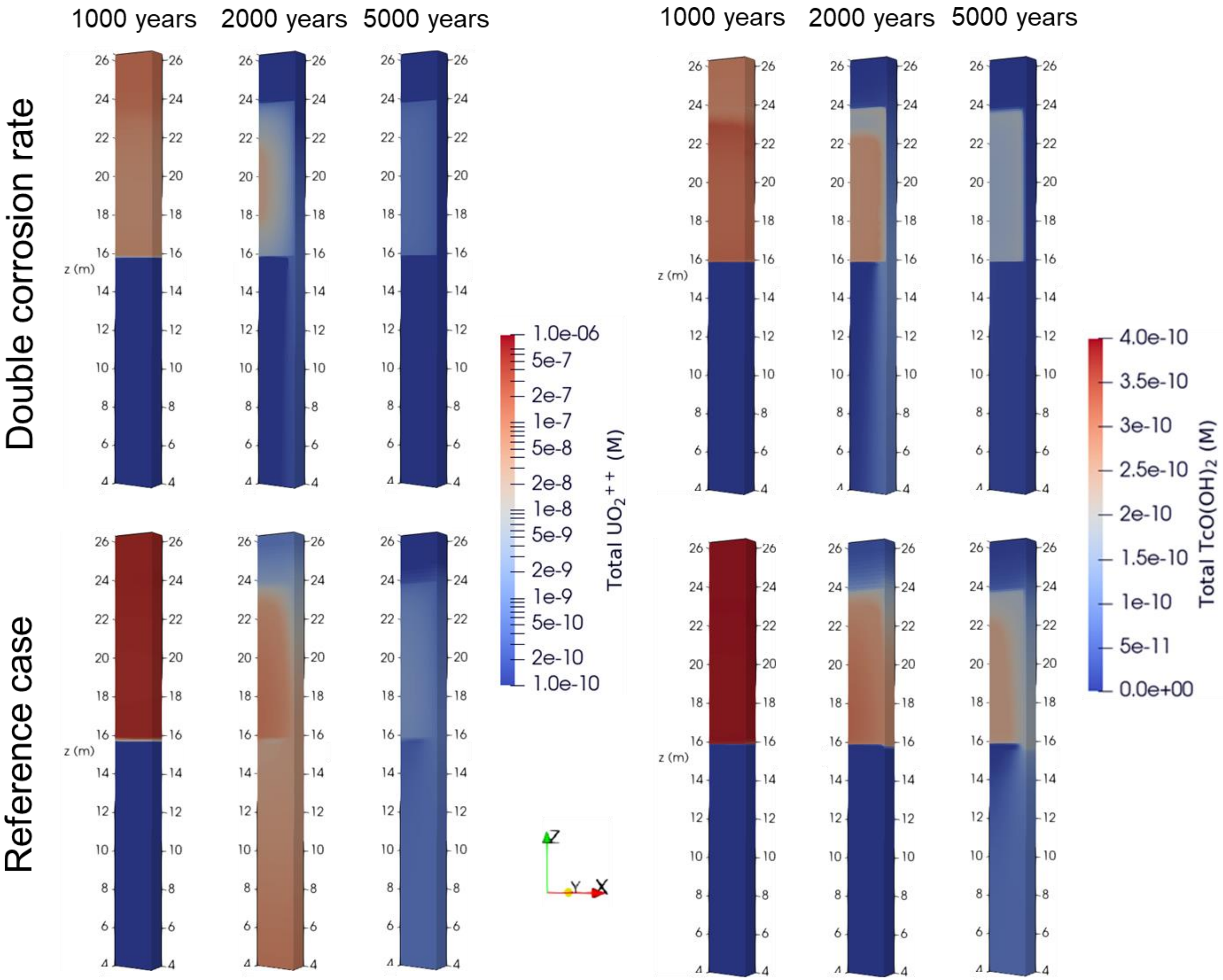

Figure 6.26: Evolution of total aqueous U and Tc (assuming Vault 8 average inventory) over 5000 years, neglecting the presence of the six HHISO containers [51]. Concentrations simulated with a doubled corrosion rate (top) are compared with the Reference case (bottom)

7 Gas Modelling

7.1 Modelling of Bulk Gas Generation

We have modelled bulk gas generation from the wastes using the Simplified Model of Gas Generation (SMOGG) software [157]. SMOGG is an enhanced spreadsheet calculator that accounts for metal corrosion and cellulose degradation to estimate bulk gas generation. There is no consideration of transport and it is assumed there is always sufficient water available, although corrosion rates for unsaturated conditions can be specified. The mass and thickness of each metal (used to calculate a corroding surface area) and the mass of cellulose are the input parameters. Different corrosion processes and rates (e.g. aerobic, anaerobic, acute and chronic) and cellulose degradation pathways, using nitrate or sulphate, can be used to simulate an evolving system.

Model outputs inform several components of the ESC. In particular, estimates of bulk gas generation support our understanding of how near-field conditions, such as saturation conditions in the vaults, may evolve over time. The bulk gas generation rate also helps to determine the rate at which radon, generated in the waste mass, will be transported to the biosphere as part of the radiological gas assessment [46].

The model for bulk gas generation represents both the trenches and the vaults [94]. The modelling period extends from 1963, marking the end of operations in Trench 1, to the year 7135, corresponding to 5000 years after the final planned disposals in Vault 12 (in 2135). The whole inventory in each trench or vault is assumed to be emplaced at the time of the end of operations in a trench or vault and then to be immediately available for gas generation. In order to maximise the production of gas, we take no account of any corrosion or degradation that occurs before emplacement.

Vaults 9 and 9a are treated together but the wastes are split into 'existing and committed' and 'future' because the existing disposals and committed wastes in both vaults will be surcharged and capped in one tranche before the latter. Thus, the following figures distinguish between 'Vault 9 + 9a committed' and 'Vault 9 + 9a future' (or 'V9+V9a C+D' and 'V9 + V9a F' on figures).

The SMOGG calculations are documented in reference [94] and the results are the focus of this subsection.

Waste and container metal corrosion

For the trenches, we model corrosion of stainless steel and carbon steel (Figure 7.1). Other metals are excluded, either due to their negligible presence in the waste inventory, or because they are expected to corrode very slowly under the conditions anticipated in the trenches, so their contribution to gas generation is minimal compared to that of the steels. presents the masses of metallic wastes modelled in the trenches [4]. In both the trenches and vaults, it is assumed that the inventory can start degrading and corroding under anaerobic conditions as soon as operations cease.

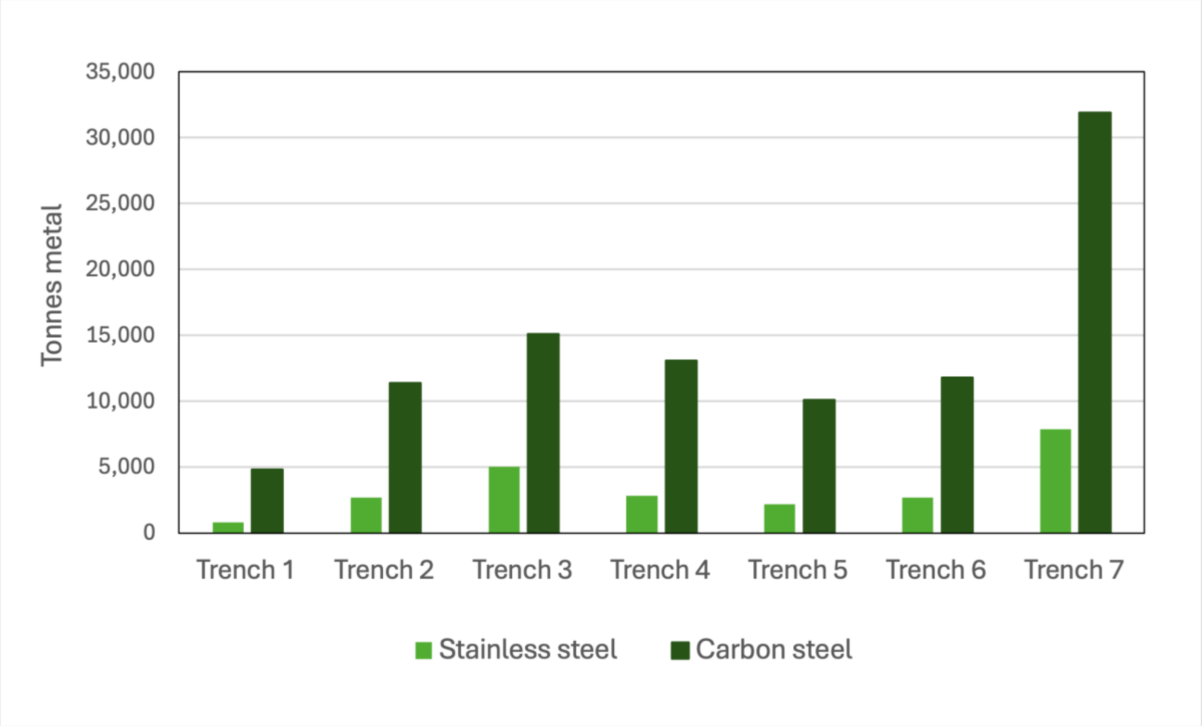

Figure 7.1: **Mass of waste metals used to estimate bulk gas generation in the trenches [4]**

For the vaults, we include stainless steel, carbon steel (waste and containers), Magnox, and aluminium in the modelling. The masses modelled for each vault are shown in Figure 7-2.

The carbon steel waste inventory includes the mass of unknown ferrous metals, which is expected to be largely carbon steel, as well as the estimated mass of steel associated with the drums and boxes used in the waste compaction process. We adopted this approach to address uncertainties in the inventory breakdown, particularly for Vault 8, and ensure a cautious representation of metal masses and associated gas generation within the vault environment.

In both the trenches and vaults, gas generation from corrosion is modelled using a single linear corrosion rate and assuming the metal is in the form of a sheet with a fixed surface area. The metal sheet is assumed to corrode from both sides. The nominal thickness is shown in Table 7.1 along with the mean of the elicited pdfs for the corrosion rates for the different environments [55, 77]. This simple geometry is not realistic as, for many items, it is likely the surface area will decrease. For example, thinner areas will effectively disappear when they are fully corroded while thicker ones will corrode for longer. However, we consider that this assumption will cautiously over-estimate the rate of gas generation compared to modelling some part of the inventory as spheres, thus a decreasing surface area, or more complex shapes.

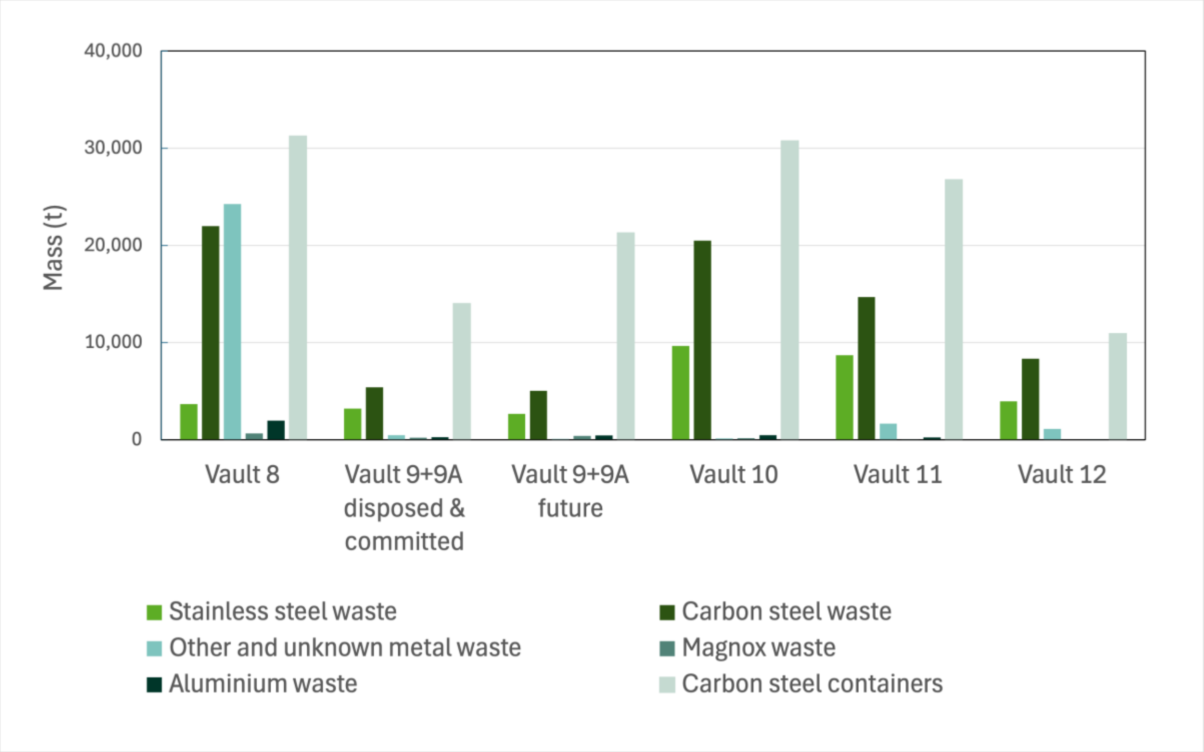

Figure 7.2: Mass of waste and container metals in the vaults [4]. Note that 'other' and 'unknown' metal is included in carbon steel waste

The nominal thickness of the HHISO containers takes account of the thinner (3 mm) walls and lid, and thicker structural elements (~12 mm) and base. The corrosion of the containers is also modelled using the higher corrosion rate for the external surface and the lower, high pH value for the internal surfaces. The initial thickness is divided *pro rata* between them.

Table 7.1: Mean corrosion rates and thickness for metals in trenches and vaults

Metal	Trench corrosion rate[1]	Vault corrosion rate[2] [158]	Nominal Thickness [93]
Carbon steel	1.87 μm yr^{-1} [75]	4.64 10^{-3} μm yr^{-1}	5 mm
Stainless steel	0.398 μm yr^{-1} [159]	4.22 10^{-4} μm yr^{-1}	2 mm
Magnox	n.d.	0.1 μm yr^{-1}	2 mm
Aluminium	n.d.	1 μm yr^{-1}	2 mm
Container (external)[3]	n.a.	0.34 μm yr^{-1} [75]	7 mm

1 Conditions are near-neutral pH, anaerobic conditions [75] [159];

2 Conditions of grouted wastes are anaerobic and pH 12.5 to 13 (termed 'early vault' in reference [158]);

3 Conditions outside the containers are unsaturated, anaerobic, near-neutral conditions [75].

Cellulose degradation

For the trenches, gas generation from cellulose degradation is a significant contribution to the overall bulk gas. As discussed in Subsection 4.3.2, the pH conditions in the grouted wastes will restrict microbial processes so cellulose degradation will not be a significant contributor to the vault bulk gas phase.

The mass of cellulose in each trench was determined from the total of paper, cotton, wood, other cellulosics, and unknown cellulosic materials reported in the inventory [4]. While certain forms of cellulose, such as paper and cotton (sometimes termed Type 1 cellulose), are generally more susceptible to microbial degradation, others, such as wood (Type 3), are considered largely unreactive due to their high lignin content [43]. We account for the unreactive proportions of the two cellulose types but the same degradation rate is used for both. The total cellulose masses are shown in Figure 7.3 for each trench.

The rate of cellulose hydrolysis was 4.50 10^{-3} y^{-1}, based on data from the LLWR Gas Monitored Trench Simulant (GMTS) experiments [160, 161] that were used to calibrate the GRM used in the 2011 ESC [53] and subsequently the SMOGG hydrolysis rate [160]. We have recently reviewed the cellulose degradation rate [52]. The revised rate of 7.50 10^{-3} y^{-1} means that the early gas generation from cellulose is faster, but more of the gas is generated during the PoA when the gas vent will be open. This would not be a cautious choice for the radon assessment (see Subsection 8.2) as it implies that the post-PoA bulk gas velocities would be lower, thus decay of radon in transit out of the repository would be higher, than with the experimental value. Therefore, we have retained the original value as used in GRM in 2011.

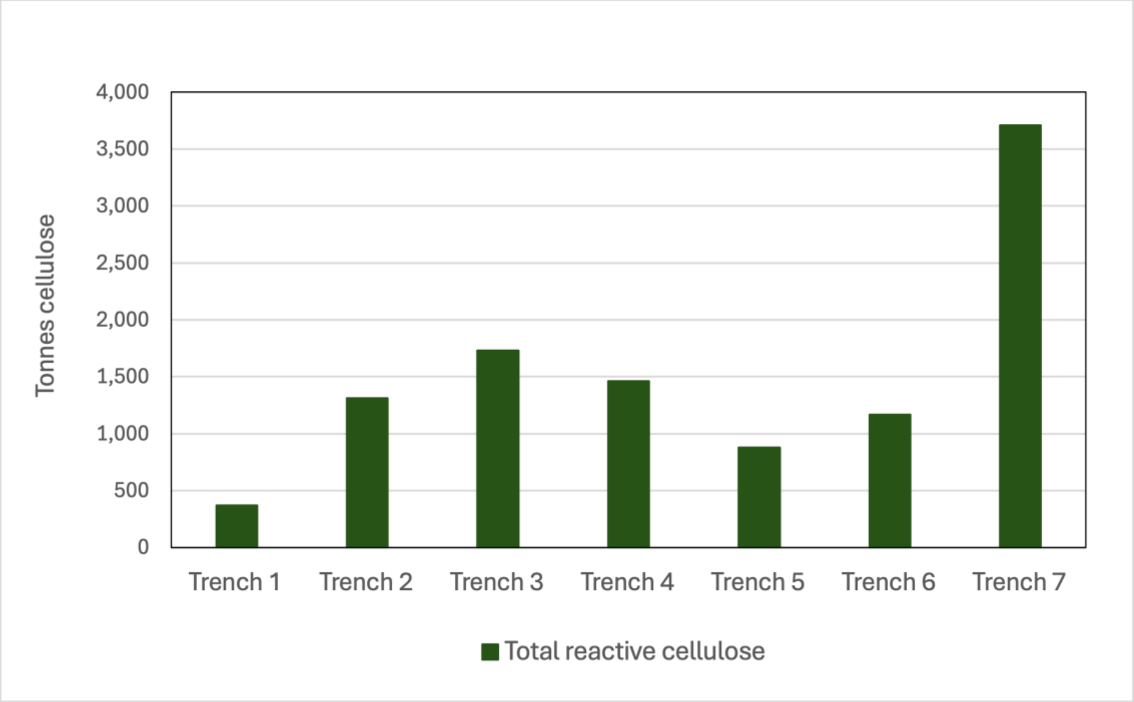

Figure 7.3: Mass of degradable cellulose considered in the trenches [94]

In modelling gas generation from cellulose degradation we assume a yield of 80% under all conditions to account for the substrate consumed to sustain the microbial populations involved in the reactions, and a 3:1 ratio of methane to carbon dioxide generation for anaerobic methanogenesis [160]. Nitrate- and sulphate-reducing conditions are also modelled, but for the quantities of nitrate and sulphate assumed to be present, these conditions only persist for a few years, so have minimal impact on the gas generation.

7.1.1 The Trenches

The calculated profile of gas generation for Trench 1 is shown in Figure 7.4. Gas generation rates are calculated in moles per year but shown in cubic metres per year, assuming standard temperature (25° C) and pressure (1 bar), to allow comparison with the GRM results [53]. In the SMOGG model, the dominant process is hydrogen generation from metal corrosion, with a smaller contribution from methane from cellulose degradation. In all trenches, until the metal is corroded, the carbon dioxide generated is consumed by reaction with hydrogen. Therefore, the methane generation rate includes a contribution from this reaction, while the hydrogen generation is slightly reduced.

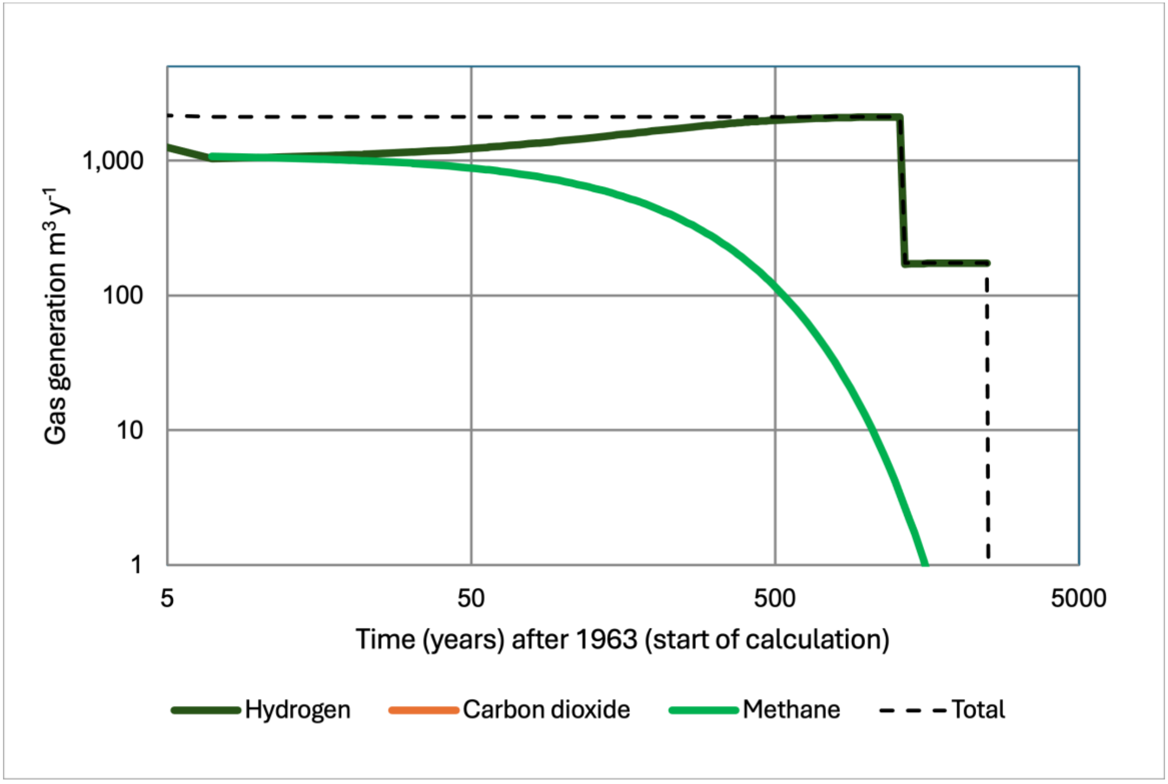

Figure 7.4: Bulk gas generation from Trench 1 calculated using SMOGG [94]

Over the first 1,000 years or so, methane generation gradually decreases, while hydrogen generation apparently increases. This is due to the gradual degradation of cellulose, resulting in less CO_2 production, thus less hydrogen consumed by the methanogenesis reaction. In fact, H_2 generation from metal corrosion remains constant, as the assumed surface area of the metal does not change, until the full thickness is corroded.

Within 1,000 years most of the cellulose has been degraded, so the subsequent gas generation is largely hydrogen from metal corrosion. A drop in hydrogen generation is seen after approximately 1,300 years, corresponding to the complete corrosion of carbon steel. After around 2,500 year the stainless steel is also completely corroded so gas generation ceases. In Trench 1, after the metal is fully corroded by 2487 years, there is still a very low continued production of methane and CO_2 (total of less than 1 mol y^{-1} or 12 dm^3 y^{-1}) from the remaining cellulose.

The dominance of hydrogen in the bulk gas modelling results is not consistent with the observations from monitoring of the trenches. The implications of the monitoring data are discussed in Subsection 4.2.1, however, there are aspects of the modelling that are simplified and may also contribute as discussed in Subsection 7.3.

The results for Trench 1 are representative of gas generation trends calculated for each of the other trenches. The total gas generation profile for all seven trenches is shown in Figure 7.5. The obvious difference in the total gas generation rate profile is the stepped increase over the first few decades resulting from the time at which the calculations begin for each trench, according to their closure date. The series of peaks in the hydrogen curve can be seen to predate each increase in methane, indicating reaction of CO_2 to generate additional methane, as in Figure 7.4.

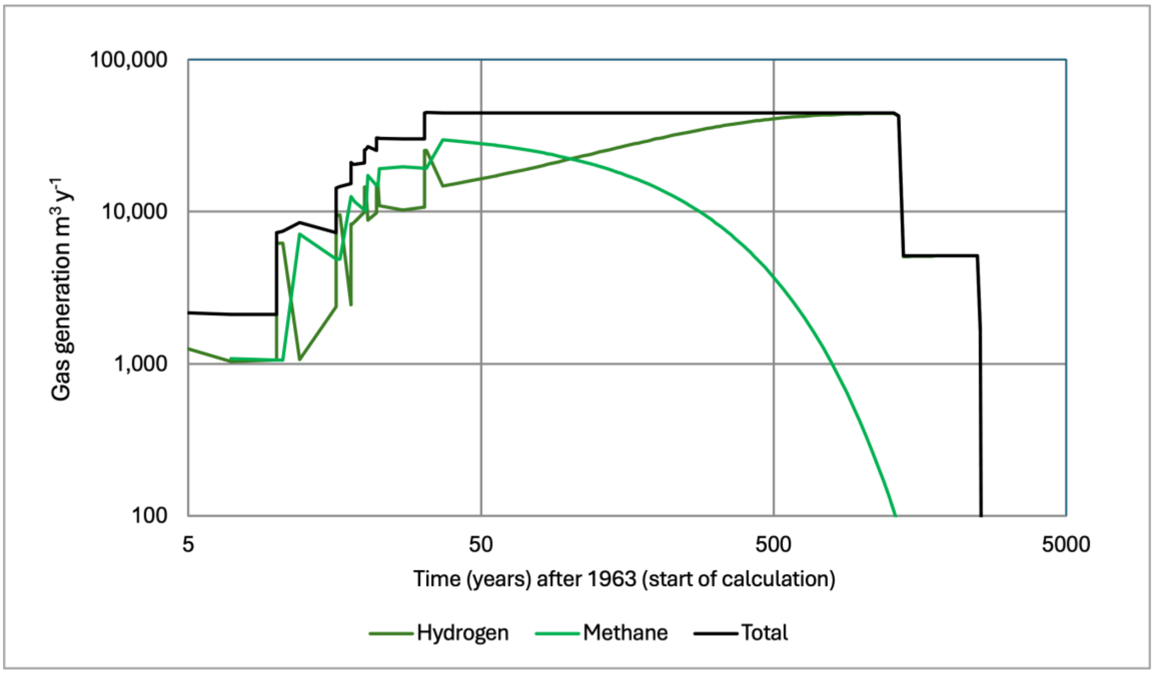

Figure 7.5: Total bulk gas generation from the trenches calculated using SMOGG [94]

The cumulative gas generation in cubic metres from the trenches is shown in Figure 7.6. Comparison with similar plots from GRM calculations for the 2011 ESC [20, p. 106] shows that the volume of gas generated in the trenches is greater in the SMOGG calculations by about an order of magnitude, and also the main period of gas generation lasts for more than 2500 years compared with less than 1000 years in the GRM calculations.

The differences in the modelling results are due to the slower corrosion rate used in the SMOGG calculations, as well as the more complete biogeochemical model used in GRM to fully account for biomass and losses of cellulose degradation products to groundwater. While the SMOGG modelling provides a cautious estimate of gas generation for use in the assessment of radon releases, in future we will need to provide more realistic results to support the engineering decisions around gas management and the design of the vent.

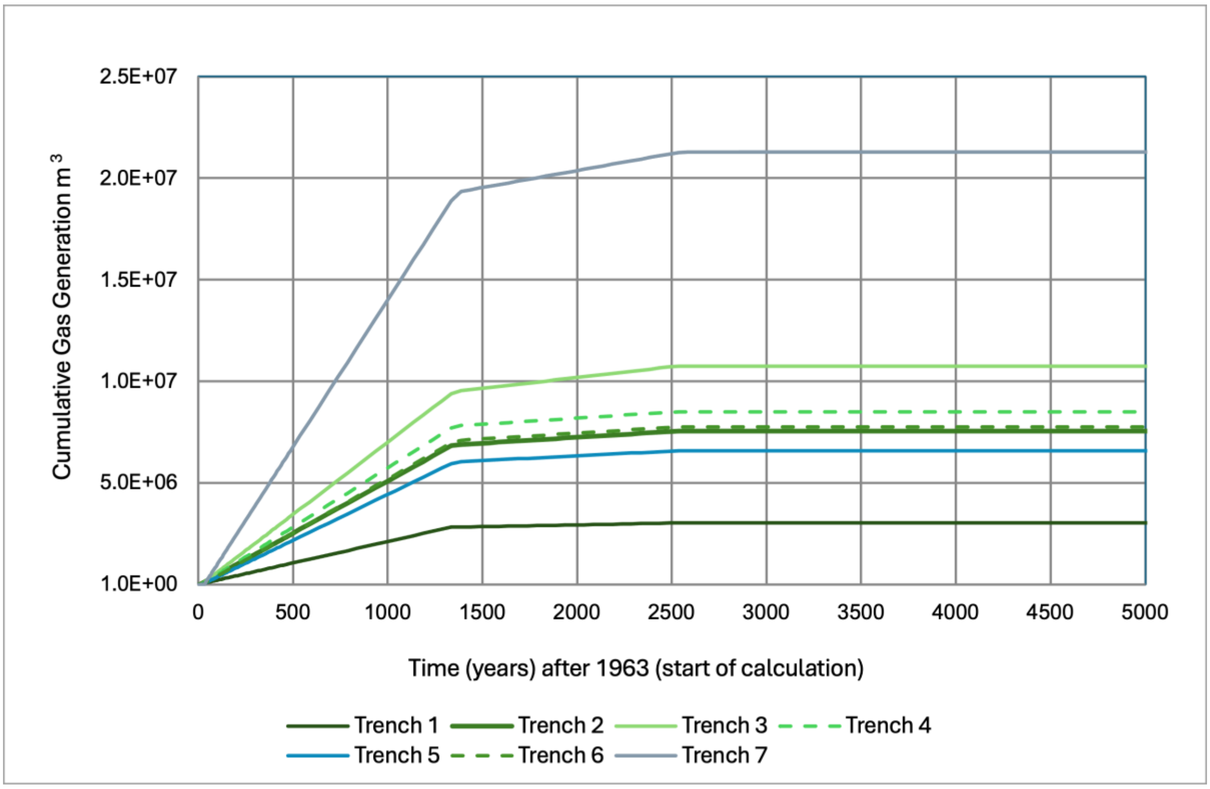

Figure 7.6: Cumulative gas generation from the trenches [94]

7.1.2 The Vaults

The calculated gas generation profile for the vaults is shown in Figure 7.7. Hydrogen generated from the corrosion of metal wastes and containers is the sole contributor.

For each vault, from the start of the calculation, gas generation rate is constant for about 1,000 years followed by a reduction corresponding to the complete corrosion of aluminium. From this time, hydrogen generation continues until beyond 5,000 years as the result of the corrosion of the containers, along with smaller contributions from corrosion of Magnox and steel wastes.

In the calculations, it is assumed that there is no restriction on corrosion due to water availability. As discussed in Subsection 6.5.1, it is possible that conditions outside the containers become very dry in the period of low infiltration rates. The water associated with the grout means that the slow corrosion of waste metals is less likely to be restricted. Consequently, the calculated gas generation from the container external surfaces (see also

Figure 6.7) may be an overestimate for the first 1000 years whereas that for the waste metals may be a better estimate.

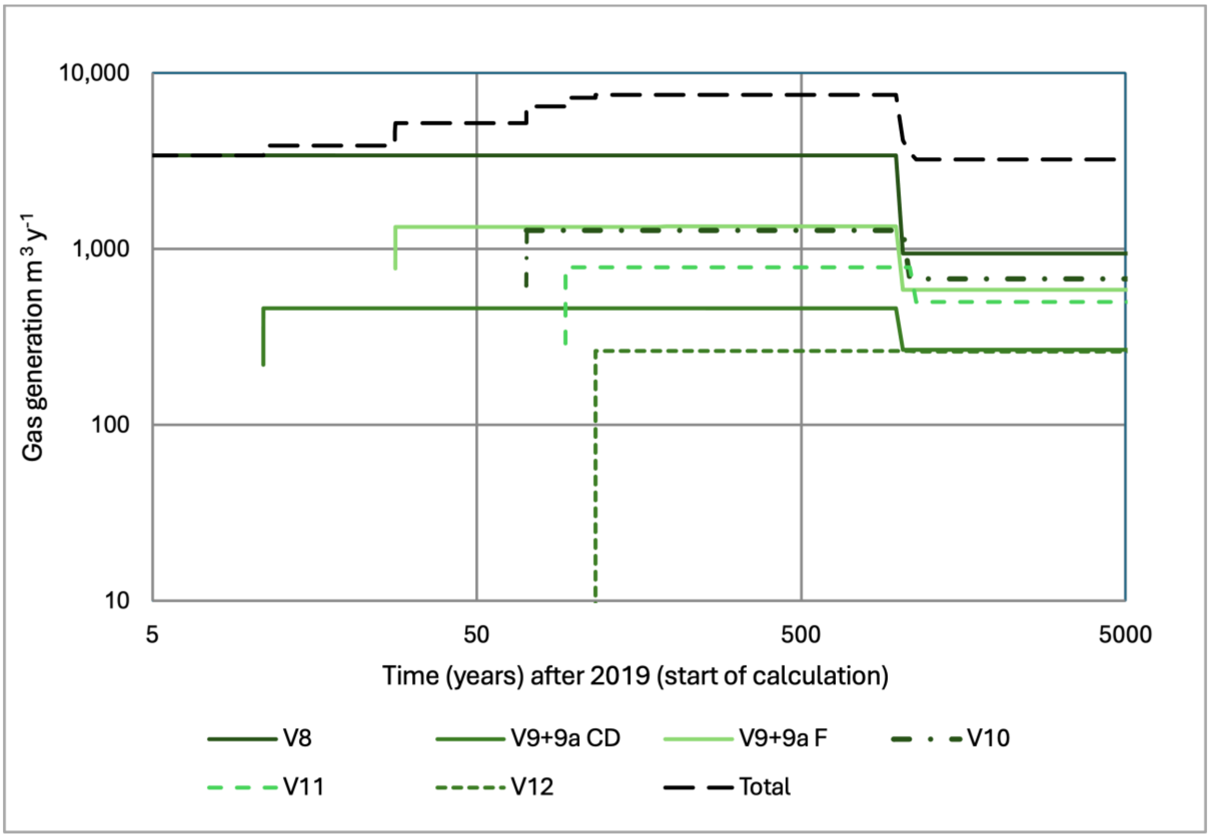

Figure 7.7: **Hydrogen gas generation from the vaults calculated using SMOGG [94]. (V: vault; CD: disposed and committed wastes in Vaults 9 and 9a; F: future wastes Vaults 9 and 9a)**

In vaults with larger aluminium inventories, however, the calculated gas generation over the first ~1,000 years is mainly due to corrosion of aluminium waste. In Vault 8, for example, more than 75% of the gas is from aluminium corrosion. In contrast, in Vault 10, only 50% of the gas is from aluminium, and in Vault 11, 40%. Uncertainty in the H_2 generation rate in Vault 8 will, therefore, be more dependent on uncertainty in the aluminium corrosion rate, and particularly whether corrosion could dry out the grout locally. This may depend on whether the aluminium is sufficiently well distributed in the containers so that there is enough water in the surrounding grout to support its corrosion, or whether its rapid corrosion rate will exceed the rate of water transport within the grout. We have not evaluated the distribution of the metals inventory at the level of detail - on an individual container basis - required to answer this question, so the uncertainty remains.

It is clear that the vault bulk gas calculation is subject to a number of uncertainties that are difficult to evaluate, but the assumptions we have made ensure we have erred on the side of caution in our calculations.

7.1.3 Changes since the 2011 ESC

As indicated by comparison of Figure 7.5 and Figure 7.7, generation of bulk gas from the trenches will dominate the repository for about 2500 years. This is an important difference from the 2011 GRM results [53] and is largely the result of substantial changes to the corrosion rates following re-elicitation to account for more recent corrosion data and the higher pH conditions in the grouted wastes [55, 77]. For example, the mean corrosion rate of carbon steel in the vaults has fallen from 1 micron per year to 5 10^{-3} μm y^{-1} for waste and 0.34 μm y^{-1} for the outside of the containers (Table 7.1). There have also been changes to the vault material inventory, and masses of steels and cellulosic wastes, in particular, have fallen significantly. Some changes are associated with the evolving future inventory, for example, lower arisings of both organic wastes and steels than previously forecast as a result of greater diversion of wastes [4]. The disposals in Vault 8 have, however, undergone some adjustments to correct a data processing error that have resulted in the metals inventory falling from 182,000 t to 50,000 t [4].

7.2 Integrated Gas Modelling for Gas Management and Engineering

We have calculated that a large amount of bulk gas will be generated after closure of the LLWR (Subsection 7.1). It is therefore important to ensure suitable management of this gas such that it does not compromise the performance of the facility. Bulk gas generation can affect safety in several ways:

- Build-up of gas pressure within the facility could disrupt the engineered barriers, particularly the barrier function provided by the BES and geomembrane layers in the cap.
- Migration of bulk gas out of the facility could provide a pathway for the rapid release radionuclides that can form gaseous species (i.e. C-14 and radon) to the biosphere.
- The bulk gases generated are also flammable, so their release could be a direct safety concern if released at a sufficient rate into e.g. a building such that they are not able to rapidly disperse resulting in the formation of a flammable gas mixture.

These effects must be addressed through suitable engineering of the facility to provide the required management of the generated gas.

To support gas management, it is first necessary to understand how generated gas will migrate through the near field of the LLWR, and the resulting gas pressure build up and fluxes and locations of gas release from the facility. We have performed two-phase flow modelling of the trenches and vaults to provide this understanding [155]. This subsection summarises this work and discusses the results but reference [155] provides the full description of the models used in the study and further results.

7.2.1 Key modelling data and assumptions

We have undertaken two-phase flow modelling using the TOUGH2 software[10] [162]. The version used includes enhancements to:

- Allow consideration of multi-component two-phase flow – this means that the different gases present or expected to be generated can be modelled explicitly, which is important in understanding the gas mix present for comparison with observations and to allow reactions that are dependent on the presence of specific gases (i.e. oxygen) to be modelled.
- Include a bespoke representation of the gas generation reactions within the waste, depending on the waste inventory (and for metals, the thickness) and the presence of oxygen and water that are both key reactants affecting the gas generation.
- Include extended two-phase flow functions allowing better representation of the variation of flow properties of the near-field materials with saturation.

The parameters required to determine gas generation and migration behaviour in the model include waste inventory and degradation rates, material properties for components described in the model, and boundary conditions such as the water infiltration rate. In addition, the assumptions and simplifications made in defining the model geometry and extent are important. The model, parameter definition and assumptions are described in full in reference [155]. Here we have summarised only the main details and the key results.

To make running simulations practicable, the models we have developed are two dimensional. So that key features are reasonably represented, the models are cylindrical and axisymmetric. We model the trenches and vaults separately so that features specific to each can be more easily represented. For the trenches, since there are no significant barriers to fluid migration between the wastes in each trench, the waste in all the trenches is modelled as a single region. For the vaults we represent each vault individually in the model so that potentially key features of the engineering around each vault can be included in the model. The geometry of each model is shown in Figure 7.8 and Figure 7.9. Note that the height of the models has been scaled by a factor of ten for convenience of presentation, so angles appear exaggerated (e.g. the top surface has a gradient of only 1:25).

---

[10] The TOUGH (Transport Of Unsaturated Groundwater and Heat) suite of software codes are multi-dimensional numerical models for simulating the coupled transport of water, vapour, non-condensable gas, and heat in porous and fractured media [162]. Developed at the Lawrence Berkeley National Laboratory (LBNL) in the early 1980s primarily for geothermal reservoir engineering, the suite of simulators is widely used in modelling gas flow at different scales for geological disposal of nuclear waste. For application to the highly heterogeneous LLWR repository, we found it necessary to eschew the more recent versions (i.e. TOUGH-MP and TOUGH3) for the older TOUGH2 running in double-precision and allowing modifications to simulate bulk gas generation.

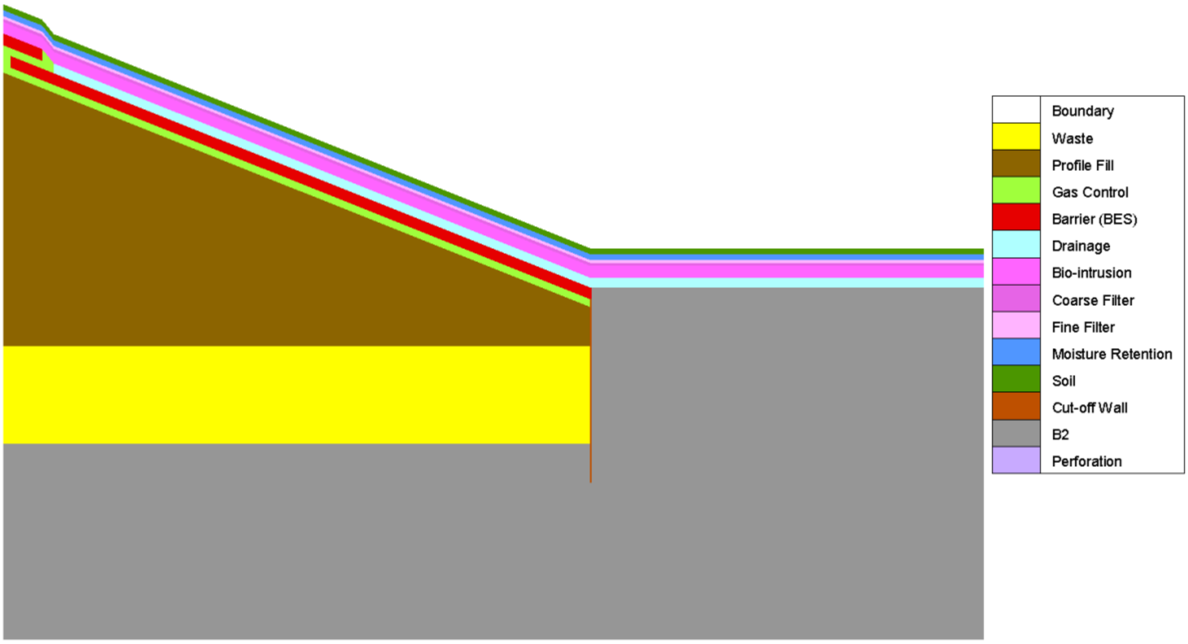

Figure 7.8: Geometry of axisymmetric model used to simulate two-phase flow in the trenches with the model axis on the left. The vertical axis has been scaled up by a factor of ten [155]

The models include all the key engineering features of the repository and its immediate surroundings. This means that we include in the model the waste, profile fill, each of the layers in the cap, the cut-off wall on the outside of the repository, and the B2 unit underneath and to the sides of the repository. For the vaults we also include separate representations of the grouted waste within containers and the 'gaps' between containers (not shown in Figure 7.9) and the individual vault bases with short 'walls' around their perimeters. A key simplification for the model of the vaults is that the relative position of each vault is not preserved, but the volume of each is. The model has been developed to represent Vaults 8 to 14, but we have not included any materials in Vaults 13 and 14 in the calculations since these vaults are not expected to be filled based on the assumed disposal inventory [4].

We expect the features of the cap to be particularly important in understanding gas migration from the repository. Each layer of material in the cap is represented explicitly, with the exception of the geomembrane since this is too thin. The properties of the geomembrane are represented implicitly by suitable modification of the properties used for the BES. A gradient is included so the height of the cap increases from the outer edge to the centre. The cap is expected to have an annular vent at its approximate centre – the cylindrical geometry chosen allows a good representation of this structure. The vent is designed with a downward gradient of the outward flow path between the barrier layers of the cap to ensure gas flow outflow while preventing water inflow.

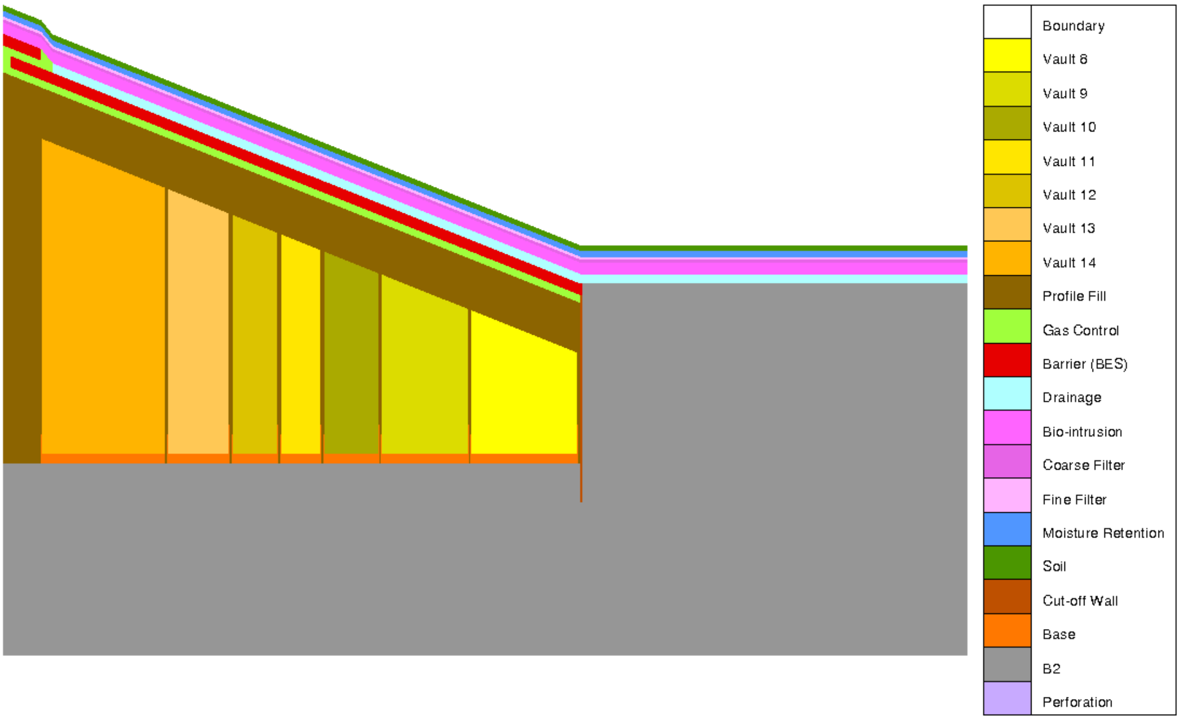

Figure 7.9: Geometry of axisymmetric model used to simulate two-phase flow in the vaults with the model axis on the left. The vertical axis has been scaled up by a factor of ten [155]

The inventory data are very similar to those used for the SMOGG calculations, as described in Subsection 7.1. Most of the degradation (i.e. gas generation) rate data are also the same as those used in the SMOGG calculations. However, for these calculations we included appropriate rate data for aerobic conditions that are expected to be prevalent initially, before the anaerobic conditions assumed in the SMOGG calculations are established. The inclusion of aerobic degradation is expected to have only a small effect on the overall gas generation, since these conditions are expected to persist for only a short period [155].

Rates and paths of fluid migration within the repository are determined by the flow properties of the materials. The key properties of the materials are their permeabilities, along with porosities and relative permeability and capillary pressure functions. Certain materials are intended to provide barriers to fluid migration, so their properties relative to the other materials are important. The main barriers to fluid flow in the repository are the BES and geomembrane layers in the cap, and the cut-off wall. In addition, the grout within packages and the concrete vault bases provide some further barriers to fluid migration. To provide an indication of the relative barriers to fluid migration provided by different repository features, the initial permeability in each part of the trench model is shown in Figure 7.10. The permeability of B2 is anisotropic, so the geometric mean is shown for this unit.

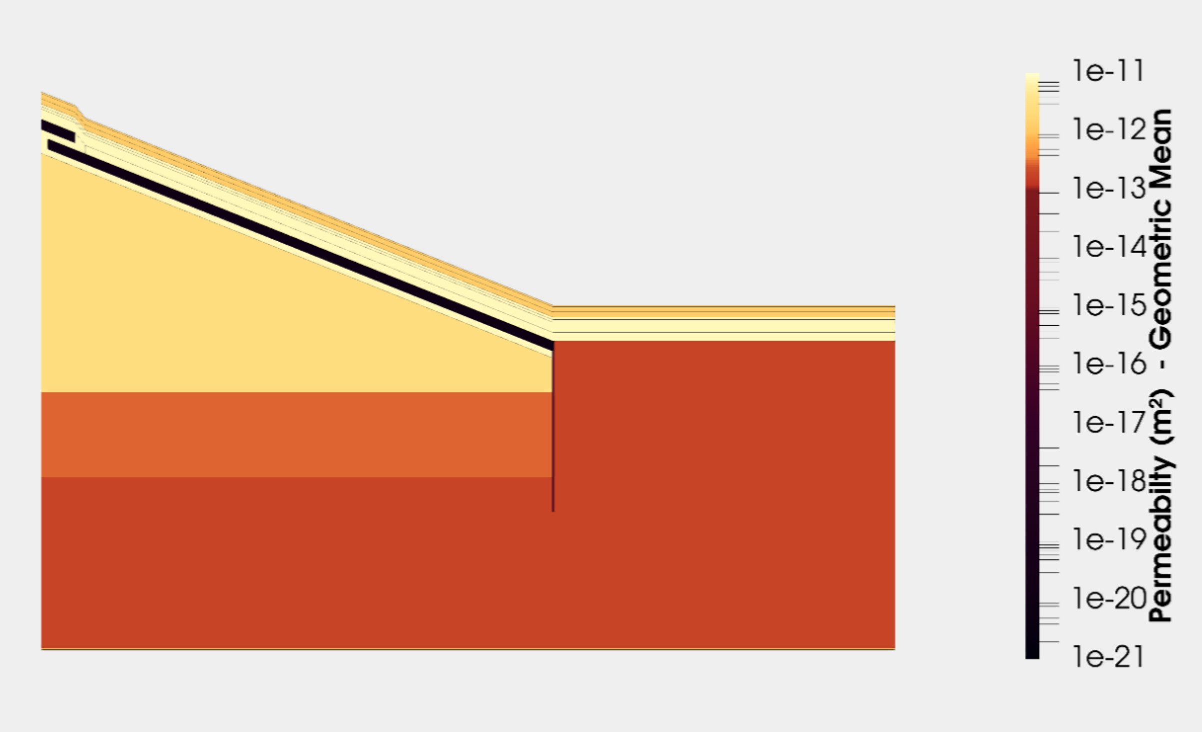

Figure 7.10: Permeability of each part of model used to simulate two-phase flow in the trenches. The vertical axis has been scaled up by a factor of ten [155]

We also recognise that the properties of the key barriers evolve significantly [12]. We represent this in the models by specifying time-varying permeabilities for the BES-geomembrane composite layer and the cut-off wall. The permeabilities of these materials are assumed to increase by several orders of magnitude over the 5,000-year period simulated [12]. We have specified the variation in the permeability of the BES-geomembrane composite layer to account for both the gradual evolution of the BES and the relatively more rapid degradation of the geomembrane.

We represent infiltration into the model by applying a water inflow rate to the top of the model. The permeability of the BES-geomembrane composite, along with the sloped surface providing drainage of the water away from the repository through the upper layers of the cap, then ensures that the expected, evolving infiltration into the repository occurs. Finally, we assume that the bottom and outer edges of the modelled region remain undisturbed, so constant boundary conditions are applied here.

7.2.2 Modelling results

Simulations using the models described above provide understanding of the pressurisation of the repository and of the gas flow paths and magnitudes out of the repository. The expectation is that, with the vent present in the cap (as shown in Figure 7.8 and Figure 7.9), gas will be released relatively easily, preventing significant pressure build up, but potentially resulting in releases of flammable and or radioactive gases at rates that may present challenges to safety. In contrast, it is expected that the impacts of focussed gas releases could be avoided by closing the vent at a suitable time, but this could result in significant pressurisation. We have run simulations with both the trench and vault models in which the vent is either left open or closed (by setting the properties and saturation of the vent grid blocks equal to those of the BES-geomembrane composite) at the end of the PoA.

As discussed in Subsection 7.1, we expect gas to be generated at a greater rate in the trenches than in the vaults for at least 2000 years. Given this, and that the volume of the trenches and vaults parts of the repository are comparable, gas build up or release are expected to be more marked when considering the trenches than the vaults. Therefore, we focus here on the modelling results for the trenches.

Considering first the pressure evolution in the trenches for both the vent open and vent closed cases. After an initial equilibration period, the maximum pressure within the repository (which at most times occurs in the BES) increases before stabilising around 1000 years after the start of the calculation (see Figure 7.11 which shows the pressure at two key locations for each case). The greatest pressure increase occurs in the BES, with lower increases and more rapid stabilisation in the underlying materials (Figure 7.11 and Figure 7.12).

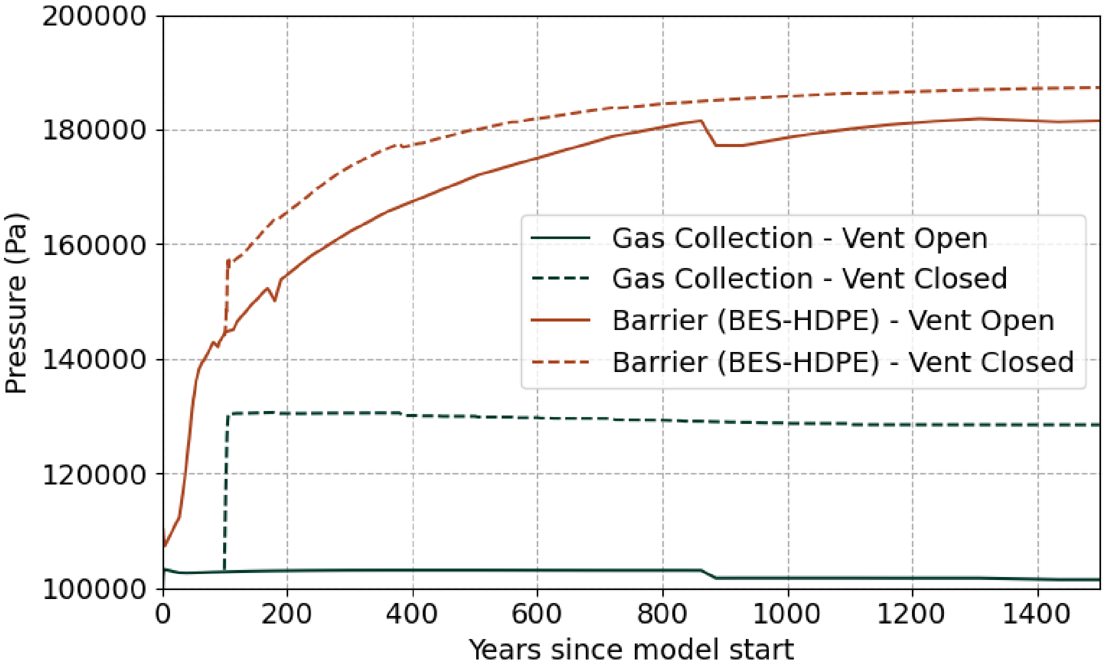

Figure 7.11: Gas pressure evolution in a grid block near the outside edge of the BES (red lines) and a grid block in the gas collection layer adjacent to the vent (black lines) for the two trench simulation cases [155]. Note that the vent is closed after 100 years, and the case are identical to that point

The maximum pressure reached in the repository occurs in the BES and is about 195 kPa. This pressure is only slightly lower for the case in which the cap remains open compared with the case in which the cap is closed. This pressure is greater than the downward pressure on the BES exerted by the overlying cap materials, so is potentially sufficient to displace the cap materials. However, the gas saturation in the BES is very low (< 1%,

Figure 7.13) so care is needed in interpreting the significance of the calculated gas pressures in this layer.

At such low saturations, gas is expected to exist dispersed and isolated in individual pores, so it is not clear that the pressure within this dispersed gas phase would have a mechanical influence on the surrounding materials at a sufficient scale to cause meaningful displacement. Furthermore, the model uses a single compound layer to represent the properties of the combination of BES with overlying geomembrane. In reality, the geomembrane can separate from the BES since gas (or water) can flow along the interface between them, allowing gas to escape more easily from the defects in the geomembrane. We have not yet investigated the implications of our description of the compound BES-geomembrane layer with detailed, small-scale modelling to determine the veracity of the results.

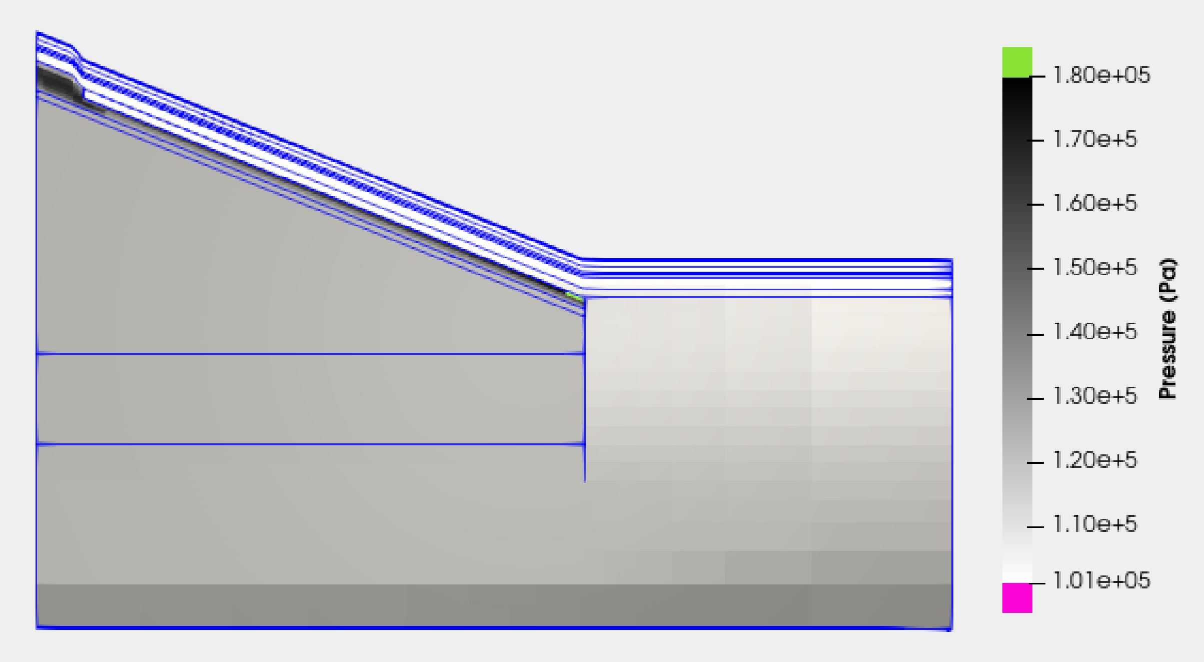

Figure 7.12: Gas pressure distribution in and around the trenches 1,500 years after closure, assuming closure of the vent at the end of the PoA. The vertical axis has been scaled up by a factor of ten [155]

Outside of the BES, the highest gas pressures occur in the gas collection layer. In contrast to the pressure in the BES, the presence of the vent has a significant effect on the maximum pressure reached in the gas collection layer. As shown in Figure 7.11 with the vent closed the pressure in the gas collection layer reaches about 130 kPa, whereas it remains below 105 kPa after the PoA if the vent remains open. The gas saturation in the gas collection layer is high, so these pressures will be exerted on the surrounding materials. However, the highest pressure reached with the vent closed is approximately the same as the downward pressure exerted by the overlying cap materials. Given the cautious approach to calculating the bulk gas volumes, this suggests the potential for displacement of, or damage to, the cap is marginal. If the vent remains open, this issue appears to be mitigated.

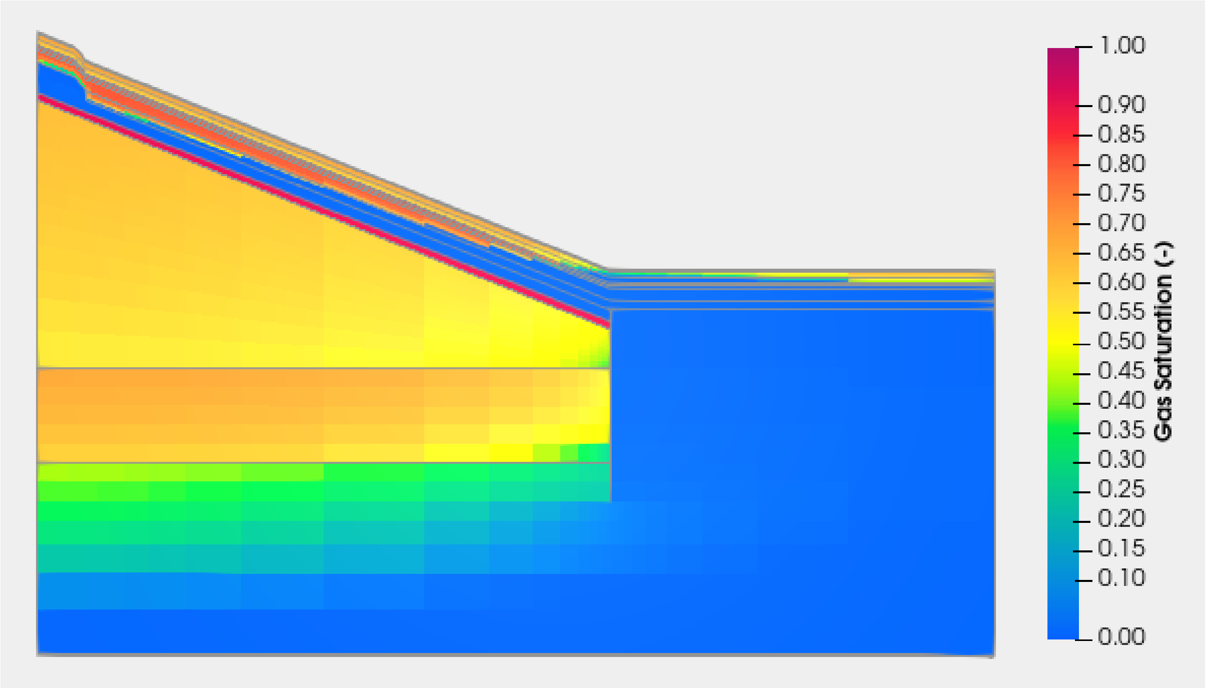

Figure 7.13: Gas saturation distribution around the trenches 1,500 years after closure, assuming closure of the vent at the end of the PoA. The vertical axis has been scaled up by a factor of ten [155]

Considering the gas flows out of the near field of the trenches, in the first 100 years (during which the vent is open) two distinct gas flow paths become established. The first path is the expected path upward from the waste, through the profile fill, into the gas collection layer and out through the vent. The second path is out of the bottom of the trenches into B2 (and to a much lesser extent out of the side through the cut-off wall), after which the gas migrates horizontally outward before dispersing more widely through B2 outside the repository area. This second path requires the build-up of a gas phase (i.e. desaturation) in B2 under the trenches (e.g. see Figure 7.13). Given the very low infiltration rate of water and significant gas generation, this desaturation is expected. However, it is notable that this results in an additional path for outflow of gas from the trenches.

The significance of the two gas flow paths and their evolution is shown in Figure 7.14. Over the first 100 years most of the gas is released via the vent. After this time, if the vent is assumed to be closed, the downward path provides the main route for outflow of gas. The gas flow rate via this route remains significant relative to the gas generation rate such that pressure build up with the repository is limited to that described above (i.e. the outflow can be accommodated via this route with only a moderate pressure rise). If the vent is assumed to remain open, gas outflow occurs primarily via the vent, resulting in lower maximum pressures compared with the vent closed case (i.e. the outflow can be accommodated with minimal pressurisation above hydrostatic conditions with the exception of the pressure in the BES).

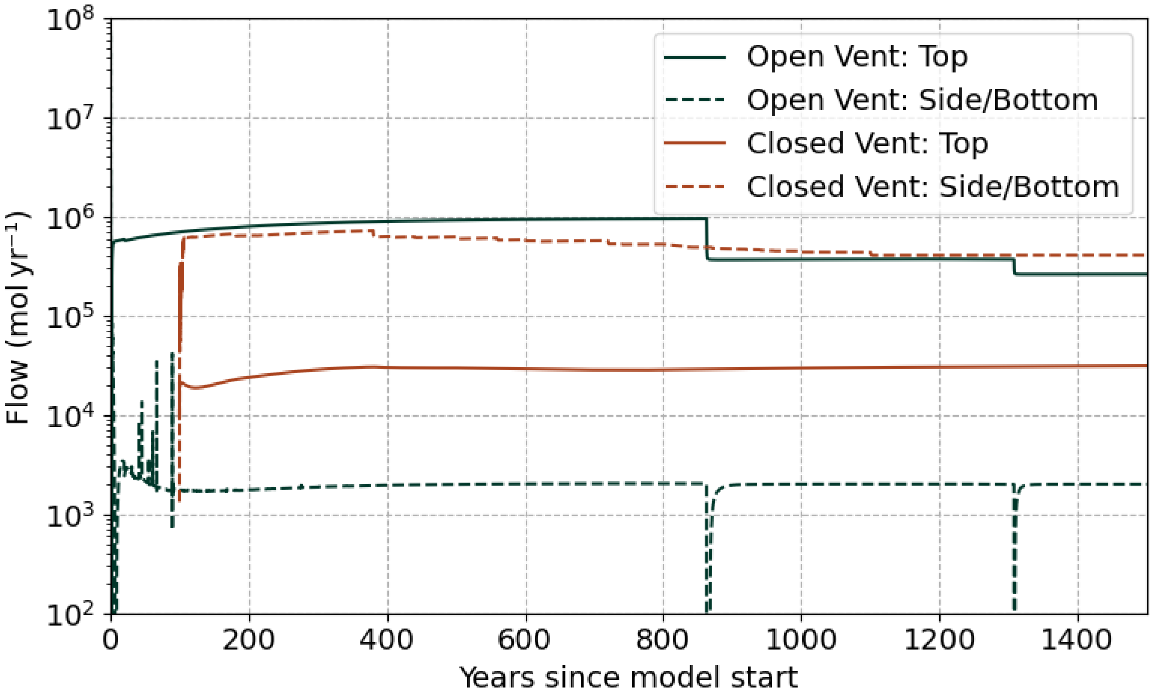

Figure 7.14: **Gas flow evolution across the bottom and outside of the trenches and across the top of the trenches for the two trench simulation cases [155]**

7.3 Discussion of the Gas Modelling Results

The SMOGG results for the trenches differ substantially from the observed gas generation provided by trench monitoring data (see Section 4.2.1). These data indicate that the gases currently being generated are predominantly methane and carbon dioxide, with only very low levels of hydrogen being measured. This discrepancy may be partly due to the current conditions under the interim cap differing from those expected after emplacement of the final cap. Specifically, it is possible that the conditions in parts of the trenches are currently aerobic, suppressing hydrogen generation, promoting carbon dioxide generation and associated consumption of hydrogen generated in anaerobic parts of the trenches. However, our understanding should improve as more monitoring data are gathered following installation of the replacement membrane over the southern trenches, and then the final cap over the northern trenches, which will ensure fully anaerobic conditions develop. This understanding should then be used to justify or revise the assumptions made in the modelling.

The SMOGG modelling is, however, simplified compared with the complex biogeochemical system of the trenches. In particular, we have cautiously assumed anaerobic conditions from the start of the calculations with no attempt to model the evolution from the early aerobic state, as was done in the GRM simulations for the 2011 ESC [53]. This simplification has the effect of overestimating hydrogen production. In addition, we assume that all the steel is available to corrode immediately. It is likely that a proportion of the metal will have been protected, for example by paint coatings on metal drums, the inside of sealed drums, and metal items disposed within other containers. This will have delayed and reduced corrosion, leading to further overestimation of hydrogen generation in the SMOGG modelling.

In addition, there is some uncertainty in the cellulose hydrolysis rate. The rate used for these calculations is a factor of three lower than recommended for the estimation of methane generation from landfills [163] and also lower than the rate recommended in other recent work [52], although it is consistent with the value used in the 2011 GRM modelling [53] that was based on gas generation experiments (see, for example, reference [138]). Such a difference can affect the composition of the gas generated initially, that is, before sufficient hydrogen is generated to react with the carbon dioxide, as well as on the duration of gas generation from cellulose degradation. We consider the degradation rate for landfills is too high because the waste composition is different and, most importantly, the temperature is lower because the amount of degradable and putrescible material is not sufficient to raise the temperature in the repository. The review [52] suggested a degradation rate 40% higher than used in this work but came too late to be used across all the affected near-field calculations

The TOUGH2 gas modelling study [155] also uses the low cellulose hydrolysis rate assumed in the SMOGG calculations. The calculated generation rates indicate a gas composition in the trenches dominated by methane, with a significant carbon dioxide presence and only minimal hydrogen for about the first 60 years of the simulation. However, after this time (as the cellulose inventory reduces) the gas composition evolves to become hydrogen rich as the availability of carbon dioxide to react with the hydrogen reduces such that there is no longer a sufficient supply to react with all the hydrogen continuing to be generated.

This study also calculates the gas generation in the vaults to be much lower than in the trenches, in agreement with the SMOGG results presented in Subsection 7.1. It is worth noting that in neither the TOUGH2 modelling nor the SMOGG modelling was any effect of the drying vaults considered in terms of potentially reduced corrosion rates. In this respect, we expect the calculated gas generation rates from the vaults to be cautious. Although the saturation in the trenches will fall, it is unlikely that humidity levels would fall to the extent that corrosion and degradation were significantly limited by water availability.

The two-phase flow modelling for the trenches indicates relatively low pressurisation in the near field irrespective of whether or not the cap vent is left open after the PoA. Higher pressures are calculated within the BES-geomembrane composite layer but, given the very low gas saturation, the implication for integrity of the low permeability barrier is unclear and will need to be further investigated. We also conclude that any consequences of gas generation identified from the modelling of the trenches will be greater than for the vaults (i.e. calculations for the trenches provide the bounding case). Further, in terms of the whole repository, the calculated results for the trenches will be cautious, since there will be no substantial barrier to gas migration between the vaults and the trenches. This means that gas generated in the trenches would be expected to spread out within the vaults, equalising pressures across the repository and reducing the maximum pressure, relative to those calculated for the trenches alone.

These results indicate that both pressurisation of the repository and the significance of different gas outflow paths from the repository depend on the assumed properties of the BES-geomembrane composite, B2 unit and possibly the cut-off wall as the main barriers in the system. Therefore, to fully understand the potential for pressurisation and possible gas releases from the repository, uncertainties in the properties of these materials need to be taken into account. In general, the elicitation of barrier properties carried out as part of the EPA [12] was considering only water flows, and multi-phase flow parameters required for gas transport modelling were not determined. As a result, we drew on other studies (e.g., references [164, 165] and see also reference [43]), which are not specific to the LLWR engineering components and do not consider their evolution, to determine appropriate multi-phase flow parameters for the modelling. This is particularly important when considering the timescales and the likelihood that multi-phase flow parameters will change in a similar way to the hydraulic properties elicited for the engineered structures.

In summary, there remains uncertainty in the rates of gas generation processes, which could significantly affect the behaviour of the system. So, while some understanding can be drawn from the work summarised above, additional work would be beneficial to provide a comprehensive understanding relating to gas. We therefore consider the current studies as an initial phase that we will build on in support of future work on design and optimisation of gas management structures (see Subsection 9.2.1).

7.4 Hazards Associated with Flammable, Explosive and Toxic (non-rad) Gases

No work was undertaken as part of the gas modelling studies reported here to consider the hazard associated with flammable, explosive or toxic gases.

Based on a previous study [136], however, we do not expect any toxic gases to be of concern. In this study [136], scoping calculations were conducted for the gas pathway for hydrogen sulphide. This gas is toxic and very flammable, with a maximum airborne concentration of 0.1 ppm (approximately 0.1 mg m^{-3}) and explosive limits in air of 4.3% to 46% by volume (Appendix C of reference [136]). GRM modelling predicted hydrogen sulphide to be present at partial pressures (normalised to the total pressure) of around 1 10^{-10} in the vaults, and between 1 10^{-4} and 1 10^{-3} in the trenches [136]. The value for the vaults is very low and hydrogen sulphide generation in the vaults can be neglected. Above the trenches, the equilibrium concentration in an enclosed structure located over Trench 7 is estimated to be 2 10^{-3} ppm, which is almost two orders of magnitude lower than the maximum airborne concentration of 0.1 ppm [136]. There is also potential for hydrogen sulphide to oxidise during migration to the surface, suggesting that concentrations are likely to be considerably lower than calculated. This study also ruled out potential hazards from carbon dioxide (toxicity) and methane and hydrogen (flammability and explosion), concluding in the latter case that hydrogen will tend to be consumed by microbial processes, thus is not considered to be a safety issue at the LLWR [136].

In the radon gas assessment, we have re-considered the hazard associated with hydrogen for the case of a house constructed over the vent. This model cautiously assumes that all the bulk gas released from the area of the vent covered by the house travels upwards into the house with no benefit taken for features of the house such as a damp-proof membrane, that could divert the gas around the walls. The purpose of the modelling is to assess the impact from radon, rather than flammable gas, and cautious assumptions for ventilation rate are used. The results indicate that a house located on the vent could build up about 0.2% hydrogen [46], compared with the 4% H_2 usually taken as the lower explosive or flammable limit (LEL) for hydrogen in air at 25 °C. For house located over a defect in the geomembrane through which bulk gas release could be focussed, the hydrogen build up is even lower at around 0.003%. This takes no account of any hydrogen consumption by microbial processes.

Although the potential for hydrogen build-up in dwellings and other buildings on the cap will be taken into account in the future consideration of gas management (see Subsection 9.2.1), these results suggest the hazard is not likely to be significant.

8 Representation in Assessments

The preceding sections have illustrated the complexity of the near-field evolution and the processes that determine the release, fate and transport of contaminants. It is not practical to represent this complexity in assessment models which instead must use a representation that encompasses the key aspects and simplifies the details in a cautiously realistic way. The following two subsections consider the representation of the near field in the two main exposure pathway models. Subsection 8.1 describes the groundwater pathway model that is used for both the radiological assessment [126] and the HRA [15]. Subsection 8.2 describes the gas pathway models for the assessment of radon and C-14-bearing gases [46].

8.1 Groundwater Pathway

The GoldSim groundwater assessment model used for the 2011 ESC [166] was updated in 2018 [167]. A key improvement introduced at that time, in response to a recommendation from the Environment Agency, was to include both the PoA and the post-PoA ('long-term') radiological assessments into a single integrated assessment model. Further improvements have been made for the 2026 ESC [126] to account for the changed conceptual model for flow and contaminant transport.

The integrated assessment model consists of a compartment flow model (CFM) to provide the water flows to the near-field model, a geosphere model and a biosphere model. The integrated model is capable of simulating contaminant release and transport during the construction and operation of the LLWR as well as during the long post-closure period.

The groundwater assessment model was also updated in 2018 to account for changes in the geological and hydrogeological models. Site investigations since 2018 have meant further changes in these areas [6] that are now represented in the assessment model, in addition to other changes reflecting improved understanding of barrier performance.

In developing a simplified representation of the LLWR, a model based on connected, well-mixed compartments for the LLWR near field has been adopted. In summary [126]:

- The near field is modelled as a series of well-mixed compartments in which average waste properties (e.g., density and porosity) are assigned to each compartment. In the 'uniform flow' model, each vault is modelled as a single component, whilst the trenches are sub-divided into a series of components.
- Water flows through the repository are modelled, accounting for infiltration through the cap as a time-varying boundary condition, and potential inflows into the repository from the surrounding geology. Water flows are calculated using a CFM that is informed by more detailed hydrogeological modelling.
- The near field is parameterised based upon the best understanding of the anticipated chemical conditions and of the evolution of the LLWR engineered barriers, which is accounted for in the CFM.

- All radiological contamination is assumed to be accessible by water.
- Radionuclides are assumed to be instantaneously released from their bound state in their associated wasteform, and immediately available for dissolution in infiltrating water.
- The rate of release to solution of some non-radiological contaminants associated with the metallic component of the waste is determined by the metal corrosion rate.
- Non-radiological contaminants associated with non-metallic wasteforms are assumed to be released to solution immediately on contact with porewater.
- Contaminants are subject to solubility limits and linear, reversible sorption parameterised appropriately for the chemical conditions in the trenches or vaults.
- Under the “uniform flow” model for the vaults, it is assumed that all porosity within the compartments is accessible to water and it is further assumed that water flows through this connected porosity.
- Under an alternative “dual porosity” model for the vaults, there are no water flows through the containers and contaminants diffuse out of the waste stacks into the gaps between the stacks. Water flows from these gaps into the underlying geology. In this model, individual stacks of containers are considered and one well-mixed compartment representing the gaps between the stacks.
- The model calculates concentrations of contaminants in near-field compartments, which become fluxes with the CFM flows between near-field compartments and thence to the geosphere compartments.

It is clear from this summary that there are several aspects of the near field for which the representation includes simplifications and assumptions. The key aspects are discussed further below.

Near-field water flows

The trenches are not currently saturated and, like the vaults, are likely to remain partially unsaturated (Subsections 3.5 and 4.2.1) for all of the period before the site is disrupted by coastal erosion. The GoldSim model treats the trenches and vaults similarly, with the model components split into an upper unsaturated compartment and a lower saturated compartment (Figure 8.1). Both compartments are well-mixed. Flows of water can then move dissolved contaminants from the saturated compartment to the compartments representing the underlying geology. The boundary between the saturated and unsaturated portions of a compartment is determined by the CFM and will move as the saturation of the vaults or trenches evolves with time.

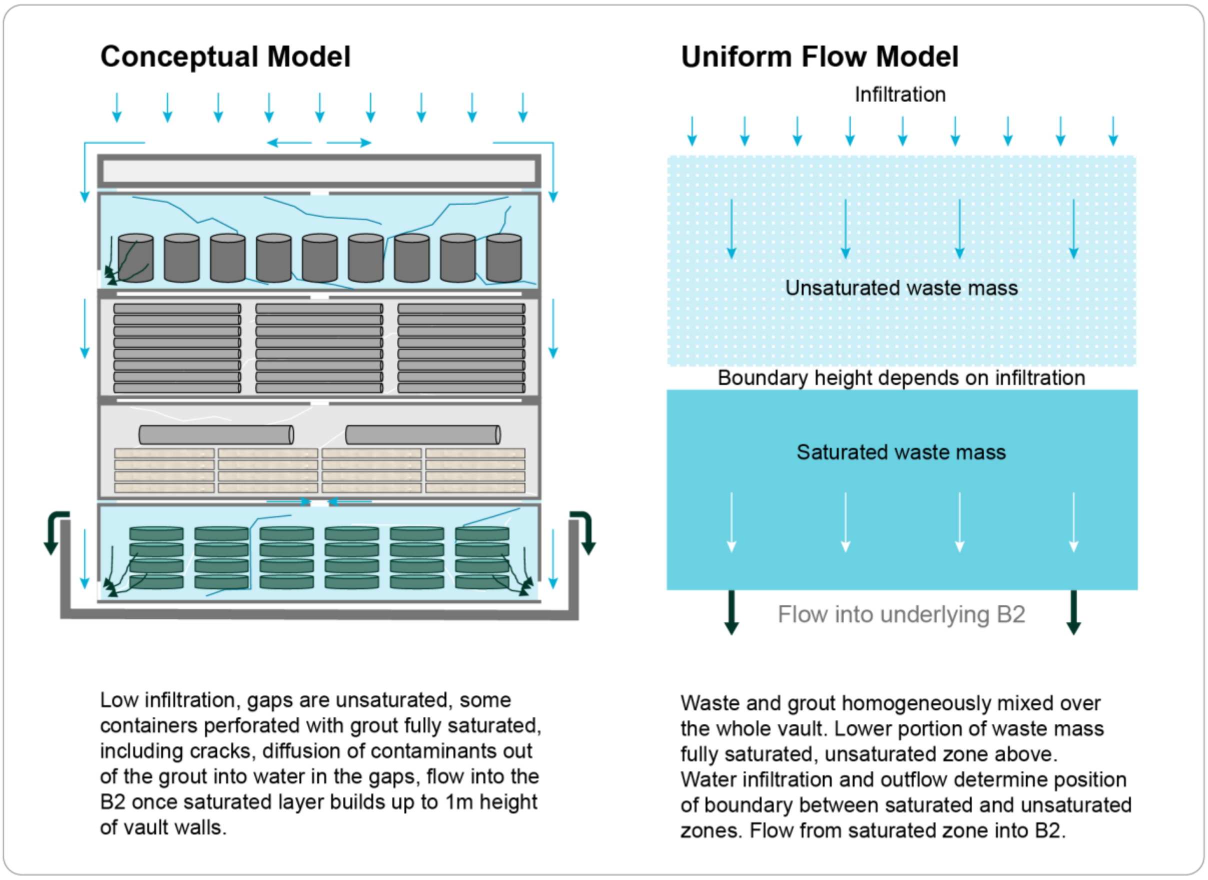

Figure 8.1: Comparison of the near-field conceptual model for the vaults and the groundwater assessment uniform flow model

This is a reasonable representation of the trenches, in which infiltration through the cap can drain more or less vertically through the porous waste and cover soils, leading to an approximate separation into saturated and unsaturated regions, as observed in the monitoring described in Subsection 4.2.1.

Infiltration in the vaults, however, is expected to flow largely through unsaturated gaps between the stacks of containers within which the grout is close to saturation initially (Subsection 3.4.1). Thus, the saturated volumes are surrounded by unsaturated gaps.

As the purpose of assessment models is to calculate transport of contaminants and thus understand system performance, rather than improve our phenomenological understanding, geometrical simplifications that accurately (or at least cautiously) represent behaviour of the key system features are acceptable. In the groundwater assessment, the bias caused by the simplified division into saturated and unsaturated portions of the vaults and the associated uniform flow of water through the waste mass can be evaluated by comparison with a 'dual porosity' model [126] that explicitly represents the grouted wasteform and the unsaturated gaps between them (Figure 8.2), as described below.

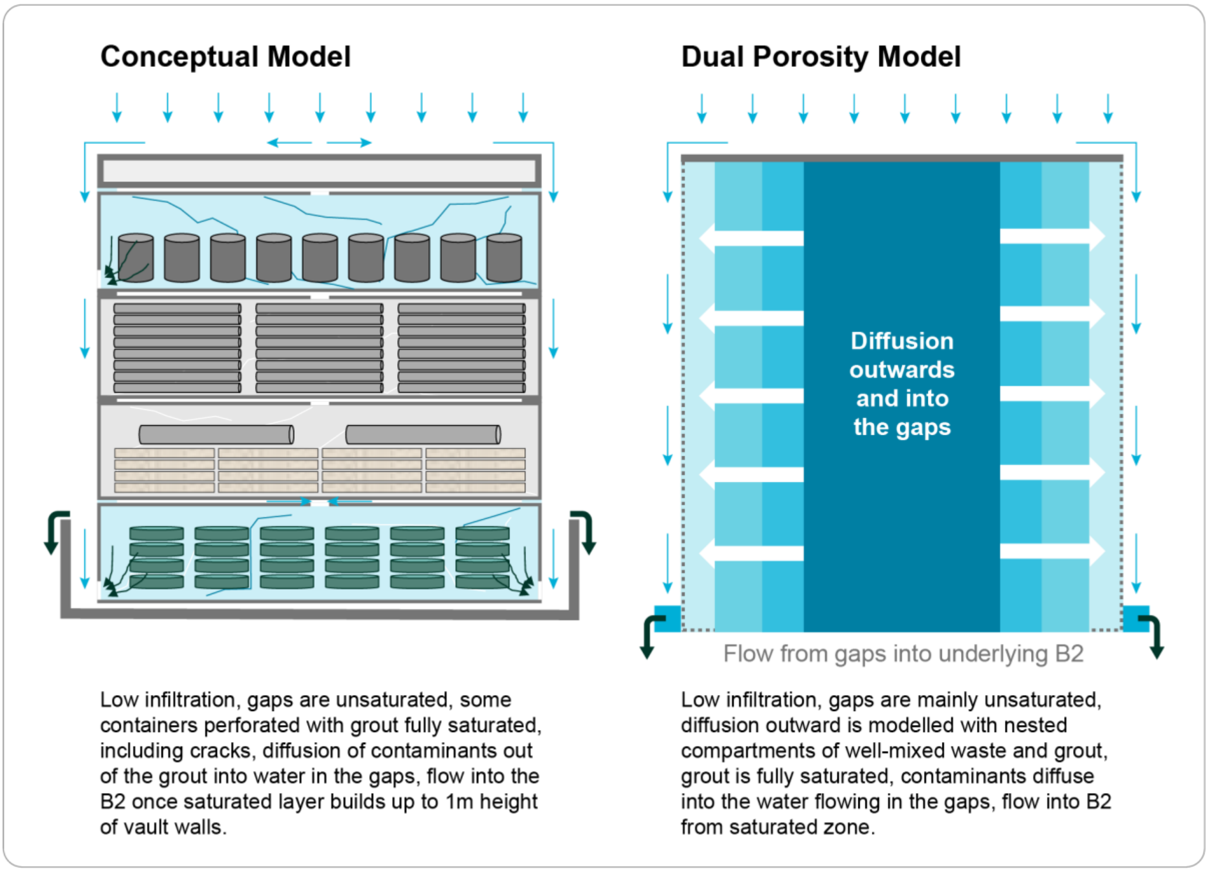

Figure 8.2: Comparison of the near-field conceptual model for the vaults and the groundwater assessment dual porosity model

With the uniform flow model (Figure 8.1), infiltrating water is assumed to flow through the entire connected pore space of the disposed wastes. While this is again moderately realistic for the porous mixture of wastes and soils in the trenches, which is fairly permeable on average (Subsection 3.3), it is a very cautious assumption for the grouted wastes. The grout, although it has around 30% porosity, has low permeability. Fully saturated grout will only support advective flows through cracks but not through the intact matrix. This model is, thus, a cautious representation as, in reality, infiltrating water will access a much smaller proportion of the waste mass.

The dual porosity model is only applied to the vaults. This model (Figure 8.2) considers flow through the gaps in the vault waste stacks, and contaminants are released from the grout by diffusion into the flowing water. Individual stacks of containers are modelled for average LLW and ILW inventories. Within the stack, there are no defined containers but a single waste plus grout block. Each stack is modelled using a set of nested compartments, but initially each compartment has the same well-mixed composition. As contaminants diffuse out into the gaps, the composition of the compartments will change. A saturated zone at the bottom of the gaps can develop as the infiltration rates increase and, from this saturated zone, flows can occur into the underlying geology. As with the uniform flow model, the presence of the containers is neglected. In addition, the grout is assumed to be initially saturated, thus contaminant release can occur immediately.

Water balance and saturation in the vaults

An important aspect of the near-field evolution in the period before geomembrane failure and the marked increase in infiltration (Subsection 3.2.1) is the water balance in the vaults. Assessment calculations, however, assume there is always water available in the vaults into which contaminants can be released (at the end of the PoA), although they will only be transported from the near field from the saturated portion of a model compartment. These calculations will cautiously overestimate the release of contaminants from the vaults after the end of the PoA.

Waste containers

In the assessment model for the vaults, we assume there are no releases to groundwater from the vaults during the PoA. This is partly because it is assumed that the HHISO containers remain largely intact for the PoA. However, there will also be very little water once the vaults are capped and any leachate will be managed during this period. After the PoA, no benefit is taken for the presence of the containers and infiltrating water has full access to the connected porosity of the grouted wastes. This applies to both the uniform flow model and the dual porosity model.

The use of strengthened containers, waste package warehousing to protect containers before disposal and CPUs once emplaced mean that future waste disposals in Vault 9 onwards will still be intact after more than 1,000 years, and potentially by the time coastal d wasteform from which contaminants could diffuse. The modelling results in Subsection 6.5 (and see also modelling of perforated containers in reference [51]) illustrate that this is very cautious when compared with the simulations in which we account for the presence of the container.

Immediately available radionuclides and other contaminants

Contaminants present in the waste can be considered to be in the “bound” state for a certain period. That is, they are physically present within the trench or vault but are not immediately available for dissolution into the porewater. For example, this represents the situation for non-radiological contaminants in uncorroded metallic waste. Contaminants are taken to be released from the bound state into an “unbound” state according to a first-order rate constant based on the corrosion rate of the metal. Once in the unbound state, contaminants are immediately available for dissolution in the porewater where they can be retarded due to contaminant-specific solubility or sorption, or transported in flowing porewater.

Other contaminants are assumed to be released sufficiently rapidly from the bound state that the release can be considered to be instantaneous. This is represented by assigning a nominally high rate constant for such releases. This is the case for all radiological contaminants in both trenches and vaults [126]. Other contaminants are assumed to be released over longer timescales, determined by the corrosion properties of metallic wastes in which they are initially present.

Sorption

In the assessment model, contaminants dissolved in porewater are subject to sorption on the soil in the trenches or the grout in the vaults. Sorption is described as an equilibrium linear, reversible process and described with a distribution coefficient (K_d) defined for the specific vault or trench chemical conditions. The K_ds can be modified by use of sorption reduction factors (Subsection 4.5.4) to account for the estimated concentration of complexants: only EDTA is considered in the trenches, but both EDTA and ISA in the vaults

In neither environment is any account taken of other sorbing substrates. In the trenches, the abundance of steel means that neglecting sorption on iron corrosion products is likely to be a cautious assumption. This is certainly the case for the vaults, given that transport of dissolved species will largely be through the unsaturated gaps that are lined with iron corrosion products. It is quite difficult to create a scenario in which leachate could somehow avoid corroding steel surfaces so such sorption could not occur. As a result, the neglect of iron corrosion products as a sorbing substrate is considered to be a very cautious assumption in the groundwater assessment and the HRA.

Treatment of C-14

Carbon-14 is released instantaneously into the 'unbound' compartment porewater. Different waste materials will release the C-14 in different forms (Subsection 4.5.2) that can undergo various reactions in the near field that partition C-14 into gas, aqueous and mineral phases. The calculation of this partitioning (Subsection 6.5.3) is based on the release and fate parameters defined for the C-14 gas assessment [46]. Partitioning was calculated for each vault as there are variations due to different proportions of C-14-bearing wastes. From this range of values, a probability distribution function was defined for C-14 releases to groundwater for application to all vaults [156].

For the trenches, microbial activity is assumed to eventually degrade all C-14 present to methane and CO_2, so that there is no groundwater release. While this is not cautious for the groundwater pathway (although it is for the gas pathway), it is justified on the basis that the inventory of C-14 in the trenches is small (0.1 TBq) compared with the vaults and there is no information about the waste materials it is associated with, thus, how it should be treated.

8.2 Radon and C-14 Gas Assessment

The models used for the assessment of radon and C-14 gas take very different approaches to representing the near field [46]. For radon, the near field is only represented as a physical system through which the inert radon is transported in the gas phase. In contrast, for the labile C-14 much more consideration is given to representing the effects of the chemical and microbial processes.

Post-PoA radon release model

The short half-life of radon means that a key aspect of this assessment is the transport of the radon between the waste and the biosphere [46]. The radon is assumed to be entrained in the bulk gas phase generated by waste degradation and metal corrosion in both the trenches and vaults.

An emanation fraction, based on empirical observations from the trenches [147] describes the proportion of the radon generated in the wastes that escapes into the unsaturated pore space from where it can be entrained in the bulk gas. For the vaults, the minimum value observed in the trenches is used in order to account for the radon needing to diffuse out of the grouted waste container into the gaps [168].

Transport of the radon through the repository to the biosphere is then based on the movement of the bulk gas phase into the profile material then the gas collection layer of the cap to the vent, or through the resistive layers of the cap once the vent is closed. Ideally, we would calculate the bulk gas velocities in a multiphase model. However, in the absence of such results, we use a simple mass balance approach.

We assume the bulk gas with entrained radon rises directly upwards through the profile material into the gas collection layer and then radially to the vent or, once the vent is closed, the nearest defect in the geomembrane (Figure 8.3). The gas flux into the gas collection layer corresponds to the rate of gas generation in the specific vault or trench and, cautiously, we take no account of any gas that may be lost from the repository through the B2 layer (Subsection 7.2.2). When the vent is open, the transit times from the different locations to the vent are estimated taking account of the concentration of the gas into the vent from the larger area of the gas collection layer (Figure 8.3 right). From this, we can estimate the maximum 'collection area' from which radon entrained in the bulk gas can be transported sufficiently quickly that it does not decay to insignificance during transport to the vent. A similar calculation can be carried out for the defects, taking account of the frequency of defects (approximately one per 400 m^2).

The bulk gas generation is calculated in the SMOGG for both vaults and trenches, as described in Subsection 7.1. As discussed there, we regard the calculation of the gas generation rates to be cautious. For the trenches, we do not account for the loss of quickly degraded waste material in the period before interim capping and, for the vaults, we ignore the likelihood that corrosion will be slowed by lack of water unavailability when the infiltration rates are low.

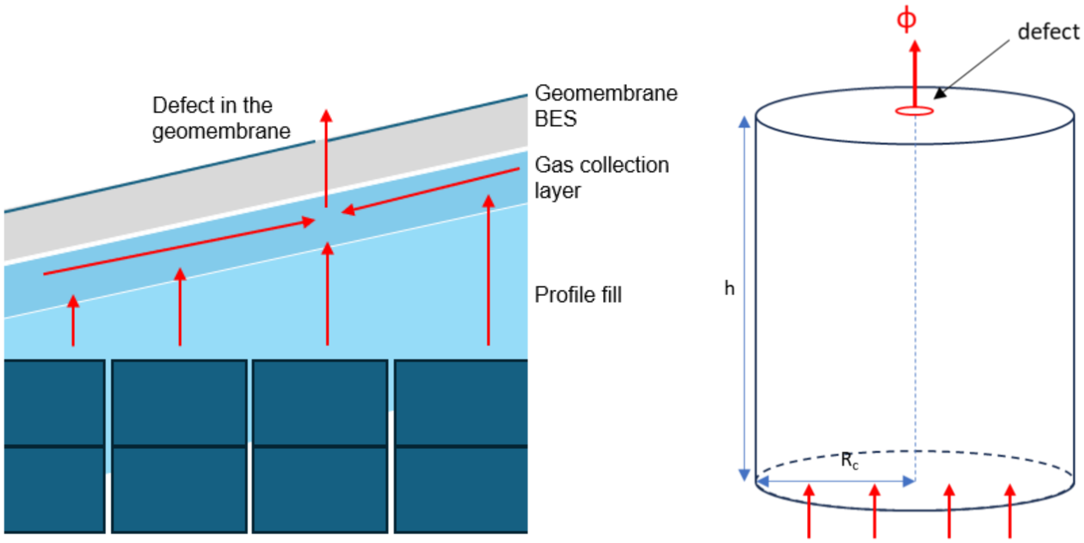

Figure 8.3: Schematic description of gas transport. Left: the assumed bulk gas pathway from the (vault) wastes, through the profile fill to the gas collection layer then radially to a defect (or the vent when it is open) in the geomembrane; right: conceptual model of gas transport in the gas collection layer with a capture zone of radius R_c, distance h to the defect, which is modelled as originating below the BES so that flow Φ through the BES and overlying cap layers is vertical into the overlying house [46]

By overestimating the gas generation rates, we increase the velocity of the bulk gas phase. This reduces the time for radon decay in transit, which in turn increases the impacts to the receptor, a person living in a house built on the cap into which the radon is released.

Carbon-14 model

In contrast to radon, the reactive nature of C-14 species means that the representation of the processes affecting C-14 speciation are as important as the representation of the physical aspects of the near-field in the gas assessment [46]. Furthermore, the half-life of C-14 is sufficiently long (5730 years) that the time for transport through the near field to the biosphere does not significantly affect its activity.

The primary releases of C-14 from waste materials may be in the form of gaseous species, mainly methane and carbon monoxide, soluble inorganic (i.e. carbon dioxide) and soluble organic species, such as acetate and formate (Subsection 4.5.1). Once released from the wastes, they will behave differently depending on the chemical environment of the vaults or the trenches. The assessment model accounts for the fate of the primary releases to determine how much of the total C-14 could be released to the gas phase.

The conceptual model for C-14 in the vaults is summarised in Figure 8.4. This shows schematically that primary C-14-bearing gas (methane) releases from the wastes are directed to the 'atmosphere' (more correctly, the gas phase, which is assumed to be released instantaneously to the biosphere), whereas all other releases are to the container porewater. C-14 released as carbon dioxide dissolves under the high pH grout conditions and reacts to form solid carbonate. The other dissolved species remain in the container porewater since we assume that the pH is too high to allow microbial metabolisation to produce further methane. Once infiltration rates rise sufficiently, dissolved species can migrate to water flowing in the gaps. Here microbial processes may result in more methane and carbon dioxide generation, possibly carbonate precipitation, or the remaining dissolved C-14 species may be released to the groundwater.

Each of these steps (blue arrows in Figure 8.4) or 'fate factors' is quantified in the C-14 assessment model based on the understanding of the chemical environment or, where this is not sufficient, by elicitation [46, 145].

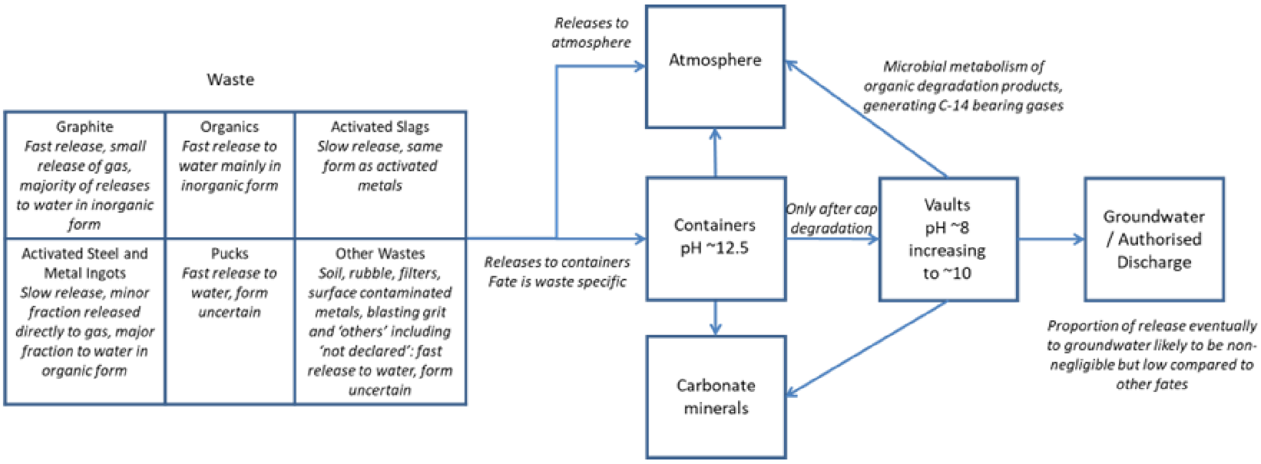

Figure 8.4: **Conceptual model used in the C-14 gas assessment for the speciation, release and fate of C-14 from LLW in the vaults [46]. A similar model is used for ILW but the waste types are slightly different (Table 4.5)**

The release rate and form of C-14 arising from the metal waste and graphite has been the subject of extensive experimentation as discussed in reference [86] and summarised for the repository conditions in Subsections 4.5.1 and 4.5.2. These rates and the proportions of gaseous and aqueous species are used directly to determine the primary release of C-14 in the gas assessment model for the vaults. For example, Table 8-1 shows the corrosion rate data that are used to determine the C-14 release rates from metals, along with the distribution of C-14 between gaseous and aqueous species. The equivalent data for graphite are given in Table 8.2.

For materials for which the C-14 form and release mechanism are uncertain or mixed (e.g., wastes in the compacted pucks), cautious assumptions are made based on our best understanding of the materials and form of the contamination. The same release rate and C-14 speciation assumptions are used in the trenches as the vaults for graphite and organics, but the steel corrosion rate is higher to account for the lower pH (Subsection 5.2.1). The trench conditions, however, do not favour retention of inorganic C-14 as calcite and it is assumed to be released as carbon dioxide. In addition, all dissolved organic species are assumed to undergo microbial reactions that generate further C-14 gas (Subsection 5.2.1).

Table 8.1: Release rate and fraction of C-14 released to gas and pore solution from activated metals wastes [46]

Parameter	Steels (LLW)	Steels (ILW)	Magnox	Aluminium
Reference corrosion rate (μm y^{-1})	0.005	0.005	0.1	1
Proportion released directly to gas	10%	10%	25%	2%
Proportion released to water (organic)	90%	90%	75%	98%

Table 8.2: Parameter values for release of C-14 from graphite [46]

Parameter	Value
Fraction of inventory available for release	5%
Release rate (y^{-1})	1.0 10^{-2}
Proportion released directly to gas	1%
Proportion released to water (organic)	30%
Proportion released to water (inorganic)	69%

The transport of gas from the near field into the biosphere is not modelled in the C-14 gas assessment [46]. Any C-14 gas generated is assumed to be released immediately to the biosphere.

The environment in the gaps between the container stacks will have a lower pH than the grout and microbial activity is more likely. In this environment, further C-14 gas could be generated from the dissolved C-14. Consequently, the processes leading to release of dissolved C-14 species into the gaps are important in determining the extent of further C-14 gas generation.

For the reference case in the C-14 gas assessment, considering the mean value for the onset of geomembrane degradation [12] implies that the geomembrane does not fail before coastal erosion [7]. In this case, the porewater C-14 is only released under the perturbed conditions of coastal erosion, the impacts of which are not accounted for in the gas assessment. In order to inform the calculation of the repository capacity for C-14, a more cautious approach is required. Thus, early geomembrane failure is used in a variant case for the calculation of capacities.

In this early geomembrane failure case, the containers are assumed to be perforated by the time that geomembrane failure results in higher infiltration rates. The containers in the vaults are treated in two populations according to their initial state and subsequent evolution.

The existing and committed populations of containers in Vault 8 and Vault 9 are cautiously assumed to be damaged due to surcharging followed by corrosion such that they no longer provide any barrier to infiltration (Figure 8.5). Dissolved C-14 species are leached from the grouted wastes and then assumed to be microbially degraded to produce further C-14 gas.

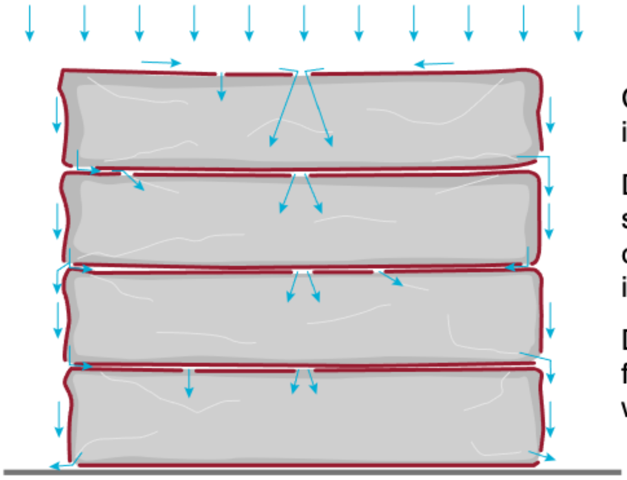

C-14 species homogeneously mixed into grout porewater in the container.

Damage due to surcharging and subsequent corrosion means that the containers provide little resistance to infiltration.

Dissolved species leached quickly from the cracked grout into flowing water and released into the gaps.

Figure 8.5: Conceptual model for release of dissolved C-14 species from the pore water in the grouted waste in surcharged HHISO containers [46]

The future wastes are disposed in the stronger containers that will not be surcharged and are protected from damage during capping by the CPUs (see Figure 8.6). As we cannot robustly estimate how many stronger containers are perforated on the timescale of interest, nor the extent of such damage, we have chosen to make an assumption that all the strong containers are perforated and that the area of the perforations is equivalent to 3% of the surface area of the sides of container. This assumption allows diffusion of dissolved C-14 species out of the grout and into the infiltrating water in the gaps to be modelling simply but explicitly in the gas assessment GoldSim model [46].

The 3% surface area of the corrosion holes is regarded as a cautious value. The surface area of a HHISO is approximately 52 m^2 and about half of this is the side walls, thus 3% is the equivalent of approximately 0.7 m^2. Reference [46] discusses this assumption in more detail and provides further justification.

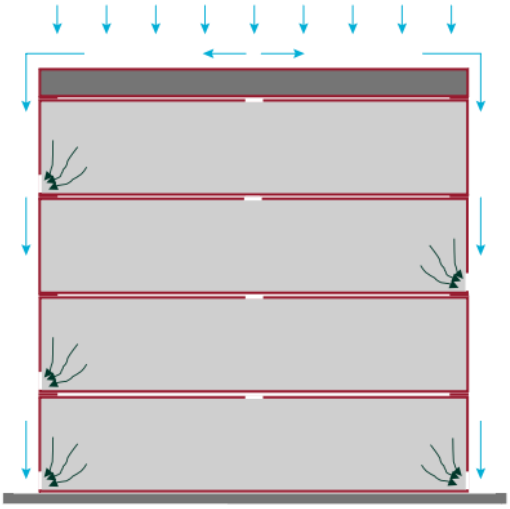

C-14 species homogeneously mixed into grout porewater in the container.

CPUs protect the containers which have only limited corrosion and few perforations and so provide resistance to infiltration.

Dissolved C-14 species can diffuse out of the grout in the containers only where perforations allow contact with infiltration flowing in the gaps.

Figure 8.6: Conceptual model of diffusion of dissolved C-14 species from the grouted waste in the stronger containers with CPUs [46]

The impact of the diffusion of dissolved C-14 from the containers after early geomembrane failure is illustrated in Figure 8.7, in particular, the prominence of 'other' wastes after geomembrane failure. There is no primary C-14 release to gas with this waste category and the releases are all to porewater, with a portion precipitated as carbonate mineral. The remainder, however, is released to the gaps after geomembrane failure and metabolised to give a sudden release of gas. As most of the 'other' waste is in the stronger containers, the release is spread in time more than for LLW 'organics' and 'pucks' that are largely in surcharged containers from which the C-14 is released more quickly.

The reference case and geomembrane failure releases are identical until the time at which geomembrane failure begins for the first strip of the cap (over Vault 8 and the northern trenches). The remaining strips of the cap begin to fail at successively later times, over about 100 years, leading to diffusion from increasing numbers of containers. The maximum C-14 gas flux occurs after geomembrane failure in this case, in contrast to the reference case, and most other cases, where the maximum C-14 gas flux is during the PoA [46].

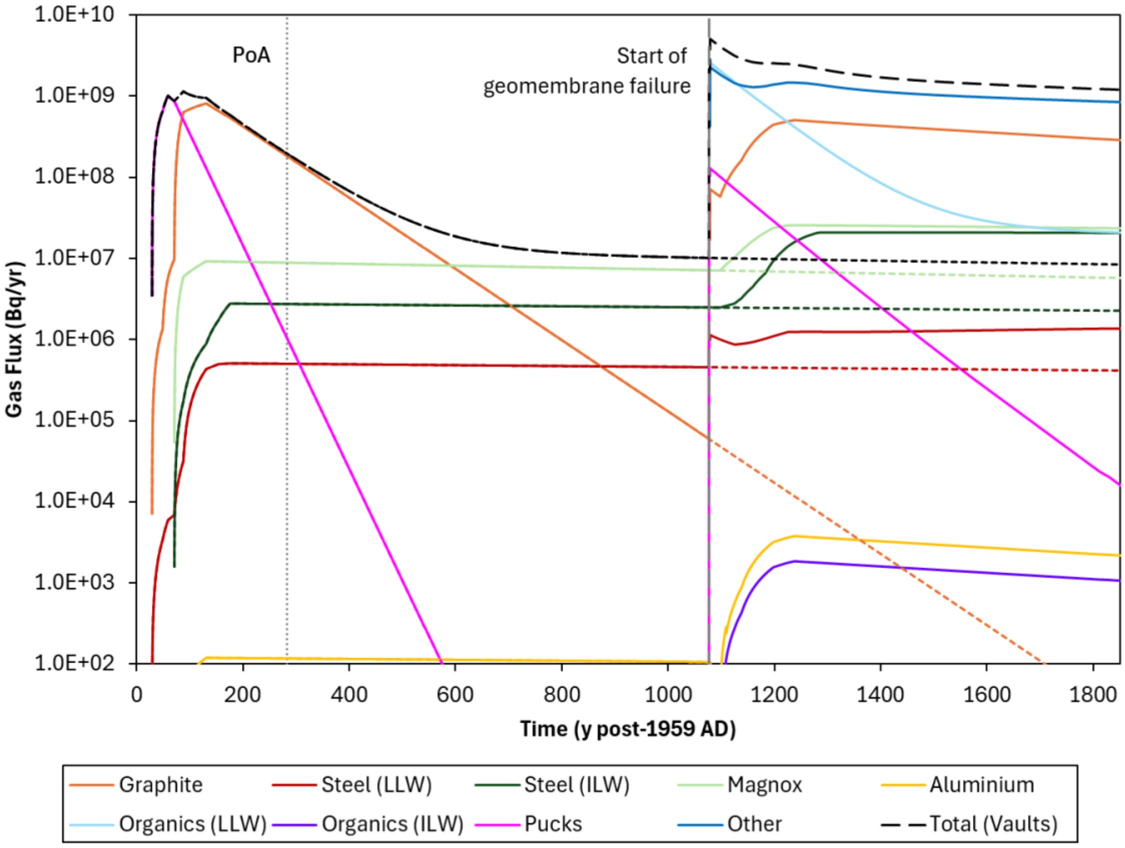

Figure 8.7: **Total C-14 gas flux from all vaults (by waste type). Early geomembrane failure case (solid lines) compared with the reference case (dashed lines) [46]**

9 Uncertainties and Future Work

9.1 Near-field Processes and Key Uncertainties

The near field provides the following main functions that limit contaminant release to groundwater and gas pathways:

- The final cap will limit infiltration to the extent that the vaults will gradually dry as more water is consumed by container corrosion and waste degradation than percolates through the cap. This state will last for one to two thousand years during which the gaps between containers will be unsaturated and there will be insufficient water flows to transport dissolved contaminants from the waste containers.
- Within the vaults, the HHISO containers, small strong boxes, CPUs and the grout will all act to limit contact of infiltrating water with the waste by diverting infiltration into the gaps between container stacks. The shielded modules will act in a similar way to divert infiltration away from the wastes.
- In the surcharged waste stacks in Vaults 8 and 9, although the containers will be deformed, they will still provide a substantial barrier to contact between wastes and infiltration (with the exception of uppermost containers with failed lids), and will still act to divert infiltration into the gaps between stacks.
- The reducing and highly alkaline chemical conditions in the grouted wastes will reduce the corrosion rate of the inner surface of the container as well as waste metals (although not reactive metals, uranium, aluminium and Magnox). Reduced corrosion will slow the release of activation products, such as C-14 from the metals. Reducing conditions will be maintained in the unsaturated gaps by corrosion of the external surfaces of the containers.
- The high pH in the grout will also restrict microbial activity to isolated niches, so that most organic wastes will degrade slowly by alkaline hydrolysis and with much less carbon dioxide generated than when microbial degradation processes are active. This limits the potential carbonation of the grout and reduction in porewater pH. Combined with the low infiltration rates, the absence of CO_2 means that the alkaline conditions will be maintained in the grout for over 5000 years.
- The reducing and near-neutral to moderately alkaline chemical conditions in the gaps between containers will allow microbial activity that may reduce the stability of some organic complexants and other species when they are released from the waste. No credit is taken for this process in the groundwater assessment.
- Water in the unsaturated gaps will be flowing over iron corrosion products that will provide a good sorbing substrate for many contaminants once released from the wastes. No credit is taken for this process in the groundwater assessment.

- The reducing and highly alkaline conditions in the grout will limit the release of uranium by maintaining low solubility and promoting sorption on the grout. The grout conditions will also stabilise the Tc(IV) oxidation state, which will sorb onto the cement grout. The grout will also provide a good sorbent for many other metal contaminants
- Monitoring of the trenches demonstrates the effect of the interim trench cap in lowering water saturation of trench waste and the contaminant release to leachate. Installation of the final cap and associated engineering will enhance this drying out still further, reducing the volume of leachate released to the underlying B2 unit.
- The chemical evolution of the trenches will result in reducing conditions established by processes of waste degradation that will continue for several thousand years. The reducing conditions will stabilise uranium through the low solubility of the U(IV) oxidation state and help to contain the trench uranium disposals.
- The conditions in the grouted waste will ensure that inorganic C-14 released from irradiated graphite and surface contaminated materials will be retained as solid carbonate minerals. A significant portion of the C-14 released as soluble organic species from activated metals will be retained in grout porewater and until the water flows in the gaps increase. We have accounted for the association between C-14 and waste materials, such as steels and graphite, in the trenches in order to take credit for the release processes from these materials.

The effectiveness and significance of the near field in minimising the release of contaminants are subject to some important uncertainties, related to the above features and processes:

- The physical evolution of the cap is important in limiting the infiltration of water. The hydrogeological evolution of the near-field engineering will also affect water inflows from the surrounding geology.
- Cap evolution and performance is partly dependent on limited differential settlement of the disposed wastes. Surcharging before capping will reduce the potential for further settlement in the trenches and surcharged containers in Vaults 8 and 9. The stronger container stacks and the shielded modules in the rest of the vaults are designed to be more resistant to structural failure that could impact the cap.
- Focussing of infiltration into the gaps between container stacks relies on the maintenance of high permeability flow paths. Some of the gaps between stacks in Vault 8 are quite large but, in the future vaults, the containers will be emplaced as closely as practical. Extensive clogging of gaps by movement of fines or chemical precipitation could potentially result in releases into surface water bodies or shallow groundwater instead of to the B2 unit beneath the repository. This may be considered in the context of general clogging of vault drainage as the same processes apply [12]. Mass balance calculations suggest widespread chemical clogging is

extremely unlikely [21, 169] and water flows are not sufficiently fast to mobilise sediment [21] unless the cap were damaged, in which case clogging within the vault would be localised.

- The physical state and behaviour of the containers depend on corrosion processes in the different environments of the gaps and the grout, both with associated uncertainties.
- The chemical form and distribution of contaminants in the waste materials is important to determining whether and to what extent physical and chemical processes may limit their release from the primary wastes into the reactive chemical system.
- The effects of physical and chemical heterogeneity in the waste and wasteform at the scale of the HHISO container are important to assumptions that are required in modelling of the near field. There are uncertainties about the impact of the biogeochemical conditions that may occur in waste initially isolated from grout and of transport through fractures in the wasteform.
- Solubility and sorption that limit the migration of the key chemically reactive radionuclides such as Tc and U in the near field are dependent on the local chemical conditions. Conditions may vary locally but the solubility and sorption parameter probability density functions describe the range of conditions expected at vault-scale.

We have not included here the uncertainty about the performance of the vent in maintaining a sufficiently low gas pressure to avoid damage to the low permeability layers of the cap. The vent design is conceptual and not optimised, but is sufficient for the purposes of the ESC. We consider that we have taken a cautious approach to treating this unoptimised vent in the gas assessments by assuming it acts to focus gas releases and impacts at this one location. This takes no account of modelling results that suggests a significant portion of the bulk gas, and entrained radon and C-14 gas, could be dispersed into the B2 unit beneath the repository (Subsection 7.2.2). Spreading of the gas releases into the B2 could allow more decay of radon and also reduce the likelihood of focussed releases into a house or a smallholding, thus reducing the impacts from both radon and C-14. The vent design will be the subject of future optimisation supported by modelling studies to ensure the uncertainty in gas pathways is reduced as far as practicable. Residual uncertainty will be taken into account once the optimised design is developed.

These main uncertainties in the physical and chemical evolution of the near field and contaminant behaviour have been considered in assessment calculations undertaken for the gas and groundwater pathways [46, 101]. Other uncertainties have been treated by appropriate underpinning work. In Table 9.1 we summarise our treatment of the key near-field uncertainties in the groundwater and gas assessments.

It is worth noting that the cautious assumptions listed in Table 9.1 that are used in response to near-field uncertainties in the same pathway will operate together. For example, for the groundwater pathway, neglect of container integrity and radionuclide release processes, application of the SEF and SRFs for complexants, which are based on cautious estimates of the concentrations of these compounds, and neglect of microbial degradation of organics in the gaps will all act simultaneously to ensure a 'compound' cautious result.

Table 9.1: Treatment of key near-field uncertainties in the assessments

Uncertainty	Treatment in the ESC
Groundwater pathway [14, 126]	
Properties of the cap and other engineered barriers	The EPA [12] has provided ranges, based on expert elicitations, for key barrier properties. These ranges are defined for different times to account for evolution as a function of time. The parameter probability density functions (pdfs) are used in probabilistic and deterministic calculations (in this case, specific values such as mean or 75% percentile are used) in the groundwater assessment. These calculations also take account of the time-dependent evolution of the other engineered barriers. The near-field modelling has simulated the effects of higher infiltration rates and heterogeneity in infiltration over the vaults.
Flow and transport properties in the vaults	In the assessment model, variations in flows have been represented across the repository using the Compartment Flow Model. Uncertainties in flows have been represented depending on the properties of the engineered barriers (as discussed above). The reference case for the groundwater assessment uses a uniform flow model in which the waste is divided into well-mixed saturated and unsaturated compartments and there is flow through the grouted wastes. The presence of the containers is neglected and the grout is represented only as a sorbing substrate that does not otherwise restrict interaction between waste and infiltrating water. These simplifications avoid the need to describe the flows within the gaps between containers vaults in detail. A variant model represents the dual porosity system of grouted wastes and gaps to examine the impact diffusive transport out of the grout could make to releases to the geosphere. However, the wastes are still well mixed within the compartments representing stacks of containers and the presence of the containers is neglected.

Uncertainty	Treatment in the ESC
Heterogeneity in chemical conditions (pH)	We have characterised the uncertainty associated with solubility and sorption parameters in probability density functions (pdfs). These pdfs are defined for small ranges of pH at a temperature of 11 °C since there will be variability in chemical conditions as well as evolution over time. The pdfs are used in the probabilistic assessment, but variant deterministic cases may use specific values, such as the means, or consider reduced sorption and 'no chemistry' [101]. The solubility and sorption parameters for vault wastes are selected for the grout pH conditions. Over a 5,000 y timescale, most of the grout will retain a pH of 12 or above (Subsection 6.5.2). The less favourable pH conditions in the gaps are not accounted for since they will not influence contaminant release from the wastes. The pdfs for solubility and sorption were defined by expert review, and account for a small range of pH (12.5 to 13.5 at 11 °C) [109]. For the trenches, the sorption and solubility pdfs were selected for near-neutral pH conditions. For the very long-term (>5000 years) a further set of pdfs was defined for pH 7.6 to 8.6 to encompass the range in pH calculated in the GRM [53] for the different trenches [114, 170], although these have not been used in the current assessment The pdfs were defined by expert review of the previously elicited values [56].
Conditions in the gaps	The low pH conditions in the gaps are expected to allow microbial activity once there is sufficient water and nutrients. While this may result in degradation of organic complexants, such as ISA, or dissolved organic C-14 species released into the gaps, forming methane and CO_2, the process is sufficiently uncertain that it is assumed not to occur in the groundwater assessment, thus maximising releases to the geosphere.
Form of key radionuclides	The association of radionuclides with waste materials is not considered in the assessment and no credit is taken for release processes: all radionuclides are immediately released from their bound state and available for dissolution.

Uncertainty	Treatment in the ESC
Physical and chemical heterogeneity in the wastes	The assessment model does not account for heterogeneity, e.g. in density and porosity, in the wastes at small-scale. These properties are assigned based on averages at vault-scale. This is justified given the isolation of wastes in individual containers separated by the unsaturated gaps. There is no consideration of chemical heterogeneity in the wastes, other than differences in the contaminant inventory between specific vaults. The heterogeneity in flows is examined by the use of the dual-porosity model [126].
Organic complexants	SEFs and SRFs have been defined for both disposed complexants (EDTA) [129] and complexes generated in the wastes (ISA) [79] to account for the potential effects of these substances on contaminant mobility. Probabilistic calculations also consider uncertainty in the strength of complexation (using defined pdfs). Deterministic calculations have considered uniformly increased complexation in the near field, or no complexation in the geosphere.
Colloids	We consider that colloids will be unstable in the high pH grout conditions, and colloids forming in the gaps (e.g. from iron corrosion products) will not enhance contaminant release from the wastes [121]. The influence of colloids in the trenches and geosphere is expected to be minor, at most, but it is also more uncertain. This is investigated with a simple colloid transport case in the assessment [126].
Gas Pathway [14, 46]	
Properties of the cap and other engineered barriers	The performance of the cap and other barriers to water flow is largely irrelevant for the gas assessment. However, the release of radon in the period before geomembrane degradation is localised by the presence of the defects which focus gas release. The frequency of defects and the factors determining the timing of geomembrane degradation (after which release of gas is uniform over the cap) were elicited as part of the EPA studies [49]. The timing of geomembrane failure, and increase in infiltration rates, determines the time at which dissolved C-14 species in the containers are released into the gaps and degraded to form

Uncertainty	Treatment in the ESC
	C-14 gas. In the reference case, there is a significant likelihood of coastal erosion occurring before geomembrane failure, removing the potential biosphere receptor for C-14 gas. To assess the impact of the release of the dissolved C-14 as gas, a case assuming early geomembrane failure is used. The results from this case are used to determine C-14 capacities.
Bulk gas generation rates	We consider the calculated bulk gas generation rates to be too high, as indicated by the inconsistency with the current gas monitoring data (Subsection 4.2.1) although we have not yet attempted to quantify the uncertainty (see Subsection 9.2). However, the gas assessment uses these rates to determine the transport velocity of the radon, so the time for decay before release into the biosphere. Less gas would reduce the velocity and allow for greater delay. Thus, the assessment takes a cautious approach to these results.
Status of the gas vent at the end of the PoA	There is some uncertainty associated with the decision to close the vent at the end of the PoA. The reference case assumed the vent is closed but the assessment has also considered the case where the vent is left open after the PoA
Association of C-14 with waste materials	The assessment makes use of release (kinetic) processes, e.g. corrosion of activated metal, slow release from graphite, to determine the rate at which C-14 is released as gas or into the grout porewater. The graphite release rate has been chosen cautiously based on experimental evidence [86]. Corrosion rate pdfs have been elicited or reviewed for relevant conditions [158] [75]. There is uncertainty about the association of a significant portion of the C-14 inventory (e.g. 'other' materials), and also about the behaviour of some materials (e.g. 'organics', which are usually ion exchange resins, or contaminated soils and rubble). This is addressed by the assumption for the less well understood materials that the C-14 is instantaneously released to gas or porewater.
Form of key radionuclides	The speciation of C-14 in graphites and steels is relatively well understood based on experimental work [86]. But C-14 released from other materials is more uncertain. Again, this is addressed by making cautious assumptions that most takes an organic form, as methane gas or dissolved small molecules,

Uncertainty	Treatment in the ESC
	such as formate and acetate, which can be metabolised to gas, thus maximising the portion that will be released to the gas phase.
Conditions in the gaps	The low pH conditions in the gaps are expected to allow microbial activity once there is sufficient water and nutrients. This may result in degradation of dissolved organic C-14 species released into the gaps. The process is uncertain but, for the gas assessment, it is cautiously assumed that 100% of dissolved C-14 species are degraded forming $^{14}CH_4$ and $^{14}CO_2$ that are then released to the biosphere.

9.2 Future Work

9.2.1 Supporting Development of a Gas Management Strategy

The discussion of the uncertainties in the bulk gas generation rates points to the requirement to develop a gas management strategy. This is also a requirement identified in Forward Issue ESC-FI-024 that arose from the Environment Agency's review of the 2011 ESC [152]. Currently, the final cap design includes a single central vent structure that allows gas release from the gas collection layer, through a break in the BES and geomembrane, to the upper layers of the cap from where it can disperse to the atmosphere (Figure 2.8).

Gas modelling carried out in 2018 [171] suggested that the overpressures arising after the PoA were small and unlikely to represent a threat to the performance of the cap. Thus, it was expected that the vent would be closed and decommissioned at the end of the PoA. The more recent gas modelling [155], taking account of the presence of the geomembrane in the final cap, has cast some doubt on whether closing the vent would be feasible.

The current vent structure is not an optimised design and, in anticipation of an optimisation study beginning after submission of the 2026 ESC, we have commissioned a study to examine potential alternative options for managing the gas [172].

In order to support the optimisation study, we expect that a further programme of gas modelling will be required. The first stage might be calculations to understand the sensitivity of the bulk gas generation calculations to uncertainties in, for example:

- waste degradation rates;
- assumptions about the initial trench inventory;
- the impact of the period before interim capping of the trenches; and
- drying conditions in the vaults.

We would also aim to include consideration of relevant data from gas generation experiments or from monitoring to provide confidence in the results.

A second stage would then develop the multiphase gas calculations reported in Subsection 7.2 in order to better understand the implications for pressurisation of the cap and, potentially, to test different gas management options.

In addition to provision of underpinning information for the engineering design requirements, a better understanding of the bulk gas generation will allow revision of the more cautious elements of the gas assessment which, in turn, should provide a better basis for C-14 and Ra-226 capacities calculations.

9.2.2 Long-term Near-field Experiment

Following the Environment Agency's review of the 2011 ESC, a forward issue (ESC-FI-018 [152]), was raised which states:

> *"…it is important that LLW Repository Ltd develop a programme of work to understand conditions within the vaults and trenches after placement of the final cap. This information is important to enhance understanding of vault and trench conditions, along with the evolution of the waste mass and surrounding near field, so as to inform the ESC. We expect this information to be gained through either in-situ monitoring infrastructure (existing or new) or via experimentation (field or laboratory based)."*

After a lengthy period of defining requirements and options [173] [174], and overcoming practical hurdles that have necessitated several design changes, we have a programme for long-term, medium-scale experiments [175] and have commenced with the initial stage of equipment testing and feasibility studies.

The purpose of the programme is two-fold, namely to:

- provide important information as evidence (including data) capable of use in future updates of the Environmental Safety Case (ESC) through improved understanding and reduction of technical uncertainties; and
- satisfactorily address the Environment Agency's extant Forward Issue 18 (ESC-FI-018) through the development of a planned experimental programme.

It was initially proposed that a small number of sealed tanks, of approximately 1 m^3, containing simulant waste streams are maintained under partially-saturated conditions whilst various aspects of their physical and chemical evolution are monitored. Subsequently, the design of the tank experimental system was refined so that the high-priority requirements could be studied in a single tank experiment. Following a prototyping phase, a long-term tank experiment would be initiated, which, it was envisaged, would operate on a timescale similar to that of an analogous gas generation experiment in Finland (~20 years) [138]. However, practical difficulties finding a location for the experiment, and the evolving needs of the ESC programme changed the requirements for the experiment.

To expediate the start of the work, a laboratory-based experimental system designed to examine the physico-chemical processes in a largely unsaturated cementitious vault wasteform was proposed [175]. The experimental design is simplified but aims to:

- Characterise the level of water saturation of LLWR grout in a system where water is accumulated at the base of the surface disposal vault.
- Examine the evolution of the pH of the standing water, as an indicator of the pH in contact with waste materials.
- Measure rates of carbon steel corrosion within the grouted waste form.
- Characterise any cellulose degradation products released from the cementitious waste form, such as isosaccharinic acid.
- Characterise any non-radiological contaminants released from the cementitious grout.
- Detect specific conservative tracer and sorbing tracer elements included as point sources in the waste form to provide data relevant to the unsaturated contaminant release model of the ESC.

The experiment does not fully represent the processes (e.g. microbiology) and features (e.g. region outside of containers) of the wider vault, which may affect both gas generation and Eh evolution. As a consequence, it will not be possible to examine the biogeochemical processes that might affect C-14 speciation.

We have the results of a series of small-scale trials which were devised to investigate [44]:

- grout properties
- cellulose placement techniques in the grout samples
- sensor positioning in the grout samples
- water uptake in the grout
- compatibility and detection of tracers with cement matrices.

Notably, the small-scale trials confirmed the saturation state of the grout following ageing is consistent with the calculated (by mass balance) value. These trials have also confirmed that the relatively small grout samples have properties, such as pore size distribution, that are consistent with the grout produced in much larger quantities by the LLWR grout plant. This means we can have confidence that the physical properties measured, and behaviours observed, in the experiments are analogous to the much larger system in the containers.

We plan to continue into the scale-up phase and are now planning the next phase of commissioning the larger-scale tanks.

10 Summary and Conclusions

This document is one of several Level 2 reports presenting the evidence that underpins our safety arguments in support of the ESC. This report summarises our understanding of the evolution of the LLWR near field, with particular focus on the water flows and contaminant release processes that will affect the groundwater and gas pathway impacts. The conceptual model developed also provides an appropriate basis to consider the release of chemotoxic contaminants.

We present summaries of a number of related work areas:

- a description of important physical features of the trench and vault disposals and the near-field engineering that may impact on evolution of the facility and the behaviour of contaminants;
- the expected physical evolution of the near-field engineering, wastes and containers;
- the evolution of water saturation and water flow through the near field;
- research forming the basis of our understanding of the near-field chemical evolution and contaminant release processes, including monitoring data;
- a conceptual model of the chemical evolution of the trench and vault disposals, contaminant release processes and the generation of gas;
- the representation of near-field hydrogeological and chemical processes that affect contaminant release in assessment calculations.

The near-field studies and environmental assessments address several requirements of the GRA [18]. In particular:

- our underpinning near-field studies demonstrate the application of good science (Requirement 4). This includes work on understanding the fundamental physical and chemical processes, inventory, modelling and experimental research studies;
- hydrogeological modelling of the near field, together with reactive transport modelling of the effects of the vault wasteform grout and container metal components, underpins our assessments (Requirement 6). Furthermore, modelling studies and reviews of international research provide a basis to define waste acceptance criteria (Requirement 13);
- the combination of hydrogeological modelling and more detailed near-field modelling of evolution of engineered barrier components also underpins our approach to optimisation (Requirement 8);
- previous and ongoing experimental and modelling studies of gas generation together with trench monitoring and chemical and hydrogeological modelling (Requirements 11 and 14) underpin our estimates of environmental impacts through gas and groundwater (Requirement 6);

- our conceptual model of the near field is based on data from near-field experimental research, including long-term experiments, international experimental programmes, our monitoring and site investigation programmes (Requirements 11 and 14). We will continue to monitor the near field in the future, so as to take into account changes that result from the repository development, and undertake further appropriate experiments to characterise the behaviour of the near field.

We have identified the key uncertainties in understanding the near-field evolution and determined those that should be addressed in further work. However, we have shown that our analysis is robust to these uncertainties. Other uncertainties are treated with the use of variant calculations in the assessments to ensure that the implications are understood. Where uncertainties have been identified because of inconsistencies between observations, for example between monitoring data and modelling results, we have considered alternative interpretations that may in turn lead to additional assessment calculations.

10.1 Evolution of the Near Field

The main physical and chemical processes that lead to the evolution of the near field and determine the release of contaminants are summarised schematically in Figure 10.1. It illustrates, for example:

- the repository may be affected be coastal erosion before cap degradation;
- the relationship of water flows to cap degradation in the vaults, whereas the trenches were wetter earlier, before capping;
- conditions in the vaults are constant over a long period, whereas the trenches are more variable;
- C-14 releases to gas occur early, especially in the trenches, but there is a second period of high release coincident with increasing water flows;
- U mobilisation coincides with increasing oxidation of the trenches.

The figure represents only approximately 3000 years from the start of repository operations in 1959 because coastal erosion followed by complete disruption of the repository is expected to occur within this timescale.

The following subsections provide a fuller summary.

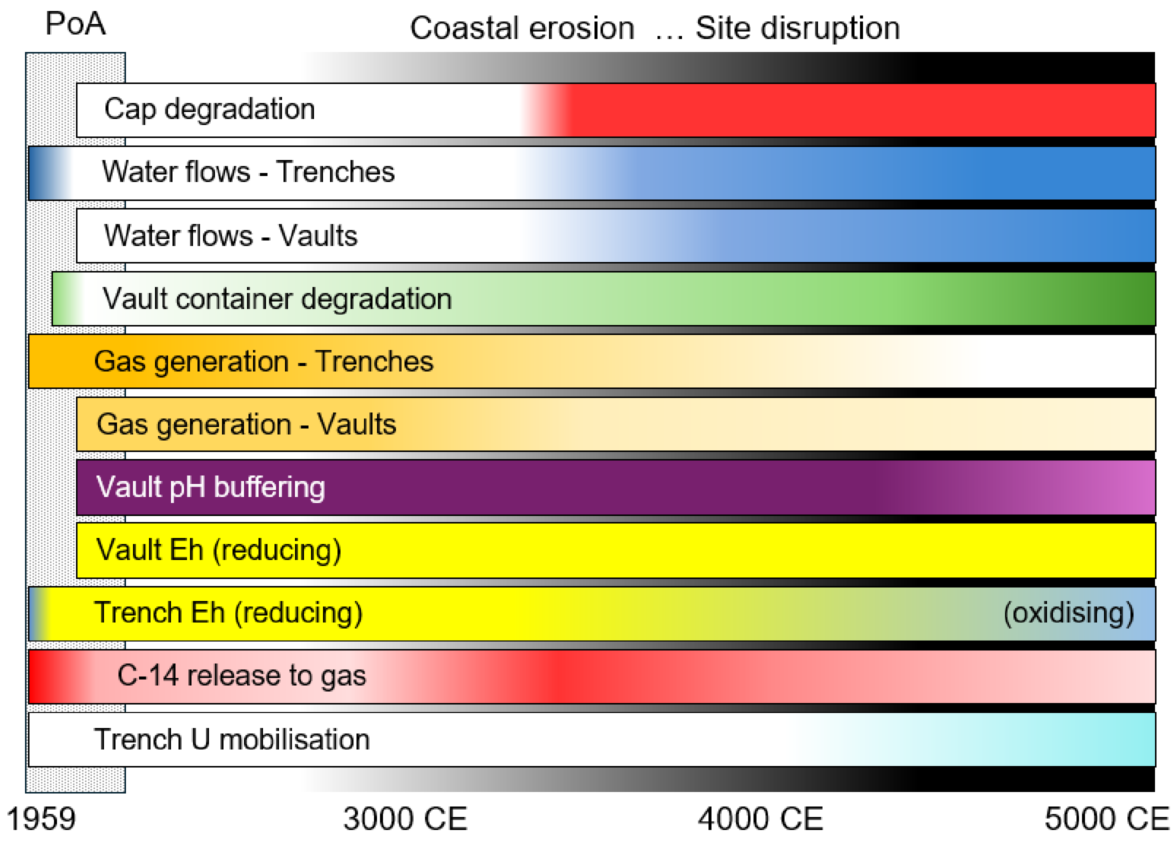

Figure 10.1: Schematic representation of key near-field processes occurring over approximately 3000 years from the start of operations (1959). The background indicates the timescale for the onset of coastal erosion while the bars indicate the key processes. Colour in the bars represents an active process, stronger colours denote more activity, whereas white denotes a process has not started or has ceased. Processes tend to switch on or off gradually, illustrated by the shading in the bars.

Physical evolution

The important processes for the physical evolution of the near field are:

- the performance and evolution of the final cap, which will determine the amount and the distribution of infiltration in the near field, and the degree of water saturation of the trench waste;
- diversion of water infiltrating the cap by the container protection units on the tops of container stacks, by the containers themselves and by the low permeability grout into the gaps between containers, thus minimising contact with the waste;
- the degradation of the trench wastes, which is coupled to chemical evolution and will influence the release of contaminants into infiltrating water;

- the degradation of the containers in the vaults as this will determine the amount of interaction between the grouted wastes and infiltrating water flowing in the gaps.

The key feature of the LLWR closure engineering is the final cap. This will largely control the extent of water ingress, especially for the vaults. Recharge below it will be very low for many hundreds of years and, combined with the cut-off wall that limits lateral flows and chemical degradation processes that consume water, will lead to a very low water table locally. The cap performance will fall slowly initially until the geomembrane starts to degrade, most likely after more than 1000 years. Over this period, the vaults will be drying out and the water table in the trenches will fall.

The complete degradation of the geomembrane before the onset of disruption by coastal erosion would lead to an approximately 500-fold increase in infiltration, recharge would increase, and the local water table would rise. After geomembrane failure, the cap performance changes very little over the next two thousand years or more.

In the period after geomembrane failure, many stronger containers will have corroded locally and have perforations in the side walls, while the surcharged containers in Vaults 8 and 9 will have more extensive damage. The grout in the containers will be variably unsaturated - more unsaturated where wastes metals have corroded - so much of the increased infiltration will initially be taken up by the grout, increasing its saturation state. Gradually, a saturated zone at the base of the vaults will be established but the gaps will still be largely unsaturated. The water table in the trenches will start to rise. By this time, more than 2000 years after closure, coastal erosion is likely to have disrupted the vaults.

We have examined the hydrogeological evolution of the near field using the program CONNECTFLOW, which has enabled a probabilistic assessment of the uncertainties in the properties of geological units and in the processes affecting the evolution of the site. Based on these models, the vaults and the trench wastes will remain unsaturated up to 3280 AD (reference climate scenario), after which the effects of coastal erosion are expected to begin to influence the local hydrogeology.

The degradation of the containers and grout will vary, depending on whether the waste stacks were surcharged or protected by container protection units, and proximity to defects in the geomembrane that will control the location of infiltration for the first 1000 years or more. Over the period before geomembrane failure, water consumption by corrosion reactions will exceed the infiltration, so that water will be available only in the vicinity of flows through defects. Containers more remote from infiltration points may not corrode as fast as those closer to the water sources. The saturation of the grout will fall as waste metal corrosion consumes water from the grout that is not replaced in the dry conditions.

In the period before geomembrane failure, release of contaminants to groundwater will be restricted due to lack of continuous water-filled pathways.

Corrosion of waste metals will affect the physical integrity of the grouted wastes, promoting cracking and forming flow paths through the grout. Once the grout is fully re-saturated, this may increase contact between wastes and infiltrating water. Corrosion of metal wastes will also be important to the release of the activation products, C-14 and Cl-36, although this is not taken into account in the groundwater assessment model.

Chemical evolution

Our conceptual model of chemical evolution of the trench and vault wastes has built upon the research and understanding developed for the 2002 PCSC and the 2011 ESC. We have drawn on developments in scientific understanding as well as the results of relevant international studies and undertaken further specific modelling studies in developing our conceptual model.

The previous near-field research and monitoring data have established the role that microbiological processes have in mediating pH and Eh conditions and gas generation in the trenches. Changes to our conceptual model largely reflect changes to:

- the repository development plans, namely surcharging the trenches before capping;
- infiltration rates, now much lower than previously considered.

For the vaults, we have updated our understanding of the chemical behaviour of the grout, however, by drawing on studies of blended cements, that is, ordinary Portland cement used in combination with large proportions of pulverised fuel ash or blast furnace slag, as well as recent experimental work on the LLWR grout. We now consider that the pH of the grout porewater will be too high, in excess of pH 12.5, to allow microbial activity within the grouted wastes. This in turn means that degradation of cellulosic wastes will be limited to abiotic alkaline hydrolysis, except in localised organic-rich niches where microbial activity may still occur, for example in the compacted pucks. As a result, bulk gas production in the vaults will be predominantly hydrogen from metal corrosion. The absence of gas production from cellulose degradation reduces the potential for carbonation of the grout by carbon dioxide. In combination with the very low infiltration rates, this means that we expect the grout porewater to remain above pH 12 in most of the grouted waste over a period of 5000 years.

We have developed a new generation of reactive transport models in the PFLOTRAN software to allow us to investigate the evolution of physical and chemical conditions. A key advantage of this software is the ability to account for the highly heterogeneous saturation conditions in the vaults. The models represent different length scales, from a single HHISO container, to a stack of containers, a section through a trench, a whole vault or the full repository. This suite of models allows us to apply appropriate discretisation for the scale of the processes being investigated.

In describing our conceptual model for the evolution of the near field, we have considered the potential for disposal of ILW in the vaults. We conclude that our analysis is robust to changes in the inventory, specifically to the material inventory, that could occur with disposal of the less hazardous ILW identified in the Stage 2 reference inventory.

The main chemical processes and phases of evolution in the trenches and vaults are summarised as follows:

- Degradation of cellulosic wastes in trench disposals will lead to mildly acidic and sulphate-reducing conditions developing early, followed by methanogenic conditions. Reducing conditions dominated by cellulose degradation will last around 1,200 years to several thousand years depending on the content of organic wastes in different trenches.
- The large quantities of corroding metal in the trenches will ensure reducing conditions are maintained even after cellulose degradation has slowed.
- In the longer-term, once corrosion has largely consumed the metal and cellulose is similarly exhausted, the chemical conditions in the trenches will tend to reflect the redox conditions associated with the iron corrosion products and minerals. There will be increased infiltration of rainwater but potentially also inflows of shallow groundwater as the cut-off wall and vault bases degrade and the surrounding water table rises in response to encroaching coastal erosion.
- Corrosion of the external surfaces of the containers will result in the establishment of reducing conditions in vaults within a few years of capping. Anaerobic corrosion of the containers as well as waste metals will result in a long period when water consumption exceeds infiltration and releases from most containers are restricted to gaseous radionuclides.
- Within the wastes, the grout porewater is initially extremely alkaline with conditions up to pH 13.5. The pH will fall slightly where infiltrating water is in contact with the grout, but in most of the grout, the conditions are expected to remain at pH 12 or above for several thousand years.
- Cellulose degradation will proceed largely by alkaline hydrolysis as microbial activity is restricted by the high pH conditions. Without microbial activity, ISA concentration will increase where cellulose is degrading, up to a limit determined by its solubility and sorption under the grout porewater conditions, and this may affect the mobility of some radionuclides and other contaminants by the formation of complexes.
- In the gaps between container stacks, the Eh is similarly very low but the pH is much less alkaline since the infiltrating water has little interaction with the grout and is mainly conditioned by contact with the bentonite in the BES layer of the cap and iron corrosion products on the container surfaces. Under pH 7 to 10 conditions, microbial activity can occur, which may result in degradation of cellulose degradation products and C-14-bearing organics released from the containers. This may affect the stability of ISA and EDTA complexes.
- While the low Eh and high pH conditions favour low solubility of uranium in the U(IV) form, the presence of ISA may increase its release rate from the grout due to the formation of ISA complexes.
- Technetium is controlled by sorption processes at low aqueous concentrations below the solubility limit of Tc(IV).

- The C-14 in the trenches is mainly released in the first few hundred years in the form of gas. For the vaults, there is an early peak of gas release but then gaseous releases fall. Most of the C-14 released from the wastes in the vaults is retained in the grout as carbonate minerals or in the porewater as dissolved organic species. In the drying vaults before geomembrane failure, most of the dissolved portion will remain in the containers without microbial degradation. Its fate depends on the relative timing of geomembrane failure and coastal erosion. When geomembrane failure occurs, there will be sufficient water to allow release from the containers into the gaps where microbial activity could result in a second, higher, peak of C-14 gas releases.

11 References

[1] Nuclear Waste Services, “2026 Environmental Safety Case for the LLWR: Main Report,” LLWR/ESC/R(26)10166, May 2026.

[2] Nuclear Waste Services, “2026 Environmental Safety Case for the LLWR: Management and Dialogue,” LLWR/ESC/R(26)10167, May 2026.

[3] Nuclear Waste Services, “2026 Environmental Safety Case for the LLWR: Site History and Description,” LLWR/ESC/R(26)10168, May 2026.

[4] Nuclear Waste Services, “2026 Environmental Safety Case for the LLWR: Disposal Facility Inventory,” LLWR/ESC/R(26)10169, May 2026.

[5] Nuclear Waste Services, “2026 Environmental Safety Case for the LLWR: Engineering Design,” LLWR/ESC/R(26)10170, May 2026.

[6] Nuclear Waste Services, “2026 Environmental Safety Case for the LLWR: Hydrogeology,” LLWR/ESC/R(26)10172, May 2026.

[7] Nuclear Waste Services, “2026 Environmental Safety Case for the LLWR: Site Evolution,” LLWR/ESC/R(26)10173, May 2026.

[8] Nuclear Waste Services, “2026 Environmental Safety Case for the LLWR: Monitoring,” LLWR/ESC/R(26)10174, May 2026.

[9] Nuclear Waste Services, “2026 Environmental Safety Case for the LLWR: Optimisation and Site Development Plan,” LLWR/ESC/R(26)10175, May 2026.

[10] Nuclear Waste Services, “2026 Environmental Safety Case for the LLWR: Waste Management Plan,” LLWR/ESC/R(26)10176, May 2026.

[11] Nuclear Waste Services, “2026 Environmental Safety Case for the LLWR: Safety Functions,” LLWR/ESC/R(26)10177, May 2026.

[12] Nuclear Waste Services, “2026 Environmental Safety Case for the LLWR: Engineering Performance Assessment,” LLWR/ESC/R(26)10178, May 2026.

[13] Nuclear Waste Services, “2026 Environmental Safety Case for the LLWR: Environmental Safety During the Period of Authorisation,” LLWR/ESC/R(26)10179, May 2026.

[14] Nuclear Waste Services, “2026 Environmental Safety Case for the LLWR: Assessment of Long-term Radiological Impacts,” LLWR/ESC/R(26)10180, May 2026.

[15] Nuclear Waste Services, “2026 Environmental Safety Case for the LLWR: Hydrogeological Risk Assessment,” LLWR/ESC/R(26)10181, May 2026.

[16] Nuclear Waste Services, “2026 Environmental Safety Case for the LLWR: Assessment of Radiological Impacts on Non-human Biota,” LLWR/ESC/R(26)10182, May 2026.

[17] Nuclear Waste Services, “2026 Environmental Safety Case for the LLWR: Implementation,” LLWR/ESC/R(26)10183, May 2026.

[18] Nuclear Waste Services, “2026 Environmental Safety Case for the LLWR: Addressing Regulatory Requirements and Feedback,” LLWR/ESC/R(26)10184, May 2026.

[19] Environment Agency, Northern Ireland Environment Agency, Scottish Environment Protection Agency, “Near-surface Disposal Facilities on Land for Solid Radioactive Wastes: Guidance on Requirements for Authorisation,” February 2009.

[20] LLW Repository Ltd, “The 2011 Environmental Safety Case: Near Field,” LLWR/ESC/R(11)10021, May 2011.

[21] Nuclear Waste Services, “LLWR 2026 ESC: Engineering Performance Assessment. Vaults and Trenches,” QRS-1895C-PR2, Version 1.6, October 2024.

[22] LLW Repository Ltd, “The 2011 Environmental Safety Case: Engineering Design,” LLWR/ESC/R(11)10020, May 2011.

[23] A. Paulley, “Design Summary Document for the Vaults,” LLWR/ESC/Mem(23)453, January 2024.

[24] Nuclear Waste Services, “Volumes of Disposed Waste,” DMF0109 v1, January 2025.

[25] URS, “Vault 8 Closure Plan: Cap Resilience Report,” URS 47071703-CRR, 2016.

[26] LLW Repository Ltd, “The 2011 Environmental Safety Case: Inventory,” LLWR/ESC/R(11)10019, May 2011.

[27] Nuclear Waste Services, “2026 Environmental Safety Case for the LLWR: Forward Inventory Methodology,” NWS/EIO-2026-003, April 2026.

[28] NDA, “2022 UK Radioactive Waste Inventory,” April 2022.

[29] LLW Repository Ltd, “The 2011 Environmental Safety Case: Waste Acceptance,” LLWR/ESC/R(11)10026, May 2011.

[30] LLW Repository Ltd, “Hydrogeological Risk Assessment for the LLWR,” LLWR/ESC/R(17)10090, Issue 2, March 2018.

[31] LLW Repository Ltd, “The 2011 Environmental Safety Case: Assessment of Non-radiological Impacts,” LLWR/ESC/R(11)10029, May 2011.

[32] Nuclear Waste Services, “Stage 2 Inventory - Volumes of Disposed Waste,” DMF0109 v1, January 2025.

[33] LLW Repository Ltd, “Review of Leachate, Groundwater and Surface Water Monitoring,” RP/DR-GEN/PROJ/00035, 2011.

[34] LLW Repository Ltd, “Environmental Monitoring Database System Data Export and Report Production,” RSP 2.21, April 2022.

[35] Serco, “Development of the Disposal Inventory - Review of Non-radiological Inventory Data,” Serco/TAS/003756/001, Issue 2, April 2011.

[36] Wood, “Representing the Chemical Behaviour of Boron in Assessment Calculations,” Wood/208727/001, Issue 2, February 2020.

[37] N. Barber and E. Henderson, “Assessment of Human Health and Environmental Impacts Associated with the Non-radioactive Component of Disposals to the LLWR at Drigg,” Nexia report (08)9442, July 2008.

[38] Nuclear Waste Services, “Trench Densities and Porosities,” DMF0120 v2, April 2024.

[39] AECOM, “DP1a Surcharge & Profile Fill – Northern Trenches Surcharge Report,” AECOM Report AEC-RDP-T1.00-RP-179, 2022.

[40] Nuclear Waste Services, “2023-24 Environmental Monitoring Summary Report,” RP-3409334.05-ENV-00185, August 2024.

[41] A. Wood, “Drigg Grouting Demonstration Project,” BNFL Project Document, 2000.

[42] AECOM, “LLWR Repository Development Programme - Tranche 1: Design Package 1b – Final Cap Detailed Design Cap Resilience Report,” AEC-RDP-T1.00-RP-130 Rev BP1, May 2023.

[43] Amentum, “Near-field Modelling of the LLWR: Task 4 – Results,” Amentum Report DEPRWD15/25, Issue 2, 2025.

[44] National Nuclear Laboratory Ltd., “LLWR Near Field Experimental Programme - Small-Scale Trials,” NNL 16731, Issue 2, February 2025.

[45] P. M. Coates, “Drigg-vault 8-bay 3 Report on Condition of LLW Containers and Compliance with Condition 4 of Extant Authorisation,” NSTS Report 5021, 2004.

[46] Quintessa, “Assessment of the Gas Pathway for the LLWR 2026 ESC: Assessment of Releases During the PoA and Post-PoA Releases and Risks,” QRS-10156B-Gas_P2, Version 2.0, May 2026.

[47] NSG, “LLWR Fine Formulation Grout Trials,” NSG Report NS6640/500/004, July 2022.

[48] Amentum, “Infiltration Through the Final Cap,” DEPRWD14/10, 21 October 2024.

[49] LLW Repository Ltd, “Trial Elicitation of Parameters Representing Performance of the Final Cap, Warrington, 4th to 5th June 2019,” LLWR/ESC/M(19)352, June 2019.

[50] Environment Agency, “The Likely Medium to Long-Term Generation of Defects in Geomembrane Liners,” R&D Technical Report P1-500/1/TR, January 2004.

[51] Amentum, “Pflotran Level 3 report, Near-field Modelling of the LLWR for the 2026 ESC: Results,” Amentum report DEPSCD39/1, May 2026 (pre-publication).

[52] J. S. Small, “Review of Cellulose Degradation Rates,” LLWR/ESC/Mem(25)476, 2025.

[53] National Nuclear Laboratory, “GRM Near-field Modelling for the LLWR 2011 ESC,” NNL(10)11233, Issue 2.0, April 2011.

[54] F. B. Neall, “Description of the Vault Near-field Conceptual Model,” LLWR/ESC/Mem(24)472, December 2024.

[55] LLW Repository Ltd, “ESC Record of Meeting: Corrosion Elicitation Workshop,” LLWR/ESC/M(21)387, May 2021.

[56] SERCO, “Elicitation of Uncertainties for LLWR,” Serco Report SERCO/TAS/E003796/010, Issue 2, 2011.

[57] Amentum, “Hydrogeological Model for the LLWR ESC,” DEPRWD14/16, October 2025.

[58] BNFL, “Drigg Post Closure Safety Case: Near-field Biogeochemistry,” September 2002.

[59] Nexia Solutions, “LLWR Lifetime Project: Review of Long Term Trench and Long Term Vault Experiments,” Nexia Solutions Report 8503, 2008.

[60] Westlakes Scientific Consulting, “BNFL Drigg Leachate Sampling and Analysis: March-april 1997,” Drigg PCSC document DTP/200, 1998.

[61] K. Clayton and D. P. Trivedi, “The Mark 2A Drigg Near Field Data Base,” BNFL Sellafield Technical Dept Memo 337, DNFSC P(92)44, 1993.

[62] LLW Repository Ltd, “Trench Cap and Cut-Off Wall Performance Review,” RP/3409246/PROJ/00314-A, 2014.

[63] Quintessa, “LLWR Trench Hydrological Management BAT: Final report,” QRS-1443ZN-R3 Version 1.0, November 2012.

[64] AECOM, “Repository Development Programme - Tranche 1 Design Package 7 - Interim Hydrological Management of the Trenches BAT Outcomes Report,” AEC-RDP-T1.00-RP-052 A 2019, 2019.

[65] Belton, “LLW Repository Ltd Trench Cap Additional Investigations: Factual Report,” Coffey report 02140AB_R_001A_ARB-Factual Report, 2014.

[66] F. B. Neall, “Updating the Model for LLWR Grout Chemical Evolution,” LLWR/ESC/Mem(2)479, May 2026.

[67] H. F. W. Taylor, Cement Chemistry, London: 2nd Edition, Thomas Telford Publishing, 1998.

[68] P. Jha, A. K. Sachan and R. P. Singh, “An Overview: Supplementary Cementitious Materials. In: Gupta, A. K. et al. (eds.), Advances in Construction Materials and Sustainable Environment, Lecture Notes in Civil Engineering,” *Springer Nature Singapore,* vol. 196, pp. 53-63, 2022.

[69] A. Clark, “Drigg LLW Container Grout/water Interactions: Petrography Mineralogy Chemical Evolution and Radionuclide Attenuation Potential (safety Case Related Characterisation and Experimental Investigation),” Drigg PCSC Document DTP/109, 2003.

[70] Nuclear Waste Services, “Properties of Raw 3:1 PFA:OPC 'LLW' Grout (Porosity and Density),” DMF0016 v1, January 2025.

[71] Amphos/RSK, “LLWR Silo Chemical Evolution (TO250): Reactive Transport Modelling - Final Report,” Report 3475_LLWR_Silo_Evolution, Version 3, February 2023.

[72] Quintessa, “pH Buffering and Carbonation in the LLWR Vaults: Insights from Thermodynamic and Reactive-transport Modelling,” Quintessa Report QRS-1443E-R1 Version 1.1, 2009.

[73] Amec Foster Wheeler, “Assessing Aspects of Near-field Heterogeneity for the LLWR,” CRM 79246, 2019.

[74] BRE, “Laboratory and Field Data for PFA Grouts,” BRE Construction Division, BRE Report 220192, 2006.

[75] Nuclear Waste Services, “Metal Corrosion Rates - Mild Steel (trenches, vaults pH 10-11, beach),” DMF0118 v1, November 2023.

[76] J. S. Small, “Status of the Understanding of Microbiology in a Silo,” LLWR/ESC/Mem(21)412, 2023.

[77] Jacobs, “Review of Metal Corrosion Rates Under Near-field pH Conditions,” DEPRWD34-TN-001 , Issue 6, September 2024.

[78] J. S. Small, “Understanding of Isosaccharinic Acid (ISA) Generation and Degradation in Cementitious Systems,” LLWR/ESC/Mem(20)396, 2021.

[79] J. S. Small, “Treatment of ISA in LLWR Assessments,” LLWR/ESC/Mem(23)447, 2025.

[80] National Nuclear Laboratory Ltd., “Review of the Formation and Degradation of Isosaccharinic Acid Under LLWR Vault Wasteform Conditions,” NNL (12) 12150, Issue 2.0, 2013.

[81] National Nuclear Laboratory Ltd., “Physical and Chemical Heterogeneity on the Container Scale,” NNL Report (09)10694 Issue 3, 2010.

[82] F. Neall, D. Bennett, A. Jones and J. Wilson, “Understanding the Evolution of the Carbon Component of the Dragon Reactor Fuel during the Post-Closure Phase of Geological Disposal,” Galson Sciences Report 1405-1, 2015.

[83] Curti, E., “Coprecipitation of Radionuclides: Basic Concepts, Literature Review and First Applications,” Nagra Technical Report NTB 97-08, 1997.

[84] S. Stead and P. Tulip, “Disposal of ‘Durable’ Containers in the LLWR Vaults,” LLWR/ESC/Mem(23)443, July 2024.

[85] LLW Repository Ltd, “The 2011 Environmental Safety Case: Assessment of Long-term Radiological Impacts,” LLWR/ESC/R(11)10028, May 2011.

[86] S. W. Swanton, B. T. Swift and M. Kelly, “C-14 Release Processes from Near-surface Disposal Facilities,” 209296-TR-01, 2020.

[87] Nexia Solutions, “LLWR Lifetime Project: Heterogeneity of the Inventory of Past and Potential Future Disposals at the LLWR,” Nexia Solutions Report (07)9126, Issue 03, 2008.

[88] National Nuclear Laboratory Ltd., “Characterisation of Uranium in a Fluoride Wasteform,” NNL Report (10) 10816, Issue 1, 2010.

[89] J. A. Berry, A. Harper and S. W. Swanton, “The release of C-14 and Cl-36 from slags in LLWR,” LLWR/ESC/Mem(10)086, 2010.

[90] F. B. Neall, “Review of the Release of C-14 from Graphite,” LLWR/ESC/Mem(20)387, 2021.

[91] Nexia Solutions, “LLWR Lifetime Project: Near Field Modelling and the Behaviour of Uranium,” Nexia Solutions Report 8372, 2008.

[92] P. J. Heard, L. Payne, M. R. Wootton and P. E. J. Flewitt, “Evaluation of Surface Deposits on the Channel Wall of Trepanned Reactor Graphite Samples,” *Journal of Nuclear Materials,* vol. 445, pp. 91-97, 2014.

[93] Nuclear Waste Services, “Metal Thickness,” DMF0181 v1, September 2024.

[94] K. Alkhateeb, “Bulk Gas and Carbon-14 Generation Modelling from the Trenches and the Vaults Using SMOGG,” LLWR/ESC/Mem(25)478 , 2026 (pre-publication).

[95] A. W. Banford, H. Eccles and M. P. Metcalfe, “Treatment and Disposal of Irradiated Graphite and Other Carbonaceous Waste,” CARBOWASTE WP 1 Review Report - UK, 2008.

[96] National Nuclear Laboratory Ltd., “Graphite Technical Guide,” NNL 15344, Issue 2, 2021.

[97] Andra, “Graphite Reference Guide: State of Knowledge,” Andra Report FR.PA.SCM.15.0026/A, 2015.

[98] B. Poncet and L. Petit, “Method to Assess the Radionuclide Inventory of Irradiated Graphite Waste from Gas-cooled Reactors,” *Journal of Radioanalytical and Nuclear Chemistry,* vol. 298, pp. 941-953, 2013.

[99] T. Lansdell and M. Newland, “Magnox Reactor Graphite Characterisation Stage 2 - Final Active Analysis Stage,” Magnox TSG (11)0801, Issue 3, 2012.

[100] SERCO, “Cl-36 Mobility in Reactor Circuits and its Potential Significance for the ESC 2011 Inventory,” SERCO/TAS/003756/008, 2011.

[101] Amentum and MCM, “Non-radiological Assessment of the Groundwater Pathway for the LLWR 2026 ESC,” DEPSCD27-TR-004, Revision 1, December 2025.

[102] F. H. Chapelle, “Chapter 13 Biodegradation and Bioremediation of Halogenated Organic Compounds in Ground-water Systems,” 2001.

[103] Nuclear Waste Services, “Landfill Gas - Trace Components Assessment,” LLWR/MON/Mem(22)010, June 2022.

[104] W. Stumm and J. J. Morgan, Aquatic Chemistry. Chemical Equilibria and Rates in Natural Waters 3rd Edition, New York: John Wiley and Sons Inc., 1996.

[105] R. Guillaumont, T. Fanghänel, J. Fuger, I. Grenthe, V. Neck, D. A. Palmer and M. H. Rand, “Update on the Chemical Thermodynamics of Uranium, Neptunium, Plutonium, Americium Technetium,” *NEA-OECD, Paris,* vol. 5, 2003.

[106] W. Hummel, G. Anderegg, L. Rao, I. Puigdomènech and O. Tochiyama, “Chemical Thermodynamics of Compounds of U, Np, Pu, Am, Tc, Se, Ni and Zr with Selected Organic Ligands,” *NEA-OECD, Paris,* vol. 9, 2005.

[107] Andra, “ThermoChimie,” 2025. [Online]. Available: https://thermochimie-tdb.com/. [Accessed 4 November 2025].

[108] E. Giffaut, M. Grivé, P. Blanc, P. Vieillard, E. Colàs, H. Gailhanou, S. Gaboreau, N. Marty, B. Madé and L. Duro, “Andra thermodynamic database for performance assessment: ThermoChimie,” *Applied Geochemistry,* vol. 49, pp. 225-236, 2014.

[109] Jacobs, “LLWR Near-field Assessment Data - Sorption Parameters,” Jacobs Report DEPSCA17/02 Rev 4, Issue 2, 2025.

[110] SERCO, “Formal Structured Data Elicitation of Technetium Solubilities and Sorption Distribution Coefficients in the Near Field,” Serco Assurance report SA/ENV-0955, Issue 1.1, 2010.

[111] Jacobs, “Development of a General Purpose Near-field Model of the LLWR – Tests of Near-field Process Models Using PFLOTRAN,” Jacobs Report 209631/02, Issue 1, 2021.

[112] Jacobs, “An Updated Conceptual Model for the Chemical Behaviour of Radionuclides in a Cementitious Geological Disposal Facility,” Jacobs Report 208886/001, Issue 2, 2023.

[113] SERCO, “Sorption of Uranium(IV) and Uranium(VI) onto LLWR Near-field Materials,” Serco Report SERCO/TAS/003623/001, 2010.

[114] Quintessa, “Review of Sorption Parameters,” Quintessa QRS-1985A-R2-NAM, 2022.

[115] Quintessa, “Solubility and Sorption Parameters: Evaluation of Uncertainty, Part 1 – Contaminants Considered in 2020 and 2022,” QRS-1985B-R1 Version 1, August 2025 (pre-publication).

[116] Quintessa, “Solubility and Sorption Parameters: Evaluation of Uncertainty, Part 2 – Additional Contaminants,” QRS-1985B-R2 Version 1 , August 2025 (pre-publication).

[117] K. Verrall, “Extraction and Characterisation of Colloids in Waste Repository Leachate,” Ph.D. Thesis, The University of Manchester, 1998.

[118] K. Baines, “Studies on Inorganic Colloids in Groundwater Samples from the Far Field of a Waste Repository,” Ph.D. Thesis, The University of Manchester, 2003.

[119] S. Allinson, “Investigation of Inorganic Colloids in the Near-field of a Waste Repository,” Ph.D. Thesis, The University of Manchester, 2004.

[120] P. Warwick, S. Allinson, K. Beckett, A. Eilbeck, A. Fairhurst, K. Russel-Flint and K. Verrall, “Sampling and Analyses of Colloids at the Drigg Low Level Radioactive Waste Disposal Site,” *Journal of Environmental Monitoring,* vol. 4, pp. 229-234, 2002.

[121] M. S. D. Read, “Role of Colloids in Radionuclide Transport at the Low Level Waste Repository,” LLWR/ESC/Mem(24)466, April 2026.

[122] LLW Repository Ltd, “Colloidal Transportation of Contaminants through Groundwater,” LLWR/MON/Mem(17)003, 2018.

[123] Nick Evans Consulting Ltd, “The Sampling and Measurement of Colloids and Associated Radioactivity at the LLW Repository Ltd: A Review,” NEC/001, Issue 5, July 2021.

[124] SERCO, “Review of the Behaviour of Colloids in the Near Field of a Cementitious Repository,” Serco report: SERCO/TAS/000475/01, Issue 02, 2009.

[125] E. Wieland, J. Tits and M. H. Bradbury, “The Potential Effect of Cementitious Colloids on Radionuclide Mobilisation in a Repository for Radioactive Waste,” *Applied Geochemistry,* vol. 19, pp. 119-135, 2004.

[126] Amentum and MCM, “Radiological Assessment of the Groundwater Pathway for the LLWR 2026 ESC,” DEPSCD27-TR-003, Revision 1.1, December 2025.

[127] T. D. Waite, J. A. Davis, T. E. Payne, G. A. Waychunas and N. Xu, “Uranium (VI) Adsorption to Ferrihydrite: Application of a Surface Complexation Model,” *Geochimica et Cosmochimica Acta,* vol. 58, pp. 5465-5478, 1994.

[128] P. Duerden, D. A. Lever, D. A. Sverjensky and L. R. Townley, “Alligator Rivers Analogue Project Final Report. 1 Summary of Findings,” OECD/NEA Report DOE/HMIP/RR/071, 1992.

[129] J. S. Small, “Update of SEF and SRF factors for EDTA for the Phase 1 and Phase 2 Assessments,” LLWR/ESC/Mem(24)460, 2026 (pre-publication).

[130] Nuclear Waste Services, “Inventory of EDTA,” DMF0077 v2, May 2025.

[131] J. O'Hanlon, “Response to the Environment Agency’s Forward Issue on Complexants,” LLWR/ESC/Mem(22)433, July 2023.

[132] AEA, “Further Experiments on the Effects of Sikament 10 and Sikament N on Plutonium Solubility,” AEA Technology Report RWMD(97)P95, 1998.

[133] M. A. Glaus and L. R. Van Loon, “A Generic Procedure for the Assessment of the Effect of Concrete Admixtures on the Retention Behaviour of Cement for Radionuclides: Concept and Case Studies,” PSI Report 04-02, 2004.

[134] NDA, “Solubility Studies in the Presence of Polycarboxylate Ether Superplasticisers,” NDA DRP LOT 2: Integrated Waste Management WP/B2/7, 2015.

[135] Environment Agency, “Guidance for Monitoring Trace Components in Landfill Gas,” LFTGN04 v 3.0, 2010.

[136] Serco, “Non-Radiological Assessment Calculations for the LLWR 2011 ESC,” TAS/003796/012, Issue 5, April 2011.

[137] L. Johnson and B. Schwyn, “Proceedings of a NAGRA/RWMC Workshop on the Release and Transport of C-14 in Repository Environments,” 2004.

[138] J. S. Small, M. Nykyri, M. Helin, U. Hovi, T. Sarlin and M. Itävaara, “Experimental and Modelling Investigations of the Biogeochemistry of Gas Production from Low and Intermediate Level Radioactive Waste,” *Applied Geochemistry,* vol. 23, pp. 1383-1418, 2008.

[139] I. R. Beadle, “Gas Monitored Trench Simulants Progress Report,” Drigg PCSC Document DTP/84, 2003.

[140] J. R. Lloyd and A. Cherkouk, The Microbiology of Nuclear Waste Disposal, Amsterdam, The Netherlands: Elsevier, 2021.

[141] T. Fenchel, G. M. King and T. H. Blackburn, Bacterial Biogeochemistry, the Ecophysiology of Mineral Cycling, Academic Press, 2000.

[142] A. Bagnoud, K. Chourey, R. L. Hettich, I. de Bruijn, A. F. Andersson, O. X. Leupin, B. Schwyn and R. Bernier-Latmani, “Reconstructing a Hydrogen-driven Microbial Metabolic Network in Opalinus Clay Rock,” *Nature Communications,* vol. 7, p. art. no. 12770, 2016.

[143] Land Quality Management Ltd, “Methane Emissions from Landfill Sites in the UK,” LQM Report 443/1 for the Department of Environment, Food and Rural Affairs, 2003.

[144] J. P. Chantona, D. K. Powelsona and R. B. Green, “Methane Oxidation in Landfill Cover Soils, is a 10% Default Value Reasonable?,” *J. Environ. Qual,* vol. 38, pp. 654-663, 2009.

[145] LLW Repository Ltd, “Assessment of Carbon-14 Bearing Gas,” LLWR/ESC/R(13)10059, 2013.

[146] J. Small, “Modelling the Partitioning and Transport of C-14 in a Microbially Active LLW Site. In: Johnson, L. and Schwyn, B. (eds.), Proceedings of a NAGRA/RWMC Workshop on the Release and Transport of C-14 in Repository Environments.”.

[147] Quintessa, “Assessment Calculations for Radon for the LLWR 2011 ESC,” Quintessa Report QRS-1443ZG-1 Version 3.0, 2011.

[148] P. Lichtner, C. Steefel and E. Oelkers, Reviews in Mineralogy, Volume 34: Reactive Transport in Porous Media, Chantilly, Virginia: Mineralogical Society of America, 1997.

[149] G. E. Hammond, P. C. Lichtner and R. T. Mills, “Evaluating the Performance of Parallel Subsurface Simulators: An Illustrative Example With PFLOTRAN,” *Water Resources Research,* vol. 50, pp. 208-228, 2014.

[150] P. C. Lichtner, G. E. Hammond, C. Lu, S. Karra, G. Bisht, B. Andre, R. T. Mills, J. Kumar and J. M. Frederick, “PFLOTRAN Web Page,” 2025. [Online]. Available: http://www.pflotran.org. [Accessed 20 October 2025].

[151] Amec Foster Wheeler, “Review of Software for Modelling the Near Field,” Report 206427/001, Issue 1, February 2017.

[152] Environment Agency, “Review of LLW Repository Ltd’s 2011 Environmental Safety Case: Forward Issues,” Issue 1, May 2015.

[153] Jacobs, “Cap Infiltration ad hoc Task,” DEPRWD15/D40, Issue 2, February 2024.

[154] Nexia Solutions, “LLWR Lifetime Project: Sorption Parameters for the LLWR Geosphere,” Nexia Solutions (08) 9451, Issue 1, September 2008.

[155] Amentum, “Bulk Gas Generation and Migration in the LLWR,” DEPSCD29-TR-01, Issue 1, May 2026.

[156] Nuclear Waste Services, “Partitioning of C-14,” DMF0141 v4.4, May 2025.

[157] Jacobs, “Specification for SMOGG Version 7.1: A Simplified Model of Gas Generation from Radioactive Wastes,” DEPSCA19-TR-01, Issue 1.1, July 2024.

[158] Nuclear Waste Services, “Metal Corrosion Rates - Early Vault,” DMF0138 v2.1, December 2024.

[159] Nuclear Waste Services, “Metal Corrosion Rates - Stainless Steel (trenches, vaults pH 10-11, beach),” DMF0117 v1, November 2023.

[160] National Nucler Laboratory Ltd., “Review of Research on Cellulose Degradation and Input Data for the Simplified Model of Gas Generation (SMOGG),” NNL (09) 8870, Issue 3, September 2009.

[161] BNFL, “Gas Monitored Trench Simulants: Progress Report,” BNFL Technical Note TN123, (referenced in the Drigg Post-Closure Safety Case, Report DTP/84, 2002), 2001.

[162] Lawrence Berkeley National Laboratory, “TOUGH: Suite of Simulators for Nonisothermal Multiphase Flow and Transport in Fractured Porous Media,” 2025. [Online]. Available: https://tough.lbl.gov/. [Accessed 4 November 2025].

[163] Intergovernmental Panel on Climate Change, “2006 IPCC Guidelines for National Greenhouse Gas Inventories,” ISBN 4-88788-032-4, 2006.

[164] SKB, “Modelling of Critical H-M Processes in the Engineered Barriers of SFR,” SKB Report TR-14-27, 2015.

[165] Jacobs, “Gas Studies Integrated Project. Conceptual Models and Data for Gas Migration from a GDF in Lower Strength Sedimentary Rock,” DEPSCA06-TR-002, Issue 1, September 2022.

[166] M. Kelly, D. Applegate, J. A. Berry, M. C. Thorne and C. P. Jackson, “Radiological Assessment Calculations for the Groundwater Pathway for the LLWR 2011 ESC,” SERCO/TCS/E003796/011, April 2011.

[167] Amec Foster Wheeler, “Revised Assessment Model for the Groundwater Pathway,” Report 205547/001 Issue 5, 2019.

[168] Nuclear Waste Services, “Radon Emanation Fractions,” DMF0152 v1, July 2025.

[169] LLW Repository Ltd, “Trial Elicitation of Parameters Representing Performance of the Drainage Layers under Vault 9a and Future Vaults, Warrington, 9th December 2019,” LLWR/ESC/M(19)367, March 2020.

[170] Quintessa, “Review of Contaminant Solubilities,” QRS-1985-R1-NAM, Issue 1, November 2021.

[171] Amec Foster Wheeler, “Bulk Gas Generation and Migration in the LLW Repository,” 206536/001, Issue 2, April 2018.

[172] Quintessa, “LLWR 2026 ESC: Engineering Performance Assessment Gas Venting Options,” QRS-1895C-R1 Version 1.0, January 2026 (pre-publication).

[173] M. Tearle and J. Small, “Proposed Near-field Experimental Approach and Potential Benefits,” LLWR/ESC/Mem(20)372, February 2022.

[174] M. Tearle and J. Small, “Future Experimental Programme: Definition of Approach & Requirements,” LLWR/ESC/Mem(21)413, 2022.

[175] J. Small and J. O’Hanlon, “Revised Scope of the Near-field Experimental Programme,” LLWR/ESC/Mem(22)432, April 2023.

Nuclear Waste Services Limited
Pelham House
Pelham Drive
Calderbridge
Cumbria CA20 1DB
UK

t +44 (0)300 369 0000
w www.nuclearwasteservices.uk

Nuclear Waste
Services

Where to find more information

You can find out more about NWS online or by contacting us directly.

About our organisation:
nuclearwasteservices.uk/about-us

You can subscribe for e-mail updates:
public.govdelivery.com/accounts/UKNDA/signup/42429

NWS Helpdesk

0300 369 0000

info@nuclearwasteservices.uk

Freepost NUCLEAR WASTE SERVICES

Follow us:

Nuclear Waste Services

@NuclearWasteServices

@nuclear_waste_services

Nuclear Waste Services

Nuclear Waste Services Limited (Company Registration No 05608448)
is registered in England and Wales with the registered office located at
Pelham House, Pelham Drive, Calderbridge, Seascale, CA20 1DB.

Part of the NDA group